Molecular Analysis of Fission Yeast Skp1, a Core Component of the SCF Ubiquitin Ligase

Anna Lehmann

Thesis submitted towards the degree of Doctor of Philosophy

University of London

University College London
Department of Biology
London, WC1E 6BT

Cancer Research UK
Cell Regulation
Laboratory
44 Lincoln's Inn Fields
London, WC2A 3PX

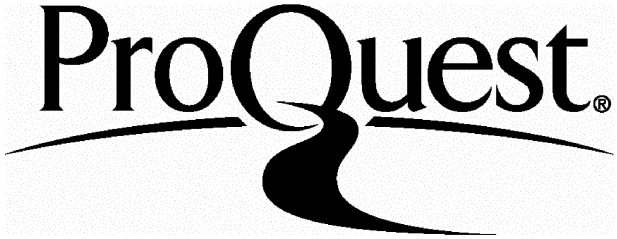

Abstract

Skp1 is a central component of the E3 ubiquitin ligase, Skp1, Cullin, F-box or SCF. It forms an adaptor bridge between a rigid cullin and the substrate specificity-determining component, the F-box. *S. pombe skp1*$^{+}$ was identified from the sequenced fission yeast genome. A deletion of the full ORF proved to be lethal as were deletions of other core components of this ligase. In order to consider a cellular role for Skp1 a temperature sensitive mutant screening analysis was carried out.

All the mutants created from this screen were sequenced and the resulting sequences showed that the alleles fell into five classes of *skp1*^{ts} mutants. Three different point mutations were obtained as were two mutations causing read through of the stop codon. Modelling of these mutations on the published structure of human SKP1 suggested that these mutations would affect F-box binding but not binding to the core SCF through Pcu1 the fission yeast cullin known to be involved in this complex.

Initial analysis demonstrated that all five types of *skp1*^{ts} mutant displayed similar phenotypes. Therefore one mutant allele, showing the most severe phenotype (*skp1*^{ts}*A7*) was chosen for further detailed characterisation. This characterisation revealed that *skp1*^{ts}A7 cells are elongated at the non-permissive temperature. This elongation can be attributed to a G2 cell cycle delay caused by activation of the DNA damage checkpoint. *skp1*^{ts}A7 cells also show abnormal chromosome segregation possibly arising from an inability to properly elongate their spindle at the restrictive temperature.

Given the results from speculative modelling, further analysis of the binding capabilities of this *skp1*^{ts}A7 mutant were analysed. This showed that Skp1^{ts}A7 was able to retain binding to Pcu1 and the majority of F-box proteins, however, binding to two F-box proteins, Pof3, an F-box involved in maintaining genome integrity and Pof1, an essential F-box, were abrogated.

The data presented in this thesis show the characterisation of *skp1*^{ts}*A7* phenotype and attempt to understand the aspects of the phenotype in the light of the interactions affected and the role for proteolysis in the cell cycle.

This thesis is dedicated to my family.

Acknowledgments

I would like to thank many people for help and support throughout my thesis. I am led to believe that for the examiners the acknowledgments are the most entertaining part of reading a thesis so I will do my best to entertain!

Firstly I would like to thank my supervisor Dr Takashi Toda for his support and encouragement and for the creation of a helpful and considerate environment in the lab that has helped to make my PhD a thoroughly enjoyable experience. I have also been fascinated to learn a great many things about Japanese culture in the process.
I would like to thank my parents for bringing me into the world, supporting me through every level of education and always spoiling me rotten. I would like to thank my brother for being older than me and showing me the way! Also for telling his friends that my PhD was about making bread.
I would also like to thank all the members of the Cell Regulation lab both past and present for being fun and interesting people to work with. In particular I would like to thank Leah for her help and patience when I was a fledgling in the lab, and Miguel Angel for being, the quiet man with the answers and for his sensitive support by e-mail now that he has left. I would also like to thank Satoshi for being the Master experimenter and Clare for her continued and unfailing enthusiasm about the SCF project and her ability to listen to me talk rubbish for hours on end and look interested.
I would also like to thank the members of the Chromosome Segregation laboratory for being fun to hang around with and organising a lot of trips to the pub and cinema and to Matt and Chris particularly for their help in reading this thesis. Chris has also asked me to thank Elvis and though I am loath to, I will do for her sake. I would also like to thank Stefan, mainly for his unforgettable impression of Ali G, but also for organising regular bracing marches across the southern countryside with Julia and co, as weekend respite from the lab.
Finally I would like to thank all my friends outside the institute in particular, "the other" Anna and Katy B for always being at the other end of the e-mail and for providing me with a second home where I can always relax and be myself, for sending me the infuriating chocolate quiz, for being willing to jeopardise their own PhD's by spending so much time writing to me!!! And for their general fabulousness. Please don't change.
Just one last thing, I would like to apologise to all the trees that got destroyed from the endless printing of draft versions of this thesis and I do hope that the de-forestation of the jungle is not exacerbated by my abundant use of paper.

Table of contents

List of Tables and Figures

Chapter 1: Introduction

Chapter 2: Identification of the components of the SCF complex in the fission yeast *S. pombe*

Chapter 3: *skp1*$^{+}$ temperature sensitive mutant screening and binding analysis

List of Figures

Chapter 4: Potential involvement of *skp1*$^{+}$ in the DNA damage checkpoint

Chapter 6: Discussion

Abbreviations

APC	Adenomatous Polyposis Coli
APC/C	Anaphase Promoting Complex
ATP	Adenosine Tri-Phosphate
BSA	Bovine Serum Albumin
Cdc	Cell Division Cycle
CDK	Cyclin Dependent Kinase
CKI	Cyclin Dependent Kinase Inhibitor
DAPI	4',6-diamidino-2-phenylindole
DNA	Deoxyribonucleic Acid
dNTPs	Nucleotide Triphosphates
DUBs	Deubiquitinating enzymes
Δ	deletion
E1	ubiquitin activating enzyme
E2	ubiquitin conjugating enzyme
E3	ubiquitin ligase
EMM	Edinburgh Minimal Medium
FACS	Fluorescence Associated Cell Sorting
5-FOA	5-Fluoro-orotic acid
g	gram
G1/2	Gap 1 or 2
GFP	Green Fluorescent Protein
HA	Hemagglutinin A
HIF	Hypoxia Inducible Factor
HU	Hydroxyurea
IP	Immunoprecipitation
LRR	Leucine Rich Repeat
M phase	Mitotic phase
mg	milligram
ml	millilitre
mM	millimolar
μg	microgram

Abbreviations

µl	microlitre
ng	nanogram
NETO	New End Take Off
ORF	Open Reading Frame
PCR	Polymerase Chain Reaction
Pof	*Pombe* F-box
RAVE	Regulator of the (H^+)-ATPase of the Vacuolar and Endosomal membranes
RNA	Ribonucleic Acid
S	Sedimentation Coefficient
S phase	Synthesis phase
SCF	Skp1, Cdc53, F-box complex
SDS	Sodium Dodecyl Sulphate
SOCS	Suppressor Of Cytokine Signalling
SPB	Spindle Pole Body
TBZ	Thiabendazole
UV	Ultra Violet light
VHL	Von Hippel Lindau
VBC	Von Hippel Lindau, Elongin B, Elongin C complex
WD repeat	Tryptophan/Apartate repeat
WT	Wild-type
YE5S	Yeast Extract 5 Supplements

Chapter 1

Introduction

The timely and selective destruction of proteins within the cell is essential for proper regulation of many processes in cell biology, in particular those requiring fast and irreversible changes in protein levels. Regulation of this kind is frequently seen in key cell cycle events and as such is highly important to the successful survival of all organisms.

The inability to control this central process of cell division can be fatal in multicellular eukaryotes such as humans, where excessive uncontrolled cell division can lead to cancer. A disruption of any part of the delicate balance of forces involved in cell cycle regulation can lead to cancer and thus the elucidation of the mechanisms governing cell division are essential to understanding this complex disease.

Unicellular organisms must copy and divide themselves in order to pass on their genetic information and create a new generation. The process of cell division is as much central to the life cycle of these organisms as it is to humans and remains astonishingly preserved in an evolutionary context. The study of unicellular eukaryotes such as the fission yeast, *Schizosaccharomyces pombe* offers a unique and simplified model for the elaboration of the essential process of cell division.

The work presented in this thesis will consider the involvement of a key class of regulating enzymes in the cell cycle, called the ubiquitin ligases. More specifically it will consider the ubiquitin ligase known as the SCF complex. It will begin with an introduction to the ubiquitin system and the discovery of the paradigm of multifactor E3 ubiquitin ligases, focusing on the role of the SCF within the cell cycle and its potential role in a cell cycle checkpoint.

1.1 The ubiquitin pathway

Intracellular protein degradation operates through the ubiquitin proteolysis system, the culmination of which in biochemical terms, is the ligation of a small protein, the 76 amino acid, ubiquitin, onto protein substrates. This occurs through a series of catalytic reactions involving three families of enzymes, known as the E1, E2 and E3 families. The attachment of a monoubiquitin moiety to a protein does not necessarily mark it as a target for destruction by the large, mechano-chemical complex, the 26S proteasome. For definitive targeting to the proteasome substrates need to acquire a polyubiquitin chain. This occurs by repeated addition of ubiquitin by isopeptide linkage to a mono-ubiquitinated substrate.

The E1 or ubiquitin activating enzyme family is responsible for the activation of ubiquitin by ATP-aided formation of a thiol-ester bond between the C-terminal glycine residue of ubiquitin and a thiol site on the E1 enzyme. Activation is followed by transfer to an E2 or ubiquitin conjugating enzyme by trans-acylation of the E2, once again creating a thiol-ester bond between the enzyme (E2) and the ubiquitin molecule. The E2 family of enzymes is capable of forming poly-ubiquitin chains joined by isopeptide linkage of lysine residue 48 of the protein, without the need for an E3. However in order to conjugate ubiquitin onto a substrate in most cases an E3 or ubiquitin ligase enzyme is required. In other cases an E3 is not required (Hershko and Ciechanover, 1992; Hochstrasser, 1996). See Fig. 1.1.1 for an illustration of the ubiquitin pathway.

E3 ubiquitin ligases fall into two categories: the HECT domain variety such as the adenovirus E6AP, or RING finger domain E3s which contain the zinc co-ordinating RING finger motif which bridges two zinc ions between a conserved cysteine/histidine rich motif (Saurin *et al.*, 1996). Some RING finger E3s are a complete ubiquitin ligase in one protein, e.g. MDM2, whilst other ubiquitin ligases consist of large groups of proteins, one component of which is a RING finger containing protein. The RING finger is required by the E3 for recruitment and interaction of the E2 (Freemont, 2000).

Once carrying a polyubiquitin chain, substrates are targeted to the 26S proteasome where they are degraded into small peptide fragments of approximately 20 amino acids. The proteasome does not degrade the attached

ubiquitin, which is de-conjugated by a further set of enzymes, the DUBs (deubiquitinating enzymes) and is recycled for further ubiquitinating activity.

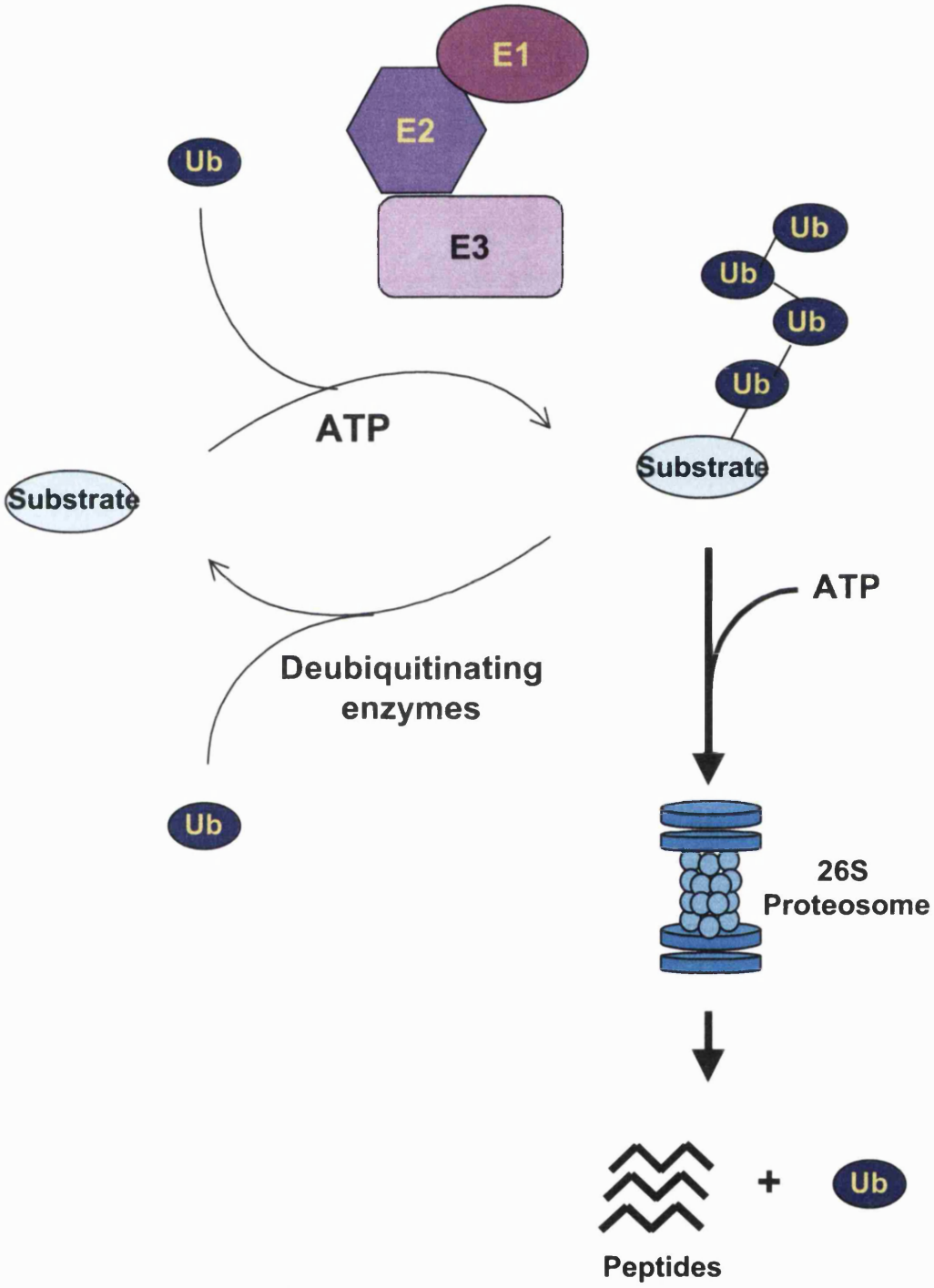

Fig. 1.1.1: The ubiquitin system
The transfer of ubiquitin onto its substrate requires the presence of an E1 ubiquitin activating enzyme, E2 ubiquitin conjugating enzyme and an E3 ubiquitin ligase. This reaction also requires ATP. Once ubiquitinated the substrate can be recognised by the 26S proteasome and degraded in an energy dependent fashion into small peptides. Ubiquitin is proteolytically cleaved by deubiquitinating enzymes and re-cycled. Ubiquitin is abbreviated to Ub in the diagram.

1.2 Ubiquitination and the cell cycle

The yeast cell cycle

A great deal of the knowledge about cell cycle regulation comes from studies carried out in yeast. The existence of genes that control the cell cycle was revealed by genetic studies in fission yeast and budding yeast. Conditional mutations in a set of genes led to the discovery of mutants that arrested at different phases of the cell cycle, whilst others could not control their division as normal and progressed through mitosis in conditions which would normally be unfavourable to the cell. The discovery of these genes, known as the cell division cycle (cdc) genes and their subsequent analysis allowed the discovery of the CDKs (cyclin dependent kinases), *cdc2* $^{+}$(fission yeast) or *CDC28* (budding yeast) and genetic components of the cell cycle checkpoints (Zachariae and Nasmyth, 1999). These kinases associate with proteins known as cyclins whose levels oscillate periodically through the cell cycle. The activity of cyclin-CDK complexes results in the phosphorylation of proteins and in the progression of cells through the different phases of the cell cycle (Fig. 1.2.1). Although initially discovered in yeast, further studies showed that these control mechanisms were universal and conserved in all eukaryotes. One major difference observed, however, between higher eukaryotes and yeast is that the yeast cell cycle is regulated by only one CDK associating with different kinds of B type cyclins, whilst in mammalian cells several different CDKs have been shown to interact with different cyclins. This presumably allows the establishment of more complex control over the cell cycle with respect to quiescent periods and division in the multicellular environment.

The association of cyclins with cyclin dependent kinases (CDKs) as the key regulators of the cell cycle was the first indication of the importance of protein regulation in the cell cycle (Doree and Hunt, 2002; Evans *et al.*, 1983). The cell cycle is underpinned by alternating phases of low and high levels of cyclin-CDK activity, a low level in G1 allowing the establishment of replication competent origins and a high level in S, G2 and M allowing the triggering of replication, prevention of origin re-firing and catalysis of entry into mitosis. The exit of mitosis is crucially dependent upon the destruction of cyclin B causing rapid

inactivation of the CDK complexes. The ability of a stable form of cyclin B, missing 90 amino acids of the N terminus, to interact with CDKs but preventing the exit of mitosis, eventually led to the conclusion that the protein contained a destruction motif (Murray *et al.*, 1989). This finding recognised the importance of proteolysis in progression of the cell cycle. The discovery of the Anaphase Promoting Complex or cyclosome (APC/C) the first of the large multi-subunit E3 ubiquitin ligases further advanced the view that proteolysis was crucial to the cell cycle (reviewed by (Zachariae and Nasmyth, 1999).

The APC/C was identified by a convergence of biochemical and genetic data from the frog, *Xenopus laevis,* and the yeast, *Saccharomyces cerevisae*. Work on fractionation of extract of *Xenopus* eggs revealed a protein complex that sedimented at 20S, was associated with proteolytic activity and this activity was cell cycle regulated (King *et al.*, 1995; Sudakin *et al.*, 1995). Studies on yeast mutants which were incapable of degrading a cyclin-β-galactosidase construct in G1, revealed five essential genes, the products of which, formed part of a large proteolytic particle much like that isolated from *Xenopus* (Irniger *et al.*, 1995). Since the recognition of the importance of regulated and specific protein destruction to the progression of the cell cycle, a further multi-component ubiquitin ligase has been discovered to be important in the release from G1 and entry into S phase. This ligase has been named the SCF complex and consists of **S**kp1, **C**dc53 (or **C**ullin protein) and the **F**-box.

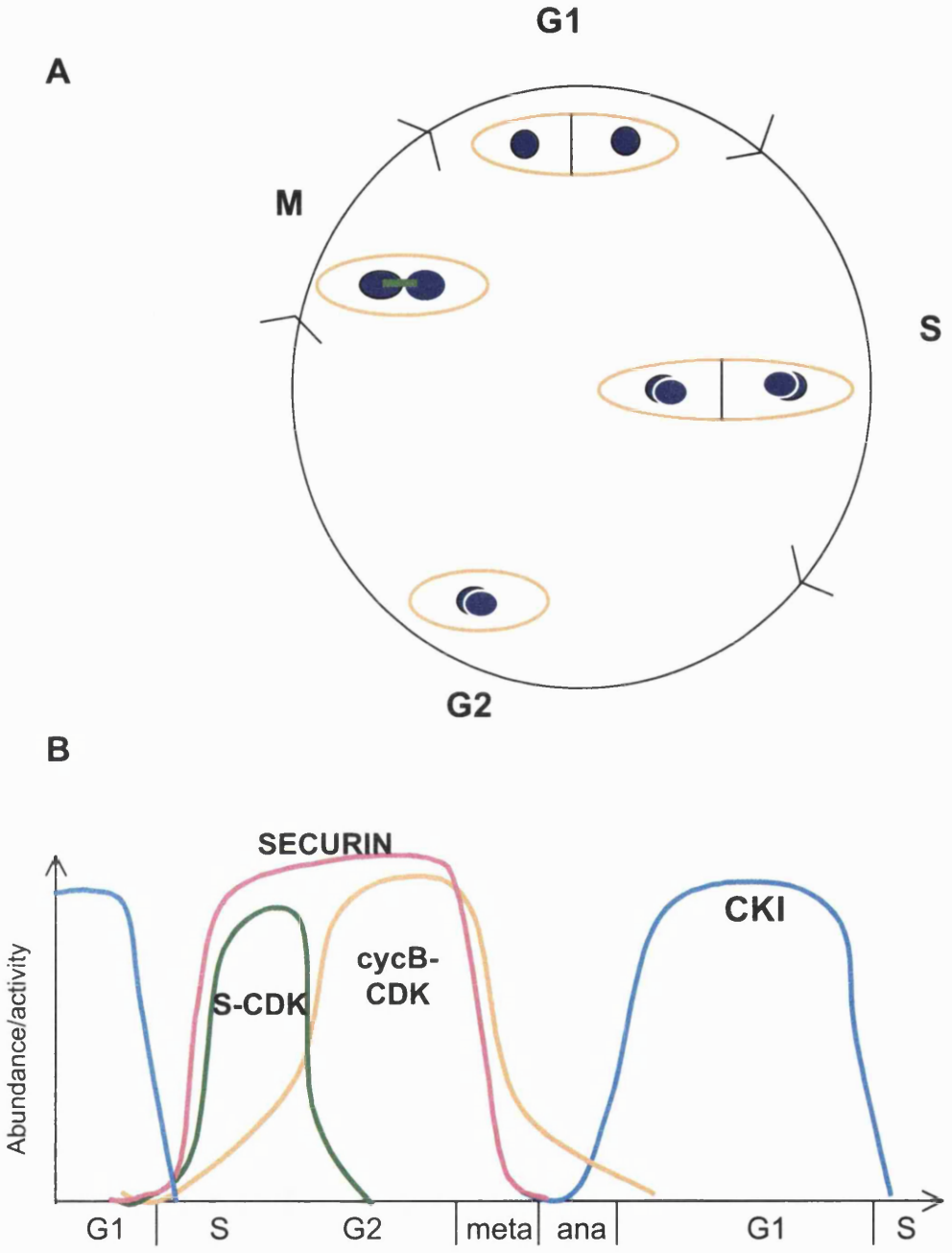

Fig. 1.2.1 The cell cycle

A The phases of the fission yeast cell cycle are represented (not to scale). In fast growing cultures the critical size for re-replication of the DNA is reached before cytokinesis is fully completed. Therefore cells enter G1 and S phase whilst still attached to their sister cell. G2 cells are short as they are the first stage of full separation. This fact is taken advantage of in the process of elutriation. See Materials and Methods.

B A generalised model of the oscillation in levels of the key regulators of the cell cycle. During G1, levels of cyclin dependent kinase inhibitors (CKI) are high. Whilst levels of cyclin B-cyclin dependent kinase (cycB-CDK) activity are low. S phase is initiated by a burst of S phase cyclin/CDK (S-CDK) and mitosis is triggered by rising levels of cycB-CDK which results in the destruction of securin allowing sister chromatids to be separated by separase.

1.3 Discovery of the SCF complex

Components of the SCF complex were first identified in budding yeast in relation to the phosphorylation-dependent degradation of the CDK inhibitor (CKI) Sic1. The temperature sensitive mutant *cdc4* is arrested at the G1 to S phase transition with a multiple budded phenotype and unreplicated DNA. These cells accumulate Sic1; deletion of Sic1 allows these cells to replicate their DNA but does not suppress lethality (Schwob *et al.*, 1994). These findings could be explained if Cdc4 forms part of a multi-protein complex that degrades Sic1 at the G1-S phase boundary.

Skp1 was initially identified independently in human fibroblasts as a binding partner of cyclin A-Cdk2 (Zhang *et al.*, 1995). The role of Skp1 as a component of a proteolytic complex was established from studies isolating *SKP1* as a multi-copy suppressor of the *cdc4* phenotype. The presence of *SKP1* in multi-copy allows Sic1 to be degraded in *cdc4* mutants (Bai *et al.*, 1996).

Studies also identified *CDC53*, the homologue of human Cullin1 (Mathias *et al.*, 1996; Patton *et al.*, 1998a) along with the E2 *CDC34*. The mutants of each of these components were shown to have a similar phenotype to *cdc4*. After much *in vivo* study in yeast, components of the yeast complex were expressed *in vitro* in insect cells and ubiquitinating activity was reconstituted (Feldman *et al.*, 1997; Skowyra *et al.*, 1997). Two years later a further component of the SCF complex, Rbx1, was isolated which highly enhanced *in vitro* ubiquitinating activity (Kamura *et al.*, 1999; Seol *et al.*, 1999; Skowyra *et al.*, 1999). Rbx1 is in fact essential to ubiquitinating activity of the ligase. It contains the RING domain which is essential for association of the E2 with the E3 (Zheng *et al.*, 2002).

Before the discovery of Rbx1, experiments *in vitro,* reconstituting the SCF, were carried out using an insect cell system to produce yeast proteins. These produced active complexes but it is unclear how this was possible in the absence of Rbx1. However, it seems likely that Rbx1 is so highly conserved that the preparations of SCF components prepared and purified from insect cells contained a functional insect version of the Rbx1 protein that could be complexed with the yeast proteins (Feldman *et al.*, 1997).

SCF^{cdc4} at the G1/S phase boundary

Subsequent to mitotic exit, all cells intending to re-replicate their DNA and divide again must undergo a period of low cyclin B-CDK activity. During this period levels of CDK activity are kept low by two mechanisms. The first mechanism is by degradation of cyclin B, which is initiated at the end of anaphase by the APC/C. The second method of lowering cyclin B-CDK activity is by the inhibition of CDKs by CKIs. For cells to progress on into S phase the CDK must be released from inhibition by CKIs allowing it to associate with S phase cyclins (see Fig. 1.2.1). In budding yeast this is where the SCF^{cdc4} comes into play. During G1 the Clns, G1 cyclins, associate with Cdc28 and result in the phosphorylation of the CKI, Sic1. This phosphorylation targets Sic1 for degradation by the SCF complex and allows progression from G1 into S phase (Bai *et al.*, 1996). A similar situation exists in fission yeast where mutants or deletions of the F-box proteins, Pop1 and Pop2, show accumulation of the CKI Rum1, which requires phosphorylation before it is degraded. Cdc18, a replication factor, is also degraded by the $SCF^{pop1/pop2}$. This replication factor is only required for the initiation of S phase and can then be degraded. Therefore the $SCF^{pop1/pop2}$ is considered to be a major factor controlling genome ploidy as accumulation of both Rum1 and Cdc18 lead to successive rounds of S phase, whilst mitosis remains inhibited by the presence of Rum1. DNA is therefore not segregated resulting in polyploid cells. (Kominami *et al.*, 1998; Kominami and Toda, 1997).

The F-box hypothesis

The discovery of the SCF^{cdc4} complex and the establishment of a motif in Cdc4 that was found in other proteins in the yeast proteome opened the door to the idea of the F-box hypothesis. The F-box is so named as it was initially identified as a motif in cyclin F (Bai *et al.*, 1996). The motif is a forty amino acid domain and is loosely conserved. The F-box domain is responsible for binding to Skp1. In most F-box proteins the F-box domain tends to be found at the N-terminus of the protein with another form of protein/protein interaction domain in the C-terminus such as WD-repeats or Leucine Rich Repeats (LRR). It is thought that

these protein/protein interaction domains bind to substrates for ubiquitin ligation (Patton *et al.*, 1998b).

The F-box hypothesis suggested that cullin, Skp1 and Rbx1 formed a central core ubiquitin ligase and this was capable of associating with several different F-box proteins in order to establish different SCF complexes, each with the ability to degrade different subsets of substrates (Patton *et al.*, 1998a; Patton *et al.*, 1998b). The finding that Cdc53, Skp1, and Grr1 but not Cdc4 were required for the degradation of G1 cyclin, Cln2 (Patton *et al.*, 1998a; Skowyra *et al.*, 1997; Skowyra *et al.*, 1999) and Cdc53, Skp1 and Met30 could together degrade Met4, a transcription factor involved in methionine biosynthesis, (Kaiser *et al.*, 2000; Patton *et al.*, 2000; Patton *et al.*, 1998a; Rouillon *et al.*, 2000) substantiated this claim. Since this initial discovery the genomes of various eukaryotes have been searched for F-box genes and many have been discovered in metazoans and yeast (Cenciarelli *et al.*, 1999; Regan-Reimann *et al.*, 1999; Winston *et al.*, 1999a).

Architecture of the SCF complex

Having identified the components of the SCF complex the next step in understanding this complex has been the establishment of how it assembles and how it relates to both substrate and the E2 ubiquitin conjugating enzyme. Crystallographic studies of the complex from human cells binding a human F-box SKP2 have gone a long way to elucidating the structure of the complex in a way that has not been possible to the same extent with the APC/C. It seems that the large cullin protein forms the scaffold platform on which all SCF complexes are built (Patton *et al.*, 1998a). The culllin structure is proposed to be relatively rigid, SKP1 binding to the cullin occurs at the cullin N-terminus, a less conserved region of the protein amongst cullin family members. Binding of the cullin to the RING motif protein occurs around the, well conserved, cullin domain at the C-terminus of the protein (Zheng *et al.*, 2002). As there are several cullin proteins in the genomes of other tested organisms (Kominami and Toda, 1997; Michel and Xiong, 1998) and each is a large protein, containing a relatively unconserved N-terminus domain and a well conserved cullin domain, the suggestion is that the N-terminus of each cullin protein could associate with a protein that performs a SKP1 adaptor role (not necessarily SKP1) but that

each C-terminus will interact with a RING protein and an E2 to form different cullin containing but non SCF ubiquitin ligases (Deshaies, 1999).
The RBX1 RING protein forms an intermolecular association in its structure with the cullin and also contains an unusual form of the RING finger enabling it to chelate a third zinc ion as opposed to the normal two zinc ions. However, comparisons of RBX1 with another RING finger E3, c-Cbl (Miyake *et al.*, 1997), show that its ability to bind to an E2 is mechanistically similar.
The SKP1 interaction with CUL 1 is meanwhile mediated through a specific protein domain known as the BTB/POZ (Broad complex Tamtrack Brick-a-brack/Pox virus and Zinc finger) domain (Aravind and Koonin, 1999). This domain is found in the N-terminus of SKP1. The F-box protein may be partly involved in mediating binding of SKP1 to CUL 1 as well. Through interaction with SKP1 the F-box is also brought into contact with the cullin (Schulman *et al.*, 2000).
The overall picture is of the cullin protein holding apart SKP1 and RBX1 at the two ends of its structure. The E3 probably does not play a part in catalytic transfer of the ubiquitin to the substrate unlike E1 and E2. There is no evidence for the formation of a thiol-ester between E3 and ubiquitin. Instead it is thought that the binding of the F-box plus substrate to the core complex orientates the substrate in order for it to be ubiquitinated (Zheng *et al.*, 2002). See Fig. 1.3.1

Fig. 1.3.1: Structure of the mammalian SCF complex
CUL1 forms the structural scaffold of the complex binding to both SKP1 and RBX1 directly and holding them rigidly apart, in order to orientate the substrate and E2 which bind at opposite ends. SKP1 forms contacts with the F-box protein through its F-box domain. RBX1 and CUL1 interact with the E2 and this is thought to bring the substrate and E2 into the right orientation for ubiquitin transfer. (Picture taken from Zheng et al., 2002)

1.4 Controlling mechanisms for E3 ubiquitin ligases

Nedd8/Rub1 covalent modification of cullin proteins

A small ubiquitin like protein usually known as Nedd8 but referred to as Rub1 in budding yeast, has been shown to be covalently attached to cullin proteins (Lammer *et al.*, 1998; Liakopoulos *et al.*, 1999). It is necessary for maximal activity of the SCF ubiquitin ligases and its site of attachment, according to structural studies, is close to the RBX1 association region (Zheng *et al.*, 2002). The exact function of this protein remains unclear. However, its attachment to the cullin proteins requires a series of enzymatic reactions similar to those involved in the activation and ligation of ubiquitin to substrates. A pair of E1-like activating enzymes and an E2 conjugation-like protein are involved in conjugation of Nedd8 to cullins (Gong and Yeh, 1999). Recently, it has been proposed that cycles of conjugation of Nedd8 onto cullin and de-conjugation off it, are essential for ubiquitination activity (Pintard *et al.*, 2003). It is claimed that Nedd8 may allow association of an E2, loaded with ubiquitin, to bind to the E3. In order for further ubiquitin-bearing E2 to be brought to the E3, Nedd8 must be detached and re-associated. The COP9/signalosome, a large complex, originally discovered in plants and containing homology to the 19S proteasome lid (Wei *et al.*, 1994), is required for removal of Nedd8 from cullin proteins (Lyapina *et al.*, 2001). Disruption of the function of this complex, by removing the metalloprotease component thought to be directly responsible for cleavage of Nedd8 from cullins, results in an accumulation of neddylated cullins and stimulated SCF activity towards some substrates (Berndt *et al.*, 2002). However it seems there are still further regulatory functions of Nedd8 and the COP9/signalosome.

Mutants in some components of the signalosome complex in *S. pombe* have shown phenotypes of slow S phase progression and mild sensitivity to DNA damaging agents (Liu *et al.*, 2003; Mundt *et al.*, 1999)). This has led to the discovery that the signalosome is associated with the *S. pombe* Cullin 4 protein, along with the Ddb1 (DNA damage binding) protein and this complex is proposed to have ubiquitin ligase activity directed towards Spd1, the inhibitor of the small subunit of ribonucleotide reductase. In human cells the signalosome has been found to be associated with CUL4A in two complexes containing

either DDB2 (DNA damage binding) protein or CSA (Cockaynes Syndrome A) protein. These complexes show ubiquitin ligase activity and are involved in responses to DNA damage (Groisman *et al.*, 2003; Liu *et al.*, 2003). *S. pombe* cullin 3 has also been found associated with the signalosome and a deubquitinating enzyme Ubp12. Zhou and co-workers suggest that the signalosome acts as a major assembly site for cullin E3 ligases. The association of the deubiquitinating enzyme at the site of assembly would prevent autocatalytic degradation of F-box or adaptor proteins whilst ligases are being built (Zhou *et al.*, 2003).

Temporal control of E3s: activator proteins versus phosphorylation

For cell cycle components timely degradation by the proteasome is highly important to achieve the kind of molecular switches observed in the progress of the cell cycle. Seeing as E3s are involved in the selectivity of the substrate it seems natural that these ligases are also subject to temporal control to bring about degradation at the correct moment. It is interesting that subunits of the APC/C and SCF have been shown to be homologous; Apc2 and 11 have similarities to cullins and Rbx1 respectively (Deshaies, 1999). It has been proposed that APC/C and SCF are distant evolutionary cousins, but this structural similarity does not appear to extend to mechanisms of control of these two ligases.

Genetic studies in budding yeast and flies identified two activator proteins which modulate APC/C activity. These proteins are both WD-repeat proteins known as Cdc20/Fizzy/Slp1 and Cdh1/Fizzy-related/Srw1 (budding yeast/drosophila/fission yeast). For simplicity these proteins are henceforth referred to using budding yeast names. Cdc20 degrades substrates at the metaphase to anaphase transition and subsequently Cdh1 takes over and degrades substrates from anaphase and during G1. Overexpression of either activator causes degradation of their substrates at any point in the cell cycle. Which protein binds to the APC/C depends on several factors. The level of Cdc20, which rises as cells enter mitosis and drops as they exit it, allowing Cdh1 to associate with the APC/C is one factor. A second is the interaction of Cdh1, whose levels are constant, with APC/C. Cdh1 binding is inhibited by phosphorylation, and binding of Cdc20 is increased by phosphorylation of the

APC/C. The binding behaviours of the activators are neatly opposed, allowing sequential association first with Cdc20 and then Cdh1, (reviewed by Zachariae and Nasmyth, (1999); see Fig. 1.4.1).

In contrast to the highly regulated cycle that appears from studies of the APC/C, SCF is not regulated at the level of the ligase but at the level of the substrate. So far the majority of substrates known to associate with the SCF are seen to be phosphorylated preceding interaction with the F-box protein of choice, (summarised by Yaffe and Elia, 2001). The fact that different F-box proteins must associate with the SCF allows one level of regulation, although it is still unclear how this is manipulated in the cell. In some respects this resembles the different activators of APC/C, Cdc20 and Cdh1. In the SCF the numbers of activators, however, are far higher and there is no established mechanism for their association with the SCF core particle (see Chapter 3 for further discussion of this). It seems likely that if the process of adaptor protein association with core particle is unregulated; then the main control over degradation of substrates is a post-translational modification that enhances their association with the F-box protein.

The most studied substrate is that of the SCF^{cdc4}, Sic1. It has now been established that Sic1 contains a series of suboptimal binding motifs known as Cdc4 phospho-degron sites (CPD) that are all capable of weak association with Cdc4. In order for rapid degradation to be triggered at least 6 of the 9 phosphorylation sites must be phosphorylated. This allows a switch-like mechanism for degradation whereby high levels of phosphorylation of the substrate must be achieved before maximal binding and thus degradation occurs. If a single optimal CPD is substituted for the 9 sub-optimal ones found in Sic1, degradation of the protein occurs but not in such a sharply defined switch like manner. The phosphorylation of the protein allows it to interact with a pocket on the beta-propeller structure of the WD40-repeat (Nash *et al.*, 2001). It therefore seems likely that all proteins that require phosphorylation for degradation, influence their own affinity for their F-box receptors. By requiring temporal control at the level of the substrate, the SCF eliminates such a strong requirement for regulation in itself and therefore increases the diversity of the substrates with which it can associate, retaining the ability to be active throughout the entire cell cycle.

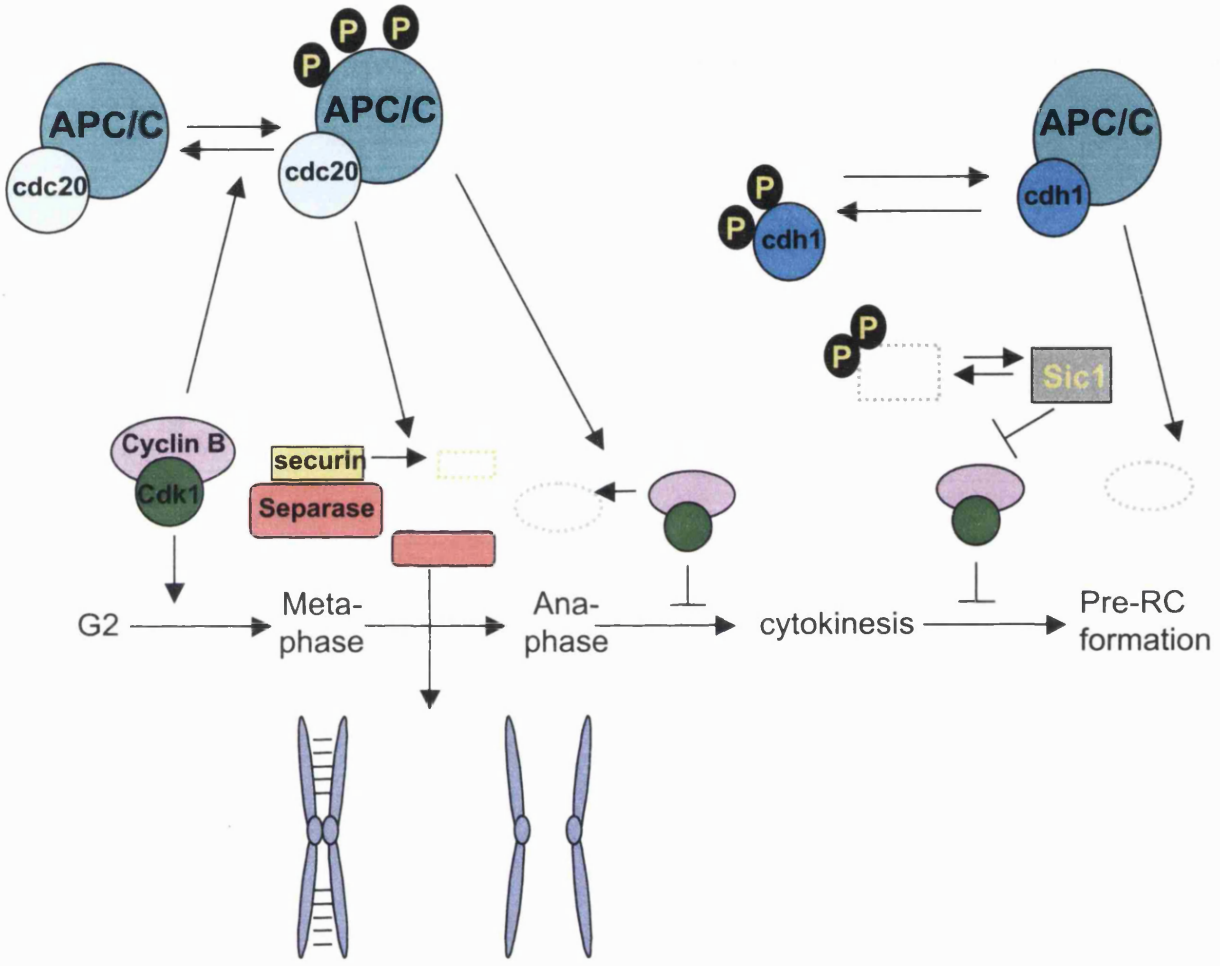

Fig. 1.4.1: Activators of the APC/C
Adapted from Zachariae and Nasmyth 1999. The APC/C is so far known to be controlled by two activator proteins. Cdc20 and Cdh1 (names from Budding yeast but homologous proteins exist in all species tested). The association of these proteins with the APC/C is thought to be sequential. In the G2-M phase association of Cdc20 with the APC/C is aided by phosphorylation of the APC/C. Targets of the APC/C Cdc20 include securin and cyclin B which leads to the progression through mitosis by separation of sister chromatids and exit of mitosis. In G1 APC/C Cdh1 takes over from APC/C Cdc20. Dephosphorylation of Cdh1 allows it to associate with APC/C and leads to the continued destruction of cyclin B necessary in G1 for the formation of pre-replication complex formation. Sic1 the budding yeast CKI is also present at this time and helps to inhibit any remaining cyclin B/CDK complexes.

1.5 SCF sets a precedent for other ubiquitin ligases based on similar architecture.

VHL

As mentioned above, ubiquitin ligase activity based on a similar format to an SCF complex but containing different cullins and different adaptor proteins are now considered almost certainly to exist. One example of this kind of ligase already exists from work carried out in human cells. The tumour suppressor gene Von Hippel Lindau (VHL) which is frequently mutated in clear cell renal carcinoma and is also associated with the rare cancer syndrome Von Hippel Lindau disease, forms part of such a complex. The VHL protein contains a motif known as the SOCS box (Suppressor of Cytokine Signalling) which is necessary and sufficient for binding to an adaptor protein with homology to SKP1, Elongin C. Elongin C is also part of a transcription elongation complex with Elongins A and B (Iwai *et al.*, 1999; Kamura *et al.*, 1998; Kile *et al.*, 2002; Lisztwan *et al.*, 1999; Stebbins *et al.*, 1999). The motif for binding to Elongin C has been further narrowed to a region of 10 amino acids that is the only shared sequence in Elongin A and VHL which both bind to Elongin C. This is referred to as the BC-box (Aso *et al.*, 1996; Duan *et al.*, 1995; Kibel *et al.*, 1995). Elongin B is also found in the Von Hippel Lindau complex, also known as the VBC complex. The Elongins in turn bind to the human Cullin 2, which is associated with RBX1. This complex has been shown to bind to and mediate the ubiquitination of hypoxia inducible factors HIF1α and HIF2 (Kamura *et al.*, 2000). In conditions of normoxia these proteins are degraded. However in conditions of hypoxia the HIFs are upregulated leading to transcription of genes related to angiogenesis (Maxwell *et al.*, 1999; Sutter *et al.*, 2000). It is interesting that clear cell renal carcinoma is commonly associated with neo-angiogenesis and it has now been shown that this is related to the mutations of VHL, which prevent, ubiquitination and degradation of the HIFs (reviewed by Semenza, 2000).

The SOCS box was originally identified in proteins that negatively regulate cytokine-inducible signalling, through the Jak/STAT pathway and thus VHL is not the only protein that contains this motif. Since it has been shown that this motif is the part of the protein necessary for binding to Elongin C, new data is

now emerging indicating that like the SCF complex the VBC complex binds multiple substrates through association with different BC box containing proteins. Furthermore it seems possible that the Elongin B/C adaptor may be able to bind more than one cullin as it has been shown to interact with Cullin 5 as well as Cullin 2 (Brower *et al.*, 2002; Kamura *et al.*, 2001). This could increase the diversity of substrates degraded by BC box proteins as interaction of the same BC box protein with different cullins could produce different substrate specificity.

Other ligases

It is now becoming clear that each of the cullin proteins is associated with ubiquitination activity. Pcu3 the *S. pombe* cullin 3 has been shown to have E3 ubiquitin ligase activity in a substrate free assay (Zhou *et al.*, 2001), whilst Pcu4 is thought to be involved in ubiquitin ligase activity to degrade Spd1, the inhibitor of the small subunit of ribonucleotide reductase (Liu *et al.*, 2003). Similarly in human cell lines, CUL4A is shown to associate with DDB2 and components of the COP9/signalosome and to have ubiquitin ligase activity (Groisman *et al.*, 2003). In the worm *C. elegans* a new protein, Mel-26, containing the BTB motif found in Skp1 for binding to Pcu1, has been identified as binding to Cul3 and a substrate Mei1/Katanin a microtubule severing protein (Matthias Peter personal communication) See Fig. 1.5.1.

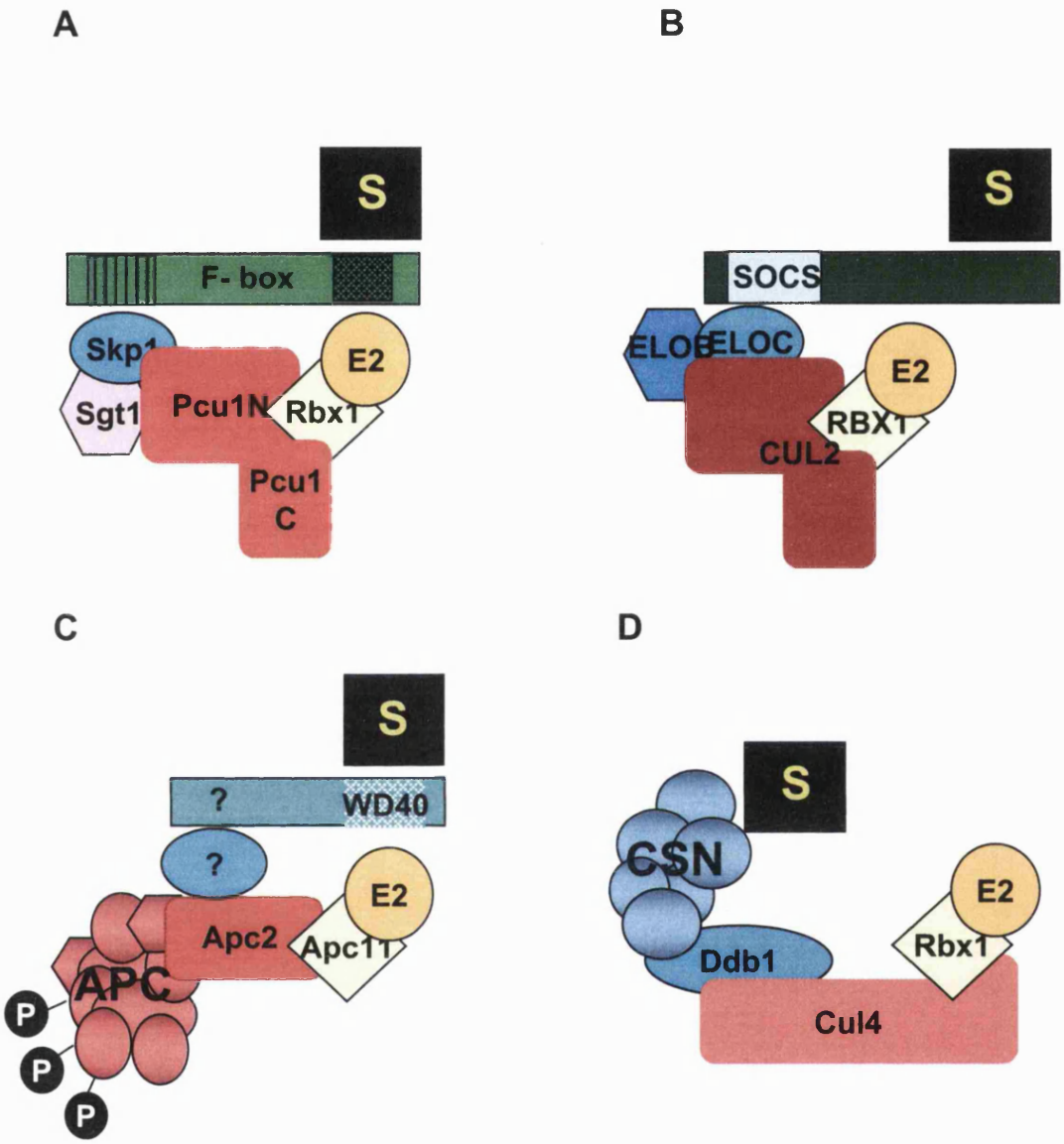

Fig. 1.5.1: The SCF as a paradigm. Different Ubiquitin ligases based on the same structure

A A cartoon representation of the SCF complex. **B** The mammalian VBC complex based on Cullin 2 as the structural backbone. Elongin B and C replace Skp1 and the B/C box containing SOCS box protein VHL acts as one adaptor protein, although other adaptors are currently emerging. **C** The homology of 2 subunits of the APC to cullin (Apc2) and Rbx1 (Apc11) has led to the suggestion that the SCF and APC/C are distant relatives. The WD40 activator proteins are seen as being akin to the F-box proteins of SCF. **D** The recently proposed ubiquitin ligase acting on Cullin 4 scaffold and involving Ddb1 and associating with the signalosome (CSN) is thought to be involved in degradation of the ribonucleotide reductase inhibitor Spd1 in *S. pombe*

1.6 SCF complexes of higher eukaryotes: far reaching roles for ubiquitin-mediated degradation

Since its initial discovery the SCF complex has been shown to be involved in many highly important cellular processes. In humans, apart from the discovery of the VBC complex and its involvement in VHL cancer syndromes, the SCF is involved in pathways as diverse as degradation of the CKI $p27^{kip1}$, cyclin E, the inhibitor of NFκB mediated signalling IκB and the NFκB precursor p105, β-catenin as well as Vpu1 a protein produced by the human immunodeficiency virus (HIV).

$SCF^{\beta TrCP}$

This SCF complex has major physiological importance as it is implicated in degrading inhibitors of NFκB, β-catenin and Vpu1. Proteins that bind to the βTrCP F-box are shown to be recognised by a short phospho-peptide motif in the substrate, DS(P)GXXS(P) (Winston *et al.*, 1999b; Yaron *et al.*, 1998). A huge number of proteins contain this motif and it is still to be elucidated how many of them are $SCF^{\beta TrCP}$ substrates.

NFκB is a heterodimeric transcription factor found in a large variety of cell types and is required for transcription of various genes in response to infection, inflammation and stress-related situations. To carry out its transcriptional activation role NFκB must be nuclear. In order to inhibit the protein its localisation signal is masked by a family of inhibitory proteins, the IκBs. This inhibition is released by IκBs' phosphorylation by the specific protein kinase IKK. The phosphorylation occurs on serines in the DSGXXS motifs of the protein resulting in recognition of IκBs by the $SCF^{\beta TrCP}$ and subsequent degradation by the proteasome (Kroll *et al.*, 1999; Suzuki *et al.*, 1999; Tanaka *et al.*, 2001). This releases NFκB which can translocate to the nucleus to promote gene transcription (reviewed by Karin and Ben-Neriah, 2000).

The NFκB transcription factor is comprised of 2 subunits that start out as precursor proteins and are proteolytically processed to form the mature proteins. One of these, p105, was demonstrated to be modified by the proteasome and is the first example of a protein that can be processed rather

than completely degraded by the proteasome. It was established that the presence of a Glycine rich repeat (GRR) poisons proteolytic destruction and is present in the p105 precursor at a position appropriate to prevent complete degradation of the protein (Orian *et al.*, 1999; Orian *et al.*, 1995). The p105 precursor of NFκB, p50, contains DSGXXS motifs and initially it was thought that processing was a function of $SCF^{\beta TrCP}$ mediated ubiquitination. The current view however, is that processing is not dependent on phosphorylation by IKK and thus is not an $SCF^{\beta TrCP}$ mediated event. p105 can also act as a cytosolic inhibitor of NFκB heterodimers and in this context is subjected to IKK phosphorylation on its DSGXXS motif and is thus fully degraded by $SCF^{\beta TrCP}$ mediated ubiquitination (Heissmeyer *et al.*, 2001; Lang *et al.*, 2003). Therefore there are dual pathways for p105 regulation.

Another important signalling molecule degraded by the $SCF^{\beta TrCP}$ is β-catenin. Once again this requires phosphorylation of the target protein at a DSGXXS motif by a kinase. Work in *Xenopus* egg extracts reveals that absence of signalling through the Wnt pathway results in continuous degradation of β-catenin whilst Wnt signalling and the subsequent presence of Dishevelled causes β-catenin to accumulate. The phosphorylating kinase in this case is GSK3β (Glycogen Synthase Kinase 3-beta), which is bound, along with β-catenin and APC (here standing for Adenomatous Polyposis Coli protein as opposed to the APC/C referred to earlier) to Axin to form a complex. The presence of Dishevelled in the cell recruits a GSK3β inhibitory factor known as GBP (GSK3β Binding Protein) and together Dishevelled and GBP prevent GSK3β phosphorylation of β-catenin. Unphosphorylated β-catenin accumulates in the cell and interacts with Tcf/Lef1 transcription factor, entering the nucleus where it performs anti-apoptotic functions (Salic *et al.*, 2000); see Fig. 1.6.1. Stabilising mutations in β-catenin are responsible for transformation of primary cells in cell culture and as such are oncogenic mutations. βTrCP has been shown to be a transcriptional target of β-catenin/Tcf complexes and consequently forms part of a negative regulatory feedback loop that can link signalling through β-catenin to the NFκB pathway. By up-regulating βTrCP transcription there can also be increased degradation of IκBs (Spiegelman *et al.*, 2000).

As well as being involved in regulatory functions in signalling pathways the disruption of which can lead to oncogenesis, the βTrCP F-box protein is also a key protein that can be hijacked by the Human Immunodeficiency Virus (HIV) Vpu1 protein. The Vpu1 protein contains a DSGXXS motif which allows it to bind to βTrCP. It is also capable of binding to the T cell receptor CD4 thus causing CD4 to become a target of $SCF^{\beta TrCP}$. Vpu1 on the other hand does not contain an attachment site for polyubiquitination allowing it to continuously bind to the $SCF^{\beta TrCP}$ without being targeted for degradation. HIV uses CD4 on the T-cell as a receptor for entry into the cell. The benefit for the virus to down-regulation of this receptor upon infection is to prevent superinfection of the T-cell, which is most probably detrimental to viral replication. This mechanism is therefore a fascinating demonstration of the way in which a virus can hijack the host's proteins for its own benefit (reviewed byKarin and Ben-Neriah, 2000).

Recently a new target of the $SCF^{\beta TrCP}$ has been identified, the F-box protein Emi1 first described in *Xenopus*. This protein can inhibit the APC/C by a method different to the checkpoint protein Mad2. Further work on this protein has shown that it contains a DSGXXS motif (Margottin-Goguet *et al.*, 2003).

SCF^{skp2} and SCF^{hcdc4}

The initial discovery of the SCF complex in budding yeast was followed up by findings in humans that it plays an essentially similar role in cell cycle regulation. The SCF^{cdc4} or $SCF^{pop1/pop2}$ in budding and fission yeast respectively were shown to degrade CKI's Sic1 or Rum1 and replication factors Cdc6 or Cdc18. Thus these two complexes are functionally homologous and are essential for normal regulation of the G1/S phase boundary. In human cells the transition from quiescence to G1 and subsequently from G1 to S phase requires the down regulation of first, the CKI $p27^{kip1}$, followed by the subsequent degradation of cyclin E from the CDK2 complexes. This process requires two SCF complexes, the extensively studied SCF^{skp2} and the recently discovered SCF^{hcdc4}. See Spruck and Strohmaier, (2002) for a review.

During quiescence the levels of $p27^{kip1}$ are inhibitory to entry into the cell cycle. Mitogenic stimulation results in sequestering of $p27^{kip1}$ in cyclinD/CDK4/6 complexes. This releases sufficient cyclin E/CDK2 to allow it to phosphorylate $p27^{kip1}$ on T187. p27 ^{kip1} phosphorylated at T187 can be recognised by the SCF^{skp2}. Degradation of $p27^{kip1}$ is also crucially dependent on the presence of CKS1, a cyclin dependent kinase associated factor (Bartek and Lukas, 2001; Ganoth *et al.*, 2001; Spruck *et al.*, 2001). Degradation of $p27^{kip1}$ by the SCF^{skp2} allows cyclin E/CDK2 levels to reach their maximal capacity required for G1. The kinase activity of cyclin E/CDK2 also allows autophosphorylation of cyclin E resulting in its recognition by SCF^{hcdc4} and subsequent degradation by the proteasome (Koepp *et al.*, 2001; Moberg *et al.*, 2001). Mutations that abolish the function of $p27^{kip1}$ are frequently found in aggressive tumours and it is therefore interesting to note that any increase in $p27^{kip1}$ degradation through increased levels of SKP2 protein could also lead to the same oncogenic effects. Increased levels of SKP2 have now been found in human lymphomas (Latres *et al.*, 2001).

For a list of SCF complexes from different organisms and their substrates see Table 1.6.1

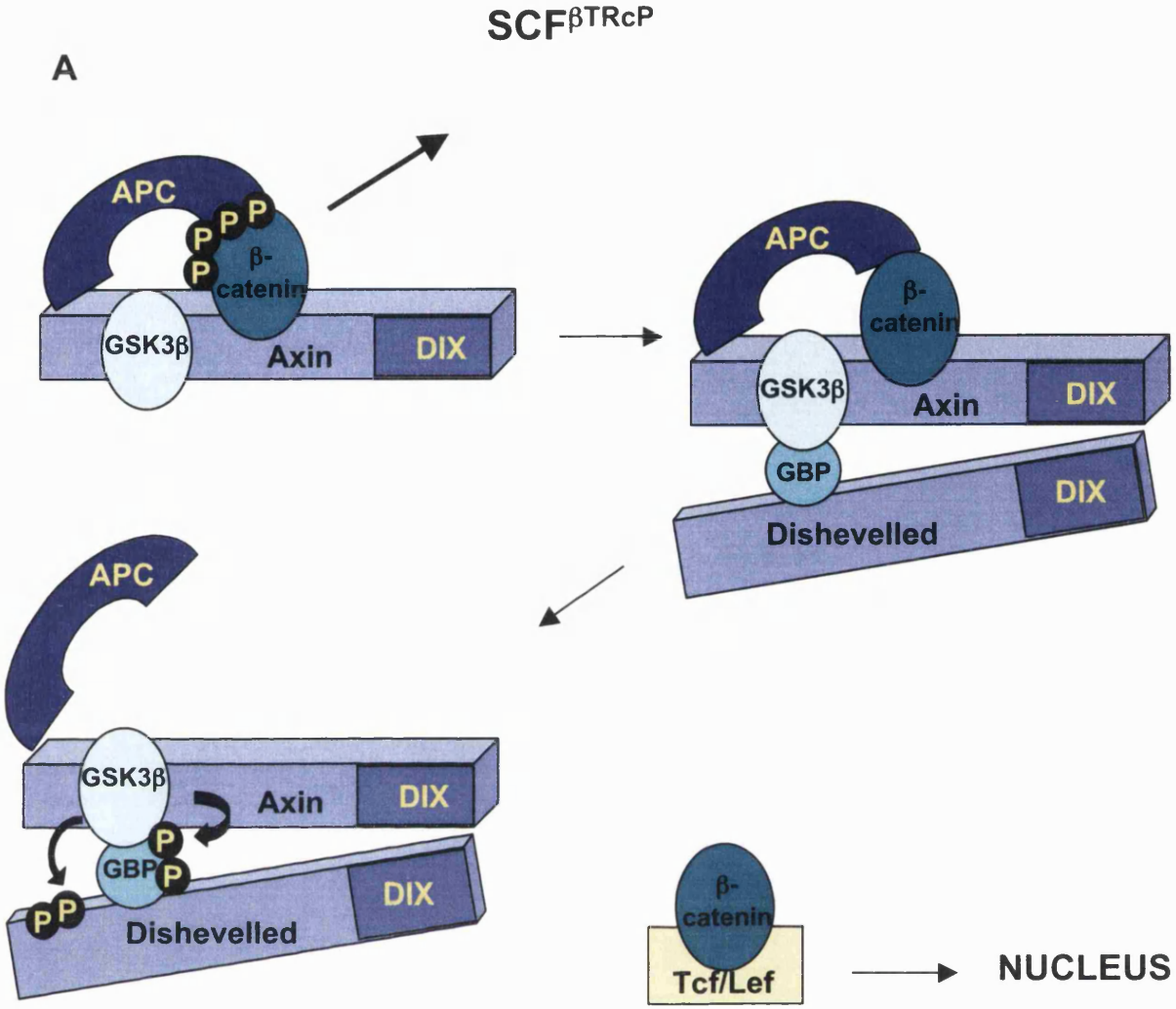
SCF βTRcP
A
APC
P P P
P
β-
catenin
GSK3β
Axin
DIX
APC
β-
catenin
GSK3β
Axin
DIX
GBP
DIX
Dishevelled
APC
GSK3β
Axin
DIX
GBP
P
P
P
DIX
Dishevelled
β-
catenin
Tcf/Lef
NUCLEUS

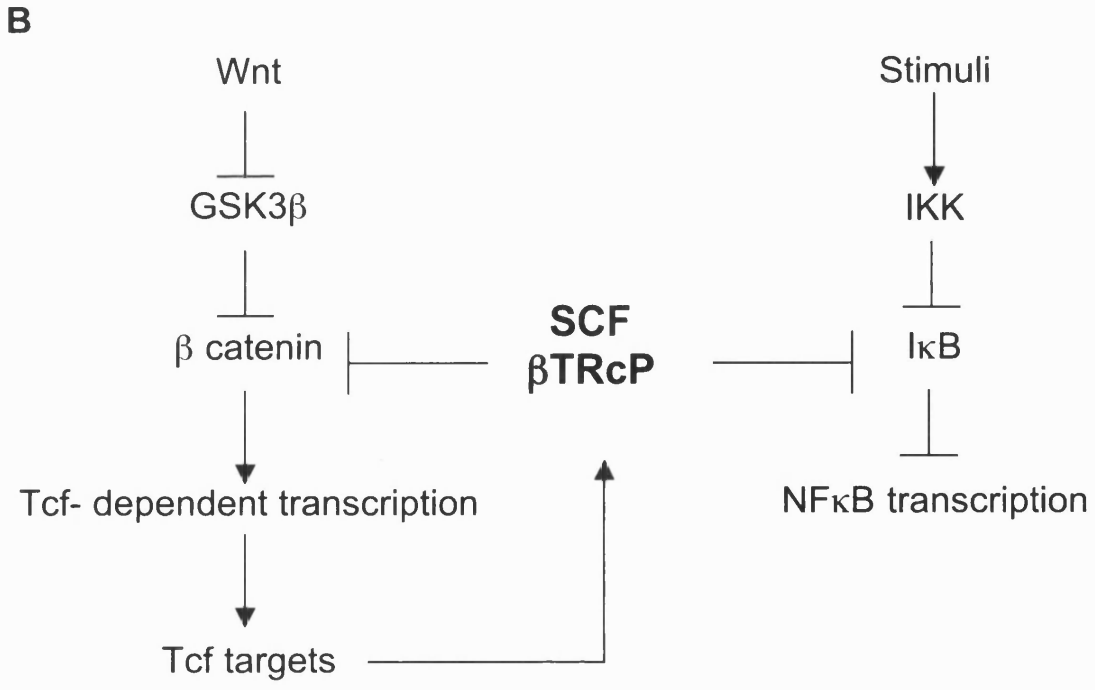
B
Wnt
GSK3β
β catenin
Tcf- dependent transcription
Tcf targets
SCF
βTRcP
Stimuli
IKK
IκB
NFκB transcription

Fig. 1.6.1: The pathways of $SCF^{\beta TrCP}$ mediated degradation.
A Adapted from Salic *et al* 2000. β-catenin is degraded when it is associated with Axin. Axin binds to GSK3β the kinase which phosphorylates the DSGXXS recognition motif in β-catenin. The result is recognition and degradation by the $SCF^{\beta TrCP}$. Upon Wnt signalling, Dishevelled binds to Axin through a domain known as the DIX domain and an accessory protein the GSK3β binding protein (GBP) also binds. This results in phosphorylation by GSK3β being diverted away from the APC protein and β-catenin. Unphosphorylated β-catenin is not recognised by the $SCF^{\beta TrCP}$ and can dissociate from the Axin/APC/GSK3β complex. It migrates to the nucleus where it can act as a transcription factor with Tcf1/Lef1.
B Adapted from Speigelman *et al.*, 2000. It is thought that the β-catenin transcription factor is involved in upregulating transcription of βTrCP F-box protein therefore resulting in a negative feedback loop for its own destruction. This would also result in crosstalk between the β-catenin pathway and the NFκB transcription pathway. The $SCF^{\beta TrcP}$ is also responsible for the degradation of inhibitors of NFκB; upregulation of $SCF^{\beta TrcP}$ would lead to increased signalling through the NF κB pathway.

Organism	ligase	adaptor	substrate	reference
H. Sapiens	SCF	SKP2	$P27^{kip1}$ & cycE	(Nakayama *et al.*, 2000; Tsvetkov *et al.*, 1999)
		βTrCP	β catenin, IκB, p105 & Vpu1	(Heissmeyer *et al.*, 2001; Latres *et al.*, 1999; Margottin *et al.*, 1998)
		hCDC4	cycE	(Koepp *et al.*, 2001)
	VBC	VHL	HIF1α & HIF2	(Kamura *et al.*, 2000)
	CUL4A, CSN & DDB2	?	?	(Groisman *et al.*, 2003)
	CUL4A, CSN & CSA	?	?	(Groisman *et al.*, 2003)
D. melanogaster	SCF	Slimb	Armadillo & Cubitus interuptus	(Jiang and Struhl, 1998)
		Archipelago	Cyclin E	(Moberg *et al.*, 2001)
S. cerevisiae	SCF	Cdc4	Cdc4, Sic1, Gcn4, Far1& Cdc6	(Blondel *et al.*, 2000; Elsasser *et al.*, 1999; Feldman *et al.*, 1997; Galan and Peter, 1999; Mathias *et al.*, 1999)
		Met 30	Met4	(Patton *et al.*, 2000; Rouillon *et al.*, 2000; Thomas *et al.*, 1995)
		Grr1	Grr1, Cln1/2 & Gic2	(Galan and Peter, 1999; Jaquenoud *et al.*, 1998; Kishi and Yamao, 1998; Skowyra *et al.*, 1999)
S. pombe	SCF	Pop1, Pop2	Rum1& Cdc18	(Kominami *et al.*, 1998; Kominami and Toda, 1997; Seibert *et al.*, 2002)
	Pcu3-type	BTB/POZ	?	(Geyer *et al.*, 2003)
	Pcu4, CSN & Ddb2	?	Spd1	(Liu *et al.*, 2003)

Table 1.6.1 Known SCF-type ligases and their substrates

1.7 Skp1 can function outside of the SCF complex

As well as the multiple functions of the SCF complex it is becoming clear from work in yeast that Skp1 is a protein which is commonly involved in complex formation. It may be that the F-box motif and BTB/POZ domains are highly adaptable motifs, making Skp1 a useful bridging protein. It is perhaps surprising that such a small and seemingly uncomplicated protein should have so many roles within the cell. Work in yeast has led the way and the tandem affinity purification system has allowed a great number of protein complexes to be elucidated. To date Skp1 has been found in complexes such as the (vacuolar) vATPase RAVE complex (Regulator of the (H^+)-ATPase of the Vaculolar and Endosomal membranes) (Seol *et al.*, 2001), the 240kDa centromeric binding complex, CBF3 ((CEN DNA)-binding factor 3) (Connelly and Hieter, 1996), an endosomal recycling complex containing the F-box Rcy1 (Wiederkehr *et al.*, 2000) and with the proteins Siah1, SIP (Siah Interacting Protein) and the F-box protein Ebi in a novel ubiquitin ligase complex lacking Cul1 (Matsuzawa and Reed, 2001). It is unclear where the functions of Skp1 will end and so far it is unclear what the role of Skp1 is in some of these complexes. That it is important to the function of these complexes is however undoubted.

Skp1 and the kinetochore

C. Connelly and P. Hieter first identified Skp1, from budding yeast, as a component of the kinetochore, in 1996. In a screen for suppressors of *ctf13-30,* a known kinetochore component, Skp1 was identified as a dosage dependent suppressor. Ctf13 was one of three components of the budding yeast kinetochore complex CBF3 which also contains Ndc10 and Cep3. All 3 genes had been previously cloned and were shown to bind to the essential CDEIII region of DNA that composes the central kinetochore region for budding yeast. Skp1 was shown to be a fourth component of this complex and required for cells to pass through G2. Skp1 binds to the F-box protein Ctf13 at the kinetochore (Connelly and Hieter, 1996). Ctf13 is unstable and it has been suggested that Skp1 is responsible for activating it to make it competent for complex formation by phosphorylation (Kaplan *et al.*, 1997; Russell *et al.*, 1999). However, Skp1 is not a kinase and is not known to specifically recruit

kinases thus it is difficult to envisage how phosphorylation of Ctf13 is dependent on the presence of Skp1. Furthermore, given Skp1's general role in ubiquitin-mediated degradation and the fact that Ctf13 is unstable, it seems more likely that Skp1 would have a destabilising effect upon Ctf13. Ctf13 degradation has been proposed to be carried out by SCF^{cdc4} (Kaplan *et al.*, 1997). However, it would be unsurprising if this were in fact a Skp1, Ctf13, mediated event of auto-degradation which has been seen with other F-boxes (Galan and Peter, 1999). More recently Skp1 has been shown to interact with the Bub1 component of the spindle checkpoint pathway in budding yeast and has been found to be responsible for its localisation to CEN-DNA, CBF3 complexes and may assist in the detection of outer kinetochore defects (Kitagawa *et al.*, 2003).
The budding yeast kinetochore is a smaller and more simple structure than the kinetochore of other eukaryotes and the elements of DNA sequence observed are not the same in budding yeast as in other eukaryotes. Skp1 in budding yeast also contains a 30 amino acid insertion sequence that is not found in Skp1 homologues. It is possible therefore that this sequence may be involved in a kinetochore function that is not conserved and is a budding yeast specific role. Skp1 has not been observed at the kinetochore in any other organism to date. However it remains a tantalising prospect that this protein, which is otherwise highly evolutionarily conserved, will be found to have a role at the kinetochore in other organisms.

Further non-SCF roles of Skp1

As well as a role at the kinetochore in budding yeast Skp1 has been isolated as part of RAVE a complex involved in regulating the assembly of the vATPase, a vacuolar membrane associated complex. Although it is clear that RAVE is involved in assembly of this enzyme it is unclear what the specific role of Skp1 might be in this context (Seol *et al.*, 2001).
The F-box protein Rcy1 in budding yeast has been shown to be involved in the recycling of proteins after endocytic internalisation of proteins. This involves the rescue of proteins internalised by endocytosis from lytic degradation in membrane bound lysosomal compartments of the cell. Rcy1 was shown to bind to Skp1 in this process and cells in which this binding was compromised were defective in recycling as were mutants in Skp1. However the process was not in

any way dependent on other components of the SCF and recycling was normal in *CDC53*, *CDC34* or *RBX1* mutants (Galan *et al.*, 2001; Wiederkehr *et al.*, 2000). This suggests that the role of Skp1 in this context is truly independent of SCF function. This proves that Skp1 has roles beyond its role in SCF mediated proteolysis and although the molecular function in these processes is often undefined it seems likely that Skp1 is a key complex forming factor for many processes.

1.8 An introduction to cell cycle checkpoints

As mentioned at the beginning of this chapter this thesis discusses the possibility that Skp1 may be somehow involved in a cell cycle checkpoint. In order to gain insight into that function a short summary of the various checkpoints that act throughout the cell cycle will be given in the following sections.

The cell cycle is known to be controlled with respect to environmental conditions. It is essential for cell survival that an accurate copy of the genetic information is passed to daughter cells. To this end, cells copy their DNA and then segregate it in chromosomal packages to two new cells. Any faults in this process of copying or segregating are detected by complex cellular signalling mechanisms and the cell cycle is regulated accordingly. Usually the cell cycle is delayed in response to defects allowing any errors to be corrected. If the damage is lethal cells may remain arrested indefinitely (in a unicellular eukaryote this essentially equates to cell death as inability to produce new cells means a lack of growth). In higher eukaryotes activation of checkpoints may result in the selective death of the cell by apoptosis (cell suicide).
The checkpoints which are highly relevant to this thesis, are the G2 DNA replication and damage checkpoint, the mitotic spindle assembly checkpoint and the spindle orientation checkpoint. There is also a restriction point in G1 of the cell cycle that is involved in commitment to the cell cycle (Fantes and Nurse, 1978). This checkpoint is generally cryptic in *S. pombe* as it is dependent on size. The critical size for re-replication and commitment to the next cell cycle is generally already achieved by *S. pombe* cells, before the completion of the

previous round of replication. This subject will not therefore be discussed further in this introduction.

G2 Checkpoints

Cells are capable of arresting or delaying DNA replication in response to two kinds of gross external stimuli. The first is problems with DNA replication resulting from certain types of external insult or difficulties with the replication machinery. The second is a response to DNA damage such as UV or γ-irradiation. In order to carry out such an arrest cells must be capable of sensing and subsequently transducing a signal from damaged or unreplicated DNA.
A number of proteins have been identified as being involved in this process. Those identified so far are regarded as transducers of signals of DNA damage. They fall into 4 distinct categories of proteins determined by the kind of conserved domains they contain. There are PCNA (proliferating cell nuclear antigen)-like proteins such as Rad1, Rad9 and Hus1 in *S. pombe* (Caspari *et al.*, 2000) and mammalian cells, RFC (replication factor C)-like proteins such as Rad17 (Griffiths *et al.*, 1995) and RFC3; BRCT domain proteins such as BRCA1 in humans and Crb2/Rhp9 in *S. pombe* and finally the PI3K-like proteins ATR and ATM in humans or Rad3 and Tel1 respectively in *S. pombe* (Bentley *et al.*, 1996). A coiled-coil protein Rad26 is also important in signalling the checkpoint in *S. pombe* (reviewed by Abraham, 2001; Elledge, 1996; O'Connell *et al.*, 2000; Russell, 1998; Zhou and Elledge, 2000)
Although the signals for activation of the checkpoint are not fully known, it was initially suggested that Rad17 would act like RFC due to significant homology between these two proteins. Therefore, Rad17 would behave like RFC toward PCNA, loading a PCNA-like structure of Rad1, 9 and Hus1 directly onto damaged DNA, leading to activation of the kinase Rad3. However, in conditions of ionising radiation it has been shown that Rad3 dependent phosphorylation of Rad26, an indicator of activation of the checkpoint, can occur independently of the PCNA-like and RFC-like proteins (Edwards *et al.*, 1999). Recent work in mammalian cells suggests that Replication protein A coating of ssDNA may be responsible for the recruitment of Rad26-Rad3 homologous complexes to DNA damage sites with subsequent phosphorylation of Rad17 being stimulated by this recruitment (Zou and Elledge, 2003).

One activity of this network of proteins is activating the effector kinases of the pathway. The effector kinases are known as Chk1 and Cds1 in *S. pombe*. Chk1 is generally responsible for responses to DNA damage in fission yeast whilst Cds1 is involved in the response to a replication block. Chk1 becomes phosphorylated by Rad3 upon activation (Walworth *et al.*, 1993; Walworth and Bernards, 1996). Activation of the effector Thr/Ser kinases results in cell cycle arrest through maintenance of the inhibitory phosphorylation of Cdc2. This phosphorylation is most probably maintained by a "double lock" mechanism that acts upon both the kinases Wee1/Mik1 and the phosphatase Cdc25, responsible for control of Cdc2 phosphorylation. Evidence suggests that Cdc25 can be phosphorylated by Chk1, on serine 216, leading to its interaction with 14-3-3 proteins and translocation to the cytoplasm rather than the nucleus where Cdc2 is found. It has also been seen that checkpoint arrest does not occur properly in a Wee1 null strain and that Chk1 overexpression results in hyperphosphorylation of Wee1 contributing to the idea that both kinase and phosphatase are involved in a G2 arrest (reviewed by O'Connell *et al.*, 2000; Rhind and Russell, 2000). The DNA structure checkpoint is therefore competent to delay cells in G2 in response to DNA damage or replication stress (see Fig. 1.8.1).

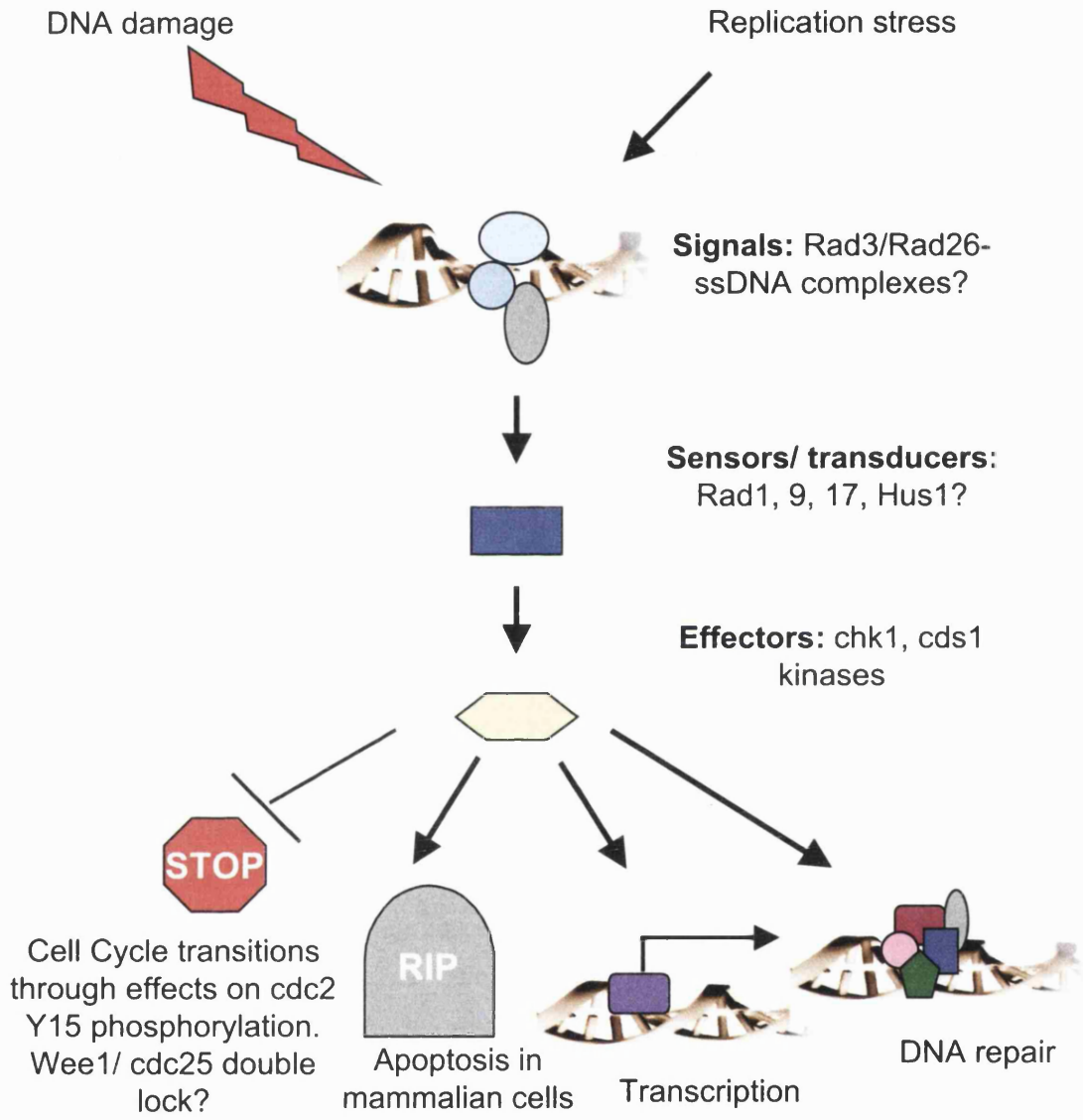

Fig. 1.8.1 The DNA damage checkpoint pathway
Adapted from Zhou and Elledge, 2000. The checkpoint is initiated by DNA damage or replication stress creating ss-DNA, which is recognised through Rad3/Rad26 complexes. Other sensing mechanisms may also involve Rad1, Rad9, Rad17 and Hus1. Activation of the pathway results in activation of the downstream effector kinases, Chk1 or Cds1, depending on what activates the pathway. The effector kinases bring about a delay in cell cycle transitions by inactivation of the Cdc2 cyclin dependent kinase. In mammalian cells apoptosis may be induced if damage is too severe. Repair of damaged DNA can also be induced. The pathway is drawn in a linear manner here for ease of representation but sensors and transducers may be recruited independently of the Rad3/Rad26 complex and subsequently interact once bound to DNA.

Mitotic checkpoints

Another major point for checkpoint control of the cell cycle is mitosis. The spindle assembly checkpoint and the spindle orientation checkpoint are responsible for surveillance allowing correct execution of mitotic processes. In order for cells to accurately segregate their DNA they must align chromosomes on a metaphase plate. This allows the organisation of the DNA in such a way that homologous chromatids are partitioned equally to the daughter cells. During this process the sister chromatids are held together by cohesin, "a molecular glue". During mitosis this cohesin is cleaved allowing the sister chromatids to segregate. Cohesion is essential for chromatids to be aligned properly and is responsible for creating an opposing force to the poleward force generated by the spindle. Once this central force is abolished sisters are free to move poleward.

Spindle assembly checkpoint

The spindle assembly checkpoint monitors the attachment of the spindle to kinetochores and ensures that there is tension between the sister chromatids. Two groups of genes were initially identified in budding yeast as being involved in the maintenance of this checkpoint, by screening for mutant yeast which fail to arrest in mitosis on the addition of spindle depolymerising drugs. Seven genes were identified, the *BUB* genes (budding uninhibited by benomyl), *BUB1*, *2* and *3* (Hoyt *et al.*, 1991), and *MAD1, 2, 3* (mitotic arrest deficient) (Li and Murray, 1991) and *MPS1*(Weiss and Winey, 1996) or *Mph1*$^{+}$ (Fission yeast). These proteins form part of a signal transduction cascade that arrests cells in response to spindle abnormalities.

It is thought that both lack of kinetochore attachment and lack of tension are capable of triggering the spindle checkpoint although in principle the two are very much related to one another as a lack of attachment results in a lack of tension. Classic experiments involving praying mantis spermatocytes demonstrated that in conditions of monopolar attachment (normally a checkpoint activating phenomenon), the application of tension to the sister chromatid with a micromanipulator and glass needle could force cells into anaphase, suggesting that tension is sufficient to release the checkpoint (Li and

Nicklas, 1995; Nicklas, 1997). However, it may be more pertinent to ask what happens when kinetochores are attached and there is no tension. This has been tested in cells which are induced to go through mitosis, without having replicated their DNA. In this case the kinetochore is always attached, however, because of the absence of sister pairs there is no tension. Under these conditions cells activate the checkpoint (Stern and Murray, 2001). Current theory suggests that there is a role for both attachment and tension in activating the checkpoint.

Signalling through the spindle assembly checkpoint is thought to initiate through the Mph1 kinase in fission yeast (He *et al.*, 1998) and this phosphorylates Mad1 in a Bub1, Bub3 and Mad2 dependent manner. A complex of Bub1, Bub3 and Mad2 and 3 is thought to be recruited to the kinetochore as a consequence. The delay to mitosis is achieved by the formation of a complex between Mad2 and various other partners and Cdc20 the activator of the APC/C. The result of complex formation is that the APC/C becomes inactive. This prevents mitosis because not only is APC/C required to degrade cyclin B for mitotic exit it is also required earlier in mitosis for the degradation of securin. Securin degradation liberates separase, a protease responsible for the cleavage of the glue between chromosomes, cohesin (reviewed by Amon, 1999; Musacchio and Hardwick, 2002). In mutants of the checkpoint proteins mentioned above (Mad1, Mad2, Mps1, Bub1, Bub2 and Bub3) a delay to mitosis can never be achieved. Cells carrying mutations in the above genes cannot delay in mitosis and exit mitosis without separating their DNA properly. In fission yeast cells the resulting phenotype is a 'cut' cell. 'Cut' cells are those with a septum placed through unsegregated DNA and 'cut' stands for Cell Untimely Torn (see Fig. 1.8.2 for a cartoon of components of this checkpoint and their arrangement at the kinetochore.).

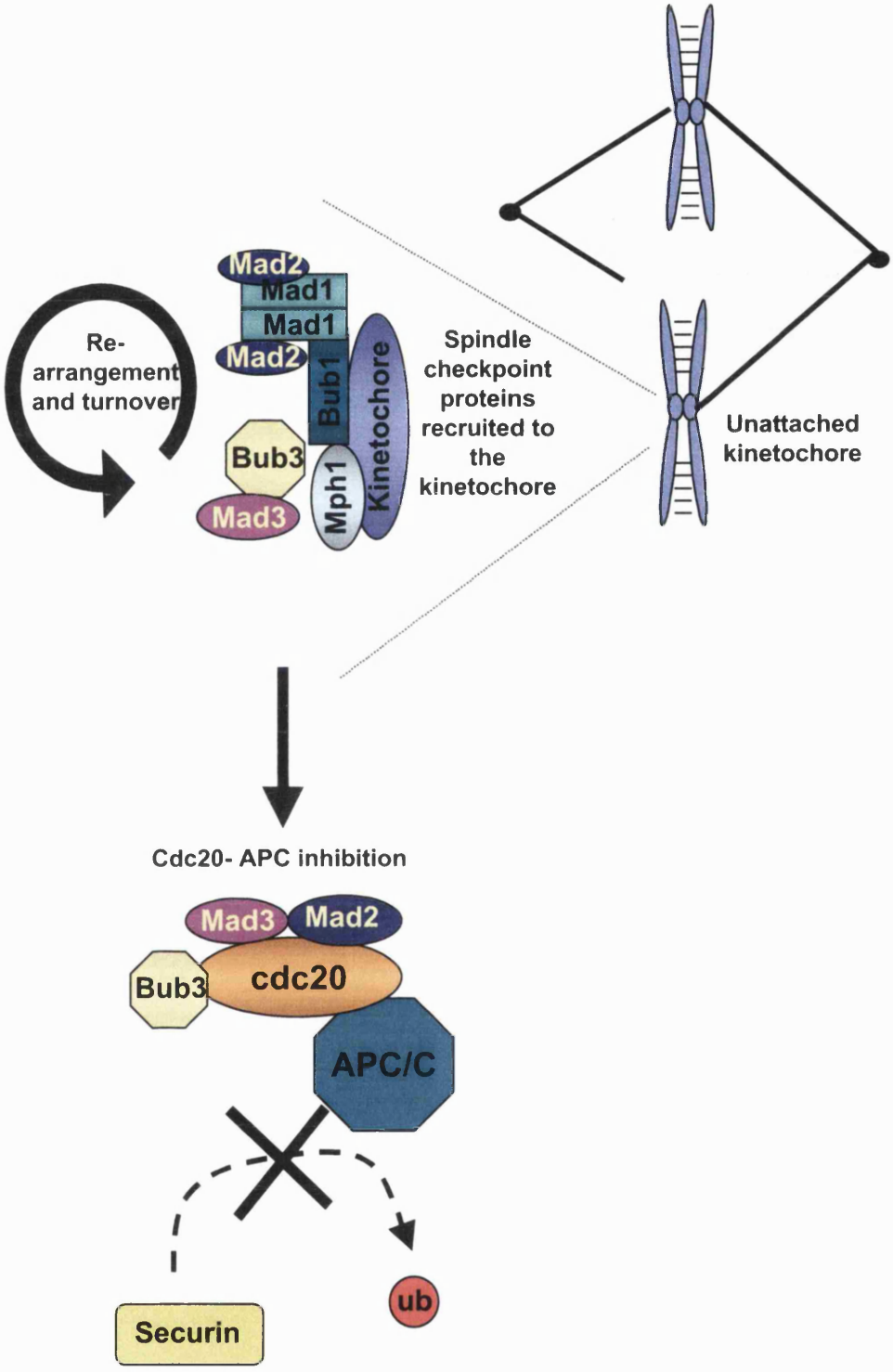

Fig. 1.8.2: The Spindle Assembly checkpoint.
Adapted from A. Amon 1999 and Millband *et al* 2002. Unattached or tensionless kinetochores allow signalling through the spindle checkpoint. The unattached kinetochore recruits components of the checkpoint which are then thought to be rearranged and turned over at the kinetochore. Some of the components bind to and inhibit the APC Cdc20 probably after interacting with the kinetochore. A complex of Mad2/ Mad3 and Bub3 binds to and inhibits Cdc20. The APC cannot therefore ubiquitinate securin and sister chromatids are not separated until the checkpoint arrest is resolved.

Spindle orientation checkpoint

In fission yeast the spindle is always orientated along the long axis of the cell. If this does not occur chromosomes are segregated in any orientation and could result in the DNA being abnormally placed with respect to the septum resulting in 'cut' cells. It was recently proposed that a checkpoint exists which delays cells until the spindle is appropriately orientated along the long axis of the cell. The mechanisms of this checkpoint are now being elaborated but signalling is thought to be initiated if astral microtubules do not interact correctly with the cortical actin ring.

S. pombe cells that have been treated with latrunculin B, which prevents polymerisation of actin and thus prevents formation of a cortical actin ring, are delayed in mitosis with a short spindle. When these cells were examined further it was found that cohesin was not cleaved and that as a consequence the spindle fails to elongate. It was found that cells lacking the transcription factor Atf1 did not delay in mitosis under the same conditions. Atf1 is activated by the Stress activated MAP kinase pathway and genes controlled by the transcription factor were found to be expressed in latrunculin B treatment conditions. The mechanism by which this delay is achieved is currently unclear. It has been claimed that the APC/C is not involved in the mitotic delay but no other mechanism for delaying the cell cycle has been proposed. As this checkpoint is a relatively recent discovery its relevance and control are as yet undefined. It is clear however, that despite the artificial conditions cells require spindles to be correctly orientated in order to progress properly through mitosis (Gachet *et al.*, 2001).

Perhaps the salient point that emerges from the examination of mitotic checkpoints is that the spindle is of vital importance in the initiation of these checkpoints. The interactions of the spindle with the DNA and the astral microtubules with the cortex are responsible for indicating to the cell the correct positioning of the DNA segregation machinery, with respect to both the cell and the DNA. Any faults in this process can have catastrophic consequences for the cell resulting in incorrect partitioning of the genetic information.

1.9 This thesis

The past few years have provided many new insights into proteolysis and its importance within the cell. When this work was initiated there was little known about the role of Skp1 outside of the SCF complex. When beginning the work described in the following chapters the aim was to create a general SCF mutant, which would allow examination of the role of the SCF with respect to the cell cycle and help in the search for further SCF substrates. For this reason we chose a central component of the complex Skp1. It has since become clear that this component may in fact be one of the more complicated members of the complex being involved in many different complexes.

The creation of *skp1* mutants has given us an opportunity to explore different aspects of the physiological relevance of this protein. This thesis describes the effects of one *skp1* mutation, *skp1^{ts}A7*, on the behaviour of *S. pombe* cells. The findings imply that Skp1 may have roles throughout the cell cycle in SCF or non SCF functions. We believe that *skp1^{+}* may have a role in the DNA damage checkpoint as the mutant activates the checkpoint. It also seems likely that the SCF may be involved in regulating some part of the spindle elongation process, ensuring that the spindle extends normally, as *skp1* mutants frequently undergo abnormal mitosis, resulting in a bent spindle which subsequently collapses.

The examination of *skp1^{ts}A7* has contributed to the conclusion that the roles of *skp1^{+}* are manifold and diverse.

Chapter 2

Identification of the components of the SCF complex in the fission yeast *S. pombe*

Introduction

In this chapter the methods involved in identifying the components of *S. pombe* SCF are described. The fission yeast genome is now fully sequenced and serves as a highly useful resource (Wood *et al.*, 2002). This was used to establish the existence of homologues of core SCF components in fission yeast. Each gene was deleted and seen to be essential for vegetative growth. A systematic search of the *S. pombe* genome was carried out in order to identify the open reading frames (ORFs) of F-box proteins of *S. pombe*. Sixteen F-box proteins were found. To assess the importance of these proteins to cellular growth each open reading frame was deleted by one step homologous recombination. Only two F-box proteins were essential whilst deletion of four F-box proteins resulted in phenotypes in the cell. The rest were fully viable.

2.1 Identification of SCF components in the *S. pombe* genome database

The identification of two F-box proteins in fission yeast in a screen of polyploidy mutants, which accumulated proteins involved in the G1/S phase boundary, (Kominami *et al.*, 1998) suggested the presence of a proteolytic complex similar to the SCF in *S. pombe.* In order to identify potential components of this complex, the *S. pombe* genome database of the Wellcome Trust Sanger Institute were searched. A BLASTP search was carried out using the protein sequence of the *S. cerevisiae* Skp1. This identified one homologue with 50% amino acid identity and 65% similarity. This protein was then used to identify the DNA sequence, which was found to be on chromosome II and contained three introns. Also present in the *S. pombe* genome are three cullin proteins (Kominami *et al.*, 1998). The first cullin is pombe cullin (Pcu) 1, which in *S. cerevisiae* is Cdc53 and forms part of the SCF complex; there are two other homologous cullins, Pcu3 and 4, these are not necessarily involved in ligase formation, (see introduction for a discussion of this.) We also identified the homologue of the small RING finger containing protein Rbx1 also known as Pip1. The gene, *rbx1*$^{+}$, was found on chromosome I, containing three introns. In budding yeast a further SCF component, Sgt1, is found in association with the SCF complex and at the kinetochore with Skp1. Its function is conserved in mammalian cells as human SUGT1 and can rescue *sgt1Δ* budding yeast cells (Kitagawa *et al.*, 1999). A homologue of *SGT1* was also found to exist in the *S. pombe* genome. The protein contains 31% homology to the *S. cerevisiae* protein. The gene was found on chromosome II containing two introns and is known as *git7*$^{+}$ (glucose inhibited transcript) due to its involvement in glucose and cyclic AMP signalling in *S. pombe* (Schadick *et al.*, 2002).
These searches suggest that homologues of all components of the SCF core complex are present in fission yeast for formation of an ubiquitin ligase complex. See Table 2.1.1 for a list of homologues

Name	aas	introns/ chr	homologues	
			S.cerevisiae	*H. sapiens*
Pcu1	767	Chr I Intr 4	Cdc53 32% Apc2 22%	CUL1 42% CUL2 33%
Sgt1/Git7	379	Chr II Intr 2	Sgt1 31%	SUGT1 38%
Rbx1/Pip 1	107	Chr I Intr 3	Rbx1/Hrt157% Apc1135%	RBX1 88%
Skp1/Psh1/ Shp1	161	Chr II Intr 3	Skp1 50% Elc 30%	SKP1A 56%

Table 2.1.1: Table of homologues of components of the SCF complex
Percentage identities of *S. cerevisiae* and *H. sapiens* proteins, to the *S. pombe* homologues, are shown.

2.2 Deletion of components of the SCF complex in fission yeast

In order to assess if Skp1 and other components of the SCF complex were essential to the growth of fission yeast cells, gene deletions were carried out. This was done in diploid cells as a deletion in an essential component in a haploid cell would result in lethality thus preventing isolation of deletion strains. Heterozygous diploid strains were created by using strains with mutations in the *ade6*$^+$ gene, which could be complemented by growth as a diploid. Each haploid strain contains a different allele of the *ade6* gene. Haploid cells carrying a single mutation turn red when grown without exogenous addition of adenine to the growth medium. Diploids carrying two different mutations achieve intragenic complementation. This complementation results in the ability to grow as a white colony on medium lacking adenine (Moreno *et al.*, 1991).
A PCR based method was used for gene deletion (Bahler *et al.*, (1998); also see Fig. 2.2.1). A DNA fragment was created containing the *ura4*$^+$ gene with 80 base pairs of flanking sequences. The flanking sequences were derived from sites on either side of the gene to be deleted, e.g. 5' and 3' to *skp1*$^+$. This DNA fragment was then transformed into the diploid cells, where the flanking sequences allow homologous recombination to occur. Colonies were selected for growth on medium lacking uracil. Growth on this medium suggests that the *ura4*$^+$ gene has now integrated into the *S. pombe* genome. In order to verify that the *ura4*$^+$ gene has integrated at the correct locus, colonies that could grow on uracil minus medium were used for colony PCR reactions. These reactions used one primer from a region just external to the gene of interest and one primer from the centre of the *ura4*$^+$ gene. Only colonies containing the *ura4*$^+$ integrated at the correct locus can produce a product from these reactions whilst those cells still containing *skp1*$^+$ cannot. From this diploids were obtained containing heterozygous deletions of *skp1*$^+$, *rbx1*$^+$, *pcu1*$^+$ and *sgt1*$^+$.

Colonies which were positive both for growth on medium lacking uracil and in colony PCR were then allowed to sporulate and tetrad analysis carried out to determine if the gene was essential for growth in haploid cells. Fig. 2.2.2 D shows that *skp1*$^+$ is an essential gene as are all other identified components of

the SCF complex (Figs. 2.2.2 A, B, C). Therefore the SCF complex seems to be essential to the cell.

Closer examination indicated that *skp1::ura4*$^+$, *pcu1::ura4*$^+$, *rbx1::ura4*$^+$ and *sgt1::ura4*$^+$ spores can germinate (Figs. 2.2.2 A', B', C', D' and D"). *skp1::ura4*$^+$ shows very limited growth and appears to undergo one cell division. *pcu1::ura4*$^+$, *rbx1::ura4*$^+$ and *sgt1::ura4*$^+$ can all undergo several cell divisions although the cells show elongation phenotypes. This suggests that *skp1*$^+$ deletion may have more severe effects for the cell causing the lethal phenotype to occur after fewer rounds of division than in the deletions of other components of the SCF.

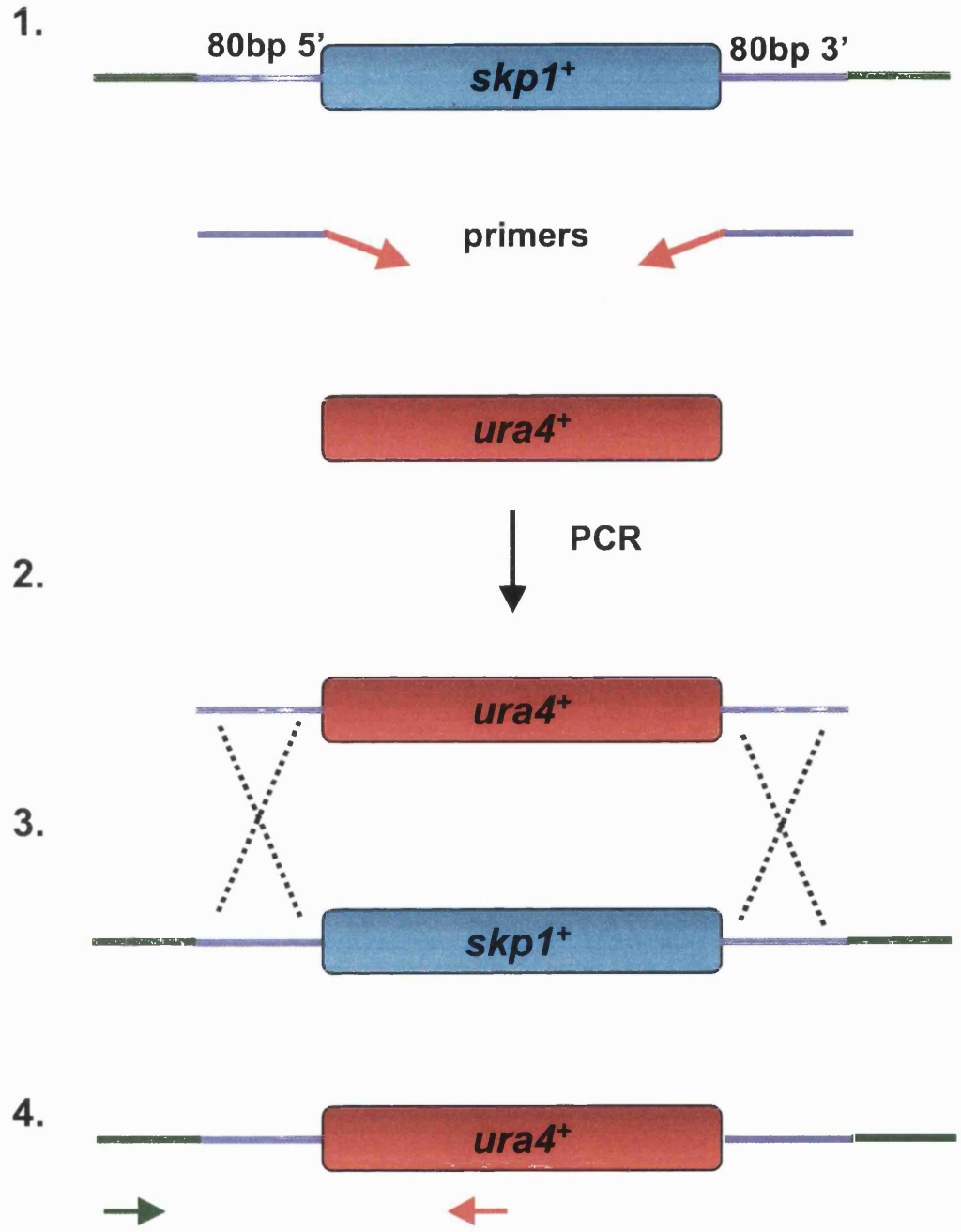

Fig. 2.2.1 deletion of genes in the *S. pombe* genome using a modular PCR based approach

1. Primers are designed containing 80bp of flanking sequence of the target gene and 20bp of *ura4*$^+$ gene.
2. The primers are used in reaction to amplify *ura4*$^+$
3. The *ura4*$^+$ gene plus flanking sequences from the target gene is transformed into yeast and recombines using the homologous sequences to remove the target gene
4. *skp1*$^+$ is replaced by *ura4*$^+$ in the genome. Green and red arrows indicate location of primers to test for integration of *ura4*$^+$ into the genome.

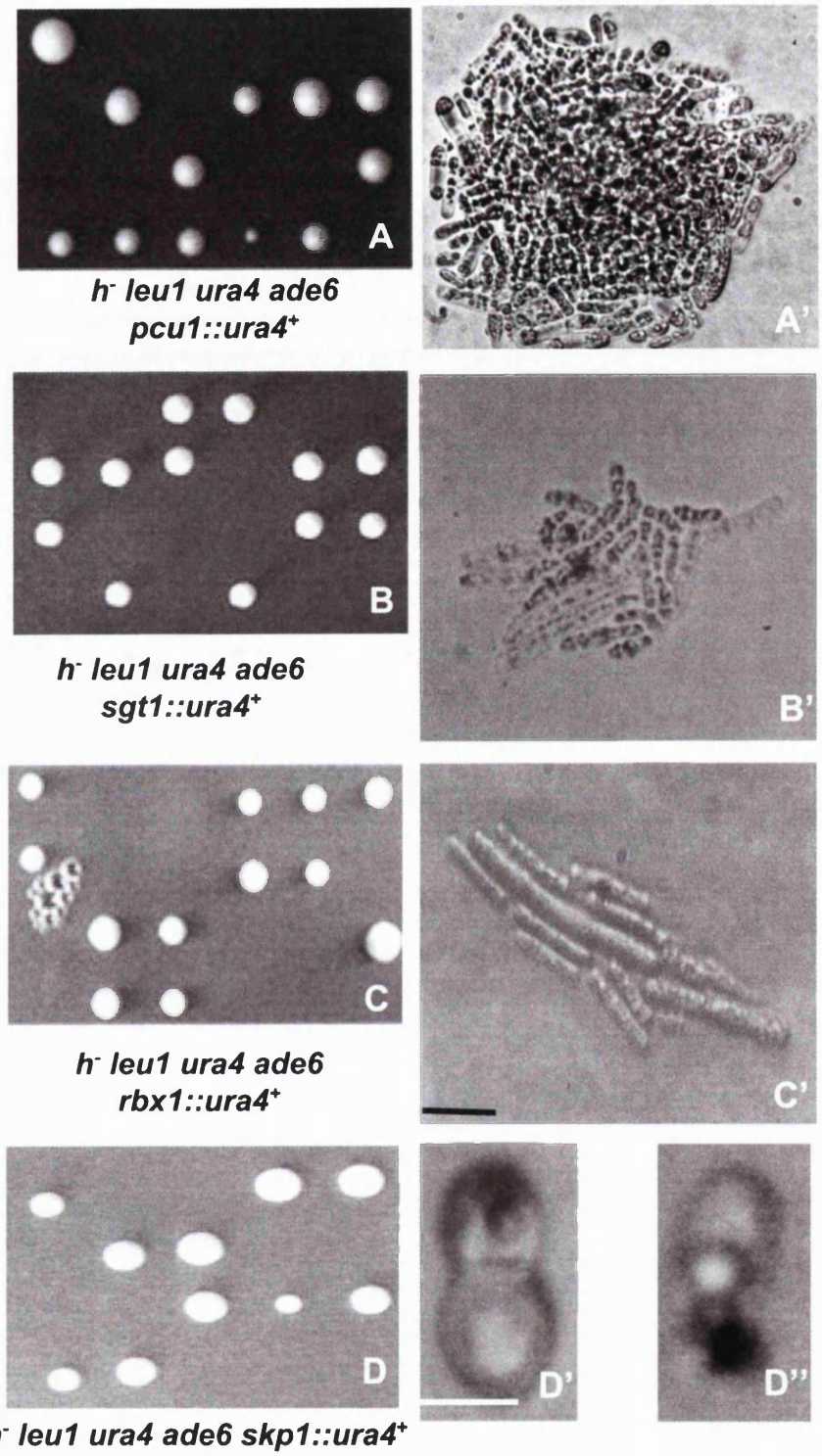

Fig. 2.2.2: Deletion of components of the SCF complex

A, **B**,**C** and **D**: Genes in diploid cells were deleted by integration of a *ura4*$^+$ marker in place of the selected gene. Colonies were selected for growth on medium lacking uracil, then sporulated. Asci were digested and tetrads dissected. A 2:2 ratio of germinated:ungerminated spores was observed and colonies which grew were unable to grow on medium lacking uracil.

A', **B'**, **C'**, **D'** and **D''**: Plates were examined for microscopic growth of colonies. Terminal phenotypes of the lethal deletions are shown. Black bar = 10μm, White bar =5 μm

2.3 Identification of the *S. pombe* F-box proteins

Skp1 binds the F-box protein through its F-box motif. This indirectly binds the substrate, to the core components of the SCF complex. The F-box is thought to create accurate positioning of the substrate for ubiquitination by the E2. A number of F-box proteins exist in each organism including sixteen in the proteome of *S. cerevisae* whilst there are twenty-six in humans and over sixty ORFs for F-boxes in the genome of the worm, *C. elegans* (Winston *et al.*, 1999a). A search was therefore undertaken to identify the ORFs of the F-box proteins in the *S. pombe* genome database at the Wellcome Trust Sanger Institute.

Searching for F-box proteins

The F-box domain from Pop1 and Pop2, and where possible previously identified F-box proteins in *S. cerevisiae,* were used to do BLASTP searches through the Wellcome Trust Sanger Centre *S. pombe* geneDB server. In total sixteen F-box proteins were identified including those already known from previous work, Pop1 and Pop2. Fig. 2.3.1 shows an alignment of the F-boxes of these sixteen F-box proteins. The consensus sequence generated by *S. pombe* F-box domains is shown at the bottom of this figure and the F-box domains are arranged in order of highest homology to this consensus motif. From this it can be seen that Pof1 and Pof11 have the most highly homologous F-box domains to the *S. pombe* consensus sequence.

Pop1, 2 and Pof1- Pof8

In previous work from this lab *pop1*$^{+}$ was cloned by complementation of double mutants *cdc2-33 pop1-364* (Kominami and Toda, 1997). Homology searches were initially undertaken using the Pop1 protein sequence to search the SWISS-PROT database. This identified *S. cerevisiae* Cdc4 as a homologue. Subsequent searches to identify further F-box proteins were carried out using Pop1 to search the Wellcome Trust Sanger Centre database. This identified Pop2 (Kominami *et al.*, 1998).

Pof1 through to Pof8 were identified, by searching the database, *S. pombe* geneDB at the Sanger Centre, using the F-box domain of Pop1 and Pop2. To

refine the search established F-box proteins from *S. cerevisiae* were used to identify proteins with sequence homology. *S. cerevisiae* Met30 and Grr1 were identified as the closest homologues of Pof1 and Pof2 respectively. Many proteins were identified using the F-box motif, in a BLASTP search, due to its loose conservation. Some of these F-box proteins contained termination codons in the middle of the F-box. These were excluded, as were any with low levels of homology. Homology was judged by the alignment score (which needed to be at least higher than 50) and the probability that this alignment score was achieved by chance (which needed to be below one and preferably below 10^{-1}). The alignment score was generated using the blosum62 matrix with the default parameters set up by the search engine.

Pof9-Pof13

Pof9 was identified, by BLASTP searches through databases, using sequence of the F-box protein from *S. cerevisiae* YBR280C. This particular *S. cerevisiae* F-box protein was found by affinity purification and mass spectrometry of Skp1 interacting components (Seol *et al.*, 2001). Pof9 had extremely high homology to YBR280C. Also found in this search was Pof10, which showed lower homology but was identified as having a well-conserved F-box. Pof10 was used as further bait in computer homology searches. This resulted in the identification of 3 further F-box proteins, Pof11, Pof12 and Pof13. Pof11 was found to have high homology to Pof1.

All F-box proteins identified by searching with Pof10 were then subjected to genome wide searches for homology to known proteins in other organisms using the NCBI BLASTP server. It was found that Pof11 had sequence homology to Met30 in *S. cerevisae* meaning that the *S. pombe* genome contains two homologues of this F-box protein, Pof1 being the closest homologue to Met30. Despite this sequence homology it does not necessarily follow that functional conservation will be maintained. The closest homologue to Pof11 from another organism was βTrCP2, a known F-box protein in humans involved in the degradation of inhibitors of NFκB (Winston *et al.*, 1999b). Pof12 has no known homologues in any other organism and Pof13 has weak homology to the F-box/kinetochore protein Ctf13 (Kaplan *et al.*, 1997;

Stemmann and Lechner, 1996) from budding yeast. These homologies are summarised in Table 2.3.1.

Fdh1

The DNA helicase hFBH1 was described in humans as a novel DNA helicase protein of the UvrD/REP family of Helicases containing an F-box in its N-terminus (Kim *et al.*, 2002). This helicase protein was used to search the databases of the Sanger centre and a homologous DNA helicase/F-box protein was identified in fission yeast containing all 7 regions of the ATP dependent DNA helicase and a well conserved F-box.

Other protein interaction domains of F-box proteins

Nine of the sixteen F-box proteins contain further motifs (Table 2.3.1 and Fig. 2.3.2). Of these nine, five are WD-repeat proteins, which includes Pop1 and Pop2. There are also two LRR proteins. Other established motifs that are found are a CAAX domain in Pof6. CAAX domains are usually indicative of membrane association and are required for prenylation of the C-terminus of the protein (Boyartchuk *et al.*, 1997). The N-terminus of the LRR protein Pof3 contains three Tetratricopeptide repeats or TPR motifs. These motifs are commonly found in proteins which interact in multi-protein complexes and aid protein/protein interaction (Blatch and Lassle, 1999). The remaining structural motif found in an F-box protein was a UvrD/REP ATP dependent DNA helicase. This F-box protein is the only known protein containing both an F-box and a DNA helicase, an enzyme rather than a protein/protein interaction domain.

Fig. 2.3.1: The F-box domain
Homology of the F-box domain in each of the *S.pombe* F-box proteins. identical residues in red, similar residues in green.

F-box	aas	motifs	*S.cerevisiae*	*H.sapiens*	Deletion phenotype	derivation
Pop1	775	WD40	Cdc4	Fbw7	Polyploid	Komminami 1997
Pop2	703	WD40	Cdc4	Fbw7	Polyploid	Komminami 1998
Pof1	605	WD40	Met30	βTrCP	Essential/germination	Harrison/Toda unpublished
Pof2	463	LRR	Grr1	?	No change	This study
Pof3	577	TPR/LRR	Dia1	?	G2 Delay	Katayama 2002
Pof4	199	None	Ela1	Elongin A	No change	This study
Pof5	348	None	Ydr360c	?	No change	This study
Pof6	872	CAAX	Rcy1	?	Essential	This study
Pof7	361	None	Hrt3	?	No change	This study
Pof8	402	None	Ufo1	?	No change	This study
Pof9	467	None	Ybr280c	Fbx9	No change	This study
Pof10	662	WD40	Ymlo88w	?	No change	This study
Pof11	506	WD40	?	βTrCP-1	No change	This study
Pof12	440	None	?	?	No change	This study
Pof13	396	None	Ctf13?	?	No change	This study
Fdh1	878	UvrD/REP helicase	?	Fbh1	G2 Delay	Kim 2002

Table 2.3.1: Deletion of all F-box proteins in the *S. pombe* genome

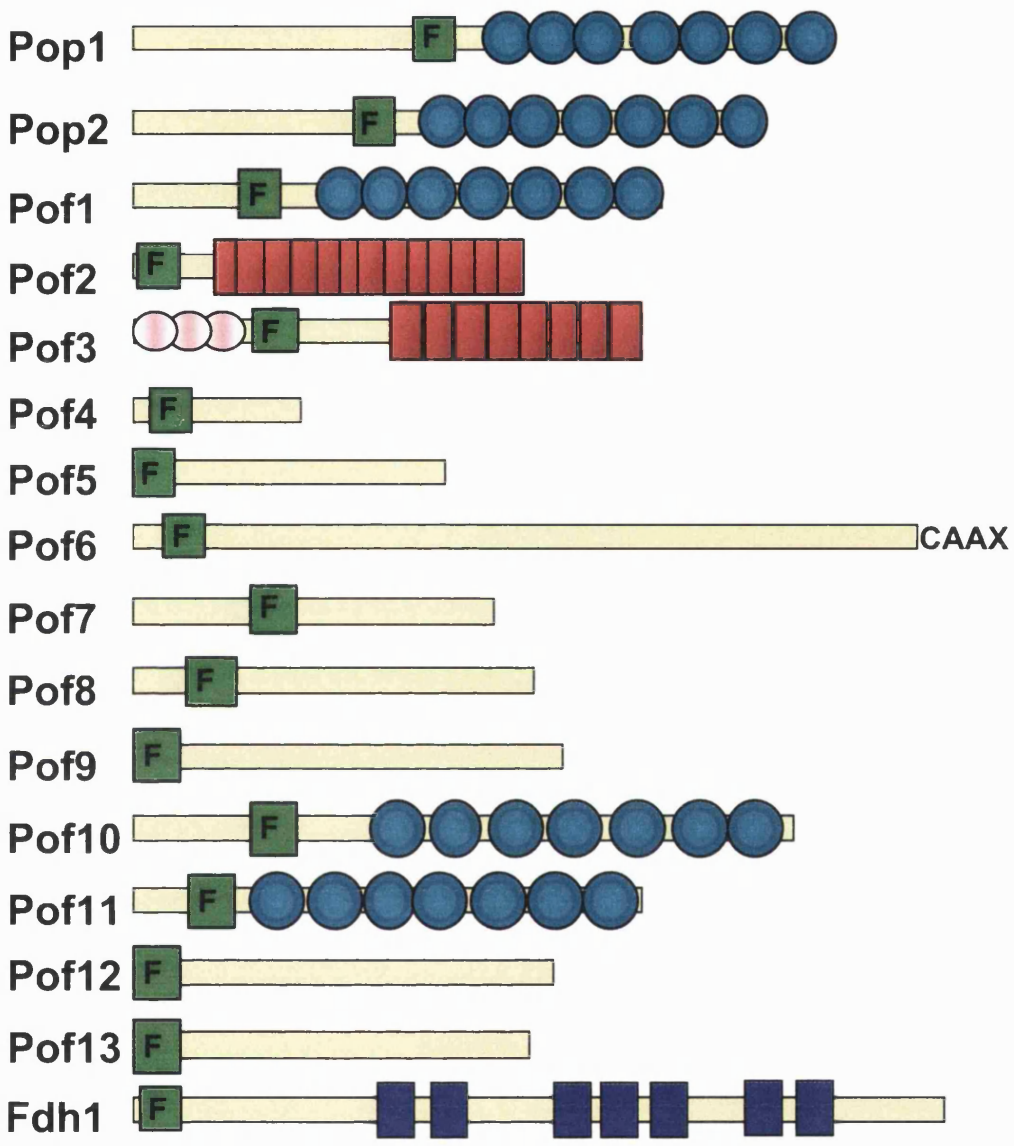

Fig. 2.3.2 : The 16 F-box proteins of *S. pombe*
The position of the 40 amino acid, F-box domain, is represented as a green square. Conserved motifs consist of WD-repeats (light blue circles), Leucine Rich Repeats (red squares), TPR repeats (pink circles), Pof6 contains a conserved C-terminal CAAX motif and Fdh1 has DNA helicase motifs (blue squares).

2.4 Systematic deletion of the F-box proteins of *S. pombe.*

All of the *S. pombe* F-box proteins described above were deleted, in a lab wide effort, by use of recombination as described earlier in this chapter (Bahler *et al.*, 1998). One copy of each F-box gene was deleted in a heterozygous diploid made from the mating of strains CHP428/CHP429 that can be selected on medium lacking adenine due to the presence of two complementary adenine mutations. These diploids are *ura4*$^-$, *ura4*$^+$ DNA fragments can therefore be integrated in place of the F-box gene. Integrants are then selected on medium lacking uracil and checked by colony PCR as described in section 2.2 and Fig. 2.2.1. Colonies, which both had a product in the PCR reaction and grew on minus uracil medium were then sporulated and tetrads dissected.
In some cases, *pof4*$^+$ and *fdh1*$^+$, the kanamycin resistance gene was used to delete the gene. As a complete collection of F-box deletion strains was desired for future work, *fdh1*$^+$ was also deleted. Deletion could be carried out in a haploid strain (the wild-type, 513: where wild-type is refered to throughout this thesis it is 513 unless otherwise stated) as the gene was known to be non-essential due to the work of Kim *et al* (Kim *et al.*, 2002).

Essential F-box proteins

As summarised in Table 2.3.1 only two F-box proteins are essential to cell growth. These are the WD-repeat containing, Met30 homologue, Pof1 and the CAAX box motif, Rcy1 homologue, Pof6.
The deletion of *pof1*$^+$ shows a very early breakdown in cell growth with spores failing even to germinate. The inviability of *pof1*$^+$ deletion cells is also seen during vegetative growth (C.Harrison and T.Toda work in progress). This essential phenotype is consistent with the requirement of Met30 for *S. cerevisiae* viability.
In contrast to the deletion of *S. pombe* Pof6 the *S. cerevisae* Rcy1 protein is not essential but cells from deletions of this protein show problems in endosomal recycling (Wiederkehr *et al.*, 2000). The Rcy1 protein forms a complex with Skp1 but not the other components of the SCF complex (Galan *et al.*, 2001). Rcy1 localises to regions of polarised growth. GFP-Pof6 tagged N-terminally shows potential localisation to the nucleus, possibly the nuclear membrane, via

the CAAX box (Fig. 2.4.1). Pof6 was also found to be essential by Hermand *et al.*, (2003) who suggest that Pof6 localises to the septum and polarised growth region. Localisation of Pof6 at septa was also occasionally seen in this study however nuclear localisation was far more frequent and prominent.

Non-essential F-box proteins

The remaining 14 F-box proteins are not essential to cell growth. Four show mutant phenotypes upon deletion. However the other ten remain unaffected in terms of morphology and are able to germinate and grow as wild-type cells in (Yeast Extract 5 Supplements also refered to as rich medium) YE5S growth medium at the optimum temperature of 30°C. The deletions are not temperature sensitive showing normal growth at 36°C and are not cold sensitive as they also grow at 18°C. The F-box protein Pof10 can cause abnormal morphology and viability loss upon overproduction and this is thought to be due to the sequestration of Skp1 away from other F-box proteins (Ikebe *et al.*, 2002). However the deletion of this protein has no observable effect on cells.

F-box protein deletions with phenotypes

The F-box proteins Pop1 and Pop2, like their mutant phenotypes, show polyploidy when deleted (Kominami *et al.*, 1998; Kominami and Toda, 1997). Deletion of Pof3 shows a G2 delay and heterochromatic de-silencing (Katayama *et al.*, 2002). The other F-box protein, which shows a defect on deletion, is the DNA helicase F-box protein Fdh1, which shows elongation phenotypes.

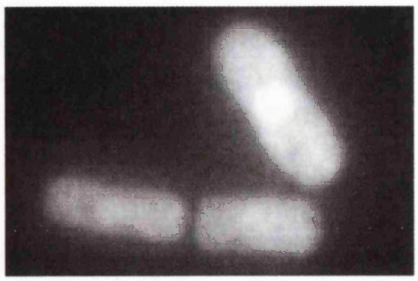

h⁻ leu1 ura4 P3nmt-GFP-pof6⁺ **-T**

h⁻ leu1 ura4 P3nmt-GFP-pof6⁺ **+T**

Fig. 2.4.1: localisation of Pof6
Strains containing N-terminally, GFP-tagged Pof6, under a thiamine-repressible promoter, at the chromosomal locus were grown at 30°C to mid-log phase. Cells were grown in the presence (repressed promoter)or absence (active promoter) of thiamine . Live cells were examined on a thin layer of agar under a coverslip with an immunofluorescence microscope.

2.5 Summary

This chapter demonstrates the existence of homologues of all the core components of the SCF complex in the *S. pombe* genome. The proteins encoded by these genes are shown to be essential to cell growth as deletions prevent growth of cells beyond a few divisions. The phenotype of the *skp1*$^{+}$ deletion is slightly different to those of the other SCF core components, appearing to cause cell death after only one division. This suggests that Skp1 may have a more important cellular role than the other components of the SCF complex in *S. pombe*. An alternative explanation is that the stability of maternally inherited Skp1 is less than that of other SCF components. Systematic identification of the ORFs of F-box proteins contained in the *S. pombe* genome using *S. pombe* F-box motifs and *S. cerevisiae* protein homologues as a query identified sixteen F-box proteins. These proteins contain an F-box motif and various other protein/protein interaction domains likely to be necessary for substrate interaction. Five proteins belong to the F-box WD-repeat family whilst two belong to the F-box LRR family. A CAAX motif and TPR motifs are also found. Finally the DNA helicase Fdh1 was found to contain an F-box motif N-terminal to its DNA helicase domain. Two proteins, Pof1 and Pof6, are essential for vegetative growth in *S. pombe*. The deletion of four other F-box proteins also has an effect on vegetative growth. These deletions result in G2 delay (Pof3, Fdh1) or polyploidy (Pop1 and Pop2).

2.6 Discussion

The existence of two F-box WD-repeat proteins in *S. pombe*, mutation of which caused accumulation of Rum1 and Cdc18 (Kominami *et al.*, 1998), suggested that an SCF complex with a function in proteolysis was likely to exist in fission yeast cells. The findings above suggest that other components, which together form the E3 ubiquitin ligase, the SCF complex, also exist. This further corroborates the idea that a fully functional complex must exist in fission yeast.

Numbers of homologues of SCF components.

Only one Skp1-like protein is found to exist in the *S. pombe* genome. Meanwhile *C. elegans* contains at least three Skp1 homologues and the genome of humans contains two. All of these organisms also contain homologues to the elongation factor, Elongin C, which has homology to Skp1 and forms part of a similar E3 ubiquitin ligase complex, the VBC complex (Lisztwan *et al.*, 1999; Lisztwan *et al.*, 1998; Lonergan *et al.*, 1998) in human cells, (see Introduction). *S. pombe* also contains an Elongin C homologue, which is not essential to cell growth (data not shown). It is interesting to note that although *S. pombe* contains three cullin proteins Pcu1, 3 and 4 it does not contain a protein with high homology to CUL 2 the cullin protein involved in binding Elongin B/C in the VBC complex of humans. This presents the possibility that a complex of this nature does not exist in *S. pombe* and that Elongin C is involved purely in a transcription elongation function in *S. pombe* and was only evolutionarily adapted to a role in proteolysis in mammalian cells. It is currently being established that ubiquitin ligase activity is associated with Cullins 3 and 4 in various organisms in different complexes. (See introduction for a description of this work).

F-box proteins in *S. pombe*

S. cerevisae (Bai *et al.*, 1996), *C. elegans* (Patton *et al.*, 1998b), and subsequently humans (Cenciarelli *et al.*, 1999) and other mammals (Winston *et al.*, 1999a) have been shown to contain many F-box proteins giving rise to the F-box hypothesis. The deletions of 14 of the 16 F-box proteins found in *S. pombe,* are not lethal to the cell whilst deletions of the core components of the SCF complex are. The possibility that the core components have individual functions separate from the SCF complex could explain this phenomenon. Instead of deletion compromising an SCF activity it could be the destruction of non-SCF function that results in lethality. An example of this is the involvement of Skp1, as a component of the CBF3 complex and possibly as a tension monitoring component with Bub1, at the kinetochore of budding yeast (Connelly and Hieter, 1996; Kitagawa *et al.*, 2003), or the involvement of Skp1 with the RAVE complex a regulator of assembly of an intracellular membrane proton pump, the vATPase (Seol *et al.*, 2001).

It is also possible that there is functional redundancy amongst the F-box proteins meaning that deletion of individual F-box proteins may not have the same effect as deleting the core components. If two F-box proteins are proposed to be involved in the degradation of a substrate, as proposed for Pop1 and Pop2 (Kominami *et al.*, 1998) with respect to Rum1, one might expect only to see the full effects of a phenotype in these cells upon deletion of both proteins. This is not, however, the case with Pop1 or Pop2 deletions, which show polyploidy phenotypes independently. In this case, it is possible that the absence of one F-box protein cannot be compensated by the presence of the other. However, the functional redundancy of the F-box proteins could be examined by creating deletions of more than one F-box gene in the same cell. The physiological relevance of this may be limited by the abnormality of cells carrying multiple deletions.

Characterised SCF systems in budding yeast and their relation to F-box proteins discovered in fission yeast

It is interesting to note that although there are homologues of each of the characterised F-box proteins from *S. cerevisae*, there are also some notable differences. The most detailed characterisation of F-box proteins in *S. cerevisiae* has been carried out on Cdc4, Grr1, Met30 and Rcy1.

The SCF^{cdc4} degrades the CKI Sic1 to allow entry into S phase from G1 (Skowyra *et al.*, 1997). A similar situation has been found in *S. pombe* where the $SCF^{pop1/pop2}$ degrades the CKI, Rum1 (Kominami and Toda, 1997).

However in the case of the direct protein sequence homologues of Met30, Grr1 and Rcy1, the case for functional homology is not as clear. The Met30 homologue is Pof1. The deletion of this protein leads to inviability as is the case in *S. cerevisiae*. Met30 is known to be involved in the transcriptional pathway that regulates Met4 abundance in the cell in response to the presence or absence of methionine (Kuras *et al.*, 2002; Rouillon *et al.*, 2000). The deletion of *met30*$^{+}$ is rescued by deletion of its substrate the transcription factor *met4*$^{+}$, which rescues the G1/S phase arrest seen in these cells. However the methionine biosynthesis pathways in *S. pombe* and *S. cerevisiae* differ considerably and there is no direct homologue of Met4 in the *S. pombe* database, therefore it is difficult to know if Pof1 and Met30 work in a similar

fashion. A pertinent question is therefore whether a functional homologue exists in *S. pombe,* despite distinct differences in the sulphur metabolism of these two organisms (Marzluf, 1997)? If such a homologue exists is it degraded by the SCF^{pof1}? A further question concerns the role of the second Met30 homologue in the *S. pombe* genome, Pof11. Could this protein be involved in a sulphur metabolic pathway also or does it function to degrade an unrelated substrate? The SCF^{grr1} in *S. cerevisiae* has been implicated in the regulation of glucose metabolism and transporters (Flick and Johnston, 1991). It is also the E3 for G1 cyclins, Cln1 and 2 (Barral *et al.*, 1995; Patton *et al.*, 1998a). These cyclins are required in passage through Start and initiation of S phase from G1. Deletion of *GRR1* although viable, leads to a build up of G1 cyclins causing pseudohyphal growth and induction of genes normally repressed in glucose rich media. The deletion of Pof2, the direct homologue of Grr1 in *S. pombe*, appears to have no effect on the cells. Although Pof2 has not been properly characterised it is likely that the importance of G1 cyclin degradation in *S. pombe* will differ due to the fact that in a wild type, rapidly growing, *S. pombe* cell, the size for Start of the next cell cycle is already achieved in the daughter cell as it is produced (Fantes and Nurse, 1978). It will be interesting to see how cells grown in conditions where the main size control point for division is G1, behave when a $pof2^{+}$ deletion is introduced.

The deletion of all known G1 cyclins in *S. pombe* gives viable cells, which are capable of oscillating through the cell cycle. In order to pass through G1 into S phase Rum1 must be ubiquitinated. It is suggested that there is an, as yet, undiscovered G1 cyclin, which is resistant to Rum1 inhibition when complexed with Cdc2 kinase. This G1 cyclin-CDK complex would be capable of phosphorylating Rum1 for ubiquitin mediated proteolysis (Martin-Castellanos *et al.*, 2000). Alternatively the continued oscillation through the cell cycle in G1 cyclin deficient mutants could suggest that the G1/S phase control point is not as important in fission yeast cells as in budding yeast. If this is the case one could postulate that the role of Pof2 in *S. pombe* may not be as important as Grr1 in *S. cerevisiae*

The F-box protein Rcy1 in *S. cerevisiae* binds to Skp1 alone. Other components of the SCF complex do not appear to be required for the function of Rcy1 in endosomal recycling, however Skp1 function is required. The deletion of the

protein results in viable cells although there are defects in recycling and a block of the endocytic pathway. The CAAX domain of the protein is required for localisation in regions of polarised growth and depends on the actin cytoskeleton (Galan *et al.*, 2001; Wiederkehr *et al.*, 2000). The difference between Rcy1 and Pof6 is immediately apparent from the fact that *pof6*$^{+}$ deletion is lethal to the cells. Localisation of Pof6 appears to be nuclear, which also differs from localisation of Rcy1. It is possible that Pof6 functions may also be independent of the SCF core complex in *S. pombe*, however it has been suggested that Pof6 may be the F-box for SCF dependent degradation of Mid2, an anillin homologue involved in the placement of the septum in *S. pombe* (Tasto *et al.*, 2003). The most basic interpretation for lethality caused by an F-box protein is that this leads to the accumulation of a substrate for proteolytic degradation that has lethal effects for the cell. As overproduction of Mid2 is not lethal to the cell it must be considered that there may be other Pof6 targets for ubiquitin degradation or that Pof6 has functions outside of an E3 role.

In order to address some of the questions concerning the SCF in *S. pombe* and due to the lethality of the core components we decided to create temperature sensitive mutants in a core component *skp1*$^{+}$, the aim being to create general SCF mutants for further analysis. The generation of these mutants and their phenotypic analysis is described in the following chapters.

Chapter 3

skp1^{+} temperature sensitive mutants, screening and binding analyses

Introduction

In the previous chapter it was established that genes encoding elements of the core SCF complex existed in the *S. pombe* genome and that their deletion was lethal to the cell. Sixteen F-box proteins were also identified and two of these were also essential to the cell.

This chapter describes mutants created using a targeted one-step PCR mutagenesis screen of *skp1*$^{+}$. This screen identified nine mutants, which fell into five categories. The recent elucidation of the crystal structure of SKP1, complexed with the F-box protein SKP2, from human cells (Schulman *et al.*, 2000) allowed the location of the mutations to be identified and their effects on the structure of the *S. pombe* protein to be considered.

We examined the prediction from the crystal structure that specific F-box protein binding but not the binding of the core elements of the SCF to the mutant protein Skp1^{ts}A7, from the strain AL2-A7, would be compromised. F-box proteins were tagged and a binding analysis was carried out between each F-box protein and Skp1 and Skp1^{ts}A7. The findings of the binding analysis indicate that binding of F-box proteins Pof1 and Pof3 is reduced whilst binding of the core component Pcu1 remains normal.

3.1 PCR mutagenesis of the *skp1*$^+$ gene

We were interested in examining Skp1 protein further as it is a core component of the SCF. Our aim was to create general SCF mutants with phenotypes that were different from those obtained through mutations of Pop1 or Pop2 F-box proteins. At the time of beginning this work other roles for Skp1 outside of the SCF complex were only loosely elaborated. It was therefore decided that as a central component in the complex Skp1 would be ideal for the creation of general SCF mutants.

The lethal phenotype of *skp1*$^+$ deletion makes it difficult to examine the protein's cellular role. For gene products that are essential to the cell it is useful to obtain conditional mutants. Haploid organisms are particularly tractable for this as the cell is dependent on only one copy of the gene and thus recessive mutations cannot be masked by the presence of a second allele. Conditional inactivation of a gene therefore gives an immediate phenotype. To further examine the role of Skp1 in fission yeast, conditional mutants were generated.

Mutagenic PCR

As mutations were desired in the *skp1*$^+$ gene it was decided to take a targeted approach and to mutagenise the *skp1*$^+$ gene in a PCR reaction. Mutagenised *skp1*$^+$ fragments would then be integrated into the genome on the basis of homology to the original gene. To create mutagenised fragments of the *skp1*$^+$ gene a special PCR reaction where the fidelity of the polymerase is lowered was used. Reduction of polymerase fidelity can be achieved by various methods (Cadwell and Joyce, 1992; Leung *et al.*, 1989), including addition of manganese or potassium ions in the reaction, or changing the concentration of the nucleotide pool. From experimental trials it was decided to use a change in nucleotide concentration as this gave a slightly smeared DNA product when run on an agarose gel, suggesting that errors were occurring in these reactions. The levels of certain nucleotides were increased to five times their normal concentration. In order to prevent biasing toward particular bases the concentration of one purine and one pyrimidine was increased.

skp1$^+$ plus three hundred base pairs of 5' upstream and 3' downstream sequence were amplified from an *S. pombe* genomic DNA library in a normal

PCR reaction. The primers used for amplification contained restriction enzyme sites allowing the gene plus flanking sequence to be subcloned into a pUR19 plasmid vector. pUR19-*skp1*$^+$ was then amplified in *E.coli* and sequenced before use as a template for subsequent PCR reactions. Mutagenic PCR reactions were carried out and the DNA fragment generated was purified.

Screening for mutants

DNA fragments were transformed into haploid cells containing *skp1*$^+$ marked at the 3' end by the *ura4*$^+$ gene, termed AL1 or *skp1*$^+$-*ura4*$^+$. Transformed cells were grown on rich medium containing the drug 5-Fluoro-orotic acid (5-FOA). This drug is an analogue of a uracil precursor, which is toxic to cells containing the *ura4*$^+$ gene, as these cells can process the drug into a toxic intermediate. Cells which have lost the *ura4*$^+$ gene, by integrating a mutagenised fragment, can grow on 5-FOA containing medium but should be unable to grow on medium lacking uracil. Cells that retain the original genotype should not be able to grow on 5-FOA, but can grow on minus uracil medium. Hence this selection medium allows for the identification of cells that have undergone homologous recombination (Fig. 3.1.1).

Fig. 3.1.2 shows a flow diagram of the screening procedure. Two separate mutagenic PCR reactions were carried out and the products of these were transformed into *skp1*$^+$-*ura4*$^+$ cells. Two hundred 5-FOA positive colonies were obtained by using all the PCR fragment generated. These colonies were replica plated onto rich medium plates containing the drug phloxine B. This is a dye that can be actively excluded by healthy cells, but defective and dying cells cannot exclude this dye and thus turn a dark red colour. Colonies on phloxine B plates were incubated at 26°C and 36°C. Those colonies that turned dark red at 36°C but remained pink at 26°C were selected and re-streaked on more rich medium plates containing phloxine B. Nine strains showed very little growth at 36°C. On examination of cells that had grown a phenotypic difference was seen between the cells grown at 26°C and 36°C. These nine strains were selected for further analysis.

Fig. 3.1.3 shows the growth of *skp1*^{ts} mutant alleles when they are streaked on rich medium plates containing the pink dye phloxine B at 26°C and 36°C. Wild-type cells grown on phloxine B plates are usually pale pink in colour and should

not be inhibited for growth. The *skp1*^{ts} mutant allele strains exhibit limited growth at 36°C and are coloured a very dark red. At 26°C they show a greater amount of growth and are capable of excluding the phloxine B dye making them pink in colour. This demonstrates that *skp1*^{ts} mutant cells are conditional mutants: their growth is dependent on temperature.

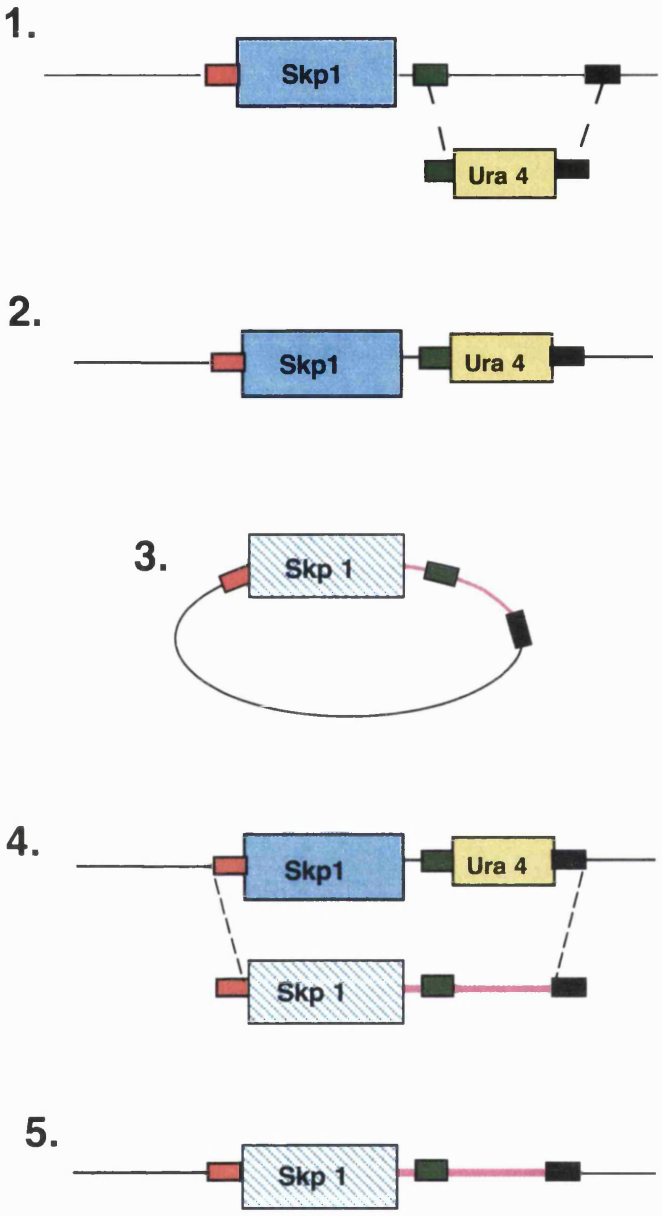

Fig. 3.1.1 : one-step targeted mutagenesis
1. Integration of the marker *ura4*$^{+}$ gene adjacent to the 5' end of the *skp1*$^{+}$ gene to yield **2.** A copy of *skp1*$^{+}$ marked at the chromosomal locus. **3.** A copy of *skp1*$^{+}$ and three hundred base pairs of downstream sequence were subcloned into a plasmid which is subjected to a mutagenic PCR reaction with primers from the red and black homology regions to create a fragment of mutagenised *skp1* used for **4.** Integration into the chromosomally marked *skp1*$^{+}$ strain. **5.** The end product of mutagenesis of *skp1* is lacking the *ura4*$^{+}$ gene marker. When recombined into the genome using the red and black homology regions the *ura4*$^{+}$ gene will be lost from the genome allowing selection on medium containing the drug 5-Fluoro-orotic acid.

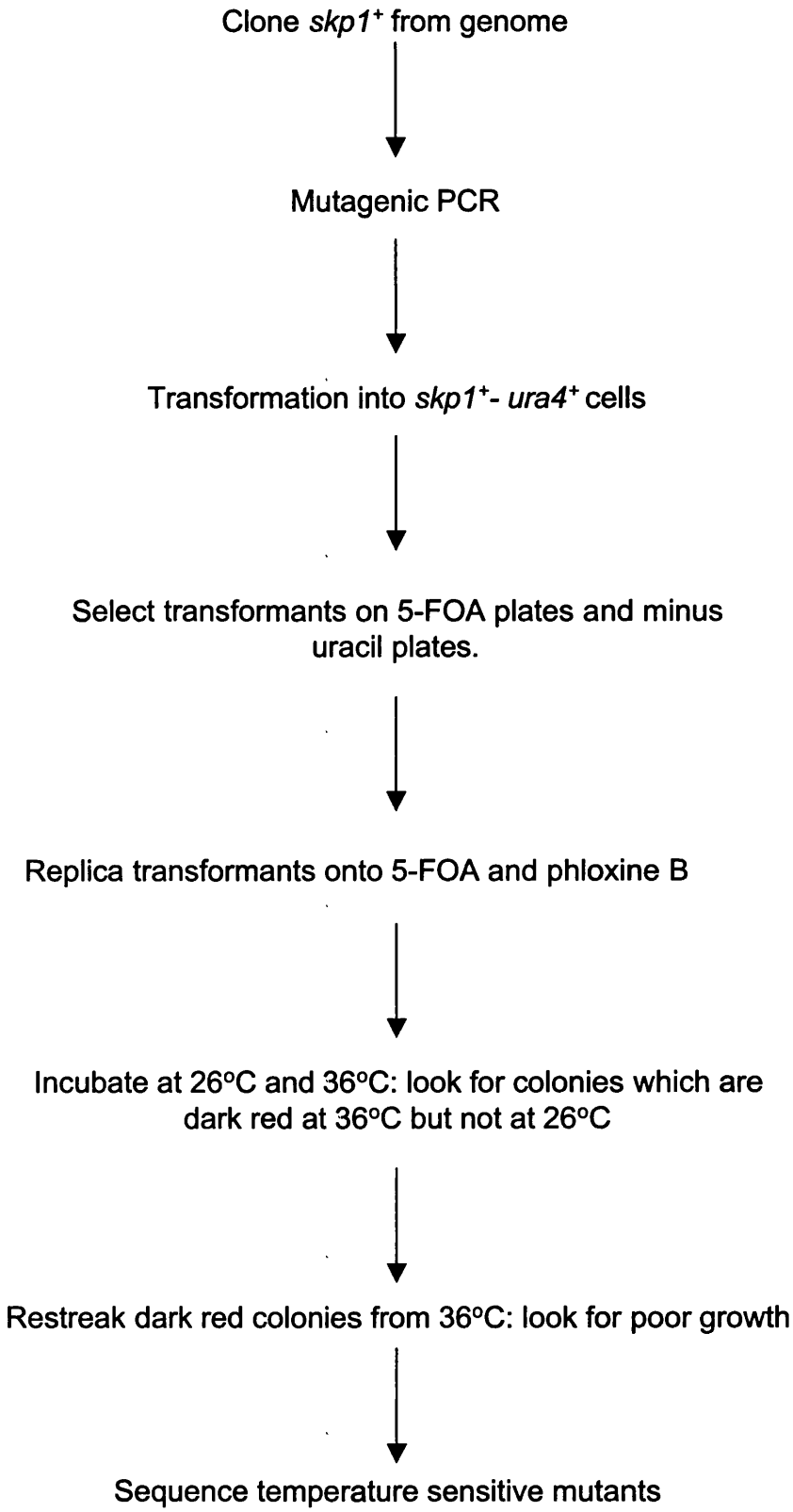

Fig. 3.1.2: Flow diagram showing the sequence of events involved in screening for *skp1* temperature sensitive mutants

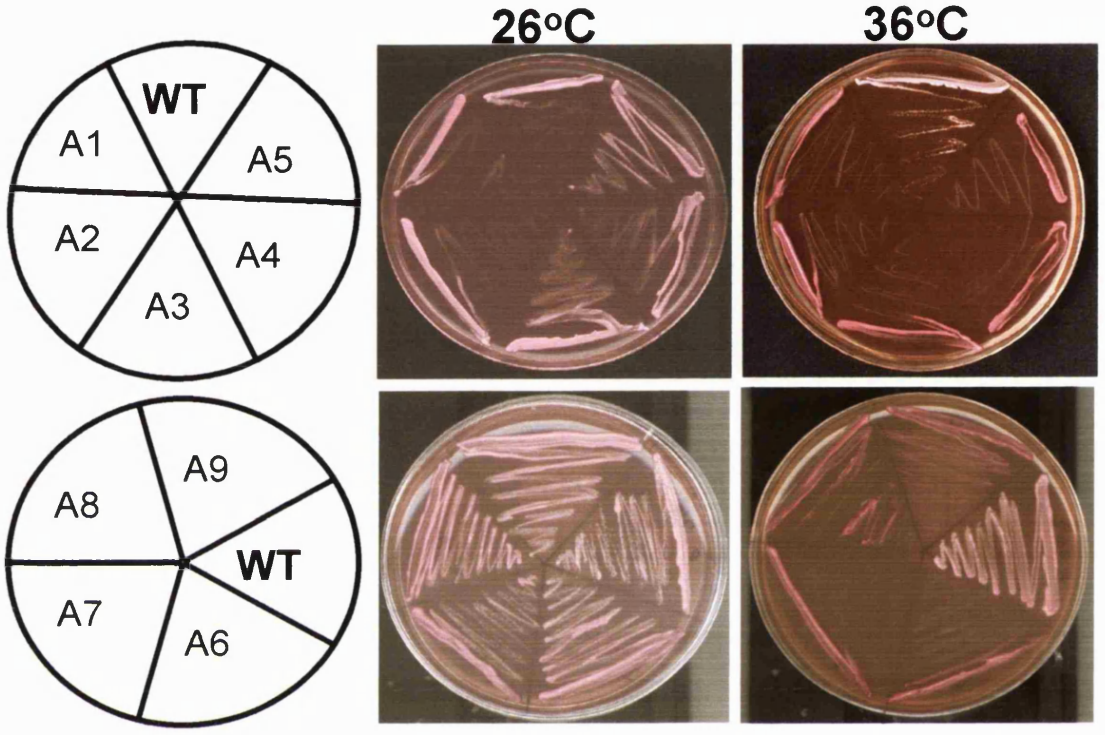

Fig. 3.1.3: Temperature sensitivity of *skp*^{ts} cells
Mutants from the screening procedure were streaked on plates containing phloxine B pink dye and incubated for two days at 36°C. Strains: 513, AL1-A1, AL1-A2, AL1-A3, AL1-A4, AL2-A5, AL2-A6, AL2-A7, AL2-A8 and AL2-A9

3.2 Distribution of temperature sensitive mutations in the *skp1* gene.

Sequencing *skp1*^{ts} mutations

In order to verify that *skp1* had been mutated sequencing was carried out. The phenotype was also checked to be dependent on the mutations and these results are detailed in Chapter 4.

Each of the nine mutants isolated was amplified using colony PCR with "Expand High Fidelity" polymerase. Primers were located five hundred base pairs upstream and five hundred base pairs downstream of the *skp1*$^{+}$ gene. Amplified fragments were then used as the template in sequencing reactions. Four primers located at 200 base pair intervals throughout the *skp1*$^{+}$ gene were used and an extra primer was used coding in the opposite direction to ensure that the 5' end of the gene was correctly sequenced.

Groups of mutants

Table 3.2.1 and Fig. 3.2.1 show the mutations created in *skp1*$^{+}$ that cause temperature sensitivity. Although there were initially nine mutants, sequencing showed there are five categories of mutants. As can be seen in Fig. 3.2.1 all of these mutations are in the C-terminal region of the protein. Within these five categories there are two main groups, point mutations and mutations in the STOP codon, which cause read through to a STOP codon seven amino acids further downstream. The point mutations are clustered within a ten amino acid region. It may be that due to the small size and essential function of this protein, it is difficult for cells to support mutations in many regions of the protein and that the majority of mutations are lethal.

The point mutations that occur are relatively conservative in nature. The changes being a Valine to an Alanine at residue 102 (AL1-A2 and AL2-A6 henceforth: *skp1*^{ts}*A2/A6*), an Isoleucine to a Threonine at residue 110 (AL2-A7 henceforth: *skp1*^{ts}*A7* unless otherwise stated) and a Leucine to a Phenylalanine at residue 113 (AL1-A3 henceforth: *skp1*^{ts}*A3*). Although these changes demonstrate differences in the size of molecules and also a change from a non-polar to a polar residue there are no drastic changes in charged residues.

Developments in the crystal structure of the human SCF complex

Work carried out in 2000 and 2002 (Schulman *et al.*, 2000; Zheng *et al.*, 2002) into the crystal structure of the SCF complex has allowed elaboration of SKP1 structure binding to the F-box protein SKP2 to a resolution of 2.8Å (Fig. 3.2.2). This demonstrates that the N-terminus of the SKP1 protein is involved in binding to the cullin protein whilst the C-terminus is involved in binding to the F-box protein. The N-terminal domain shows similarity to a BTB/POZ domain (Aravind and Koonin, 1999) with the C-terminus of the protein forming an extension of two helices. The last two helices of the BTB/POZ domain and the two helices of the extension form the regions of contact with the F-box protein. Of these four helices, helix 5 and 6 of the BTB/POZ domain are thought to form core contacts with all F-boxes whilst helices 7 and 8 are thought to form different contacts with the F-box depending on which F-box protein is binding. *S. pombe* Skp1 has 75% similarity to the human version (Fig. 3.2.1). This figure also demonstrates the location of the F-box contact residues as dots under the alignment. These were identified in the structural analysis (Schulman *et al.*, 2000).

Modelling the *S. pombe* mutations onto the crystal structure of human Skp1

Due to the high homology between Skp1 in *S. pombe* and *H. sapiens* it has been possible to map the mutations created in *S. pombe* Skp1 onto the human structure and postulate how these mutations may affect the function of Skp1 in binding either to its associating F-box proteins or Pcu1. Fig. 3.2.3 shows the position of the C-terminal extensions added onto the Skp1 protein. From this diagram it is possible to conceive that the extension mutations may interfere with helix 8 and its interface with an F-box protein.

Fig. 3.2.4 shows how the point mutations in *skp1*^{ts} strains would affect the structure. All three mutations occur in helix 5. Each of the residues shows a high degree of conservation between species. The V102A mutation occurs at a core contact residue for F-box binding. The loss of the side chain may make the distance for binding at this point too far, loosening contact with the F-box protein. The other two mutations do not occur in residues involved in directly contacting the F-box. However examination of the region suggests that this is a

densely packed, hydrophobic area of the protein. The introduction of a bulky aromatic side chain in the L113F mutant, *skp1^{ts}A3*, is likely to disrupt the packing in this area of the protein. The I110T mutation of *skp1^{ts}A7* is also part of this hydrophobic region. This change introduces a polar amino acid with a hydroxyl group into the centre of a hydrophobic region, which could potentially disrupt the structure of this region and thus the binding to F-boxes. Further observation shows that the *skp1^{ts}A3* mutation is in the same location as a previously characterised *S. cerevisiae* mutant *skp1-4*; this mutant contains a leucine to serine change and produces a G2 arrest phenotype characteristic of cells defective in the Skp1 kinetochore function of *S. cerevisiae* (Connelly and Hieter, 1996). The *S. pombe* Skp1 however has not so far been shown to have a role at the kinetochore.

Allele	Mutation type and comment
A1, A4, A5	STOP → Gln. Read through stop codon to a stop codon a further 7 amino acids downstream
A2,A6	Val102 → Ala point mutation. A6 has a further mutation in the 3'UTR
A3	Leu113 → Phe point mutation
A7	Ile110 → Thr point mutation
A8, A9	STOP → Ser. Read through stop codon to a stop codon a further 7 amino acids downstream

Table 3.2.1: Mutations in temperature sensitive *skp1* alleles
All strains contain an *h⁻ leu1 ura4* background.

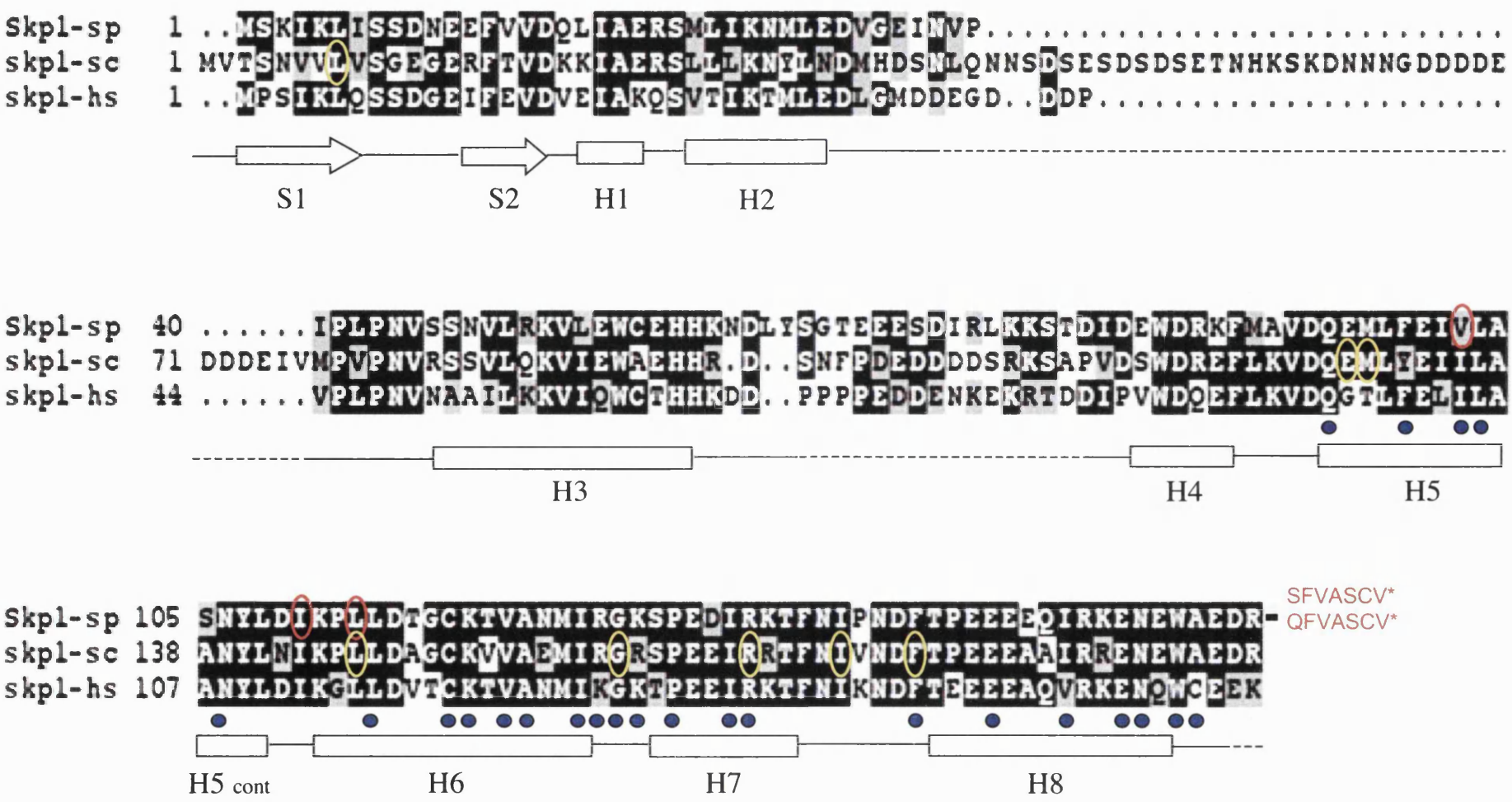
Skp1-sp 1 ..MSKIKLISSDNEEFVVDQLIAERSMLIKNMLEDVGEINVP.....
skp1-sc 1 MVTSNVVLVSGEGERFTVDKKIAERSLLLKNYLNDMHDSNLQNNSDSESDSDSETNHKSKDNNNGDDDDE
skp1-hs 1 ..MPSIKLQSSDGEIFEVDVEIAKQSVTIKTMLEDLGMDDEGD..DDP.....
S1
S2
H1
H2
Skp1-sp 40 .....IPLPNVSSNVLRKVLEWCEHHKNDLYSGTEEESDIRLKKSTDIDEWDRKFMAVDQEMLFEIVLA
skp1-sc 71 DDDEIVMPVPNVRSSVLQKVIEWAEHHR.D..SNFPDEDDDDSRKSAPVDSWDREFLKVDQEMLYEIILA
skp1-hs 44 .....VPLPNVNAAILKKVIQWCTHHKDD..PPPPEDDENKEKRTDDIPVWDQEFLKVDQGTLFELILA
H3
H4
H5
Skp1-sp 105 SNYLDIKPLLDTGCKTVANMIRGKSPEDIRKTFNIPNDFTPEEEEQIRKENEWAEDR-
skp1-sc 138 ANYLNIKPLLDAGCKVVAEMIRGRSPEEIRRTFNIVNDFTPEEEAAIRRENEWAEDR
skp1-hs 107 ANYLDIKGLLDVTCKTVANMIKGKTPEEIRKTFNIKNDFTEEEEAQVRKENQWCEEK
SFVASCV*
QFVASCV*
H5 cont
H6
H7
H8

Fig. 3.2.1: Comparison of the homologues of Skp1 from fission yeast, budding yeast and humans

Identical residues are shown in black, similar residues in grey. The *S. cerevisiae* protein contains a 30 residue insertion not found in fission yeast or humans. The helices and domains from the human crystal structure are represented beneath the alignment. F-box contact residues (blue dots) are present mainly in the C-terminus (B. Schulman *et al.*,2000). Known temperature sensitive mutants in Skp1 from budding yeast (yellow circles) are *skp1-12* L8G, *skp1-1* E129G, *skp1-2* M130V and F176S, *skp1-4* L146S, *skp1-11* G160R and R167K, *skp1-3* I172N (C. Bai *et al.*,1996; C. Connelly and P. Hieter, 1996). The three point mutants created from the screen in *S. pombe* *skp1^{ts}A2/A6* V102A, *skp1^{ts}A3* L113F and *skp1^{ts}A7* I110T are shown in red as are the C-terminal extension mutants.

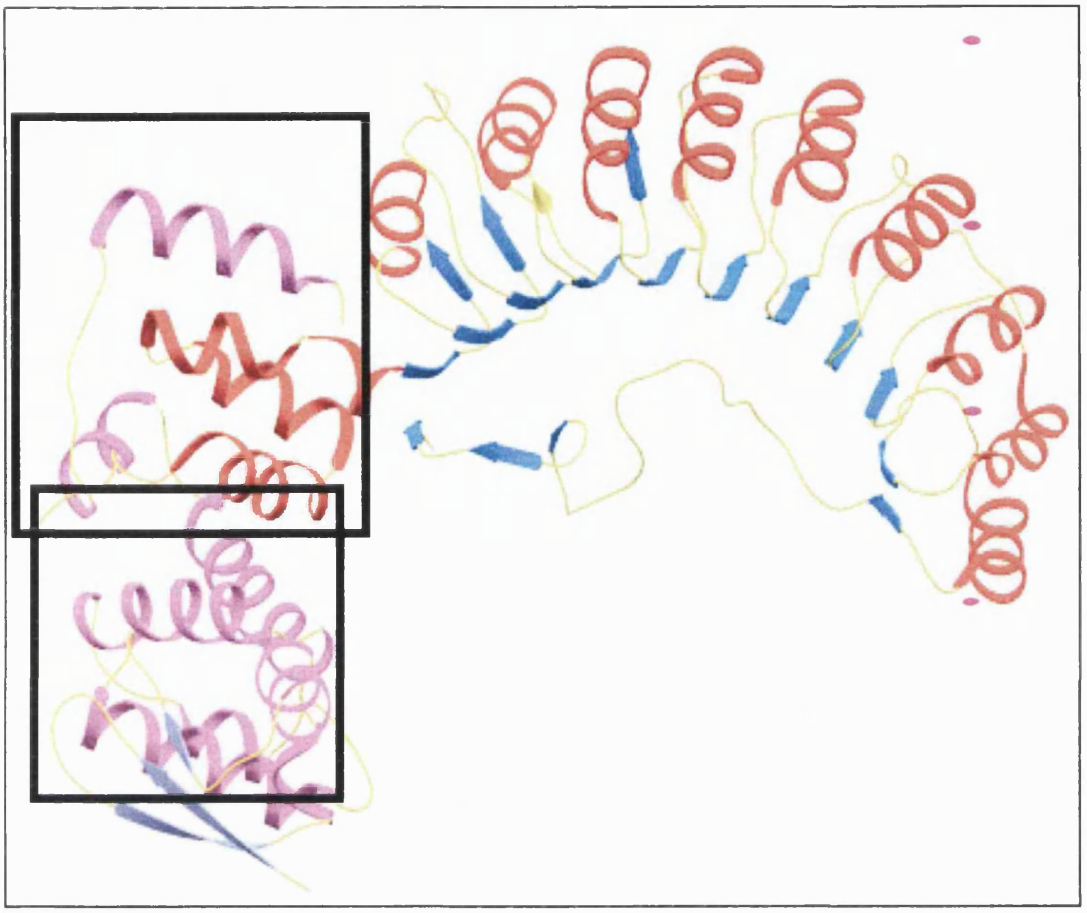

Fig. 3.2.2: Crystal structure of human SKP1 binding to the human F-box protein SKP2
SKP1 helices shown in purple and β-strands in blue. SKP2 helices shown in red and β-strands in blue. Black squares are regions where *S. pombe* mutations have been created and are enlarged in the next two figures.

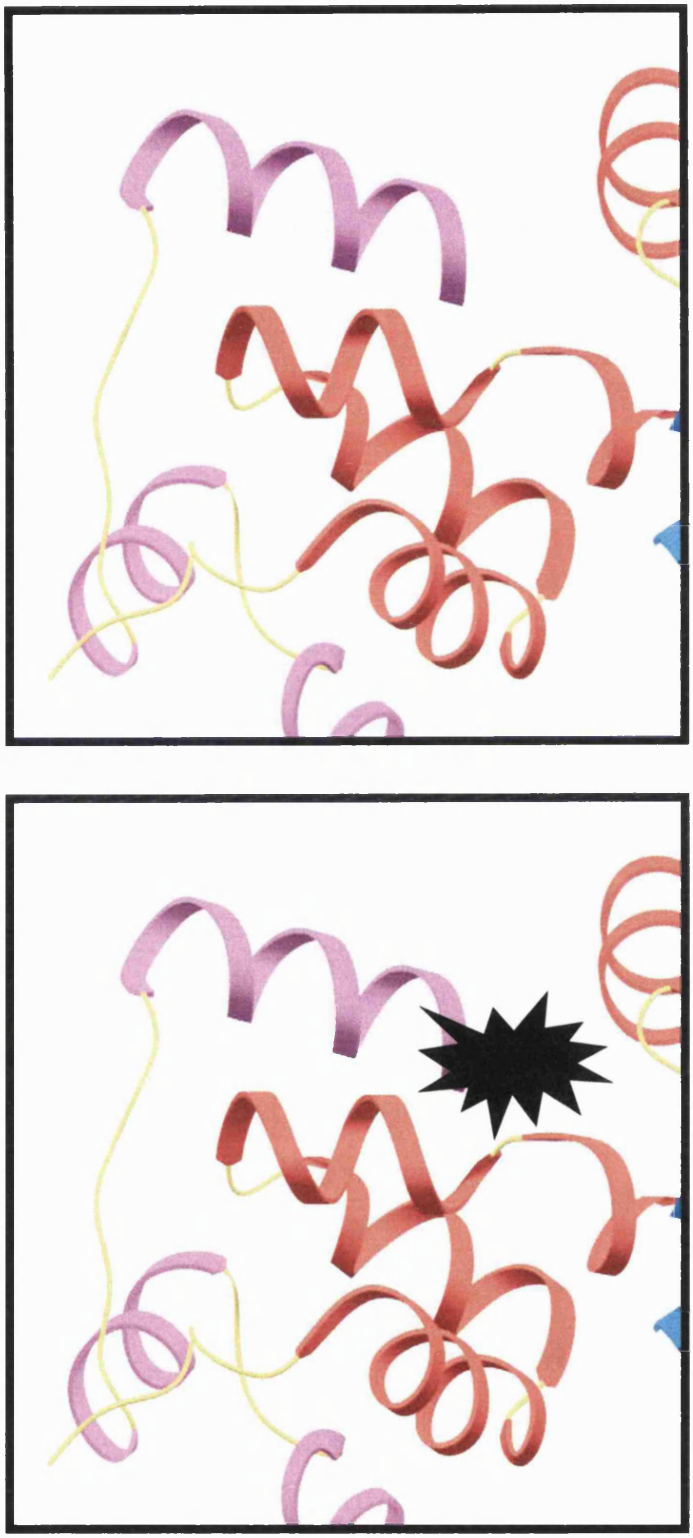

Fig. 3.2.3 : The C-terminus of SKP1 interacting with the F-box of SKP2 from humans

Upper SKP1 C-terminus in purple. N-terminus SKP2 (F-box) in red. Lower black star represents the amino acids added upon read-through of the STOP codon of Skp1. The proximity of these to the F-box (red helices) is proposed to affect binding of SKP1 to an F-box protein.

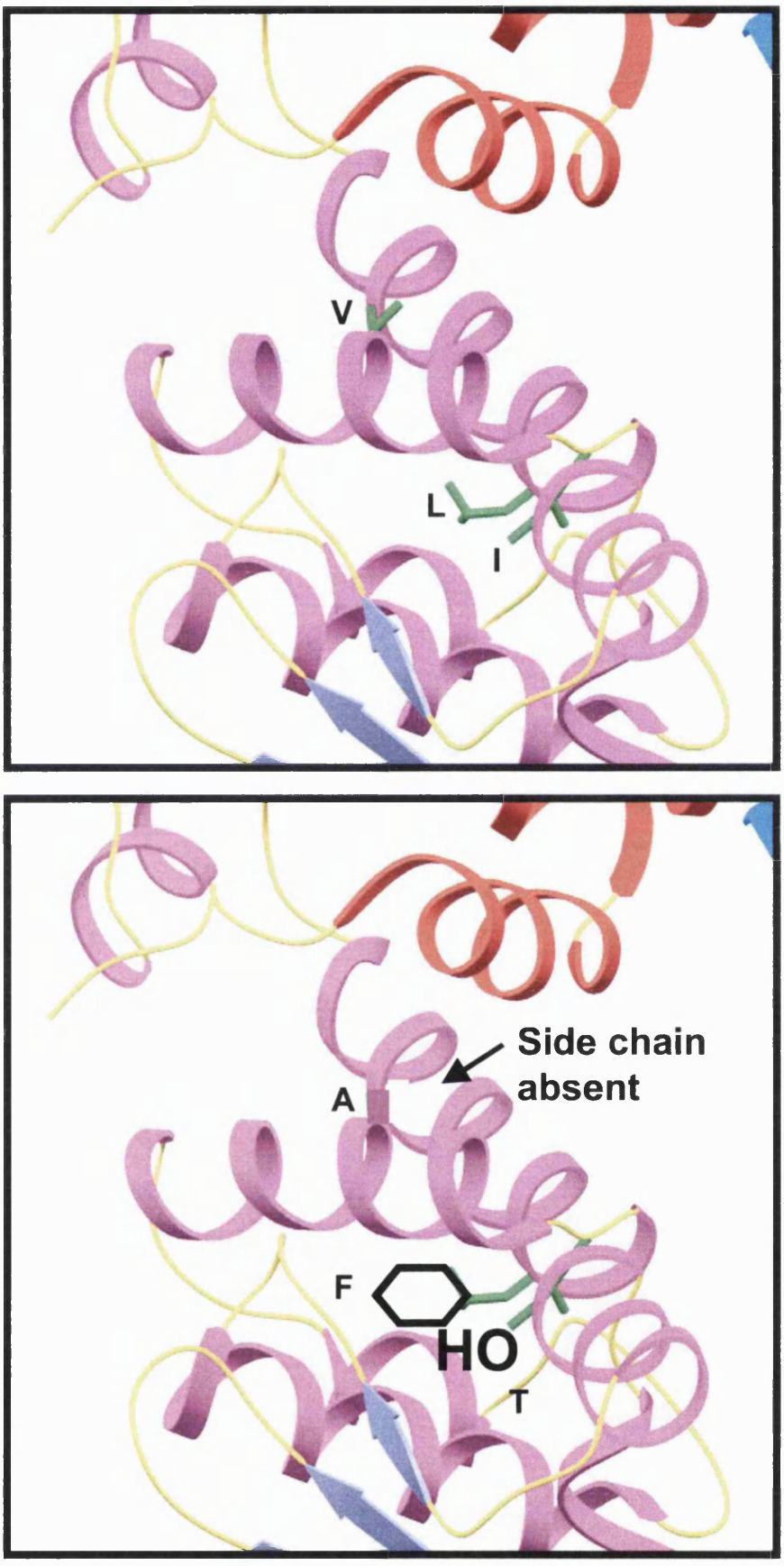

Fig. 3.2.4: Central region of SKP1
Upper shows the position and side chain orientation Valine 102, Isoleucine 110, Leucine 113 all in green.
Lower shows changes in these side chains that occur in *skp1*^{ts} point mutants, V102A, I110T and L113F.

3.3 Epitope tagging of each F-box protein

In order to assess if the phenotype of *skp1*^{ts} strains was dependent on compromised binding interactions with other components of the SCF complex, as predicted by the structural modelling, it was decided to check physical interaction of Skp1 with each of the F-box proteins and the fission yeast SCF cullin, Pcu1. As shown in the following chapter the phenotypes of all the *skp1*^{ts} strains were similar for all mutant alleles created. The allele *skp1*^{ts}*A7* was chosen as representative and used for further experiments.
Pcu1 and each of the F-box proteins were C-terminally tagged with 13 copies of the myc epitope at the chromosomal locus by homologous recombination. Pof6 contains a CAAX domain in its C-terminus. This prevents tagging at the C-terminus as this domain is usually prenylated followed by proteolytic cleavage; this cleavage is critical to the function of CAAX containing proteins. Pof6 was therefore tagged at its N-terminus with GFP under the strong thiamine-inducible promoter. This promoter was used under repressing conditions, with thiamine present in order to produce expression at low levels. For the DNA helicase Fdh1 no clones tagged at the C-terminus were obtained. It was therefore tagged with GFP at the N-terminus in a similar manner to Pof6. For certain F-box proteins it was not possible to obtain tagged clones at either the N or the C-terminus: these were Pof4 and 11. This suggests that both the N and C-termini of these proteins are disrupted by the presence of a tag in some way that prevents the function of the protein or possibly that these are not real genes (i.e. pseudogenes).

3.4 Production of polyclonal anti-Skp1 antibody

In order to detect Skp1 in the cell, polyclonal antibodies were created. The yeast *skp1*$^{+}$ was cloned into an expression vector carrying six copies of the histidine tag (6XHis). This construct was expressed in bacteria (Fig. 3.4.1A). The protein was in the soluble fraction of bacterial lysates and was purified on Nickel columns. Purified 6XHis-Skp1 was injected into two rabbits. Two anti-sera were generated and the resulting antibodies were tested for immuno-reaction against protein extract from yeast and against the original purified

extract. Both sera could recognise Skp1 but one was far superior at detecting the protein. Fig. 3.4.1B (lane1) shows the antibodies of the superior anti-serum can detect a band slightly larger than 20 kDa, and the predicted size of Skp1 in wild-type extracts is 19.3 kDa. This band was expected to shift to 25 kDa when the protein was tagged with three copies of the Hemagglutinin epitope (3HA) at the N-terminus under the thiamine-inducible promoter (Yamano *et al*., 2000). Significantly the levels of the 25kDa band were sensitive to the presence or absence of thiamine (lanes 3 and 4). It was therefore concluded that these antibodies were competent to detect Skp1 in yeast cell lysates. A yeast lysate from *skp1^{ts}A8* strain was also tested for detection of Skp1 with these antibodies. The protein was found to be present although levels were lower than the wild type.

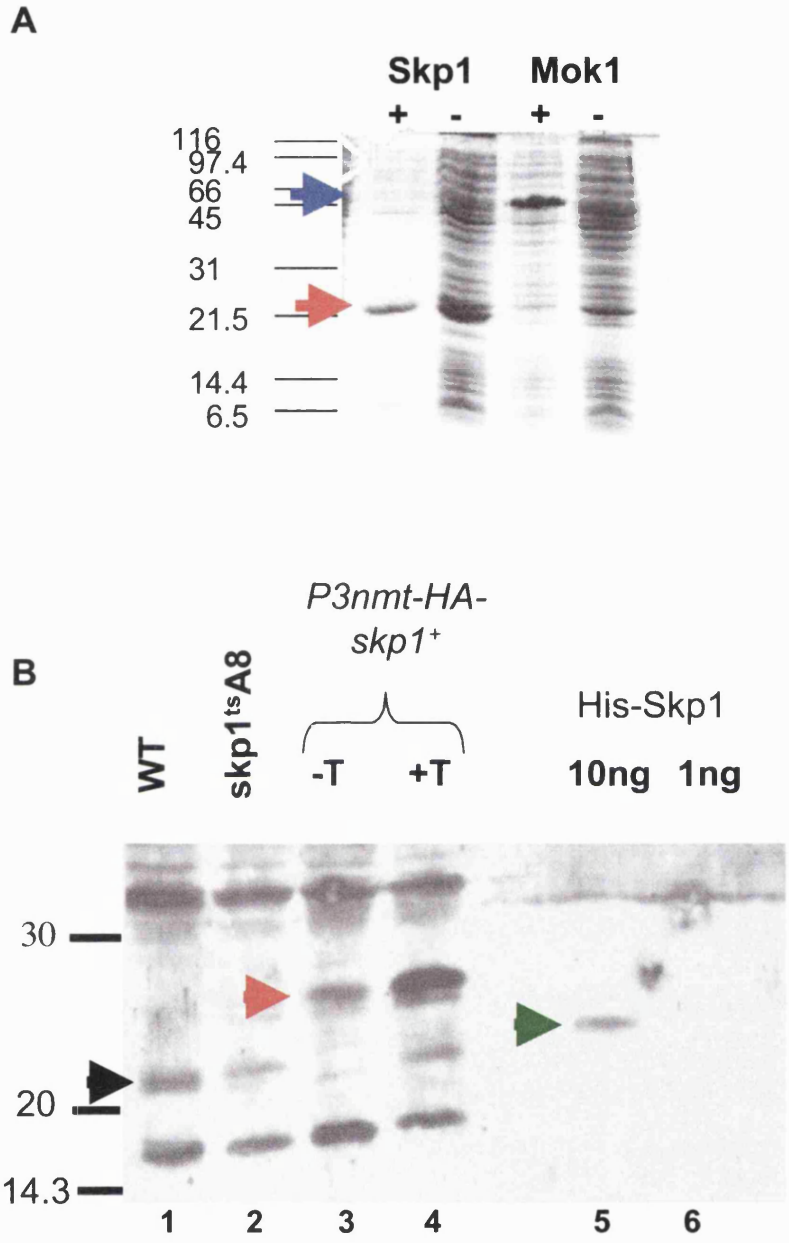

Fig. 3.4.1: Skp1 antibodies detect Skp1 on a western blot.
A *pET14b-6xhis-skp1*$^{+}$ expressed in *E. coli*. Extract prepared from 1ml of *E. coli* culture by pelleting cells and direct addition of SDS from induced (+) and uninduced (-) cultures are shown. Mok1 a previously created construct is expressed as a positive control. **B** 30μg protein extract from WT(513), *skp1*^{ts}*A8* (AL2-A8), N-terminally HA-tagged Skp1 under a thiamine-repressible promoter (Skp1nmt) and bacterially purified recombinant His-Skp1 proteins were detected on a western blot with antibodies purified from rabbit.
Endogenous Skp1 is marked by a black arrow and runs at ~21KDa, the HA-tagged protein is marked by a red arrow and the His-tagged protein by a green arrow. Levels as low as 10ng of protein can be detected by the antibody

3.5 Comparisons of F-box binding in *skp1*$^{+}$ and *skp1*^{ts}*A7* strains

For binding analysis wild-type and *skp1*^{ts}*A7* cells containing a tagged F-box protein or tagged Pcu1 (see strain list; sub–heading: F-box tags, for full genotypes in Materials and Methods section) were grown at 26°C overnight until mid-log phase. Cultures were then shifted to 36°C for 4 hours in order for the *skp1*^{ts}*A7* phenotype to become apparent, after which protein extracts were prepared. These protein extracts were then used for immunoprecipitations. In all cases polyclonal Skp1 antibodies were used to pull down proteins and the presence of F-box proteins or Pcu1 was then detected by anti-myc or anti-GFP western blotting.

Skp1 and Pcu1 binding

Fig. 3.5.1 shows the binding of Skp1 or Skp1^{ts}A7 to Pcu1. Pcu1 appears as two bands, the slower migrating form being modified by the small ubiquitin like protein Nedd8 (Osaka *et al.*, 2000). This neddylation is essential for function of SCF ubiquitin ligases and is seen in all SCF complexes defined so far. The structural analysis of the complete SCF complex (Zheng *et al.*, 2002) shows that human NEDD8 binds to the cullin in a region close to the binding site of the E2 and it has been proposed that neddylation occurs in order to assist E2 recruitment into the SCF complex (Kawakami *et al.*, 2001). It is therefore unsurprising that Skp1 associates with both the neddylated and unneddylated forms of the protein. The levels of binding of Pcu1 appear to be unaffected in the mutant *skp1*^{ts}*A7*. This suggests that the assembly of the core elements of the SCF complex are unaffected by the point mutation that this allele carries. In fact Fig. 3.5.3, a quantitative analysis of the binding, suggests that binding to Pcu1-myc in *skp1*^{ts}*A7* may even be slightly increased as the amount of Skp1^{ts}A7 pulled down is not as large as the amount of wild-type Skp1 and the amount of Pcu1 present is higher than in the wild-type background. The continued binding of Pcu1 to Skp1 was predicted from the assignment of the mutation site I110T in Skp1^{ts}A7, as described above in section 3.2.

Skp1 and F-box binding

Wild-type Skp1 could be immunoprecipitated with the tagged F-box proteins (Figs. 3.5.1, 3.5.2 and 3.5.4). The levels of F-box proteins present in the protein extract varied, with Pofs 5, 7, 8 and 10 being higher in abundance than the majority of the other F-box proteins. As the F-box is known to be a Skp1 binding domain, the binding of all the F-box proteins we have identified by genome searching verifies they contain a genuine F-box and are likely to be real SCF components, despite the low conservation to the consensus F-box sequence observed in some of these proteins (See Chapter 2 Fig. 2.3.1). The levels of binding are quantified in Fig. 3.5.3. It is noticeable that the abundance of the protein within the cell always exceeds the amount bound to Skp1 (compare input to IP Figs. 3.5.1 and 2). Furthermore, abundance of the Pof protein within the cell is not necessarily a predictive factor for the amount of F-box that binds to Skp1 (compare the levels of Pof8 and Pof9 in the input and IP Fig. 3.5.2).

Skp1^{ts}A7 binding to F-box protein

The binding of the majority of F-box proteins to Skp1^{ts}A7 showed little difference to the binding of wild-type Skp1. Notably although all F-box proteins continued to bind to Skp1, the levels of binding of Pof1 and Pof3 F-box proteins was markedly reduced. This may be significant as Pof1 is essential to cell viability and Pof3 is essential for the maintenance of genome integrity. (Fig. 3.5.1: compare lanes *pof3-myc* and *skp1^{ts}A7 pof3-myc*; also Fig. 3.5.1: compare lanes *pof1-myc* with *skp1^{ts}A7 pof1-myc*). The binding of Pof3 shows a particularly significant reduction in binding to Skp1^{ts}A7.

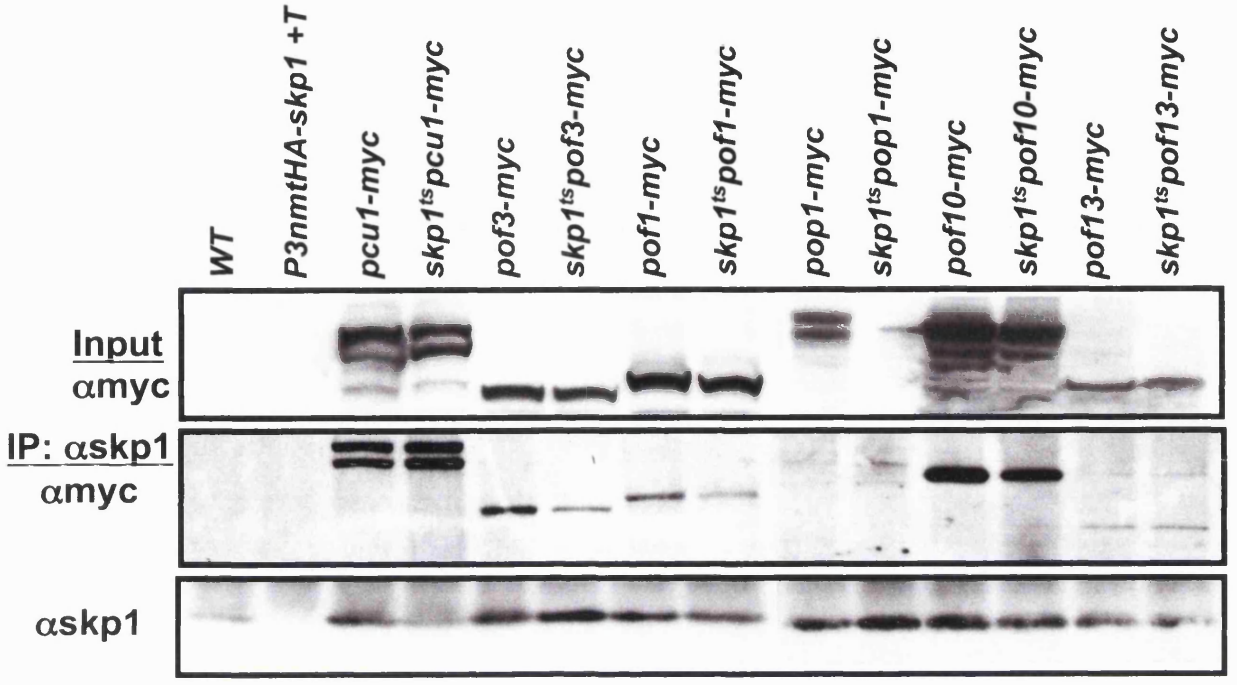

Fig. 3.5.1: Immunoprecipitation of Skp1 and Skp1^{ts}A7 with myc tagged F-box proteins

Strains were grown at 26°C overnight and shifted to 36 °C for 4 hours. Protein extracts were made and 30μg used for western blot analysis, 2 mg were subjected to immunoprecipitation procedures. Strains used, in lane order as follows: 513, Skp1 nmt, SKP414-17, AL74, SKP510, AL76, CLP9, AL84, SKP410-15, AL80, AL91, AL120, AL89 and AL131

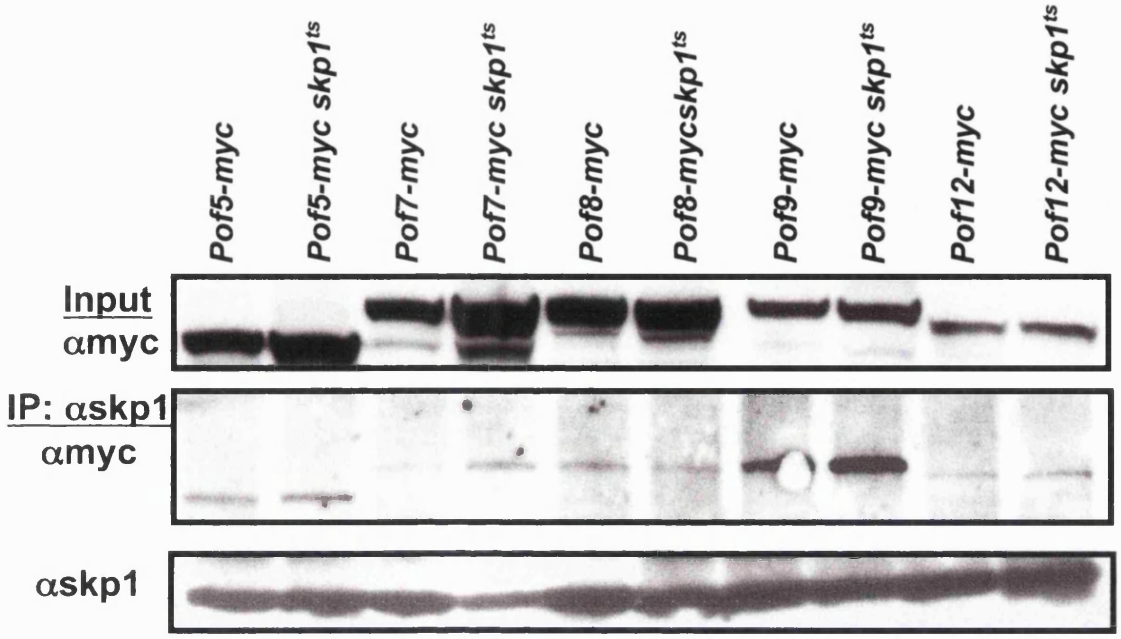

Fig. 3.5.2 : Immunoprecipitation of Skp1 and Skp1^{ts}A7 with myc tagged F-box proteins

Strains were grown at 26°C overnight and shifted to 36 °C for 4 hours. Protein extracts were made and 30μg used for western blot analysis, 2 mg were subjected to immunoprecipitation procedures. Strains used, in lane order as follows: AL95, AL126, AL87, AL127, AL98, AL124, AL90, AL123, AL92, and AL129

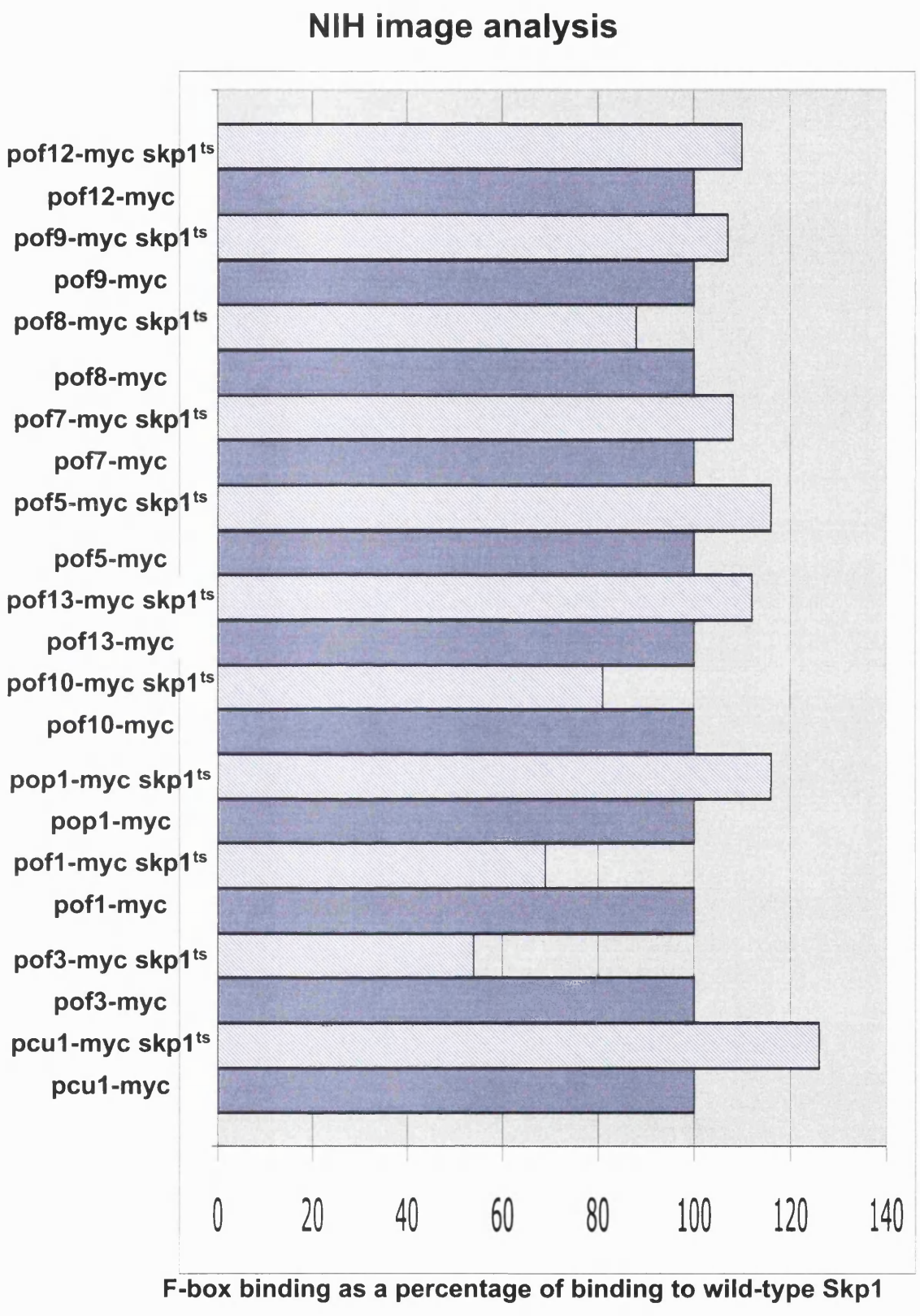

Fig. 3.5.3 NIH image analysis of bands from immunoprecipitations
NIH image was used to calculate the intensity of the bands from immunoprecipitation. The mean pixel density was taken for each band and equalised to the background of the blot by measuring pixel density in a region of identical size below the band.The background was then subtracted from the measurement for the band. Measurements are given as a percentage where binding to wild-type Skp1 is taken to be 100%.

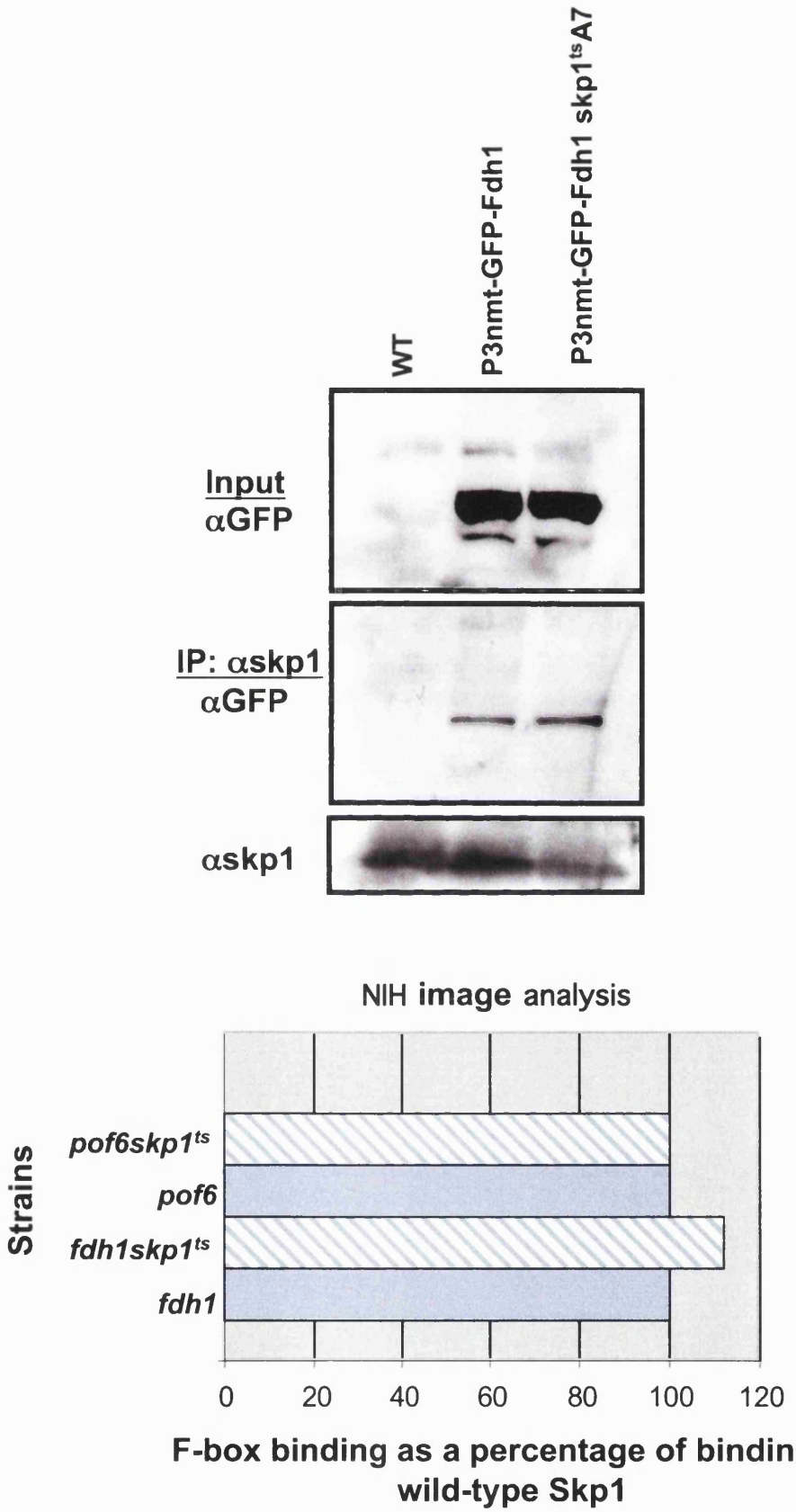

Fig. 3.5.4 : Immunoprecipitation of Skp1 and Skp1^{ts}A7with GFP-Fdh1
Strains were grown at 26°C overnight and shifted to 36 °C for 4 hours. Protein extracts were made and 30μg used for western blot analysis, 2 mg were subjected to immunoprecipitation procedures.
Western blots were subsequently analysed by NIH image and the intensity of the bands at 36°C in WT and mutant cells compared. Strains used: 513, AL182 and AL177

3.6 Summary

In order to further assess the role of Skp1 in the cell a screen to isolate temperature sensitive mutants in the *skp1*$^{+}$ gene was carried out. This screen yielded nine mutants, which fell into two major groups. The first group are those mutants that contained a mutation in the STOP codon adding an extra seven amino acids onto the protein. The second group was a set of point mutants. Using the crystal structure of human SKP1 it was possible to assess how these mutations may affect *S. pombe* Skp1 protein structure. The location of the mutations suggests that they were likely to affect F-box-binding, core helix number 5 of the protein, where there is a region of densely packed hydrophobic residues but would not affect the N-terminal Pcu1 interacting domain. Fig. 3.6.1 shows a summary of the regions affected by mutation in the Skp1 protein of *S. pombe*.

The existence of a functional F-box in each of the proteins encoded by the ORFs identified in Chapter 2 was verified by co-immunoprecipitation of Skp1 with each individual F-box protein. The ability of Skp1 to bind to the cullin protein Pcu1 was also examined. A comparative analysis of the binding of the F-box proteins to both Skp1 and Skp1^{ts}A7 demonstrated that although Skp1^{ts}A7 was capable of maintaining binding to all of the F-box proteins, binding to two important F-box proteins, Pof1 and Pof3, was visibly reduced. Skp1^{ts}A7 showed no such reduction in binding to Pcu1 suggesting that the core complex of SCF components remains intact in these cells as predicted by the structural analysis.

Fig. 3.6.1 : Summary diagram of regions affected by mutations on a model of *S. pombe* Skp1
Regions affected are shown in black. Skp1 N-terminus is at the bottom of the diagram and the C-terminus at the top. The black arrow indicates the F-box binding groove.

3.7 Discussion

Effects of mutation on binding to other proteins

In order to examine the role of the SCF complex in the cell and its potential substrates it was decided to target a central component of the complex for mutational analysis. Bearing in mind the fact that Skp1 may be required to bind to several factors in order to create several different SCF complexes it is perhaps surprising that the mutational analysis did not provide a diverse array of mutations but a collection of mutations in a small region of the gene. Comparison of the protein to the human crystal structure reveals that the mutations are contained in a region close to the C-terminus. Pcu1 the cullin protein, which forms the scaffold of the SCF complex is thought to bind to the N-terminus of the protein. The mutations that were not lethal occurred in helix 5 and 8 of the Skp1 protein. These are regions shown to be involved in F-box binding. It is therefore predicted that the mutants created should have defects in binding to F-box proteins but maintain intact binding to Pcu1. In order to test this prediction the F-box proteins in the *S. pombe* proteome were checked for their ability to bind to wild-type and mutant Skp1.

Skp1 and Skp1^{ts}A7 differences in the binding to F-box proteins. A reason for a defective phenotype?

In creating temperature sensitive mutants of *skp1*$^{+}$ it is important to assess how this would impact on the formation of the SCF complex as a whole. If *skp1*^{ts} mutants caused the disruption of the entire SCF complex then it is likely that all substrates would accumulate. This would lead to inviability as deletion of each of the core components is lethal to the cell and so too are deletions of two F-box proteins. This suggests that there is residual activity of the SCF complex in the *skp1* temperature sensitive mutants. The structural data in this chapter suggests that binding to Pcu1 and thus the rest of the core components of the SCF complex should be unaffected in the *skp1*^{ts}*A7* mutant. However we predicted that defective F-box binding will occur. Indeed this is true for two F-box proteins, Pof1 and Pof3, which are affected in the mutant *skp1*^{ts}*A7*.
The binding of F-box and substrate to the core complex is probably the main role of Skp1 rather than a direct involvement in ubiquitination. It is interesting

therefore that binding to the F-box is not totally abolished but is in two cases reduced and this suggests that some degradation of target substrates could still be possible. The ability to degrade a known SCF substrate is tested in Chapter 4.

If it is the case that substrates are still degraded by the SCF complex containing defective Skp1, the fact that a defective phenotype is seen in these cells suggests that the cell is extremely sensitive to the levels of target proteins, if a reduction by half of F-box binding to Skp1 can cause a phenotype in cells. The binding of two F-box proteins is affected therefore the phenotype of *skp1* temperature sensitive mutants could result from the combination of slight accumulation of more than one substrate.

The binding of Pcu1 to Skp1 appears to increase rather than decrease in *skp1^{ts}A7* strains. This also opens the possibility that Skp1 can be sequestered in SCF complexes in the cell when it may have other functions away from the SCF. The increased binding to Pcu1 may mean that there is insufficient free Skp1 in the cell for carrying out non-SCF functions.

A further question relating to F-box binding relates to the factors that may make some F-boxes bind more than others. It was wondered if an increased ability of the F-box proteins Pof1 or Pof3 to bind Skp1^{ts}A7, would we be able to rescue the *skp1^{ts}A7* mutant phenotype. Pop1 F-box shows increased binding to the *skp1^{ts}A7* mutant. It was therefore a possibility that if we substituted the F-box of Pop1, with increased binding, into one with reduced binding, Pof3 or Pof1 the *skp1^{ts}A7* mutant phenotype would be rescued.

The protein sequences of the F-boxes was examined in order to look for similarities in those F-boxes that did not bind and those that did. We noticed some conserved residues in the F-boxes of Pof1 and Pof3 that were not conserved in Pop1. These 3 F-box regions were aligned with the human F-box protein SKP2 in order to locate the position of key SKP1 binding contacts that have been elaborated for the SKP2 protein (Fig. 3.7.1). It was observed that the F-box similarities of Pof3 and Pof1 were in core F-box binding residues. A domain swap was attempted using the F-box regions of Pop1 and Pof3 so far this has not been possible. Fig. 3.7.2 shows a scheme of how this experiment was attempted.

F-box proteins with respect to combinatoriai control

The SCF complex operates by targeting substrates for ubiquitin-mediated degradation. The core part of the complex is thought to be involved in orientating the E2 with respect to the substrate (Zheng *et al.*, 2002). Different substrates are recruited to the SCF complex through the F-box domain. The numbers of F-box containing ORFs present in a variety of genomes (Cenciarelli *et al.*, 1999) implies that the SCF complex has a diverse array of targets as each F-box appears to recruit several proteins for degradation (Patton *et al.*, 1998b). The *S. pombe* genome like other genomes investigated contains a wide variety of F-box containing ORFs with several different protein/protein interaction motifs. This therefore suggests that in *S. pombe* as with other organisms there are a variety of different substrates.

With many F-box proteins present in a genome the mechanism of temporal control of ubiquitination by SCF complexes has become an outstanding question. In some situations proteins are phosphorylated before degradation (Skowyra *et al.*, 1997) however not all known SCF substrates have been shown to be controlled in this manner. The SCF is thought to be active throughout the cell cycle but what is of interest is when and how various F-box proteins become associated with the core complex and whether the F-box is recruited into the complex with substrate pre-bound prior to association. Work in *S. cerevisae* suggests that F-box binding to the core complex leads to the auto-ubiquitination of the F-box with subsequent degradation (Galan and Peter, 1999; Mathias *et al.*, 1999). This provides a feedback loop of negative regulation. Recent work has suggested that stability of assembled SCF complexes could be regulated by association with de-ubiquitinating activity of the COP9/signalosome-Ubp12. SCF complexes would be assembled in the presence of the signalosome and associated de-ubiquitinating enzymes (Ubp12) and are, by this mechanism, temporarily protected from auto-catalytic degradation (Zhou *et al.*, 2003). Although this system explains the assembly of these complexes, what is still not clear is how and when these complexes become disengaged from the signalosome? What is also unknown is how a de-ubiquitinating enzyme could selectively protect F-box proteins from auto-ubiquitination but leave their substrates for degradation untouched.

The presence of 16 F-box proteins in the *S. pombe* proteome leads to the question of how and when these F-box proteins associate with Skp1. Does this occur in a similar manner to the association and assembly in other organisms? As the F-box motif is loosely conserved one feasible explanation for temporal control is that there is competition between F-box proteins for binding to Skp1. Those with the most highly conserved binding motifs possibly being the most tightly bound but therefore degraded faster due to auto-ubiquitination, whilst those with more loosely conserved motifs may be more stable and thus able to bind when the concentration of the highly conserved F-box proteins is low. Pof10 is seen to be a highly stable F-box protein and it has been suggested that overexpression of this protein can displace Pop1 in binding to Skp1. Overexpression of Pof10 resulted in a Pop1 phenotype and the effects of this overexpression could be removed by co-overexpression of Skp1 (Ikebe *et al.*, 2002). This contributes to the idea that in *S. pombe* as well as auto-ubiquitination and regulation by the signalosome, F-box proteins have a competitive relationship with one another with respect to binding to Skp1.

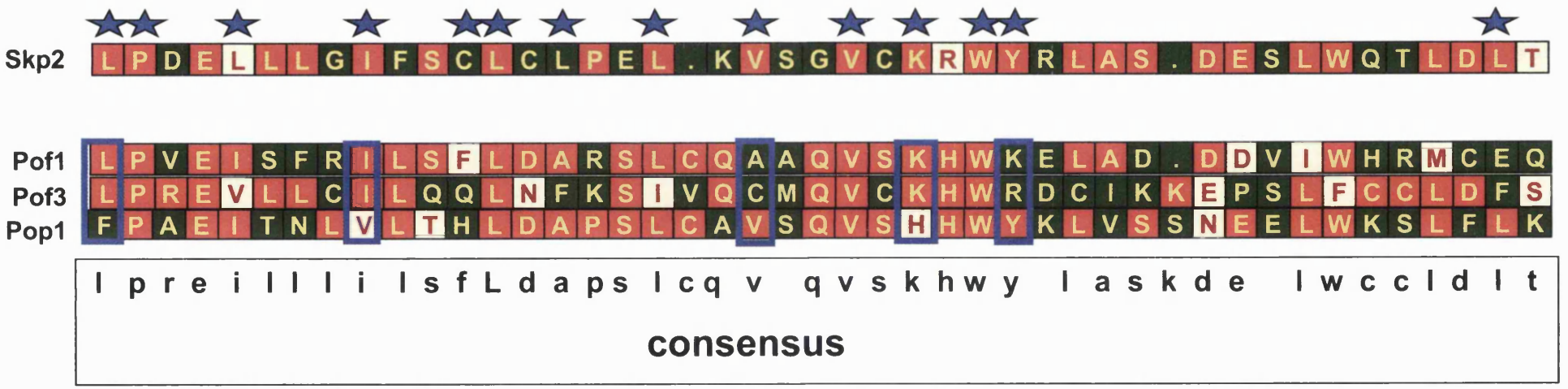

Fig. 3.7.1: The differences of Pof1 and Pof3 compared with Pop1 in core Skp1 binding residues
SKP2 F-box from humans was used to indicate core F-box binding residues when Pof1, Pof3 and Pop1 F-boxes were aligned with the SKP2 F-box. Identical residues in red. Similar residues in green. Non-identical residues in cream. Blue stars represent core F-box contact points of SKP2 with SKP1 from the human crystal structure of Skp1/Skp2. Blue boxes represent core F-box binding residues which are the same in Pof1 and Pof3 but different in Pop1.

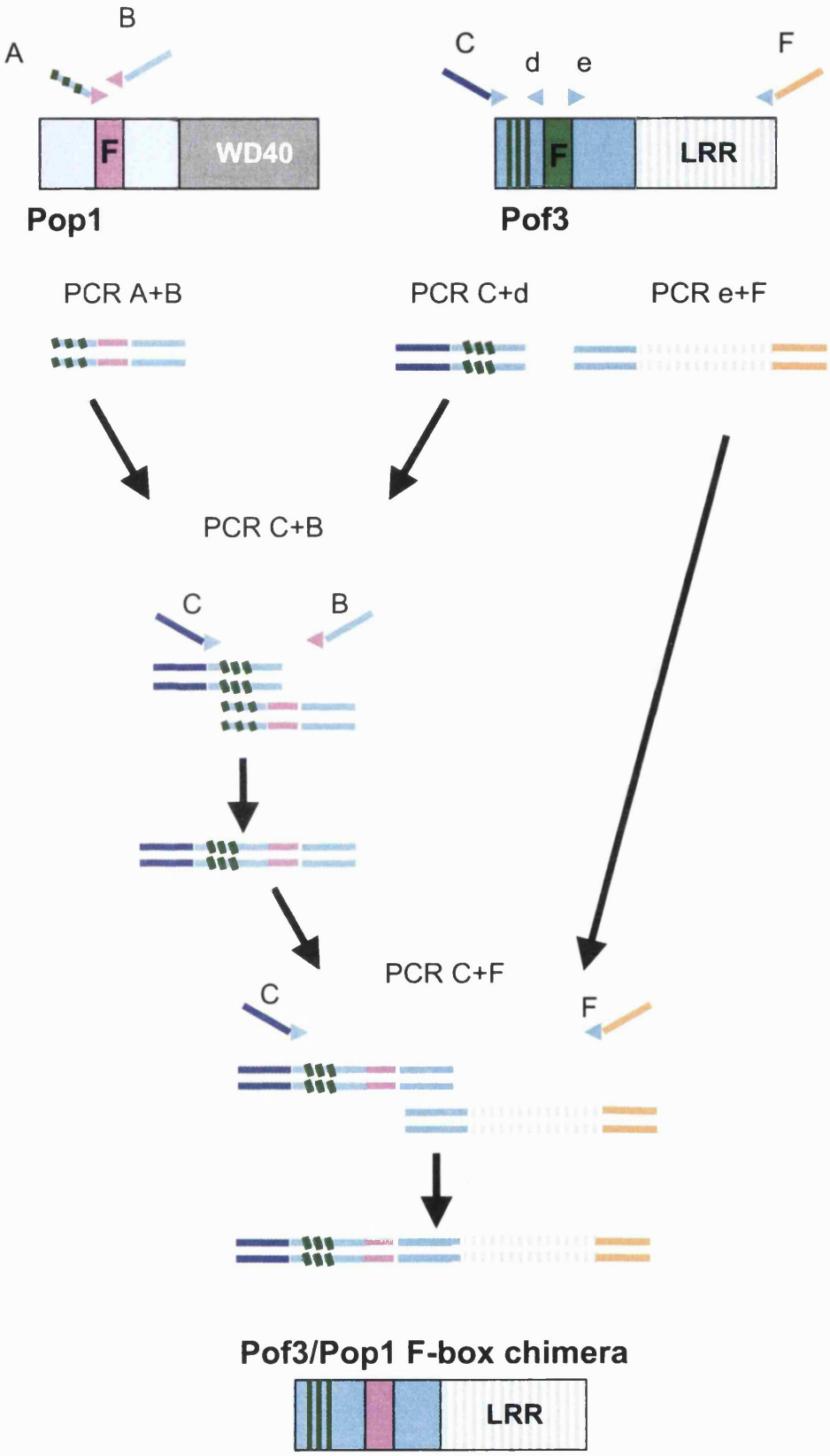
A
B
F
WD40
Pop1
C
d
e
F
F
LRR
Pof3
PCR A+B
PCR C+d
PCR e+F
PCR C+B
C
B
PCR C+F
C
F
Pof3/Pop1 F-box chimera
LRR

Fig. 3.7.2 A Scheme for PCR based generation of F-box protein chimeras

This process involves generation of different fragments of F-box proteins which are then joined together by fusion PCRs.

PCR A+B uses long primers with sequences of homology to Pof3 in the regions flanking the F-box. The front section of these primers contains in frame homology to Pop1 F-box. The resulting product should contain *pop1*$^+$ F-box flanked by *pof3*$^+$ homology.

PCR C+d uses a long primer to regions upstream of and including the 5' region of the the *pof3*$^+$ gene and a short primer from the very edge of the *pof3*$^+$ F-box towards the 5' end of the gene. This creates a fragment of DNA corresponding to the N terminus of the Pof3 protein up to but excluding the F-box. There is also a region of flanking homology to the chromosome around *pof3*$^+$ for re-integration of the finished construct in to the S. pombe genome.

PCR e+F is similar to PCR C+d but creates the 3' region of the gene corresponding to the C terminus of the protein. This fragment begins from the F-box and extends through the LRR region and incorporates a region of homology to the 3'UTR of *pof3*$^+$ again for re-integration into the genome.

PCR C+B fuses fragments created from A+B and C+d and

PCR C+F fuses fragments from C+B to fragments from e+F.

Any product generated from this reaction could theoretically be transformed into fission yeast to produce a chimeric F-box protein. However, fusion PCRs were unsuccessful and if successful did not produce sufficient quantities for transformation into yeast which requires 1/2μg DNA as a minimum.

Chapter 4

Potential involvement of *skp1*$^{+}$ in the DNA damage checkpoint.

Introduction

In the previous chapter a biochemical approach was taken to characterise *skp1* temperature sensitive mutants. In order to further understand the behaviour of *skp1* temperature sensitive cells, the physiological aspects of their phenotype were investigated. This chapter describes some of these characteristics.

One of the most prominent features of the temperature sensitive phenotype was elongation of cells. Investigation of the DNA content of the cells revealed an accumulation of cells with a 2C DNA content, thus suggesting that the cells are delayed in the G2/M phases of the cell cycle.

Eukaryotic cells possess checkpoint mechanisms in S/G2 and M phases of the cell cycle known as the DNA structure checkpoint and the spindle assembly checkpoint respectively. These allow cells to delay their cell cycle in conditions where DNA replication or mitosis would be detrimental to the cell. One of the potential reasons for a G2 delay in cells would be activation of these checkpoints, which in turn prevents progression through the cell cycle. This chapter investigates this idea and proposes that at 36°C the DNA damage checkpoint is activated and that this leads to the elongation phenotype displayed by *skp1*^{ts}*A7* cells.

4.1 *skp1* temperature sensitive mutants have an elongation phenotype

In order to gain some insights into *skp1*$^{+}$ function the physiological characteristics of the *skp1* mutants were examined. This included analysis of cell morphology, DNA structure, viability at 36°C, verification that the temperature sensitive phenotype is dependent on a mutation in the *skp1*$^{+}$ gene and analysis of DNA content at 36°C.

Mutant morphology

Mutant cells were grown in a rich medium, liquid culture; for 8 hours at 36°C and examined using a light microscope in order to observe the cell morphology. Fig. 4.1.1 A shows examples of these cells from each category of mutant allele (Chapter 3). The average length of a dividing fission yeast cell is ~12μm (Fantes, 1977; Nasmyth *et al.*, 1979). As can be seen from Fig. 4.1.1 A each of the mutant strains was considerably longer than 12μm, with perhaps the exception of *skp1*^{ts}*A8,* which appears to exhibit some slightly elongated and bent cells. In order to examine the progression of this elongation event, *skp1*^{ts}*A7* cells from a culture synchronised in G2 by elutriation were measured (details of centrifugal elutriation are given Chapter 7 section 7.2). Only unseptated cells were measured for cell length. Fig. 4.1.1 B shows that after 8 hours at 36°C *skp1*^{ts}*A7* cells were considerably longer than those grown at 26°C and unseptated cells were reaching a length of over 20μm. This increase in size seems to be a continuous progression as unseptated cells at 5 hours were already reaching sizes of 14μm.

Mutant Chromosomal Structures

skp1^{ts}*A7* cells from growth at the restrictive temperature (36°C), were fixed in formaldehyde and stained with DAPI (4',6-Diamidino-2-phenylindole), which binds specifically to DNA. Cells were examined with a fluorescence microscope and DNA was visualised. Fig. 4.1.2 A shows *skp1*^{ts}*A7* cells after 0 hours and 8 hours growth at 36°C. At 0 hours cells contain no abnormal DNA structures. After 8 hours growth however some 'cut' cells begin to appear (Fig. 4.1.2 A right). This occurs when the chromosomes fail to separate but cell division

continues resulting in the septum cleaving the undivided nucleus into two. Samples of different mutant strains were counted for numbers of 'cut' cells (Fig. 4.1.2 B). All the mutant alleles contained 'cut' cells to some extent, *skp1^{ts}A3* containing the highest percentage. Cells that become 'cut' are inviable as the cleavage of the nucleus is fatal to the cell. The presence of 'cut' cells probably contributes to the inviability of *skp1^{ts}* mutants at higher temperatures (see below).

Mutant viability

Fig. 4.1.2 C shows the viability of mutants after they have been grown at the restrictive temperature (36°C) and then returned to the permissive temperature (26°C). This experiment shows the changes that occur in *skp1^{ts}A7* mutant cells are irreversible as *skp1^{ts}A7* loses viability after being grown at 36°C for 8 hours and it cannot recover growth or colony forming ability at 26°C.

Temperature sensitivity, inviability and elongation phenotypes are all due to the mutations in the *skp1^{+}* gene.

In order to ensure that the physiological changes seen in *skp1^{ts}* mutants were due to the mutations in the *skp1^{+}* gene, *skp1^{ts}A7* was first backcrossed to a strain containing a *ura4^{+}* marked wild-type copy of *skp1^{+}* to look at the recombination frequency of the wild-type marker allele and the temperature sensitive phenotype. Fig. 4.1.3 A shows that after mating and sporulation all tetrads dissected have a 2:2 ratio of wild-type/*ura4^{+}* versus temperature sensitive/*ura4^{-}* suggesting that there is no recombination between the *skp1^{ts}A7* and *ura4^{+}* alleles and thus the temperature sensitivity is linked to the *skp1* allele.

Secondly *skp1^{ts}A7* cells were supplied with a wild-type copy of the *skp1^{+}* gene on a plasmid. Fig. 4.1.3 B shows that the elongation phenotype of *skp1^{ts}A7* strain is alleviated by the addition of a wild-type *skp1^{+}* gene on a plasmid as compared to addition of a vector alone. The wild-type gene also relieves growth deficiency at 36°C (Fig. 4.1.3 C). From these results it can be concluded that the mutations in the *skp1^{+}* gene are responsible for the temperature sensitivity and elongation phenotype of *skp1^{ts}* cells at 36°C. The growth rescue exhibited in the presence of the plasmid copy of *skp1^{+}* also allows the conclusion that the

mutation in *skp1^{ts}A7* is recessive. It is feasible that these rescue effects are due to a highly increased dosage of the Skp1 protein present through overexpression. In order to fully verify that *skp1^{ts}A7* is a recessive mutation the effects of the mutation would have to be examined in a heterozygous diploid carrying one copy of wild-type Skp1.

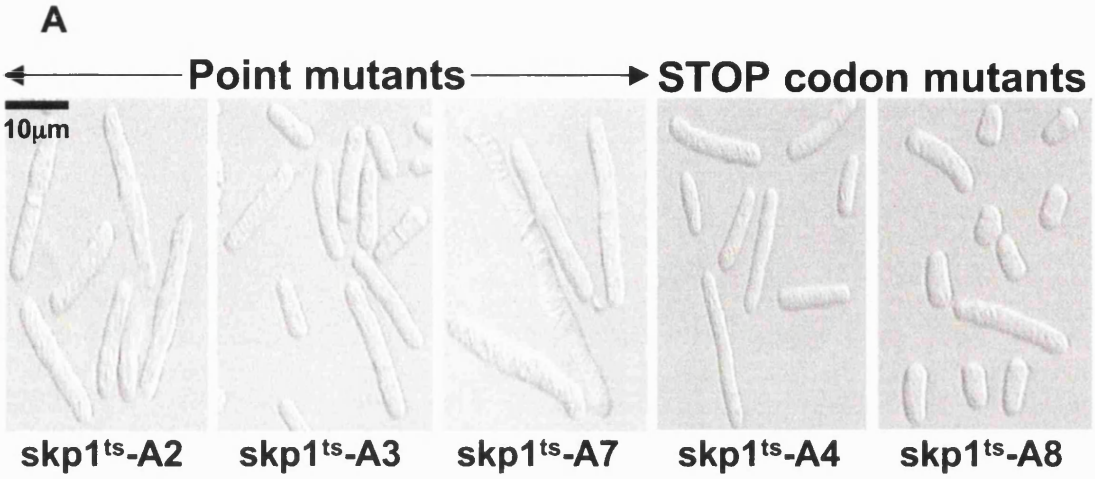

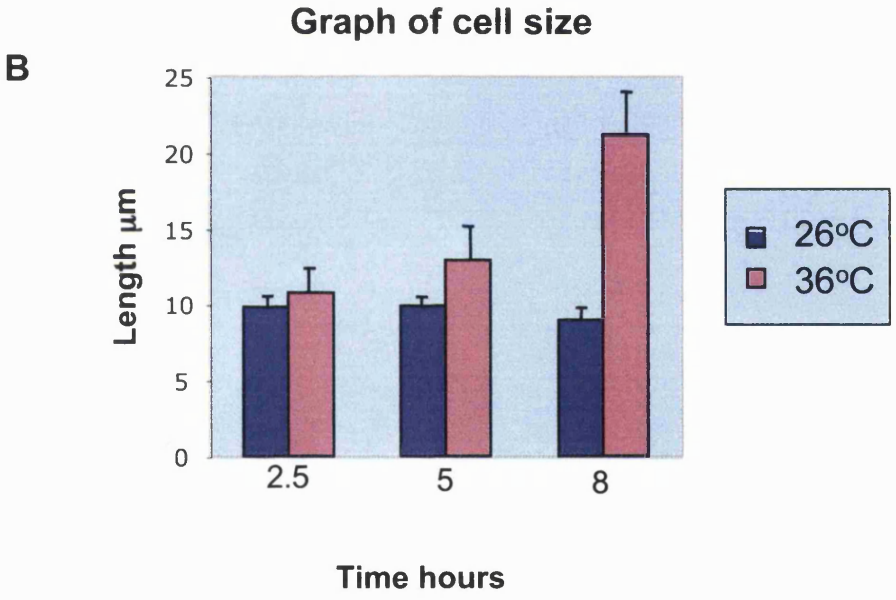

Fig. 4.1.1: Skp1 temperature sensitive strains at 26°C and 36°C
A Cells were grown in rich medium to mid-log phase overnight at 26°C. Cultures were shifted to 36°C for 8 hours. Live cells were examined. **B** *skp1^{ts}A7* cells synchronised in G2 by elutriation were followed through subsequent cell cycles. Samples fixed in formaldehyde were examined by light microscopy and their length at 2.5, 5 and 8 hours after shift up to 36°C was measured. (Strains:AL1-A2, AL1-A3, AL2-A7, AL1-A4, and AL2-A8)

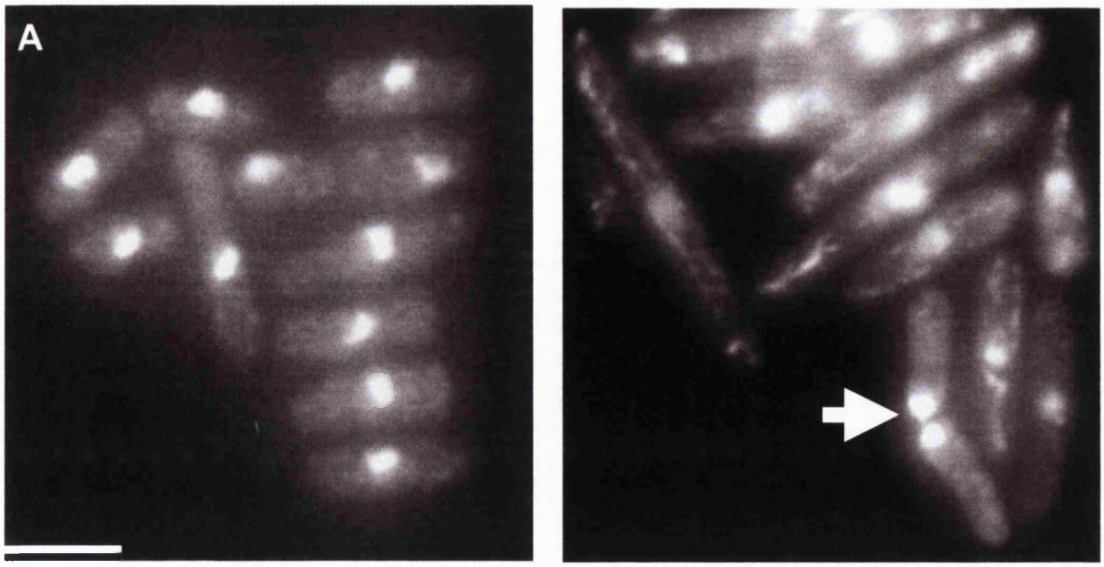

B

skp1 ts	A2	A3	A4	A7
% cut cells	8.75	15.5	5	8

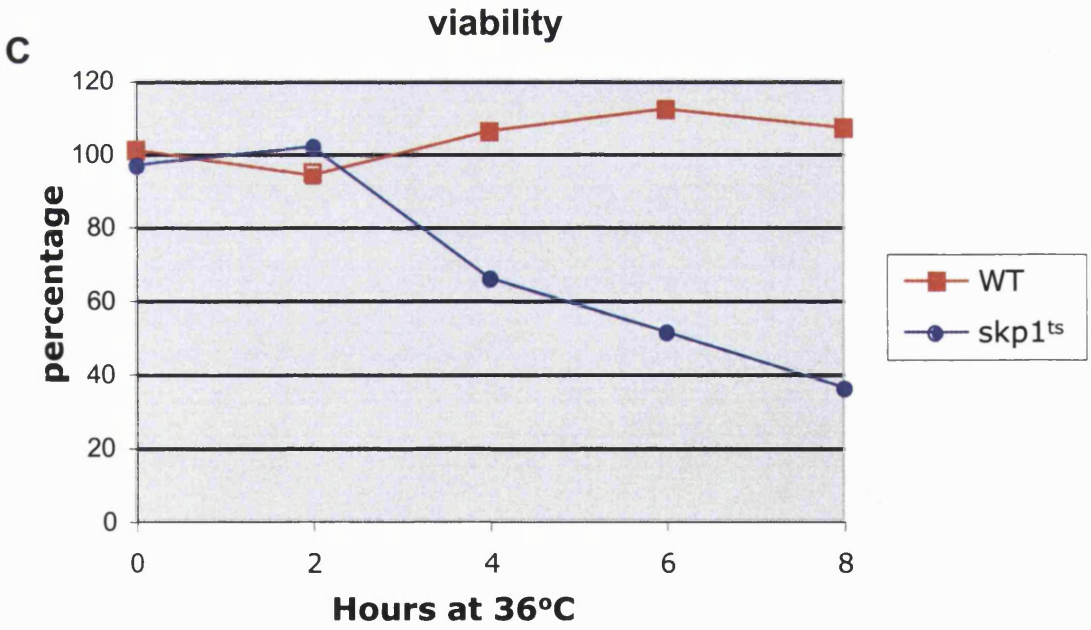

Fig. 4.1.2: Properties of *skp1^{ts}A7* cells
Cells were grown overnight at 26°C and shifted to 36°C for 8 hours. Samples fixed with formaldehyde were stained with DAPI and examined under the microscope. White bar represents 10μm **A** *skp1^{ts}A7* DNA at 0 hrs and at 8hours. **B**. Table of the number of 'cut' cells in different *skp1^{ts}* mutant alleles. **C** *skp1^{ts}A7* cells used to assay the viability of cells after they had been grown at 36°C.

Cross: *h⁻ leu1⁻ ura4⁻ skp1ts-A7* **X** *h⁺ his7⁻ leu1⁻ ade6-M210 skp1-ura4⁺*

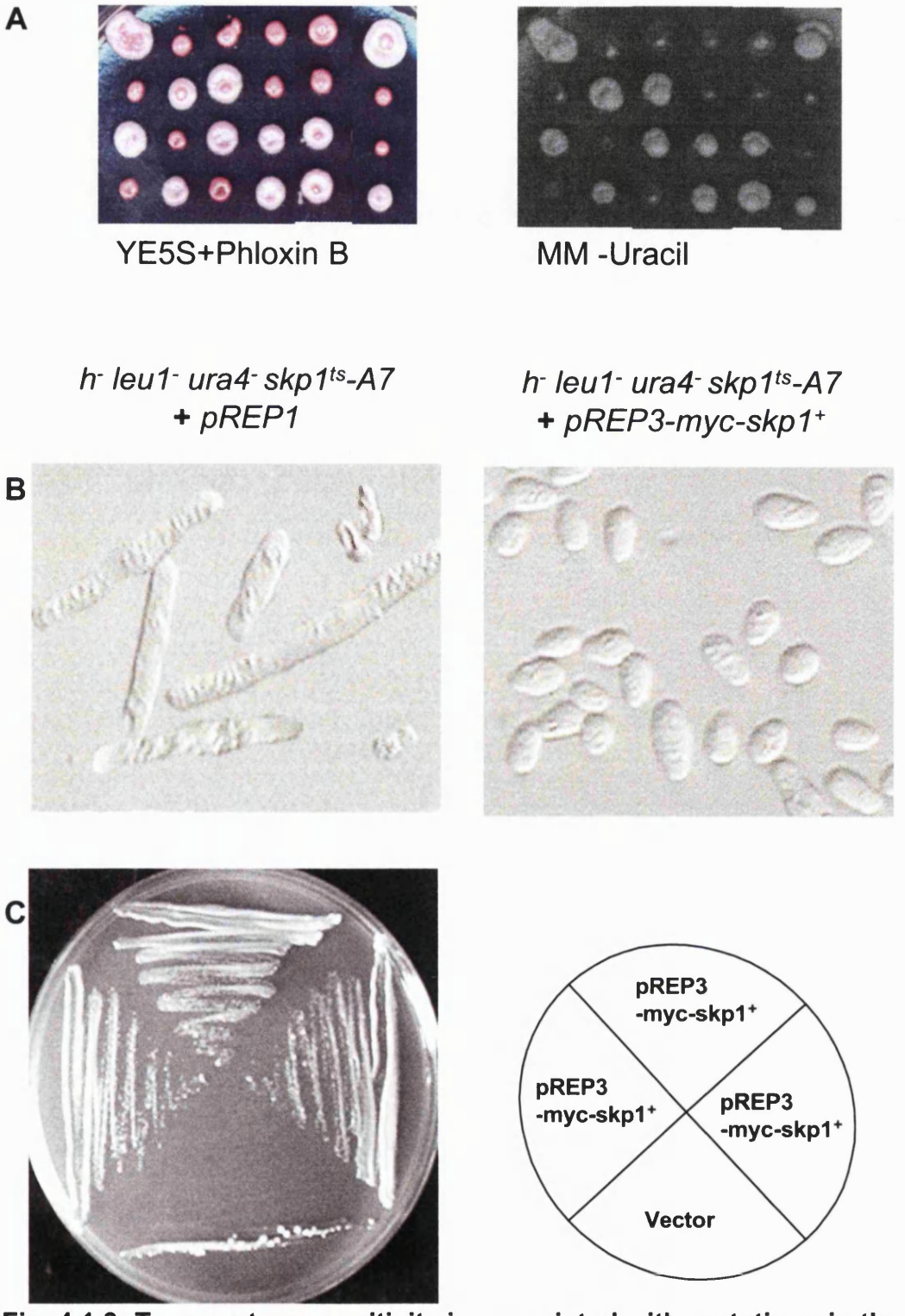

Fig. 4.1.3: Temperature sensitivity is associated with mutations in the *skp1⁺* gene.

A backcross between *skp1tsA7* and a WT strain containing the *skp1⁺* gene marked by the *ura4⁺*gene. Left segregation of the temperature sensitivity: YE5S+ phloxine B medium at 36°C, 3 days; right segregation of the ura4 marker: EMM -uracil medium at 26°C, 3 days. **B** *skp1tsA7* transformed with, vector-left, plasmid containing *skp1⁺*. - right **C** *skp1tsA7* cells transformed with the indicated plasmids were streaked and incubated for 2 days at 36°C.

4.2 Rum1 is not accumulated in *skp1^{ts}A7* mutants

Polyploid cells frequently show elongation and general enlargement due to repeated advancement through S phase without intervening mitoses allowing the cell to continue growing without reducing in size (Moreno and Nurse, 1994). The previously discovered F-box proteins Pop1 and Pop2 show polyploidy and elongation upon mutation/deletion due to the accumulation of Rum1 and Cdc18 (Kominami and Toda, 1997). It was decided to check if the effects of elongation seen in *skp1^{ts}* cells were caused by a defect in the pathway involving degradation of Rum1.

Elongation of *skp1^{ts}A7* cells is not due to polyploidy

In order to ascertain the DNA content of *skp1^{ts}A7* cells and check for polyploidy *skp1^{ts}A7* cells were grown at the restrictive temperature for 12 hours. Samples were stained with Propidium Iodide and processed in a Fluorescence Activated Cell Sorter (FACS). Fig. 4.2.1 A shows the DNA content of the cells after 12 hours remains stable at 2C. *S. pombe*, although a haploid organism spends the longest fraction of each cell cycle in G2 (Nurse *et al.*, 1976). A 2C DNA content therefore represents a normal DNA content for *S. pombe* cells. Although the DNA content of *skp1^{ts}A7* cells remains at 2C the cell size increases. This increases the forward scatter of light by the cells and is reflected in the rightward shift on the (Forward SCatter) FSC-H axis in the FACS dot plots (Fig. 4.2.1 A). These plots represent the DNA content as the absorbance of light by propidium iodide stained DNA, against the cell size represented by the forward scatter of light by the cells.

Deletion of *rum1^{+}* has no effect on the DNA content of *skp1^{ts}A7* cells

To further verify that the accumulation of Rum1 is not affecting *skp1^{ts}A7* cells the ORF of *rum1^{+}* was deleted in *skp1^{ts}A7* cells by mating with a *rum1Δ* strain. *rum1Δ* strains are sterile and therefore the strain carried a plasmid bearing a copy of *rum1^{+}* gene to allow entry into G1 and mating. The strain created was named Rum1Δ (see strain list) and for clarity will be refered to as *skp1^{ts}A7 rum1Δ*. The DNA content of the *skp1^{ts}A7rum1Δ* cells, after incubation at 36°C,

was measured by FACS analysis. Fig. 4.2.1 B shows that there is no change in the DNA content in these cells. If cells do not go through successive rounds of DNA replication, it is still possible that the presence of Rum1 could cause elongation by inhibiting cyclin B-Cdc2 complexes thus preventing cells from entering mitosis. However as shown in Fig. 4.2.1C, the cell size plots from FACS analysis show that cells continue to elongate even when Rum1 is deleted. Thus Rum1 does not cause cell cycle arrest in *skp1^{ts}A7* cells.

Rum1 does not accumulate in *skp1^{ts}A7* cells

To further confirm the independence of the temperature sensitive phenotype from Rum1 its accumulation in *skp1^{ts}A7* cells at the restrictive temperature was assessed. Two cultures of *skp1^{ts}A7 rum1-HA* cells (strain name: AL158), where Rum1 is expressed from the endogenous promoter, were grown at restrictive and permissive temperature. Samples were prepared for western blotting with 12CA5 anti-HA antibodies. Fig. 4.2.2 shows that Rum1 does not accumulate in *skp1^{ts}A7* at the restrictive temperature of 36^{o}C.

From the above experiments it was concluded that despite the SCF$^{pop1/pop2}$ being responsible for Rum1 degradation by the proteasome the *skp1^{ts}A7* mutant is not affected in its ability to degrade Rum1. This is further corroborated by the finding in the previous chapter that Pop1 binding to Skp1 in the *skp1^{ts}A7* mutant is unaffected.

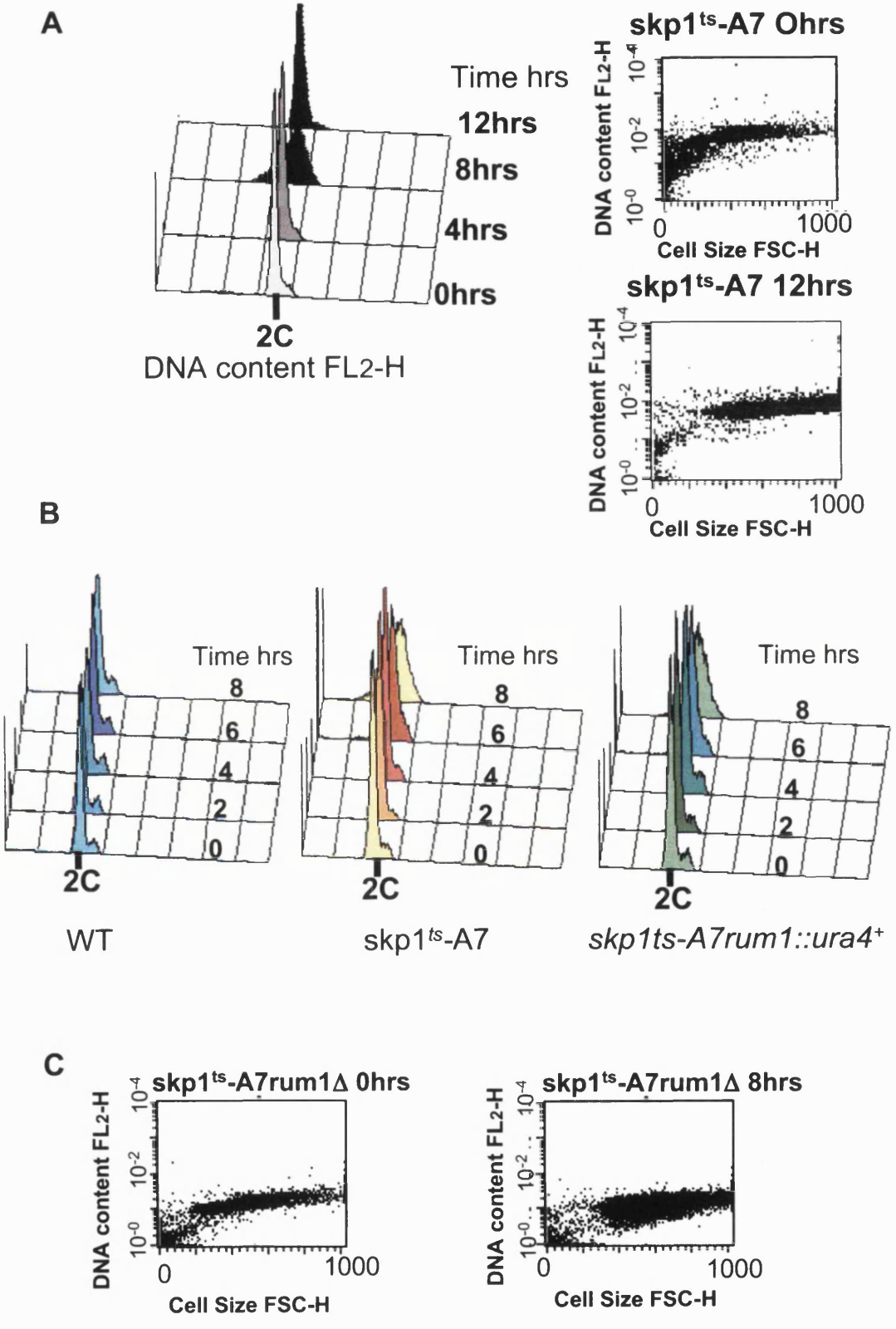

Fig. 4.2.1: *skp1^{ts}A7* cells elongate but have a G2 DNA content
All strains were grown to mid-log phase shifted to 36°C and fixed in ethanol. Cells were treated with propidium iodide and DNA content and cell size were measured. **A** DNA content and cell size of *skp1^{ts}A7* after 12hrs at 36°C. **B** DNA content 0-8hours comparing *skp1^{ts}A7* and *skp1^{ts}A7rum1Δ* (Strain name: Rum1Δ). **C** *skp1^{ts}A7rum1Δ* cell size at 0 and 8 hours.

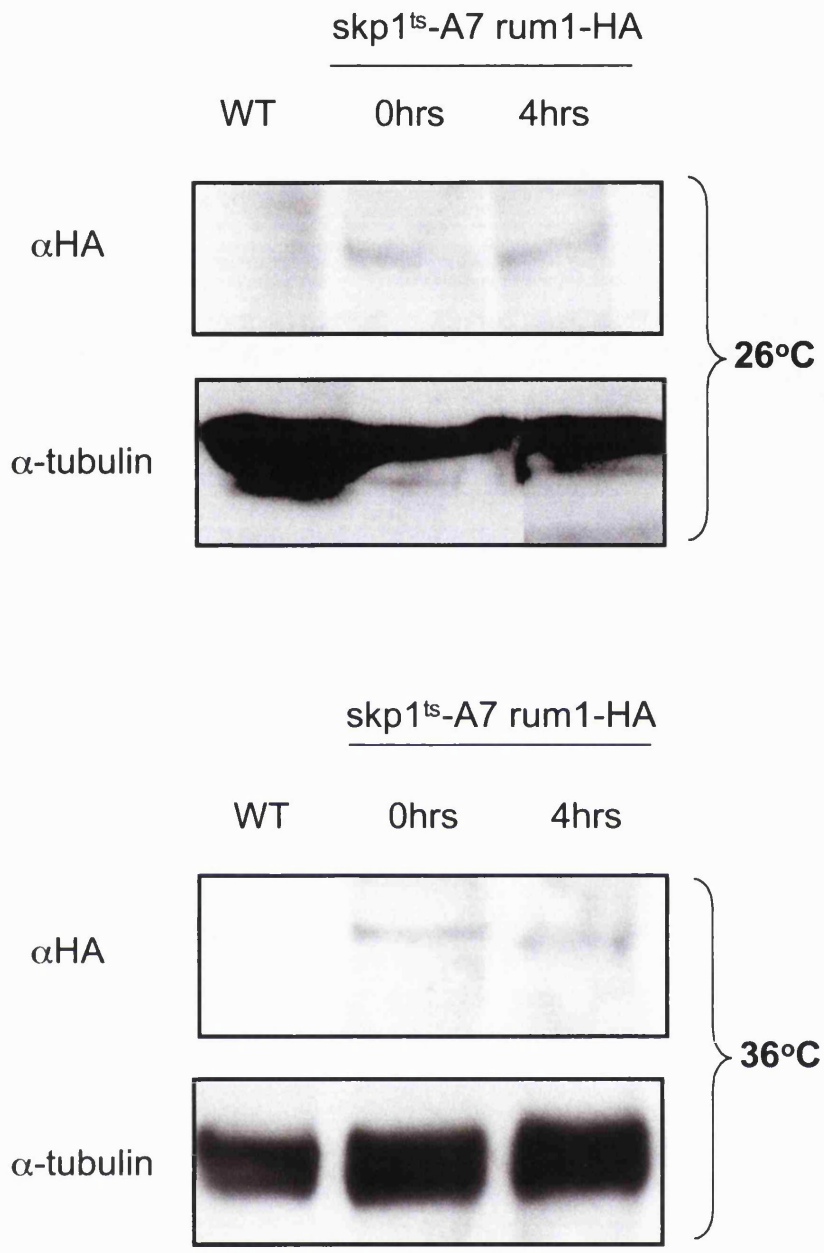

Fig. 4.2.2: Rum1 does not accumulate in *skp1^{ts}A7* cells
skp1^{ts}A7 mutants containing an endogenous copy of *rum1^{+}* tagged with 3HA epitopes (Strain name: AL158) were grown overnight at 26°C. The culture was then split and half grown at 26 and half at 36°C for 4 hours. Samples of protein extract were made, run on a gel and blotted for the presence of Rum1-HA using anti-HA antibodies. The same blot was re-probed with antibodies against α tubulin to ensure equivalent loading of samples.

4.3 The DNA damage checkpoint is activated in *skp1^{ts}A7* mutants

Checkpoints are a mechanism of delaying the cell cycle in response to situations of stress. Several checkpoints have now been identified in yeasts; the intra S phase replication checkpoint and the DNA damage checkpoint, collectively referred to as the DNA structure checkpoint are two such checkpoints, (reviewed by Elledge, 1996; Hartwell and Weinert, 1989). The checkpoint acts in S phase and G2 to delay cells in response to DNA replication problems (intra S phase checkpoint) or in response to extrinsic DNA damage (DNA damage checkpoint) and arrests cells before entry into mitosis (see Introduction and Fig. 1.8.1). As *skp1^{ts}A7* cells have a G2 delay but show no polyploidy it was considered that a checkpoint could be activated. In order to examine this further, cells were synchronised in G1 to examine progression through a complete cell cycle and assess when defects first occur.

Synchronisation of *skp1^{ts}A7* cells

skp1^{ts}A7 cells were synchronised by nitrogen starvation. This arrests cells in the G1 phase of the cell cycle. Cells were arrested in nitrogen free medium overnight (14hours) after which they were re-introduced into rich medium and shifted to 36°C. Cells were processed for septation, viability and FACS analysis. Fig. 4.3.1 A shows that cells have a lag phase after which septation occurs at 4 hours. If septation is taken as an indication of completed mitosis this implies that *skp1^{ts}A7* cells can undergo mitosis at 36°C. Concomitant with this septation viability is seen to drop (Fig. 4.3.1 A, 4 hours). This suggests that at 36°C mitosis and subsequent attempts at re-entry into the cell cycle are lethal for these cells. Fig. 4.3.1 B shows the DNA content of *skp1^{ts}A7* cells following the shift to 36°C as measured by FACS analysis. Comparing wild-type and *skp1^{ts}A7* shows that the progress into S phase at 36°C in *skp1^{ts}A7* cells appears to be delayed (compare 1, 1.5, 2 and 2.5 hours time points). This suggests that at 36°C *skp1^{ts}A7* cells are stalled in entry to S phase, which may eventually impact on their entry into mitosis.

This experiment suggests that although defects of *skp1^{ts}A7* cells become apparent in mitosis they could occur earlier in the cell cycle. FACS analysis from nitrogen starvation suggests that *skp1^{ts}A7* cells undergo S phase later

than wild-type cells and this may be indicative of defects in this part of the cell cycle. It is possible that these defects lead on to the subsequent delay in G2 resulting in elongation of the cells. Potentially cells that do not delay in G2 enter mitosis in inappropriate conditions, i.e. with partially replicated or damaged DNA and hence lose viability.

Deletion of DNA damage checkpoint components leads to the disappearance of the elongation phenotype of *skp1^{ts}A7* cells

The DNA damage checkpoint initiates signalling through the PI3K- like kinase Rad3 (Bentley *et al.*, 1996). Activation of this pathway leads to the eventual activation of the downstream kinase Chk1 (Walworth *et al.*, 1993). The pathway is thought to be bifurcated in that if initiated in S phase by faulty replication, signalling leads to activation of Cds1 as the downstream kinase, rather than activation of Chk1. This is activation of the replication checkpoint rather than the damage checkpoint. The activation of Chk1 results in maintenance of tyrosine15 phosphorylation of Cdc2 and consequently this kinase remains inactive and G2 is maintained (see Fig. 1.8.1 for a summary and refer to Chapter one for a more detailed introduction to the DNA damage checkpoint). In order to ascertain if the G2 delay in *skp1^{ts}A7* cells is related to activation of the DNA structure checkpoint deletions of the checkpoint components *rad3^{+}*, *rad9^{+}*, *rad26^{+}*, *chk1^{+}* and *cds1^{+}* were created in a *skp1^{ts}A7* background. These strains were created by mating deletion strains, where the checkpoint gene was deleted from the chromosomal locus by the *ura4^{+}* gene, with *skp1^{ts}A7* strains which were *ura4^{-}*. (See strain list; sub-heading: checkpoints, in the Materials and Methods section for full genotypes of the chekpoint gene/temperature sensitive mutant strains). Heterozygous diploids were selected and sporulated after which tetrads were dissected. Cells which were temperature sensitive and could grow in the absence of uracil were examined for morphology. It was found that *skp1^{ts}A7* cells were no longer elongated at 36°C in a "checkpoint deletion" background Fig. 4.3.2 A. For *rad9Δ* and *rad26Δ* the effects were the same as *rad3Δ* and *chk1Δ* (data not shown). However in the case of the *cds1^{+}* kinase, the downstream component of the intra S checkpoint, deletion shows no change in the elongation phenotype compared to *skp1^{ts}A7* alone (Fig. 4.3.2 A,

far left panel compared with far right panel). This strongly suggests that the DNA damage checkpoint is responsible rather than the intra S replication checkpoint for the elongation phenotype of *skp1^{ts}A7* cells. In addition to this *skp1^{ts}A7* mutant cells are not sensitive to growth in the presence of sublethal doses of HU (data not shown). Cells defective in the intra S phase checkpoint show high levels of sensitivity to HU (Murakami and Okayama, 1995). This contributes to the conclusion that *skp1^{ts}A7* cells are not defective in the intra S phase checkpoint.

Partial rescue of *skp1^{ts}* phenotype in checkpoint deletion strains

A further interesting observation was made from the *skp1^{ts}A7* strains carrying checkpoint gene deletions, is that there is a partial rescue of temperature sensitivity. Cells from wild-type strains and *skp1^{ts}A7*, *rad3Δ*, *skp1^{ts}A7 rad3Δ*, *skp1^{ts}A7 chk1Δ* and *skp1^{ts}A7 cds1Δ* strains were grown at 26°C to mid-log phase, counted and serially diluted and spotted on plates. The first spot contained 10^5 cells and each spot thereafter containing 10 fold fewer cells. These plates were incubated at 26 and 36°C. Fig. 4.3.2 B shows that *skp1^{ts}A7* strains containing a DNA damage checkpoint gene deletion grow better than the *skp1^{ts}A7* strain at the restrictive temperature. The cells are also a paler pink colour than *skp1^{ts}A7*. *cds1$^+$* deletion appears to further reduce growth on plates

.

Elongation phenotypes are seen upon reintroduction of *rad3$^+$* into *skp1^{ts}A7rad3Δ* cells

To confirm that signalling of the DNA damage checkpoint is responsible for the elongation phenotype seen in *skp1^{ts}A7*, a copy of the *rad3$^+$* gene on a plasmid, under the control of the thiamine-inducible promoter and also under the control of the weaker thiamine-inducible promoter was reintroduced into *skp1^{ts}A7* cells. In *skp1^{ts}A7rad3Δ* cells the wild-type *rad3$^+$* gene caused a return to the G2 delay phenotype as seen in *skp1^{ts}A7* cells at 36°C. This effect was not seen when cells were transformed with an empty vector Fig. 4.3.3 A. This confirms that *rad3$^+$* and the DNA damage checkpoint are responsible for the elongation phenotype of *skp1^{ts}A7* cells.

$chk1^+$ is phosphorylated in $skp1^{ts}A7$ cells after four hours at 36°C

$chk1^+$ is the effector kinase of the DNA damage pathway (Walworth *et al.*, 1993). During activation of this pathway this kinase becomes phosphorylated. This phosphorylation can be visualised by a shift in mobility on an SDS-polyacrylamide gel and consequently can be used as a read out of the activation of the DNA damage pathway (Walworth and Bernards, 1996). This method was therefore used to assess whether the DNA damage checkpoint was activated in $skp1^{ts}A7$ cells. $skp1^{ts}A7$ strains carrying a 13xmyc epitope tagged Chk1(Strain: AL144) were used for this experiment. A wild-type strain carrying the same epitope tag as $skp1^{ts}A7$ cells was also used (Strain: SKP467-13). Strains were treated either with a temperature shift of 4 hours or a UV treatment. UV treated strains were allowed to recover for 30 minutes before preparation for western blotting. All samples were run on a specialised SDS-polyacrylamide gel containing an increased level of acrylamide to bis-acrylamide (see Materials and Methods) which allows the mobility shift to be visualised more clearly. Wild-type strains treated with UV show a band just above the Chk1-myc band that corresponds to the phosphorylation mobility shift of Chk1-myc. $skp1^{ts}A7$ maintained at 36°C for 4 hours also clearly shows a phosphorylation band that is not visible in the same cells maintained at 26°C for 4 hours (Fig. 4.3.4 B). Wild-type cells grown at 36°C do not show this slower migrating band (data not shown). This experiment shows that the Chk1 protein is activated at 36°C in $skp1^{ts}A7$ cells and thus the DNA damage checkpoint is activated.

Other $skp1^{ts}$ alleles created in a *rad3* deletion background show more severe phenotypes when $rad3^+$ is introduced.

As $skp1^{ts}A7$ cells are partially rescued in a *rad3Δ* background we endeavoured to create stronger *skp1* temperature sensitive alleles in a *rad3Δ* background. This was achieved using the same method described in Chapter 3, although the optimal conditions for mutagenesis on this occasion required the use of 10xdGTP rather than five times increase of one purine and one pyrimidine. The mutated $skp1^+$ gene fragment included a kanamycin marker and was introduced into a strain that was already *rad3::ura4*$^+$. Two temperature sensitive mutants

were isolated by this method. These strains were back-crossed to a *rad3*$^{+}$ strain and in both cases, like the original *skp1*^{ts}*A7* mutant, the temperature sensitive phenotype was heightened in the presence of *rad3*$^{+}$. Fig. 4.3.4 C shows the chromosomal defects in the new allele *skp1*^{ts}*94* when grown at 36°C for 4 hours in the presence (Strain: TP619-94-5D) or absence (Strain: TP619-94-2D) of the *rad3*$^{+}$ genetic background. Also shown is the percentage of 'cut' cells counted in a sample of three hundred, in either the *rad3*$^{+}$ or *rad3Δ* background. The percentage of 'cut' cells, a lethal phenotype, is increased almost two-fold in a *rad3*$^{+}$ background. This strongly suggests that the checkpoint involvement of *skp1* is not an allele specific phenotype. Furthermore although the G2 delay phenotype appears to be dependent on *rad3*$^{+}$ in *skp1*^{ts}*A7, skp1*^{ts}*94* does not have an elongation phenotype but is still influenced by the presence or absence of *rad3*$^{+}$. The increased severity of phenotypes seen when *rad3*$^{+}$ is present in *skp1*^{ts} cells suggests that activation of the DNA damage checkpoint is detrimental to the cell. One possibility is that cells unnecessarily activate the checkpoint in the absence of SCF function. Therefore removing the ability to signal the checkpoint somehow improves the ability of these cells to survive with mutations in the *skp1*$^{+}$ gene.

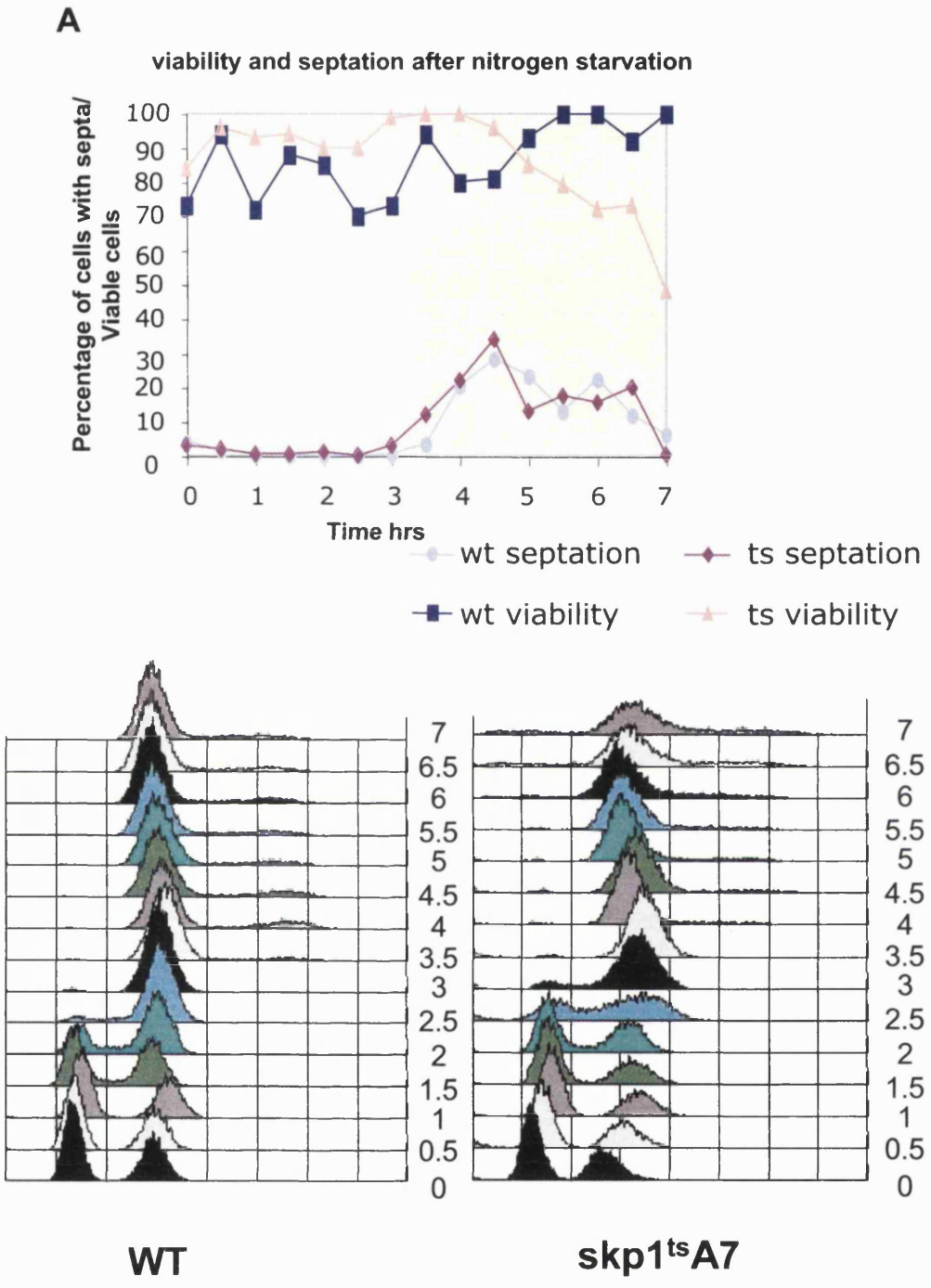

Fig. 4.3.1: Cell cycle progression after nitrogen starvation.
skp1^{ts}A7 cells were synchronised in G1 by nitrogen starvation for 14hrs followed by release at 36°C into nitrogen rich medium.
A Cells were counted and plated for viability assays and fixed in formaldehyde followed by staining with calcofluor for visualisation of the septum. **B** Samples were taken every half hour and fixed in ethanol. Subsequently they were treated with propidium iodide and their DNA content measured by FACS.

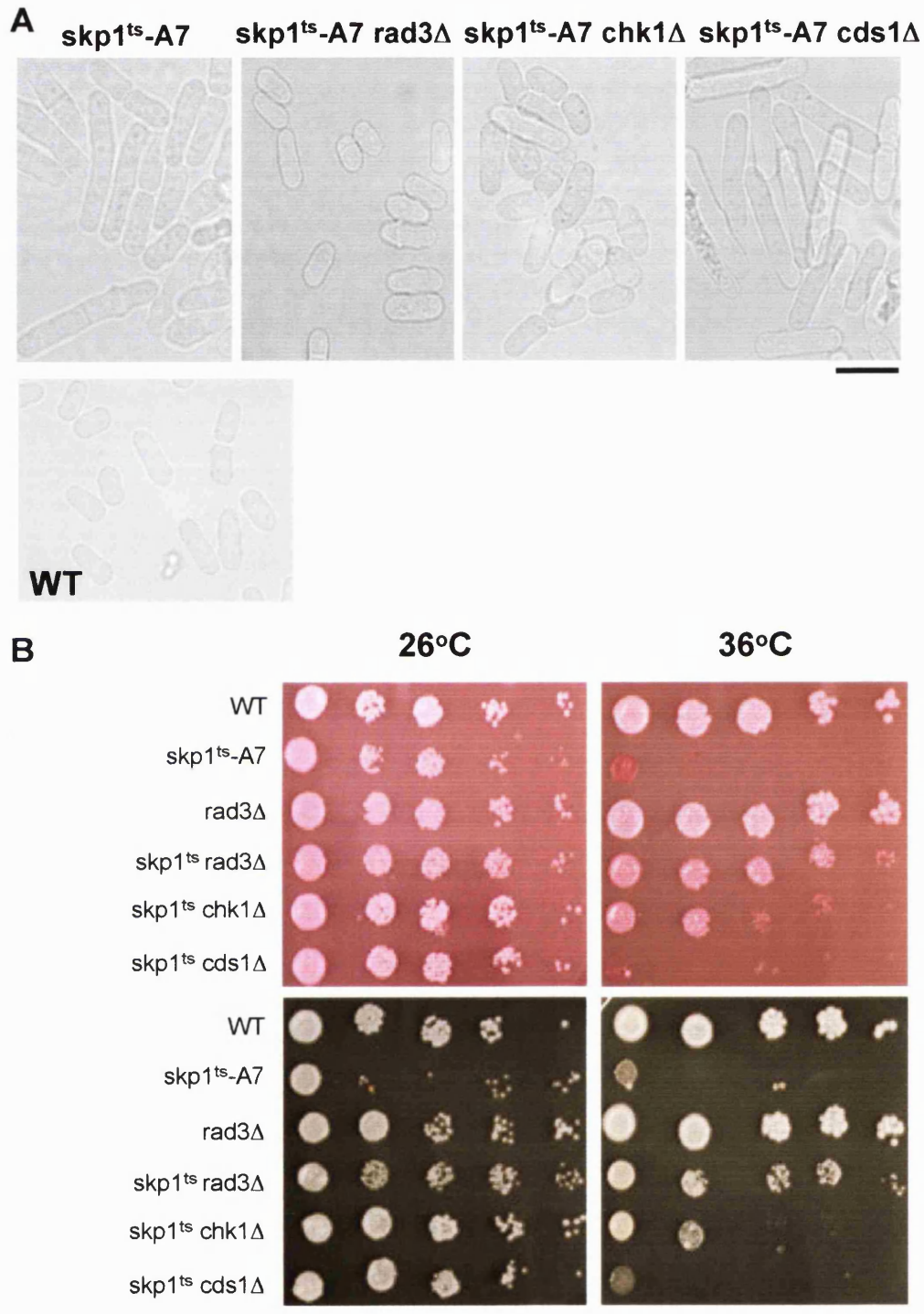

Fig. 4.3.2: Deletion of checkpoint genes in a *skp1^{ts}A7* strain can eliminate the elongation phenotype of these cells at 36°C and causes a partial rescue of temperature sensitivity.

A Cells were grown overnight at 26°C shifted to 36°C for 4 hours and then viewed live in medium under a light microscope. Black bar equals 10 μm. **B** Cells were grown in liquid medium overnight, counted and serially diluted so that the first spot on the plate contained 10^5 cells and the last contained 10 cells. Cells were plated on either rich medium containing phloxine B (upper panel) or rich medium without phloxine B (lower panel). All plates were incubated for 2 days at the stated temperatures. (Strains, in order from top to bottom of plate: 513, AL2-A7, SKS1, AL22, AL59, AL64.)

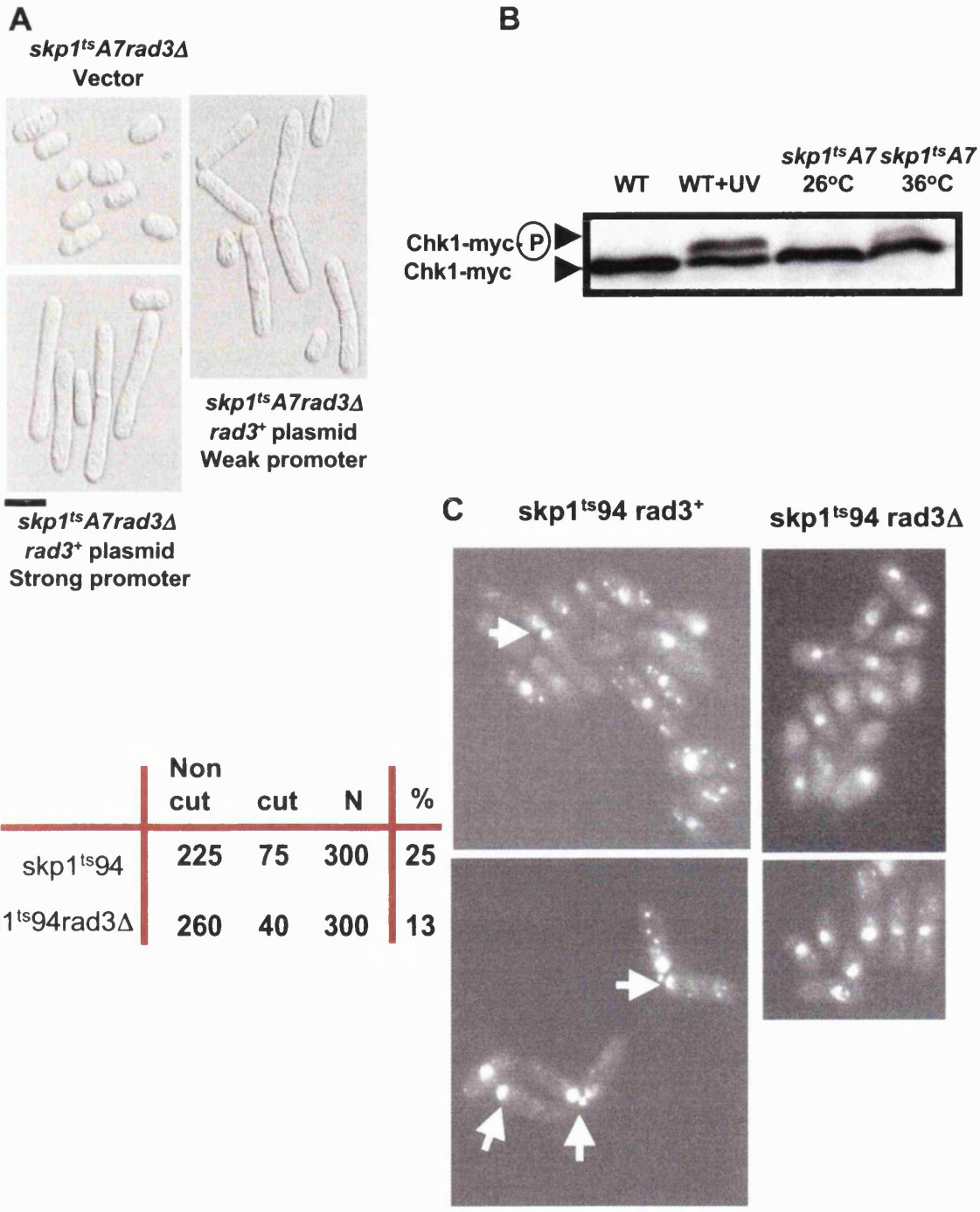

	Non cut	cut	N	%
skp1ts94	225	75	300	25
skp1ts94rad3Δ	260	40	300	13

Fig. 4.3.3: The DNA damage checkpoint is responsible for the elongation phenotype of *skp1tsA7*

A *skp1tsA7rad3::ura4+* (AL22) cells were transformed with a plasmid containing *rad3+* under either a strong or weak promoter. Black bar represents 10 μm. **B** WT (SKP467-13) or *skp1tsA7* cells containing Chk1 tagged with 13myc epitopes at the chromosomal locus (AL144) were grown at 26°C. Cultures were split and half the WT culture treated with UV. Half the *skp1tsA7* culture was grown at 36°C for 4 hours. Extract was prepared for western blotting and run on a 200:1 Acrylamide:Bis gel. **C** *skp1ts94* (TP619-94-5D) (left) and *skp1ts94rad3::ura4+* (TP619-94-2D)(right) cells were grown overnight to mid - log phase at 26°C and then shifted to 36°C and grown for a further 8 hours. Cells were fixed in formaldehyde and stained with DAPI. The presence of 'cut' cells (septated without DNA division) was quantitated.

4.4 The F-box protein/DNA helicase *fdh1*$^{+}$

As detailed in Chapter 2 an F-box protein exists in the genome of *S. pombe* that contains an F-box and all 7 domains of the UvrD/REP ATP dependent DNA helicase. The work of Kim *et al.*, (2002) established that this protein contains a functional DNA helicase activity and Fig. 3.5.4 demonstrates that the F-box allows it to bind to Skp1 in *S. pombe*. Cells deleted for this F-box protein show a G2 delay phenotype and elongation, similar to that described for the *skp1*^{ts}*A7* mutants. It is a possibility therefore that the phenotypes of *skp1*^{ts}*A7* might be dependent on *fdh1*$^{+}$ function. It was decided to compare the *fdh1Δ* and *skp1*^{ts}*A7* strains more closely to see if the phenotypes were related in any way.

The *fdh1Δ* phenotype

fdh1^{+} was deleted from the chromosomal locus in a haploid strain (Strain: Fdh1Δ) by integration of the kanamycin resistance gene as described in detail in Chapter 2. Cell morphology was examined. The cells showed a diverse array of sizes many were wild-type, some were extremely elongated and some were both longer and wider than wild-type. Compared to the *skp1*^{ts}*A7* phenotype there was a less uniform elongation phenotype (Fig. 4.4.1 A). It is possible that these long, fat cells are diploids caused by an occasional failure in M phase. However, Fdh1 is a DNA helicase and is likely to be involved in DNA replication or repair processes. It therefore seems likely that these cells are, like *skp1*^{ts}*A7* cells, are delayed in G2 by a checkpoint.

UV sensitivity of *fdh1Δ* and *skp1*^{ts}*A7*

DNA helicases are implicated in various DNA based activites in the cell including replication, recombination and repair of DNA. Thus it seemed possible that *fdh1Δ* is sensitive to DNA damage and the elongation phenotype may be indicative of cells accumulating damage. As *skp1*^{ts}*A7* cells also have an elongation phenotype and have a checkpoint related defect (see sections above) it was decided to assess the UV sensitivity of these cells.

skp1^{ts}A7 sensitivity to UV was first assessed at 26°C, the permissive temperature for *skp1^{ts}A7* strains. Three hundred cells per plate were exposed to varying levels of UV irradiation and incubated for 4 days at 26°C. Colony forming ability was counted. Fig. 4.4.1 B shows that *skp1^{ts}A7* cells did not show increased sensitivity to UV. It is of interest to note that at 26°C *skp1^{ts}A7 rad3Δ* strains are less sensitive to UV than a single *rad3^{+}* deletion. This suggests that not only can *rad3Δ* suppress some aspects of the phenotype of *skp1^{ts}A7* cells but that *skp1^{ts}A7* can suppress some of the defects that normally occur in a *rad3Δ* cell. A known suppressor of the *MEC1* deletion, the *rad3^{+}* homologue in budding yeast, is *SML1*, an inhibitor of ribonucleotide reductase (Zhao *et al.*, 2000). Since cullin based ligases, centred around the cullin Pcu4, have recently been linked to the degradation of Spd1, an RNR inhibitor in *S. pombe*, in conjunction with the COP9/signalosome and Ddb1 (Liu *et al.*, 2003) suppression of *rad3Δ* by *skp1^{ts}A7* is a highly interesting finding. However, this must be taken in context of the evidence that so far Pcu1 is the only *S. pombe* cullin proposed to bind to Skp1 and that experimental evidence from Liu *et al* (2003) suggests that Skp1 is not present in a complexes containing Pcu4.

A second experiment at 26°C with the *fdh1Δ* strains shows that *fdh1Δ* is also not sensitive to UV and behaves similarly to wild-type (Fig. 4.4.1 C). Deletion of checkpoint components in both *fdh1Δ* and *skp1^{ts}A7* strains increases sensitivity to UV. *fdh1Δ rad3Δ* (Strain: TP612-10D) cells show much increased sensitivity whilst *fdh1Δ chk1Δ* (TP624-10B) cells show intermediate sensitivity. This may be due to the fact that the removal of *rad3^{+}* prevents signalling through both the DNA damage and replication checkpoints whilst deletion of *chk1^{+}* only abrogates the damage checkpoint. Cells are still capable of sensing problems in replication and can arrest in a *cds1^{+}* mediated manner.

UV sensitivity of *skp1^{ts}A7* and *fdh1Δ* strains was examined after incubation at 36°C for 4 hours. This was to allow activation of the *skp1^{ts}A7* phenotype. Under these conditions *skp1^{ts}A7* still shows wild-type levels of sensitivity to UV exposure, as does *fdh1Δ* (Fig. 4.4.1 C). The *fdh1Δ* strain was incubated at this temperature in order to compensate for the possibility of temperature effects.

fdh1Δ cells did not show any change in sensitivity at 36°C. Despite activating the DNA damage checkpoint at 36°C (see above) the *skp1^{ts}A7* mutant did not lose viability compared to wild-type in conditions of UV exposure. Perhaps the activation of the checkpoint prior to UV exposure may even protect these cells. This could occur by initiating repair or replication processes specialised to UV damage limitation before insult. This would be analogous with the spindle assembly checkpoint where overexpression of Mph1, the initiating kinase, makes cells resistant to damage by TBZ.

The conclusion that neither *skp1^{ts}A7* nor *fdh1Δ* is sensitive to UV exposure supports the idea that cells lacking in *skp1^{+}* function may activate the checkpoint unnecessarily. If *skp1^{ts}A7* had undergone prior DNA damage, which resulted in activation of the checkpoint, then further insult through UV might make these cells inviable.

Skp1 and Fdh1 can form an SCF complex in *S. pombe*

Skp1 can form complexes with F-box proteins lacking other SCF components such as Pcu1, Rbx1. These do not have an ubiquitin ligase function. It was tested whether Fdh1 can form part of an SCF complex, by performing immunoprecipitations in a *pcu1^{+}-13myc GFP-fdh1^{+}* strain (Strain: AL179). Antibodies to the myc tag were used to pull down Pcu1 with protein A sepharose beads. Western blotting for GFP was subsequently carried out. From the crystal structure of the human SCF complex (Zheng *et al.*, 2002) it is known that an F-box protein does not directly bind to a cullin. The fact that Pcu1-myc is capable of pulling down Fdh1 thus suggests that Fdh1 can form part of an SCF complex and that Skp1 must be present for this association (Fig. 4.4.2).

The elongation phenotype of *skp1^{ts}A7* and *fdh1Δ* is additive

skp1^{ts}A7 and *fdh1Δ* both show elongation phenotypes. If these elongation phenotypes were initiated from a similar cause then it would be expected that a *skp1^{ts}A7 fdh1Δ* strain would not show additive phenotypes. To test this a double mutant strain containing both the *skp1^{ts}A7* mutation and an *fdh1^{+}* deletion was made (Strain:AL181). Double mutant strains were examined for cell morphology at permissive and restrictive temperatures. Fig. 4.4.3 A shows the phenotype of

each of the single mutants and the double mutant. *skp1^{ts}A7 fdh1Δ* cells appear to be longer than *fdh1Δ* alone at 26°C and after four hours at 36°C. In order to verify this, two hundred cells of each single mutant and the double mutant were measured for length and the mean cell length was assessed. Fig. 4.4.3 B shows that at both 26°C and 36°C *skp1^{ts}A7 fdh1Δ* cells were longer than the single mutants. The standard deviation from the mean is high for *skp1^{ts}A7 fdh1Δ* cells as might be expected for a highly heterogenous population, the distribution of the cell populations is shown in Fig. 4.4.3 C. Although a large population of cells in the double mutant fall into the same size category as *fdh1Δ* and *skp1^{ts}A7* single mutants, the majority of the cells in the double mutant fall into the larger size categories compared to the single mutants. Although the difference in the means is not statistically significant this could be due to the larger amount of size variation seen in *skp1^{ts}A7 fdh1Δ* cells. It is therefore suggested that the elongation phenotype seen in each of the single mutants is from an unrelated cause and that the phenotypes are additive when combined. The fact that the Skp1^{ts}A7 continues to bind to Fdh1 at the restrictive temperature contributes to this conclusion (Fig. 3.5.4).

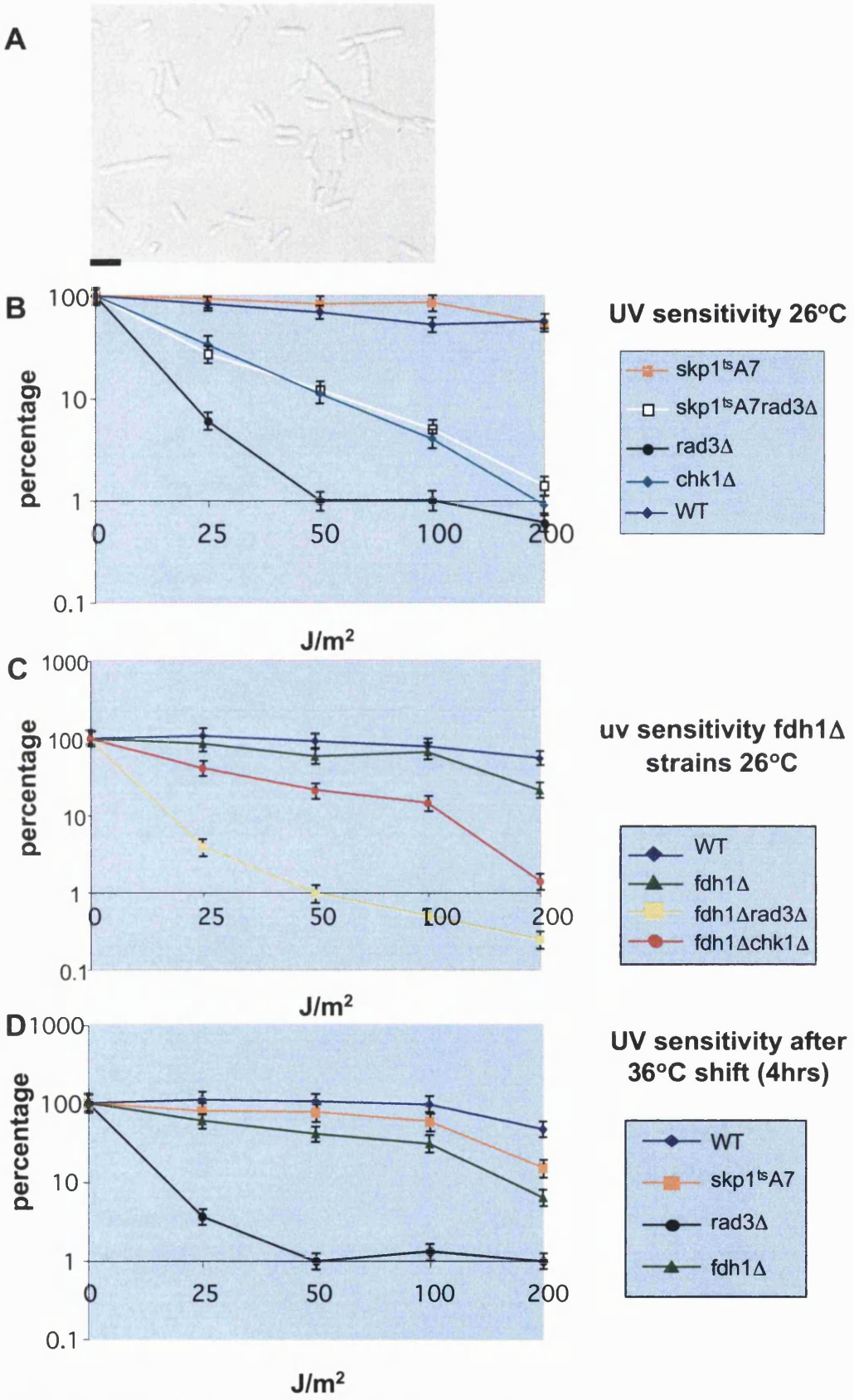

Fig. 4.4.1: *Fdh1Δ* cells have elongation phenotypes.
A *fdh1Δ* cells were grown to mid-log phase at 30°C and viewed under a light microscope. Black bar is equal to 10 μm. **B**,**C**, **D** Cells were counted and plated at 300 cells per plate. The plated cells were then subjected to UV irradiation of varying intensities. Colonies growing on the plates after 4 days were counted. Error bars are standard error on the mean from two independent experiments. **B** *skp1ts* strains at 26°C, **C** *fdh1Δ* strains at 26°C, **D** After shift up to 36°C for 4 hours before plating. (Strains: AL2-A7, AL22, SKS1, Chk1Δ, Fdh1Δ, TP612-10D, TP624-10B, WT-513)

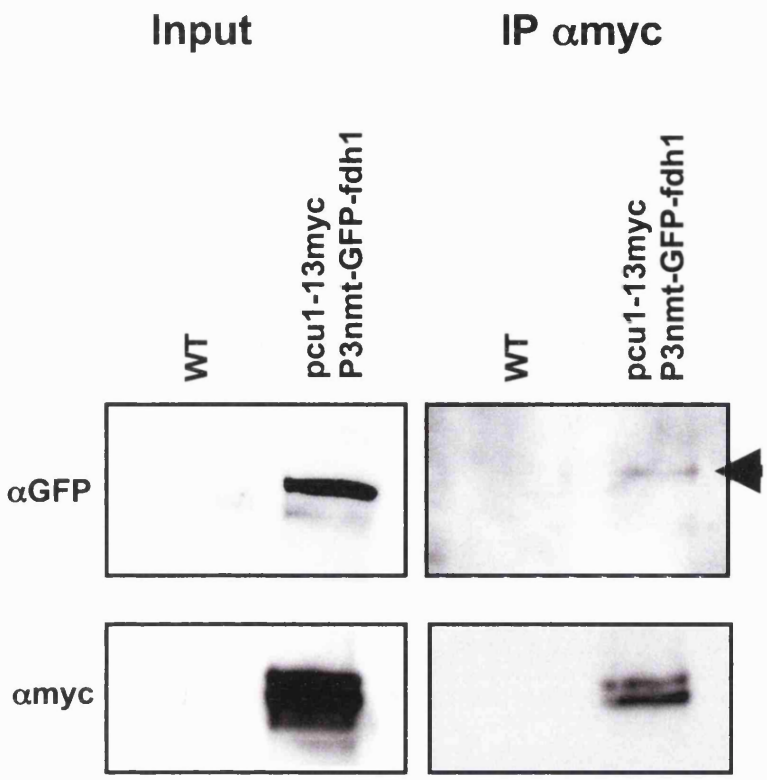

Fig. 4.4.2: Fdh1 can form an SCF complex.
Protein extract was made from wild-type and *pcu1⁺-myc GFP-fdh1⁺* (AL179) and 30μg run on a western blot, left panels. 2mg of the same extract was used for immunoprecipitation with anti-myc antibodies and then immunoblotted for the presence of GFP-fdh1, right panels.

A

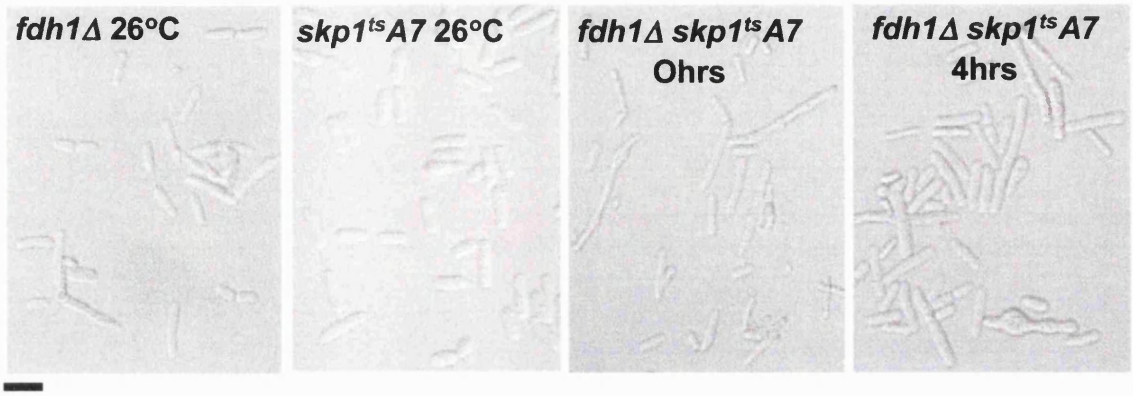
fdh1Δ 26°C
skp1tsA7 26°C
fdh1Δ skp1tsA7 Ohrs
fdh1Δ skp1tsA7 4hrs

B

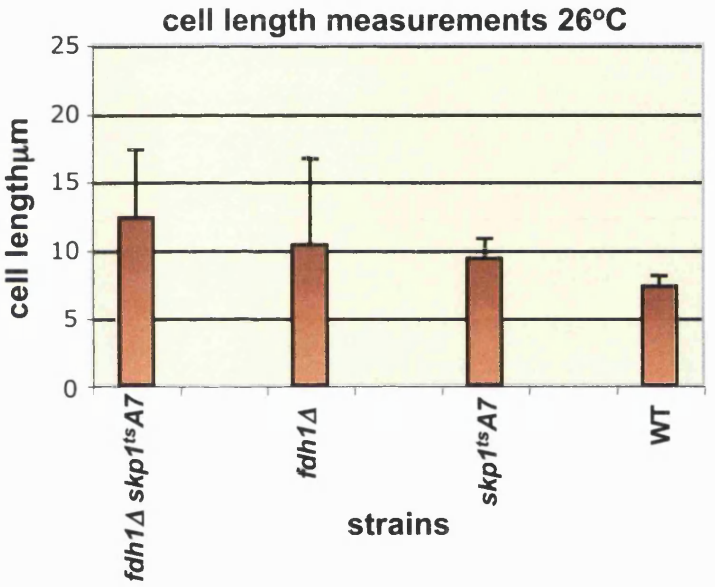
cell length measurements 26°C
cell lengthμm
25
20
15
10
5
0
fdh1Δ skp1tsA7
fdh1Δ
skp1tsA7
WT
strains

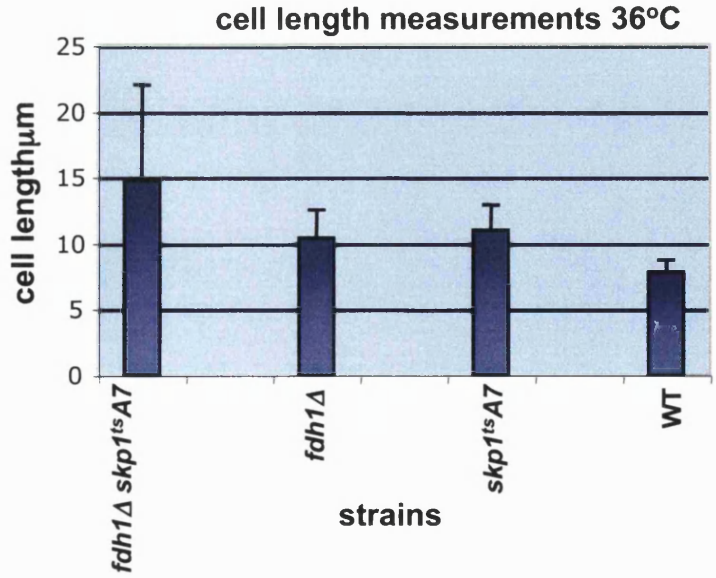
cell length measurements 36°C
cell lengthμm
25
20
15
10
5
0
fdh1Δ skp1tsA7
fdh1Δ
skp1tsA7
WT
strains

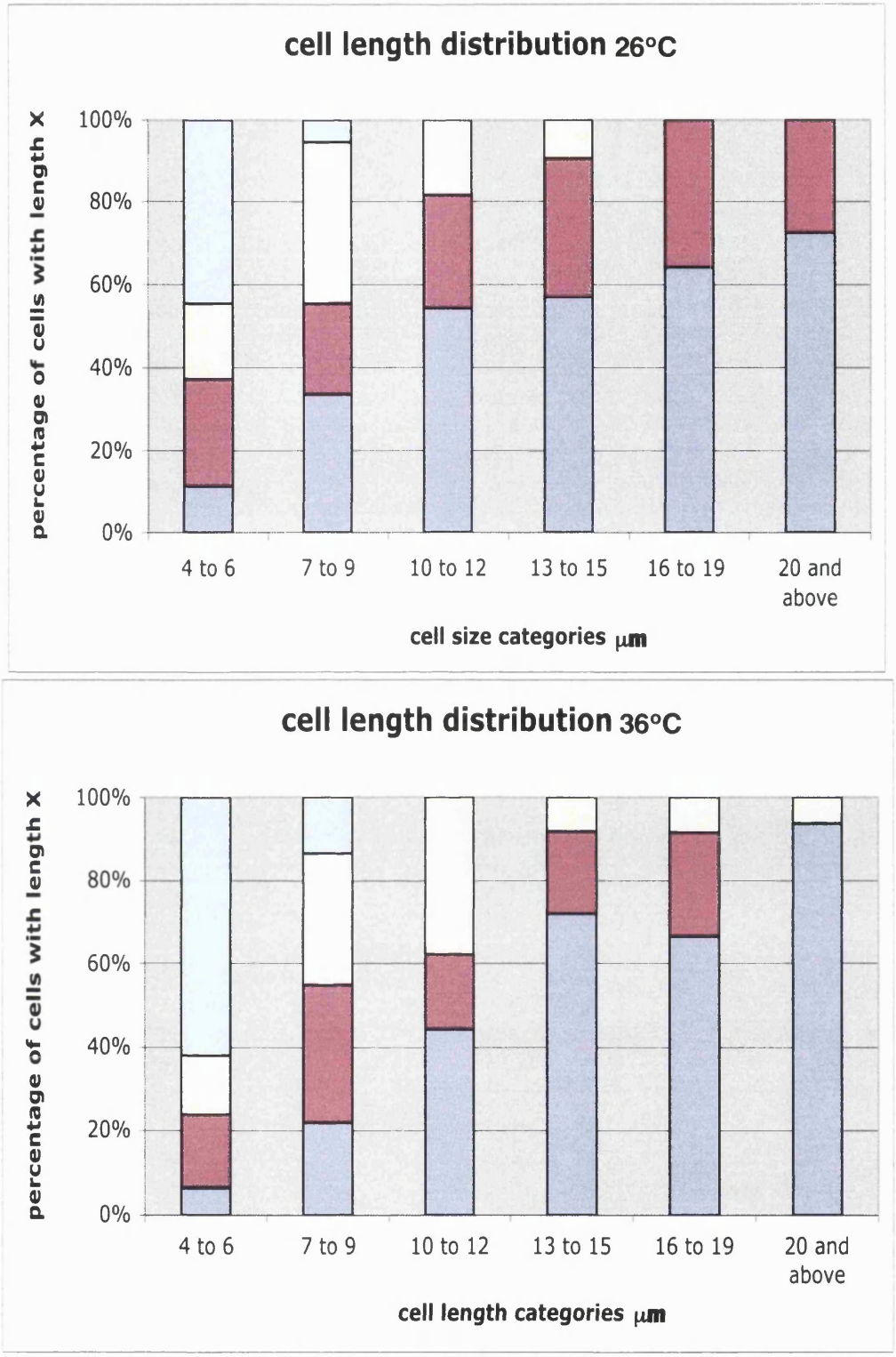

Fig. 4.4.3: *fdh1Δ* and *skp1^{ts}A7* have additive phenotypes
A Cells were grown at 26°C overnight and shifted to 36°C for 4 hours. Samples were fixed with formaldehyde and viewed under a light microscope. Black bar represents 10μm. **B** Cell length from samples taken after growth at 26°C and 36°C to activate the temperature sensitive phenotype of *skp1^{ts}* mutants. Mean measurements of 200 cells are presented. Error bars represent standard deviation from the mean. **C** The percentage of cells falling into each size category was plotted. The majority of the largest cells are formed by the double mutant *fdh1Δ skp1^{ts}A7*. (Strains: AL181, Fdh1Δ, AL2-A7, 513)

4.5 Summary

This chapter has further examined the physiological implications of mutation to *skp1*$^{+}$. The *skp1*^{ts}*A7* strain shows reduced viability at 36°C and has a prominent elongation phenotype. This was shown not to be related to previous elongation phenotypes seen in *pop1* and *pop2* mutants as *skp1*^{ts}*A7* cells were not polyploid after incubation at the restrictive temperature. Also unlike *pop1* and *pop2* mutants *skp1*^{ts}*A7* cells did not accumulate Rum1, the CKI target of the SCF$^{pop1/pop2}$. This suggests that SCF$^{pop1/pop2}$ function is intact in *skp1*^{ts}*A7*. Further investigation of the *skp1*^{ts}*A7* elongation phenotype demonstrated that it was dependent on the presence of the *rad3*$^{+}$, *rad9*$^{+}$, *rad26*$^{+}$ and *chk1*$^{+}$ DNA damage checkpoint genes. Surprisingly, removal of the ability to signal the DNA damage checkpoint partially alleviates the temperature sensitive phenotype. This leads to the suggestion that *skp1*^{ts}*A7* cells at the restrictive temperature activate the checkpoint unnecessarily. *skp1*^{ts}*A7* strains were not sensitive to UV induced DNA damage and could form SCF complexes with the F-box protein Fdh1 a UvrD/REP family, ATP dependent, DNA helicase. It was thought this helicase could be involved in DNA damage repair or replicative processes. If interaction between Skp1 and Fdh1 was abolished or affected in *skp1*^{ts}*A7* mutants this could lead to activation of the DNA damage checkpoint. However, the additive phenotypes seen upon deletion of *fdh1*$^{+}$ and in the *skp1*^{ts}*A7* strain, indicate that the elongation phenotype of the *skp1*^{ts}*A7* mutant is probably not due to a failure of the SCF^{fdh1} function.

4.6 Discussion

Activation of checkpoints without damage, an analogy with the spindle checkpoint.

The partial rescue of *skp1*^{ts}*A7* strains by deletion of the DNA damage checkpoint suggests *skp1*^{ts}*A7* cells activate the checkpoint unnecessarily. This would explain some of the phenotypes seen. This is similar to a particular situation involving the spindle assembly checkpoint. Activating the spindle assembly checkpoint, activates *mph1*$^{+}$ kinase which results in mitotic arrest by inhibition of the APC/C. If *mph1*$^{+}$ is activated by overproduction, the APC/C is

inhibited regardless of any damage to the spindle (Hardwick *et al.*, 1996; He *et al.*, 1998; Kim *et al.*, 1998). This leads to extra resistance to spindle damaging agents.

A similar situation could be envisaged for *skp1^{ts}A7* cells where a substrate of the SCF is involved in signalling the DNA damage checkpoint. Inactivation of the SCF by the *skp1^{ts}A7* allele leads to accumulation of this substrate and promotes checkpoint activation. This would therefore act in an analogous manner to overexpression of *mph1^{+}*, activating the DNA damage checkpoint without DNA damage. In turn this would lead to phosphorylation of Chk1 kinase and downstream inactivation of cyclinB-Cdc2 complexes, with the final result that cells elongate. According to this model deletion of the DNA damage checkpoint should lead to a removal of the elongation phenotype. This was observed when the *rad3^{+}* gene was deleted in *skp1^{ts}A7* cells. This suggests that Skp1 or the SCF may be involved in regulating the function of the DNA damage checkpoint (Fig. 4.6.1).

The state of the DNA damage checkpoint in *pof3Δ* cells

In the previous chapter it was noted that binding to the F-box protein Pof3 was reduced to half normal levels in *skp1^{ts}A7* strains. Deletion of *pof3^{+}* creates a G2 delay in cells. Previous investigation showed that the delay is dependent on the DNA damage checkpoint similar to *skp1^{ts}A7* cells. Pof3 is involved in the maintenance of genome integrity as strains deleted for *pof3^{+}* show lagging chromosomes, heterochromatic de-scilencing and reduced fidelity of minichromosomal maintenance. As these two mutants share this similarity and Pof3 binding is reduced in *skp1^{ts}A7* this suggests that perhaps the phenotype of *skp1^{ts}A7* cells is mediated through abrogation of an SCF^{pof3}. In direct contrast to *skp1^{ts}A7* strains, which are partially rescued by DNA damage checkpoint deletions, *pof3Δ* strains are synthetically lethal with any deletion of a DNA damage checkpoint component (Katayama *et al.*, 2002). It is therefore difficult to reconcile the idea that *skp1^{ts}A7* may act through an SCF^{pof3} mediated pathway despite the similarities of the two mutants.

Pof3 function in the DNA damage checkpoint and the implications of loss of binding in *skp1^{ts}A7* cells

pof3Δ cells like *skp1^{ts}A7* cells activate the DNA damage checkpoint. How these cells activate the DNA damage checkpoint is unknown but one proposal is that it is due to accumulation of a substrate which can damage DNA. In *skp1^{ts}A7* cells the same substrate may accumulate to lesser levels (as Pof3 binding is only 50% reduced). A threshold effect could occur. Mild accumulation of the SCF^{pof3} substrate damages DNA sufficiently to induce the DNA damage checkpoint. The remaining 50% of SCF^{pof3} is sufficient to degrade a proportion of substrate preventing serious DNA damage occurring. In this case activation of the checkpoint should not be detrimental to the *skp1^{ts}A7* cell. It is therefore difficult to explain the partial rescue seen in *skp1^{ts}A7rad3Δ* cells. In a *pof3Δ* strain the cell is reliant on activation of the checkpoint to allow it to survive to the next cell cycle. If the phenotype of *skp1^{ts}A7* cells is mediated through abrogation of SCF^{pof3} function, *rad3* deletion would not partially rescue cells as seen in Fig. 4.3.2.

An alternative to SCF^{Pof3} involvement in DNA damage checkpoint activation is action of Pof3 in a non-SCF capacity. Inability to bind Pof3 in *skp1^{ts}A7* cells could free Pof3 for its checkpoint role. This could not explain how the checkpoint becomes activated in a *pof3Δ* strain but could explain the phenotype of *skp1^{ts}A7* cells. Pof3 activates the checkpoint alone and reduced Pof3 binding to the core SCF in a *skp1^{ts}A7* cell leads to an increased role in signalling the checkpoint unnecessarily. Deletion of *rad3^{+}* alleviates this by preventing signalling of the checkpoint resulting in the partial rescue phenotype observed in *skp1^{ts}A7 rad3Δ* cells. Any residual temperature sensitivity could be attributed either to lack of function of an SCF^{pof3} or another SCF complex, for example SCF^{pof1} (the Pof1 F-box also shows reduced binding to *skp1^{ts}A7* see Chapter 3). It would be interesting to assess whether proteins accumulate in *skp1^{ts}A7* cells and if so which ones. Protein accumulation in a *pof3Δ* cell has not been observed so far thus preventing a conclusive identification of a substrate. Elucidation of which proteins, if any, accumulate in *pof3Δ* and *skp1^{ts}* cells is crucial to future work in this area.

Fdh1, Pof3 and Skp1, three proteins with potential checkpoint functions.
Another possibility for SCF involvement in the DNA damage checkpoint is the DNA helicase, F-box protein, Fdh1. Abrogation of function of a DNA helicase is likely to cause DNA damage, unless the protein function is redundant. As deletion of *fdh1*$^{+}$ results in a G2 delay in some cells, this suggests that Fdh1 evokes the DNA damage checkpoint response. However deletion of checkpoint components in an *fdh1Δ* background is not lethal to the cell and like *skp1*^{ts}*A7* appears to result in partial rescue of the elongation phenotype. It was therefore interesting to assess if the phenotype of *skp1*^{ts}*A7* was related to loss of function of SCF^{fdh1}. However Skp1^{ts}A7 can still bind to Fdh1 at the restrictive temperature and additive phenotypes are seen when *skp1*^{ts}*A7* and *fdh1Δ* are combined, suggesting SCF^{fdh1} is not compromised. Although binding between Skp1^{ts}A7 and Fdh1 are not compromised in the *skp1*^{ts}*A7* cells it is still possible that some function of SCF^{fdh1} is compromised in *skp1*^{ts}*A7* mutants.
It would be interesting to assess whether a triple mutant of *skp1*^{ts}*A7*, *pof3Δ* and *fdh1Δ* is viable in order to see if all three phenotypes are additive. It is possible that Pof3 and Fdh1 function is related and that one compensates for the absence of the other. A combination of *pof3Δ* and *fdh1Δ* together was found to be inviable by examination of crosses of *pof3Δ* with a *rad3Δ fdh1Δ* strain Fig. 4.6.2. *pof3Δ rad3Δ* cells die with different phenotypes to *pof3Δ fdh1Δ*. *pof3Δ rad3Δ* cells are 'cut' and form very small colonies whilst *pof3Δ fdh1Δ* still form elongated cells. The triple deletion appears to die in a manner similar to *pof3Δrad3Δ* suggesting that *pof3Δ* affects the cell most severely. The lethality of *pof3Δ* and *fdh1Δ* combined produces the possibility of hetero and homodimeric F-box complexes, which have previously been suggested for the SCF$^{pop1/pop2}$ (Kominami *et al.*, 1998; Seibert *et al.*, 2002). If degradation of substrates required either homodimer complexes of Pof3 or Fdh1 or a heterodimer complex one could postulate that when binding of Pof3 to Skp1^{ts}A7 is reduced, Fdh1 compensates. Deletion of *fdh1*$^{+}$ in this situation would worsen the *skp1*^{ts}*A7* phenotype leaving it dependent on residual Pof3 binding.

One further issue regarding Fdh1 function is whether it has ubiquitin ligase activity and if so is this ligase function separated from DNA helicase activity or whether the two are required together. A domain analysis of this protein could resolve this.

The activation of the DNA damage checkpoint in *skp1^{ts}A7* and *pof3Δ*, the similarities of the *fdh1Δ* phenotype to the *skp1^{ts}A7* phenotype and the possession of intrinsic DNA helicase activity in Fdh1 suggest these three proteins are involved in the DNA damage checkpoint. The capacity in which these proteins function and whether they have a novel function in initiating checkpoint activity, is unclear. Recent work by Zou and Elledge (Zou and Elledge, 2003) seems to indicate a requirement for ssDNA as the crucial signal for DNA damage checkpoint signalling. The proposal that *skp1^{ts}A7*, *pof3Δ* or *fdh1Δ* could be involved in checkpoint activation would therefore need to encompass the idea that ssDNA intermediates were generated in these mutants.

Residual *skp1^{ts}A7* temperature sensitivity

This chapter has investigated the elongation phenotype of the *skp1^{ts}A7* strain and its interaction with the DNA damage checkpoint pathway. There are further phenotypes of *skp1^{ts}A7* which are observed when these elongated cells finally enter mitosis. These phenotypes explain why *skp1^{ts}A7* cells remain partially temperature sensitive in the absence of the DNA damage checkpoint. These mitotic phenotypes are investigated more thoroughly in the next chapter.

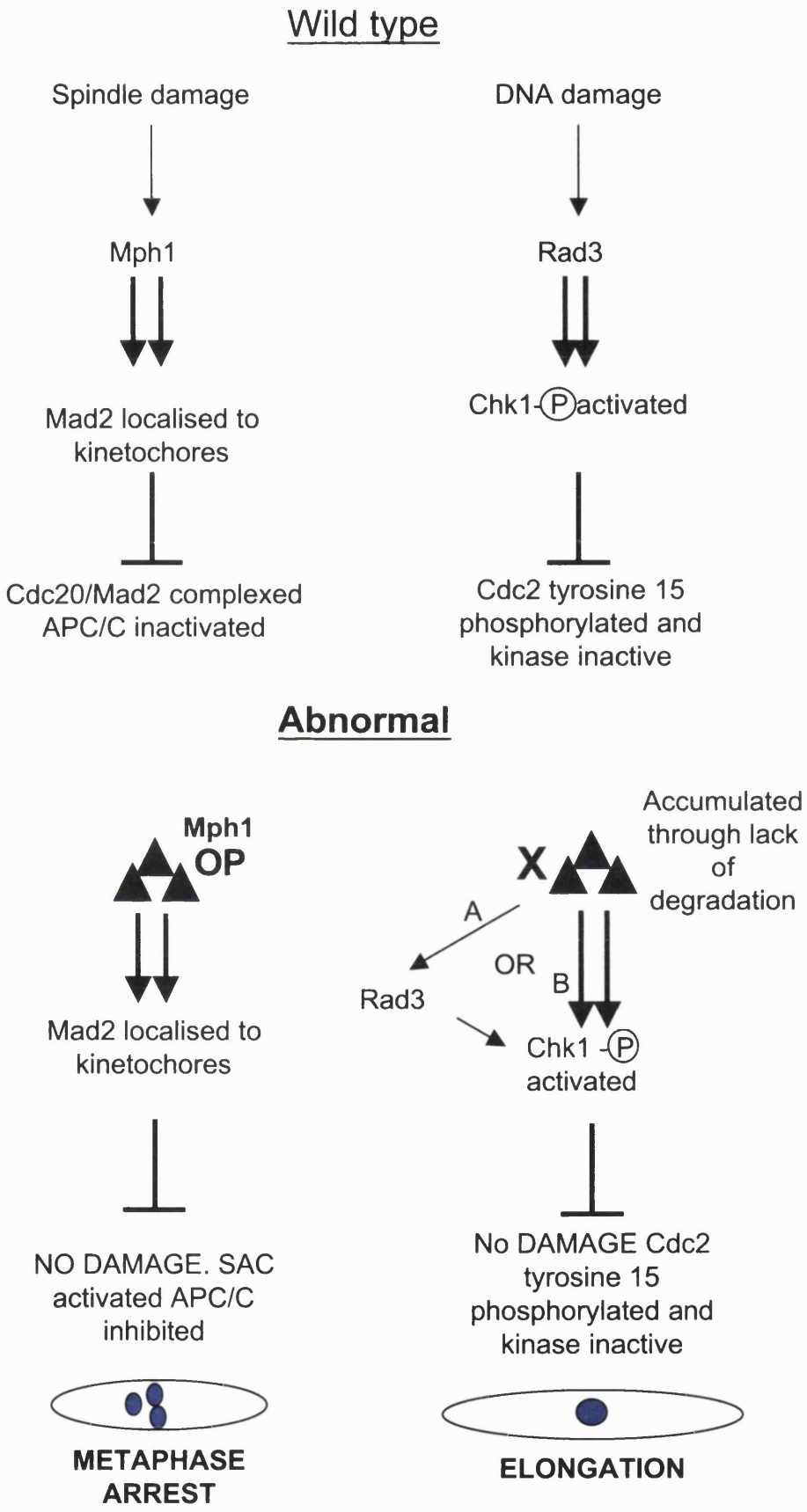

Fig. 4.6.1: A scheme showing how accumulation of a substrate of the SCF could lead to checkpoint activation
By analogy with the spindle assembly checkpoint and overproduction of Mph1 it is possible to envisage how accumulation of a substrate could activate the DNA damage checkpoint.

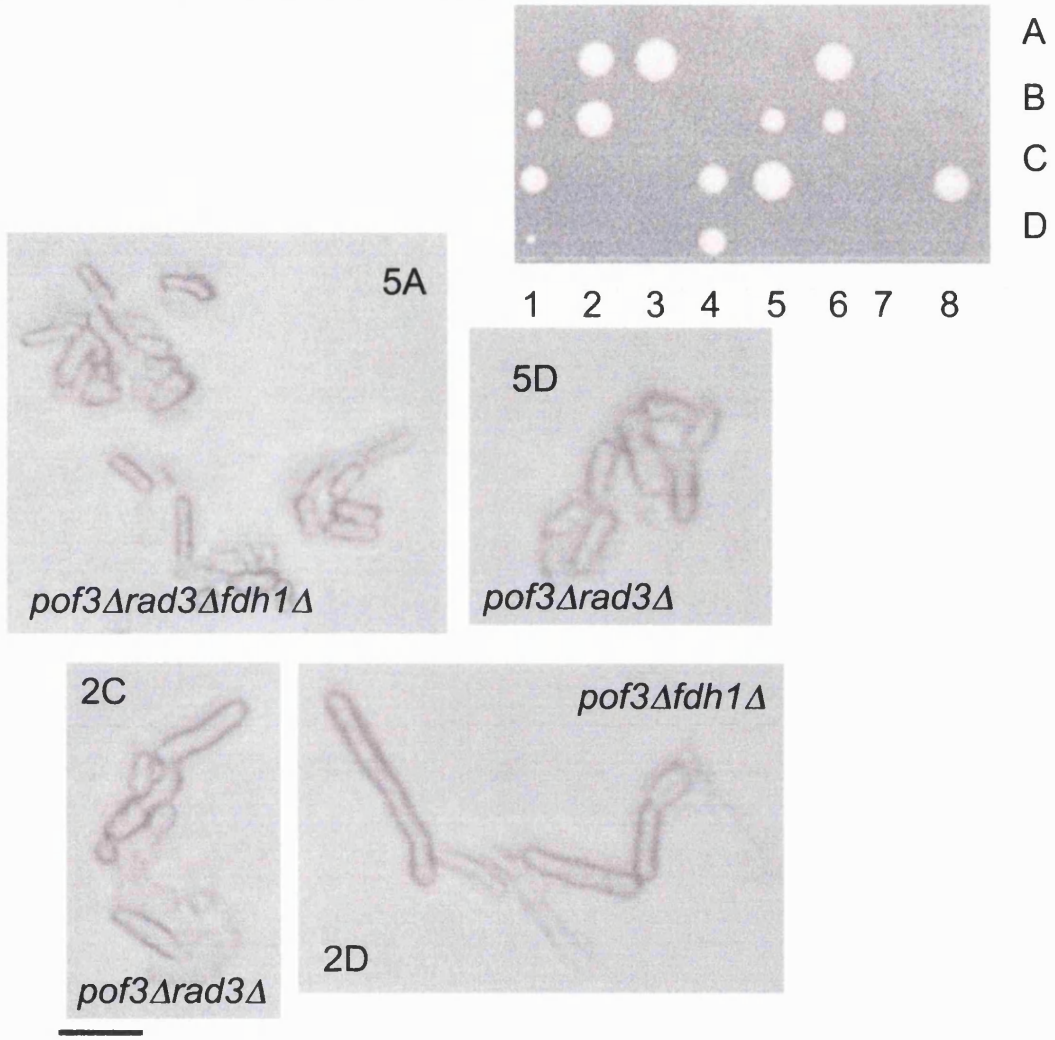

Fig. 4.6.2: A genetic cross between *pof3Δ* and *fdh1Δrad3Δ* shows *pof3Δfdh1Δ* is lethal.

A genetic cross between *pof3Δ* and *fdh1Δrad3Δ*. Where two viabile colonies were present these were tested for kanamycin sensitivity and growth on uracil minus medium. Tetrad 5 contained two *ura4*$^-$ colonies indicating that neither contained deletions for *pof3*$^+$ or *rad3*$^+$. The smaller viable colony was kanamycin^r and contained long cells, indicating it was deleted for *fdh1*$^+$. The other viable colony was kanamycin^s and therefore *fdh1*$^+$. Assuming Mendelian segregation we concluded that one of the inviable microcolonies is *pof3Δrad3Δ* (which is known to be lethal from the work of Katayama et al (2002)) the remaining colony must therefore contain all 3 deletions and this appears to be inviable. Tetrad number 2 also contained two viable colonies one was kanamycin^r, therefore must contain an fdh1 deletion but was also *ura4+*. Cells were short suggesting this was *fdh1Δrad3Δ* (as *rad3Δ* suppresses cell elongation in *fdh1Δ* (data not shown)). The other viable colony was *ura4*$^-$ and kanamycin^s suggesting that none of the genes deletions was present. From this it was concluded that one of the inviable colonies contained *pof3Δrad3Δ* (known to die with a cut cell phenotype, Katayama et al (2002)). the other inviable microcolony, which showed long cells was *pof3Δfdh1Δ*. The combination of two elongated cell phenotypes was assumed to be most likely to produce an elongated terminal phenotype, different to the 'cut' terminal phenotype seen in *pof3Δrad3Δ* combinations .

Chapter 5

The defective spindle phenotype of *skp1^{ts}A7* mutants implicates the SCF in mitotic activities.

Introduction

The *skp1^{ts}A7* mutation activates the DNA damage checkpoint and the cells delay in G2. However these cells do eventually enter mitosis and this chapter addresses the mitotic defects seen in the *skp1^{ts}A7* mutants. Elongated *skp1^{ts}A7* cells were seen to contain aberrant mitotic spindles and large astral microtubules. It seems likely this phenotype is related to the decreased viability of *skp1^{ts}A7* cells at 36°C.

The anillin homologue Mid2 was recently established as a substrate of the SCF (Tasto *et al.*, 2003). Mid2 is involved in cytokinesis and this chapter also considers whether this protein is accumulated in *skp1^{ts}A7* cells and whether it is related to the mitotic phenotypes seen in these cells.

5.1 *skp1* temperature sensitive cells show mitotic phenotypes

As mentioned in Chapter 4 *skp1*^{ts}*A7* cells have abnormal chromosomal structures and accumulate defective and 'cut' cells at 36°C after 8 hours. Attempts to segregate these abnormal chromosomes are likely to result in irreversible loss of viability. To understand the *skp1*^{ts}*A7* phenotype more thoroughly the abnormal DNA structures were examined in more detail. The microtubules of *S. pombe* change throughout the cell cycle and these changes in the cytoskeleton are well characterised (Fig. 5.1.1). One of the best methods to monitor a cell's progress through mitosis and the cell cycle is through observation of its cytoskeleton. Since microtubules are required for accurate segregation of chromosomes to the daughter cells some chromosomal aberrations may be caused by defects in the mitotic spindle function.

Observation of *skp1*^{ts}*A7* cells in asynchronous culture

skp1^{ts}*A7* cells were grown to mid-log phase at 26°C in rich liquid medium, shifted to 36°C and grown for a further 8 hours. An incubation of this length of time allows the full effects of the *skp1*^{ts}*A7* mutant phenotype to become visible. It is possible that these phenotypes take a long time to emerge due to the delays in earlier phases of the cell cycle. Samples were taken and processed for immunofluorescence, and stained with anti-tubulin antibodies. Fixed cells were mounted in glycerol mounting medium containing DAPI and examined under a fluorescence microscope. Different kinds of phenotypes were quantified by counting two hundred cells in a field of view chosen at random on the 8 hour time point slide. In asynchronous culture the vast majority of cells were elongated in length and contained interphase microtubules (>70%). A small percentage of elongated cells contained short mitotic spindles and a further fraction were septated with mis-segregated DNA. The mis-segregated DNA category included phenotypes where the spindle was placed through the DNA or where different proportions of DNA were present in each daughter cell or where all the DNA was in one daughter cell and none in the other daughter. The remaining cells were short with disorganised microtubules (Fig. 5.1.2).

As asynchronous cultures only contain a portion of cells in mitosis and dead cells were not counted in this analysis it was decided to examine whether abnormal phenotypes accumulated over time.

Observation of *skp1^{ts}A7* cells in synchronous culture

Cells were synchronised in G2 by centrifugal elutriation released at 36°C, followed for up to 7 hours, fixed and stained for anti-tubulin immunofluorescence. Fields of cells were counted to check for the appearance of abnormal DAPI staining structures as detailed in Fig. 5.1.3. By the end of the time course almost 50% of the cells had accumulated mitotic chromosomal defects. This occurred around 4 hours after release from G2, after the first attempt at mitosis (see Fig. 5.1.3 B). Examples from the 2 hour, 5 hour and 7 hour time points are shown in Fig. 5.1.4. Cells with mis-segregated DNA and abnormal mitotic spindles from the 5/7 hour time points are shown. Cells from the 2 hour time point show normal mitotic phenotypes and post anaphase arrays. *skp1^{ts}A7* cell can therefore be said to accumulate mitotic phenotypes which begin to emerge after the first mitosis at 36°C, implying wild-type Skp1 is involved in normal mitosis.

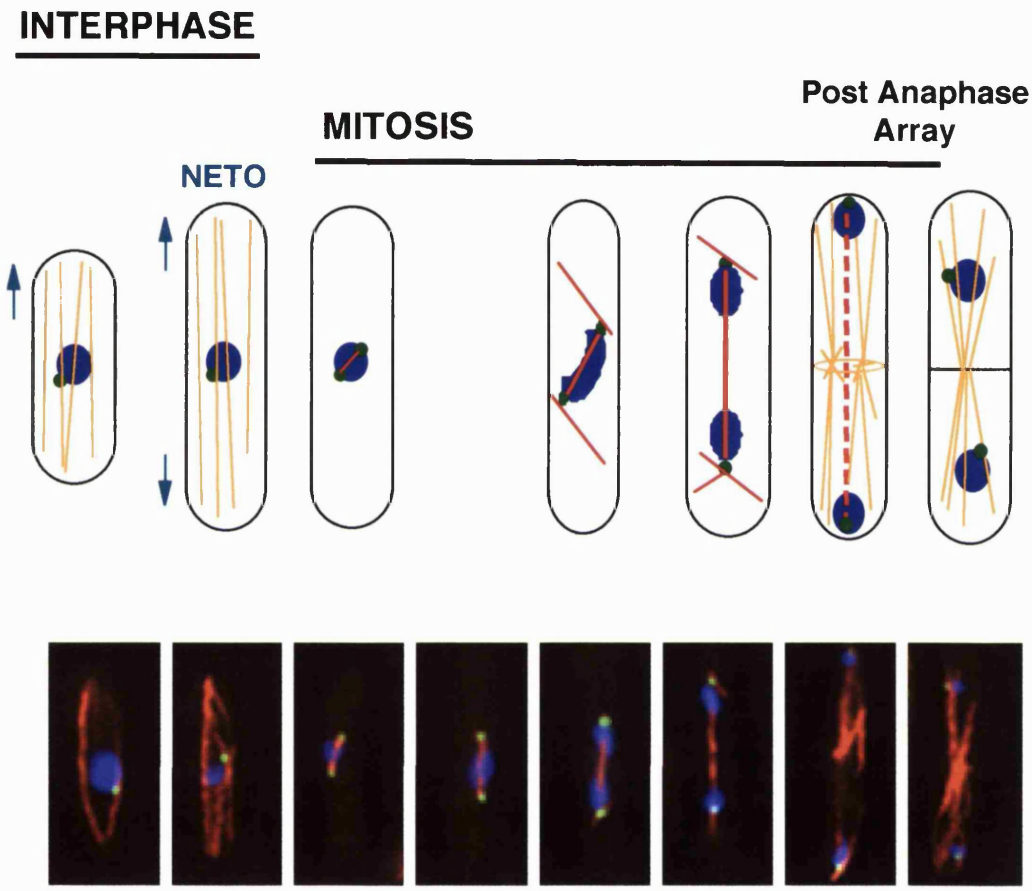

Fig. 5.1.1: The microtubule organisation of fission yeast throughout the cell cycle

Upper panel shows a cartoon of the microtubules. Lower panel shows wild-type cells fixed in methanol and stained for microtubules (anti-tubulin-red), spindle pole bodies (anti-sad1-green) and DNA (DAPI-blue).

In interphase cytoplasmic microtubules form parallel arrays extending along the axis of the cell. These break down at mitosis and the mitotic spindle forms. After mitosis two microtubule organising centres nucleate a post anaphase array of microtubules.

Figure adapted from L. Vardy 2001

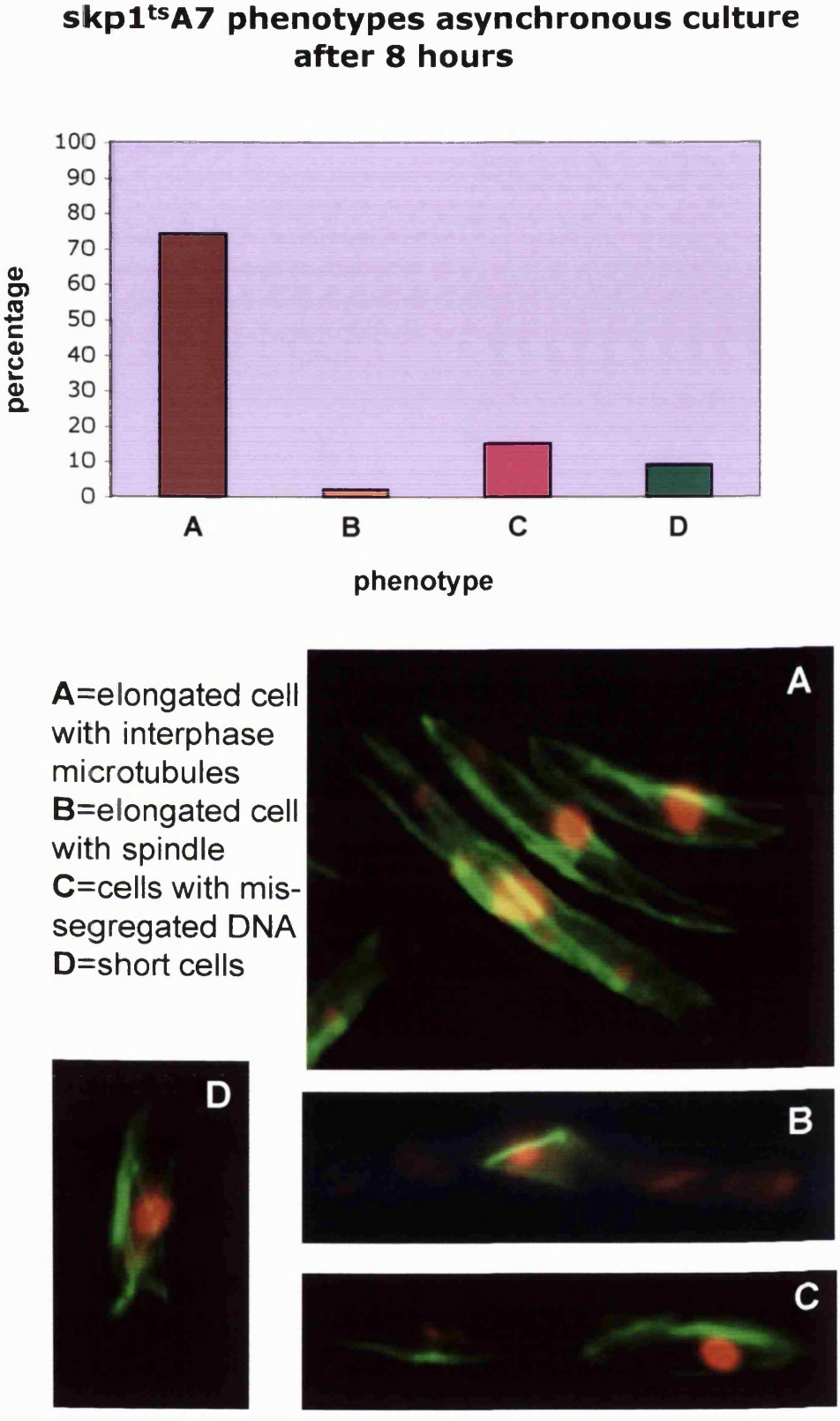

Fig. 5.1.2: *skp1^{ts}A7* cells have assorted phenotypes
Asynchronous cultures of *skp1^{ts}A7* were grown for 8 hours. Cells were fixed with methanol and stained with anti-tubulin and DAPI. Cells were categorised: **A** elongated cells in interphase; **B** elongated cells in mitosis with a spindle; **C** cells which have been through mitosis and have mis-segregated their DNA; **D**, short cells.

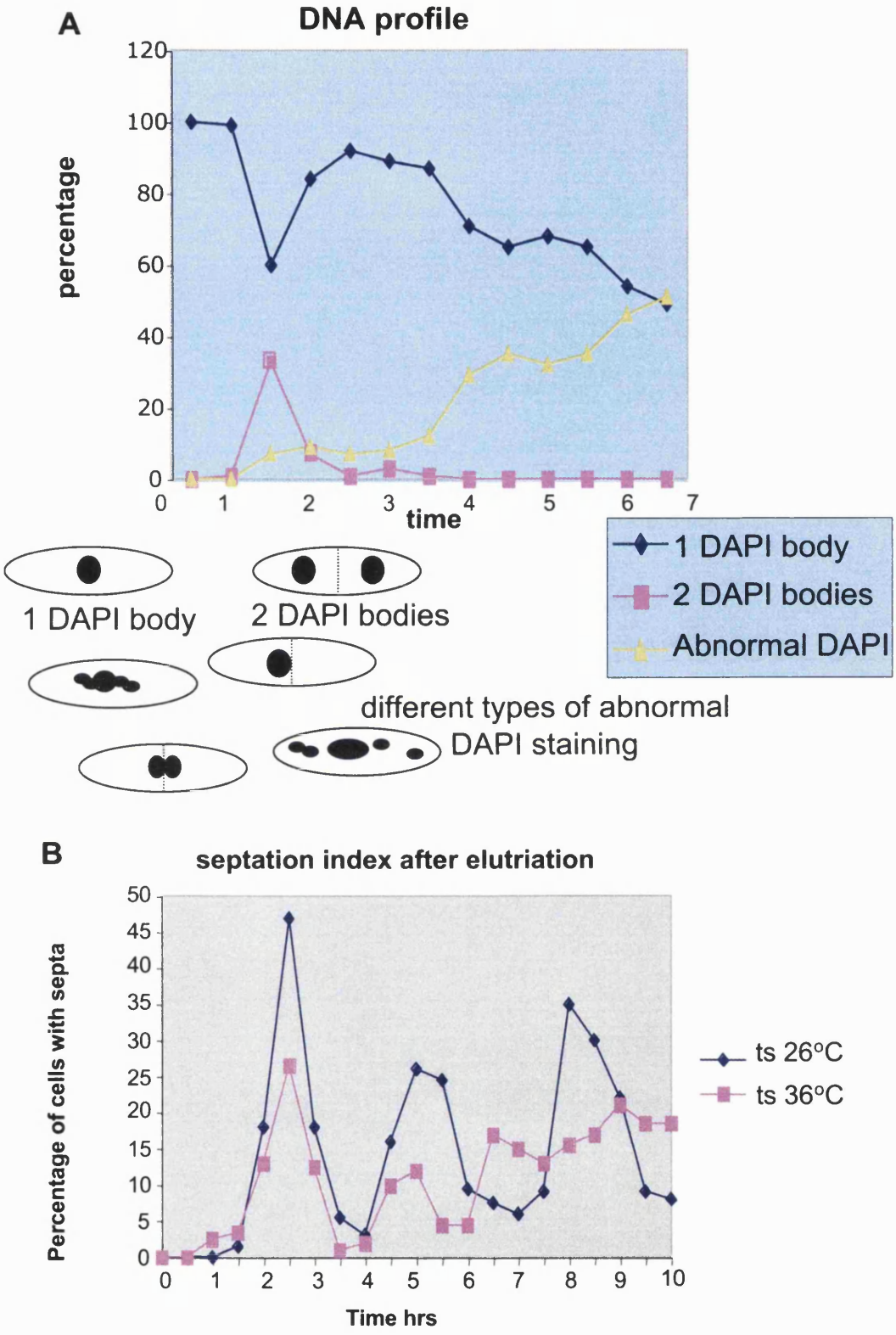

Fig. 5.1.3: Synchronous cultures of *skp1^{ts}A7* accumulate mitotic phenotypes

A Cells synchronised by centrifugal elutriation were shifted to 36°C and sampled regularly. Samples were fixed in methanol and stained with anti-tubulin antibodies and DAPI. Cells were examined under a fluorescence microscope and counted for different mitotic phenotypes. **B** Septation data of samples from the elutriation. Cells are fixed in formaldehyde and then stained with calcofluor. 200 hundred cells were counted per time point.

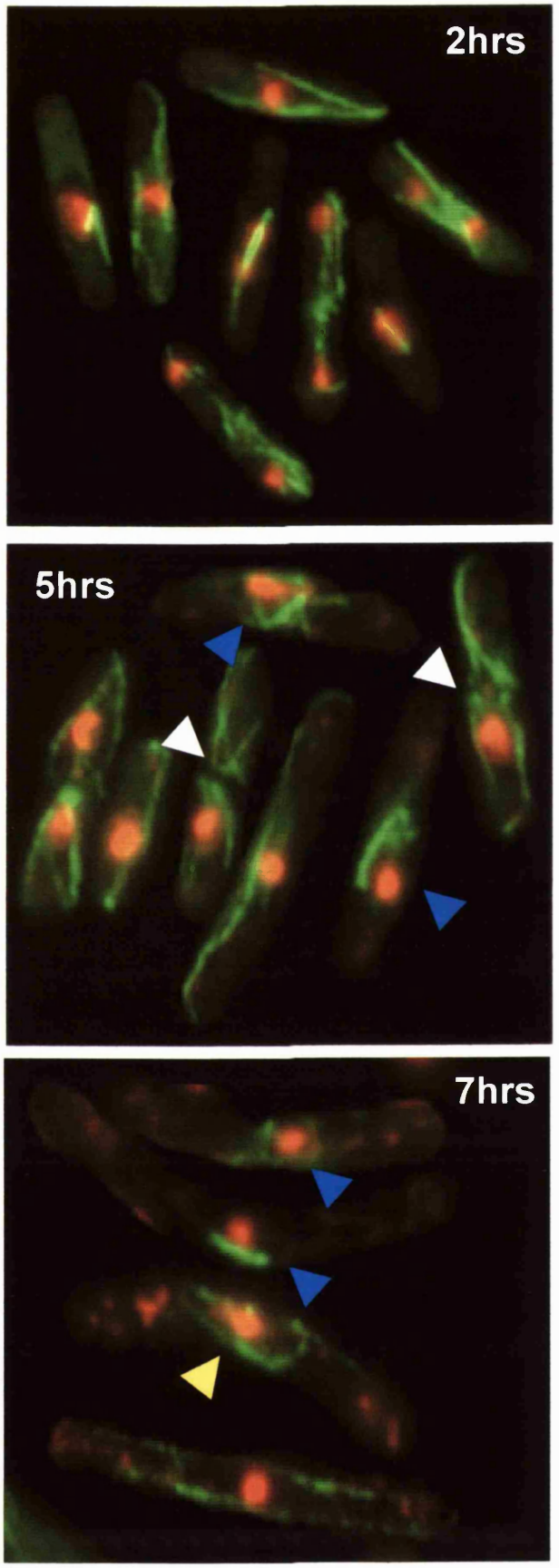

Fig. 5.1.4: Chromosome mis-segregation in *skp1^{ts}A7* cells
Cells were elutriated to obtain a G2 population and placed at 36°C for 7 hours. Samples from 2,5 and 7hr time points. At 2hrs normal mitoses are seen. After 5 hours abnormal mitoses are evident (blue arrowheads) as is mis-segregated DNA (white arrowheads). At 7 hrs there are further mitotic phenotypes (blue arrowheads) and one cell shows a bent spindle (yellow arrowhead).

5.2 Live image analysis of *skp1^{ts}A7* microtubules at 36°C

In budding yeast Skp1 is part of the CBF3 complex that is essential for the function of the kinetochore and binds to the CDEIII element of the budding yeast kinetochore (Connelly and Hieter, 1996; Kaplan *et al.*, 1997; Kitagawa *et al.*, 2003; Stemmann *et al.*, 2002). Although the kinetochore of budding yeast is somewhat different to that of fission yeast, it remains a highly intriguing possibility that Skp1 could be involved in fission yeast kinetochore function. Mutations in *skp1^{+}* could affect this potential role, therefore it was decided to examine the basis for the defective DNA phenotypes seen in *skp1^{ts}A7* cells. The kinetochore is required for the formation and maintenance of the mitotic spindle. Therefore it was decided to examine the mitotic spindle of *skp1^{ts}A7* cells. Microtubules were labelled with GFP in *skp1^{ts}A7* fission yeast cells, by integration of a plasmid expressing GFP-tagged α-tubulin (Atb2) under the control of the thiamine-inducible promoter (Strain: AL108). After 4 hours at the restrictive temperature the cells were examined live on a pre-warmed microscope stage. Cells with a short mitotic spindle were selected for analysis and filmed as they progressed through mitosis. Frames were taken every 30s. Fig. 5.2.1 shows a phenotype observed in three or more of every ten *skp1^{ts}A7* cells filmed live undergoing mitosis. The *skp1^{ts}A7* mitotic spindle begins the process of elongation (Fig. 5.2.1 90s- 690s) but then begins to bend abnormally (Fig. 5.2.1. 810s). Bending continues (Fig. 5.2.1.900s-1020s) until the spindle forms a complete circle (Fig. 5.2.1 990s) and finally the spindle collapses (Fig. 5.2.1. 1050s).

Having observed mitotic spindles bending in a live cell we next verified that it was similarly present in fixed cells. Previous assessment of fixed cells had been carried out using a single plane for photographing cells. The spindle can bend in 3 dimensions in the *S. pombe* cell and thus it is difficult to observe bent spindles in single plane photographs. Laser Scanning confocal microscopy was used to take photographs of cells and the series of pictures taken on different planes were then merged to build a more 3 dimensional picture of the spindle in the cell. Fig. 5.2.2 A shows very clearly bent spindles at different stages of mitosis. It appears that the spindle forms a sphere corresponding to the location of the nucleus. Astral microtubules are clearly visible at the ends of the spindles

and are elongated compared to those normally observed in wild type cells. The astral microtubules are nucleated from the spindle pole bodies (SPBs) at the ends of the spindles and it appears that the two poles of the spindle are moving together and not apart in the later stages of mitosis. These phenotypes are examined in more detail in the next section.

Skp1 in the *skp1^{ts}A7* mutant is reduced in its binding to Pof3 (Chapter 3), and so the observed phenotype could be due to loss of SCF^{pof3} function. *pof3Δ* cells were therefore checked for bent spindles by confocal microscopy but no bent spindles were observed in 5 fields of view containing approximately 100 cells each. Since bent spindles were not observed in *pof3Δ* cells this effect in *skp1^{ts}A7* cells is unrelated to loss of Pof3 binding in *skp1^{ts}A7* cells. Fig. 5.2.2 B shows *pof3Δ* cells from confocal microscopy at different stages of mitosis displaying normal spindle morphology.

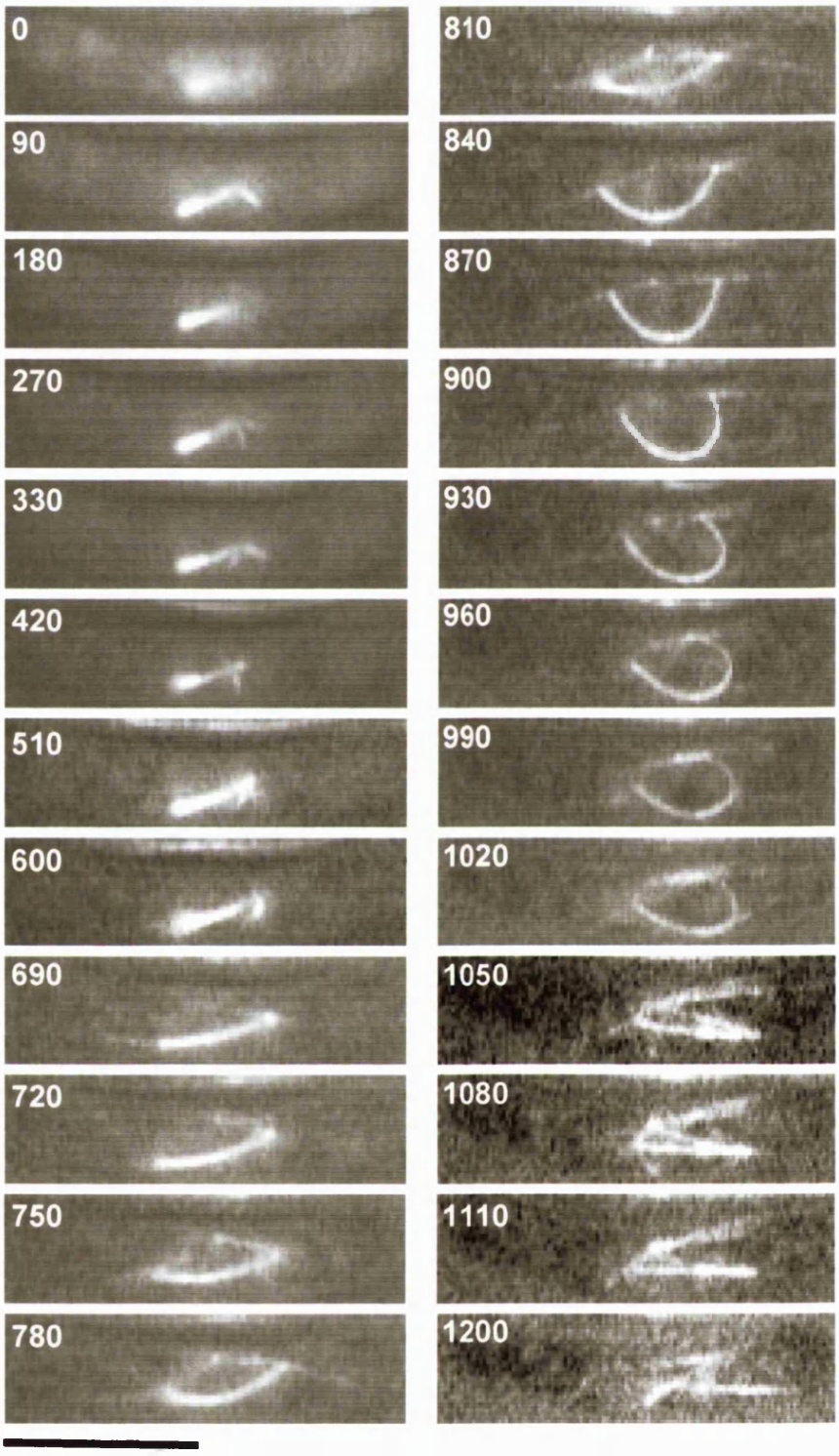

Fig. 5.2.1: *skp1^{ts}A7* cells undergoing mitosis live at 36°C
skp1^{ts}A7 containing an α-tubulin *atb2^{+}-GFP* plasmid (AL108) were filmed undergoing a live mitosis at 36°C using a fluorescence microscope. Frames were taken every 30 seconds (not all are shown for ease of display). Black bar represents 10 μm

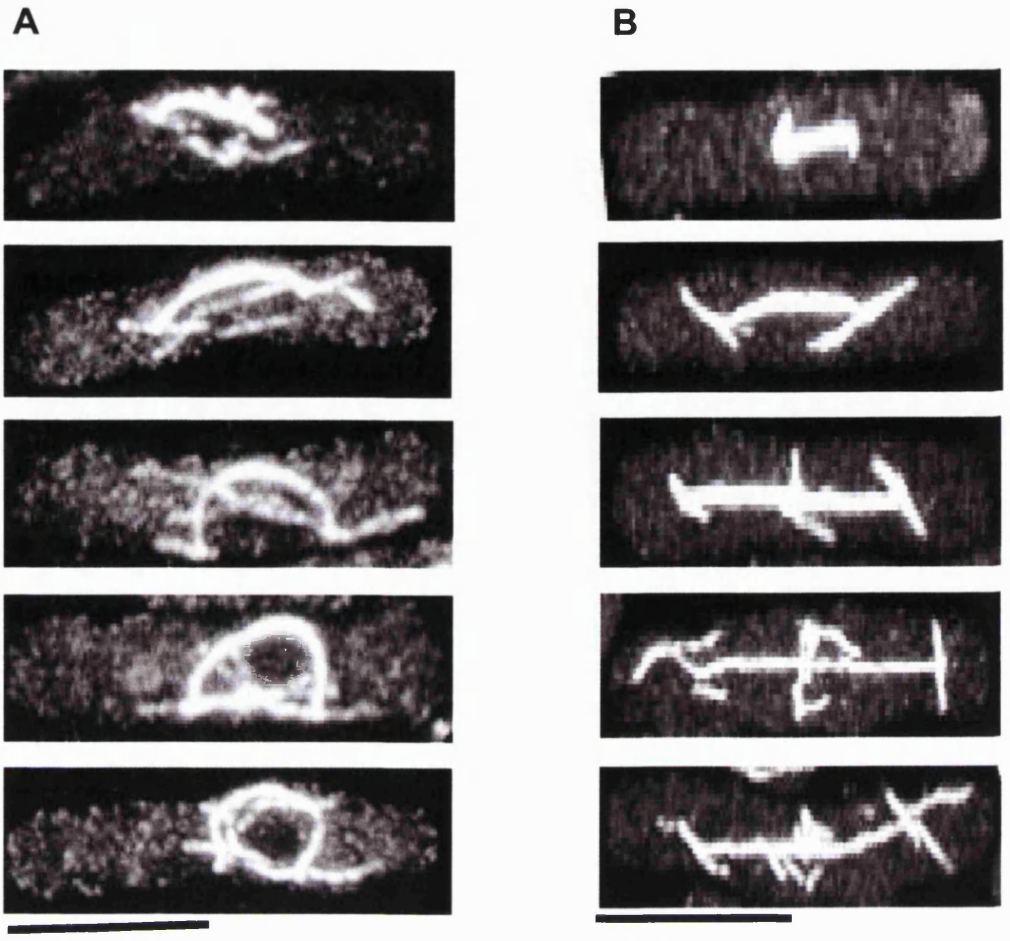

Fig. 5.2.2: *skp1^{ts}A7* cells show bent spindles in mitosis but *pof3::ura4^{+}* cells do not

A *skp1^{ts}A7* or **B** *pof3::ura4^{+}* cells were grown for 4 hours at 36°C, fixed in methanol and stained with anti tubulin antibodies. Cells at different stages of mitosis were selected for examination and images were taken on a confocal microscope. Reconstructed cells were compiled from a Z stack of 10 slices through the cell. Black bar represents 10μm

5.3 Spindle pole bodies in *skp1^{ts}A7* strains at 36°C

The SPBs of *skp1^{ts}A7* appear to move together in late mitotic cells where the spindle is bent. In normal cells SPBs move towards the poles during anaphase and are partly involved in driving this movement through polymerisation of microtubules which are nucleated from them (Ding *et al.*, 1997; McIntosh *et al.*, 2002). Thus the location and movement of the SPBs in the mutant was examined further. A *skp1^{ts}A7* strain containing an endogenously CFP tagged *cut12^{+}* was used for the purpose of examining the SPBs. Cut12 is a known SPB marker (Bridge *et al.*, 1998).

skp1^{ts}A7cut12-CFP cells (Strain: AL149) were observed undergoing live mitoses at 36°C. Cells were observed from various stages in mitosis. Those with just separating SPBs or with SPBs at a short distance from one another were generally chosen for observation. SPBs began by moving apart as expected (Fig. 5.3.1 15s-135s). The inter-SPB distance increases from 5.7μm to 7.41μm. However after 150s the SPBs started to recoil back towards each other and the centre of the cell (Fig. 5.3.1 A marked by a red arrow). They finally return to within 1.71 μm of each other. The velocity of this movement towards the cell centre was ~1.8μm/min (Fig. 5.3.1 B) which is slightly faster but approximately the speed (1.4μm/min $^{+}$- 0.2) of microtubule extension during phase 3 of fission yeast mitosis, spindle elongation (Nabeshima *et al.*, 1998). The results shown here confirmed the aberrant behaviour seen through observation of the mitotic spindle.

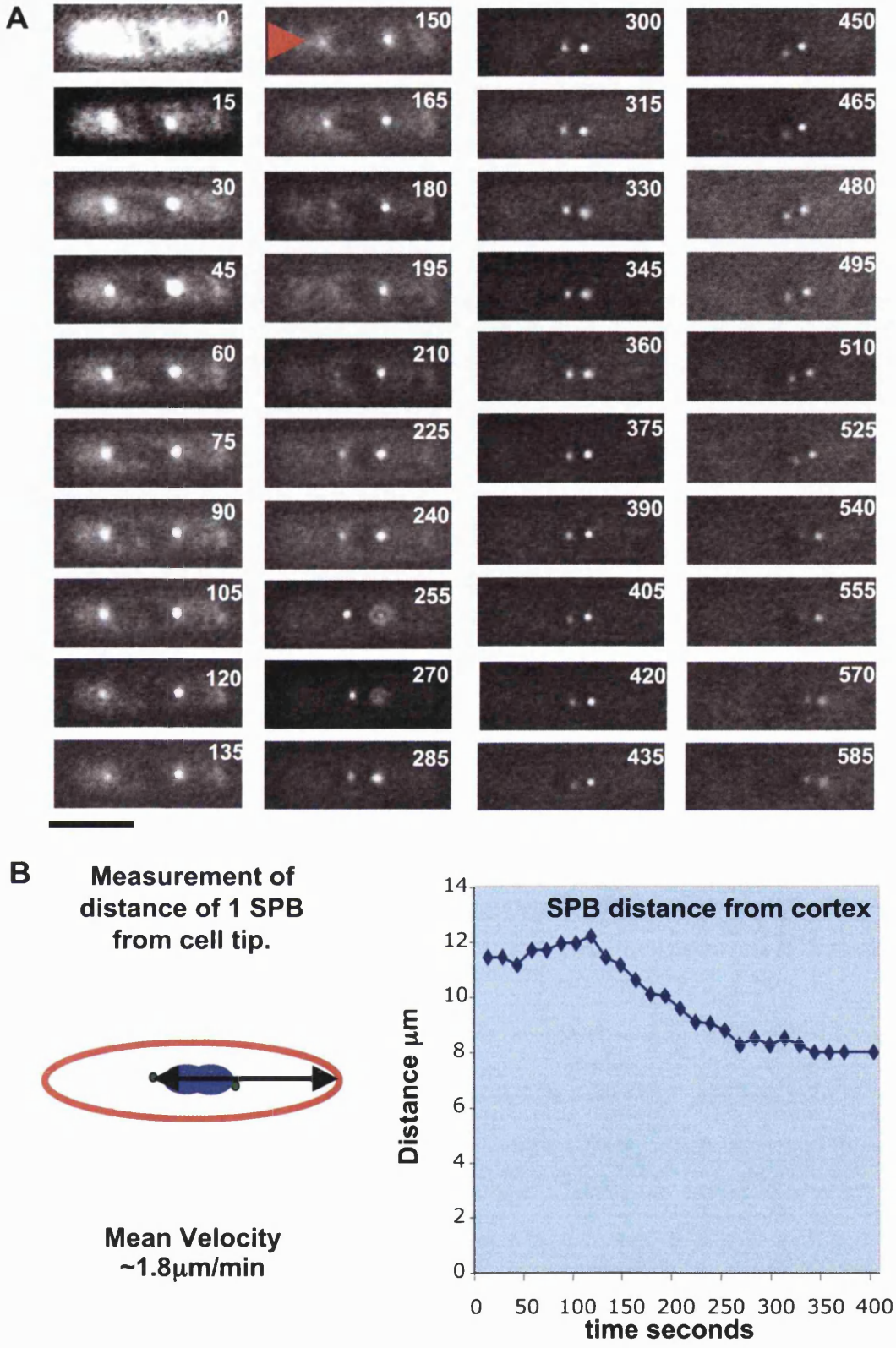

Fig. 5.3.1:*skp1^{ts}A7* cells with bent spindles show reversed spindle pole movement

A *skp1^{ts}A7* cells containing Cut12 tagged with CFP in the chromosomal locus (AL149) were filmed undergoing live mitosis using a fluorescence microscope. Frames were taken every 15 seconds. The red arrow marks the point at which SPB's begin to converge. **B** The distance of one SPB from the tip of the cell was measured as represented in the diagram and plotted against time. The velocity of SPB movement during mitosis was measured from the gradient of the line.

5.4 Does the nuclear membrane prevent spindle elongation?

Films and still images of SPB movement and spindle elongation suggested that the path of the spindle follows the edge of the nucleus. The movement of the SPBs looks like an elastic recoil motion as the SPBs get to a certain point, then cannot stretch further and start to move back again. One of the features of yeast mitoses is that they are closed mitoses, whereby the nuclear membrane does not break down whilst the chromosomes are being separated (Kubai, 1975). This means that the spindle must penetrate through the nucleus, nucleated by the SPB which is partly embedded in the nuclear membrane at mitosis (Ding *et al.*, 1997). One way to explain the aberrant spindle movement seen in *skp1^{ts}A7* cells is that the spindle is restrained by the nuclear membrane and thus prevented from elongating. The nuclear membrane was examined by following the GFP tagged *cut11^{+}* protein, a known nuclear membrane protein (West *et al.*, 1998). A *skp1^{ts}A7 cut11^{+}-GFP* (AL190) strain was examined using a confocal microscope and the resulting images are shown in Fig. 5.4.1 A. In all cells observed with a bent spindle the merged images show that the nuclear membrane and the spindle are precisely co-localised (yellow) with additional astral microtubules outside of the nuclear periphery. It appears from this analysis that the nuclear membrane of *skp1^{ts}A7* cells becomes severely distorted during mitosis and that it is stretching until it can extend no further. After a certain threshold, the microtubules inside the nucleus begin to grow around the periphery of the nucleus rather than extending laterally down the central axis of the cell. One conclusion that could be drawn from this is that in wild-type cells Skp1 may be involved in coupling changes in the nuclear membrane during mitosis to spindle elongation (see Discussion below).

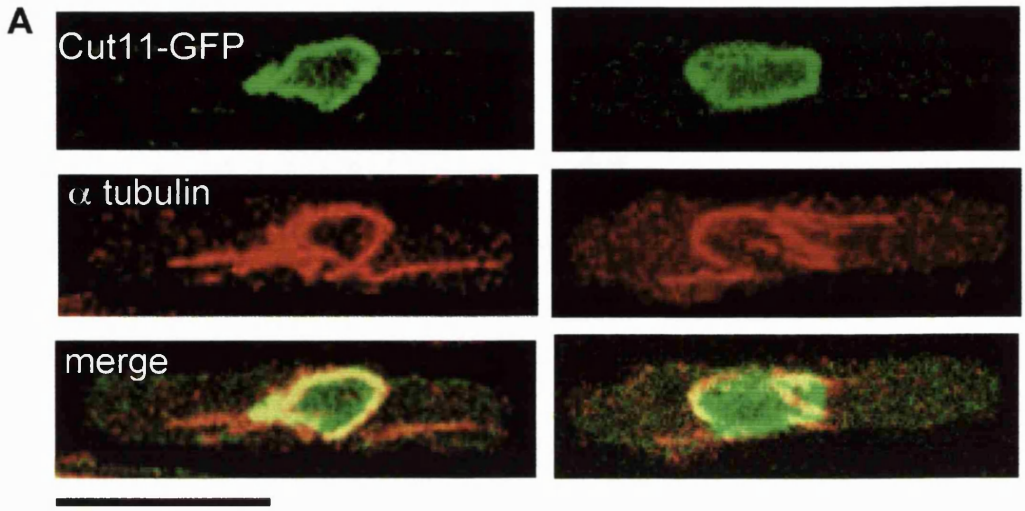

Fig. 5.4.1: Spindle elongation appears to be constrained by the bounds of the nuclear envelope in *skp1^{ts}A7*

skp1^{ts}A7 cells containing *cut11^{+}* nuclear envelope marker tagged with GFP at the chromosomal locus (AL190) were grown for 4 hours at 36°C, cells were fixed in methanol and stained with anti-tubulin. Cells were examined using a confocal microscope and those containing a bent spindle were photographed. Black bar represents 10μm

5.5 The astral microtubules of *skp1*^{ts}*A7* cells

Analysis of confocal sections of tubulin-stained *skp1*^{ts}*A7* cells showed very prominent astral microtubules. Astral microtubules are rarely seen in wild-type cells fixed with methanol and stained for anti-tubulin. However in *skp1*^{ts}*A7* cells the astral microtubules are very large even in cells with short spindles (Fig. 5.5.1). In wild-type cells two astral microtubules are sometimes visible, which are thought to be involved in anchoring the spindle in the correct orientation with respect to the long axis of the cell (Gachet *et al.*, 2001). In *skp1*^{ts}*A7* cells with elongated spindles (bent or straight) there are highly developed networks of astral microtubules. It is unclear if these networks anchor the spindle to the cortex as they seem thoroughly entangled (Fig. 5.5.1). The length of these astral microtubules in *skp1*^{ts}*A7* cells with short spindles and the extensive networks in cells with long spindles suggests that the astral microtubules are more stable. This could relate to the length of the cells. Part of the role of astral microtubules is to search for the cortical actin ring to anchor onto. The increased length of the cell may require the astral microtubules to grow further in order to find the cortex and anchor the spindle correctly. An alternative explanation is that elongated astral microtubules are related to some SCF function that is abrogated in *skp1*^{ts}*A7*. It would therefore be important to observe how astral microtubules behave in other grossly elongated cell types. This could be investigated in *cdc25*^{ts} cells after they have been blocked in G2 by incubation at 36°C, and then released at the permissive temperature. They would then undergo mitosis at a large cell size, and their astral microtubules could be examined for similarities to the astral microtubules of *skp1*^{ts}*A7* cells.

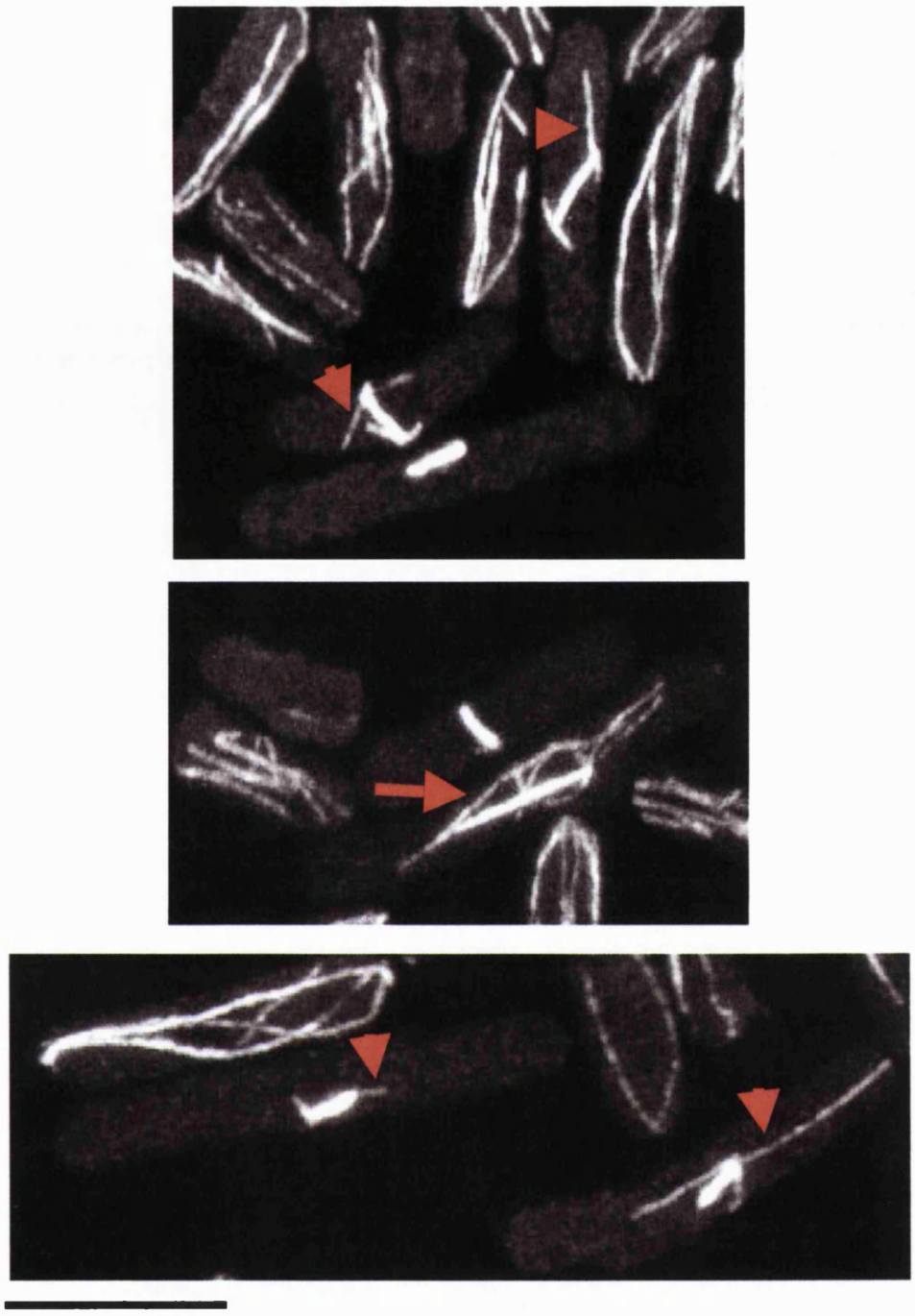

Fig. 5.5.1: *skp1^{ts}A7* cells have stable astral microtubules
Asynchronous *skp1^{ts}A7* cells grown for 8 hours at 36°C were fixed in methanol and stained with anti-tubulin antibodies. Cells were examined under a confocal microscope and Z stacks composed of 10 slices through the cell were compiled. Red arrowheads indicate prominent astral microtubules. Red arrow shows a long spindle with complex astral network. Black bar represents 10μm.

5.6 Mid2 and *skp1^{ts}A7*

The recently discovered anillin homologue Mid2 is a septin regulating protein involved in cytokinesis. Accumulation of the protein is cell cycle regulated both transcriptionally and post-translationally. It was shown to accumulate in proteasome mutants and is suggested to be an SCF target (Tasto *et al.*, 2003). As Mid2 is involved in cell division it was assessed if accumulation of this protein was involved in the *skp1^{ts}A7* mitotic phenotypes. To investigate this a *skp1^{ts}A7* strain carrying a deletion of Mid2 was created. *skp1^{ts}A7 mid2Δ* (AL164) cells were treated for immunofluorescence with anti-tubulin staining. Cells were examined with a fluorescence microscope capable of imaging through the Z axis. Merged images show that *skp1^{ts}A7 mid2Δ* cells still contain bent mitotic spindles as shown in Fig. 5.6.1 A.

Overexpression of Mid2

Mid2 overexpression creates rounded cells with depolarised actin (Tasto *et al.*, 2003). This finding was replicated and Mid2 was also overproduced in *skp1^{ts}A7* cells at 36°C. Because Mid2 is suggested as an SCF target it was questioned if overproduction in an SCF mutant would affect the cell.

Mid2 was expressed under the control of the thiamine-inducible strong promoter in *skp1^{ts}A7* cells (Strain: AL166). At 36°C when Mid2 was expressed strongly by the removal of thiamine the temperature sensitive cells became round as in Mid2 overexpression in a wild-type strain rather than giving the characteristic elongated phenotype of *skp1^{ts}A7* cells (Fig. 5.6.1 B). It therefore seems that Mid2 overproduction at 36°C can suppress the *skp1^{ts}A7* elongation phenotype from occurring. It remains to be tested if the DNA damage checkpoint is still activated.

Mid2 levels

In order to assess if there was accumulation of endogenous Mid2 in *skp1^{ts}A7* cells the *mid2^{+}* gene was C-terminally tagged with the HA epitope. *skp1^{ts}A7 mid2^{+}-HA, mid2^{+}-HA* (see strain list; sub-heading: Mid2 experiments in the Materials and Methods section) and a wild-type untagged strain were grown to

mid-log phase at 26°C then shifted to 36°C for 4 hours and protein extract was prepared for western blotting. Fig. 5.6.1 C shows that Mid2 is not particularly accumulated in *skp1*^{ts}*A7* cells although there is perhaps a very small amount of accumulation. It seems likely that the degradation of Mid2 by the SCF is, therefore, not affected in *skp1*^{ts}*A7* cells and is unlikely to be the cause of the aberrant spindle morphology observed.

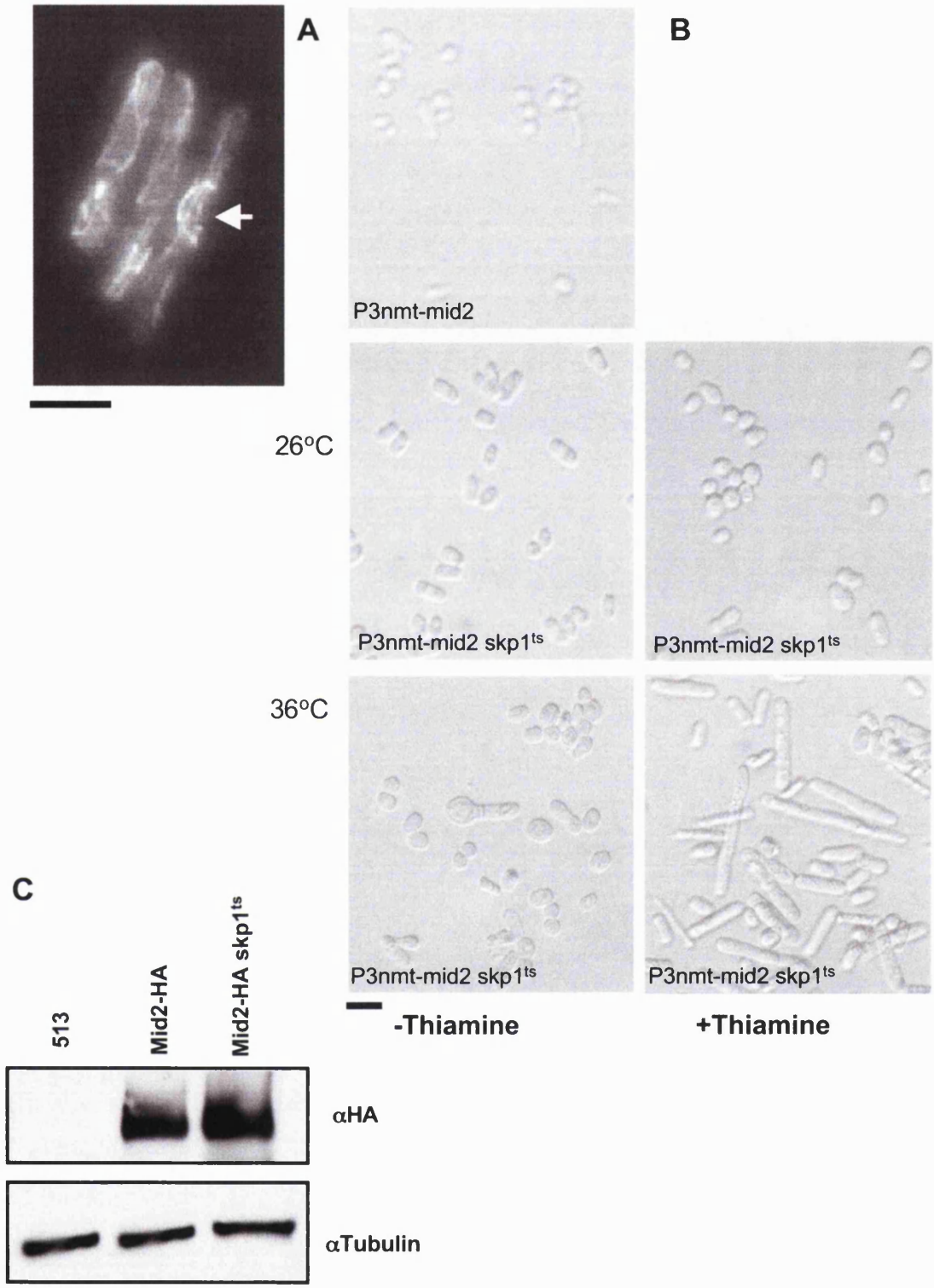

Fig. 5.6.1: *mid2*⁺ deletion, overexpression and protein levels in a *skp1ts*A7 strain

A *skp1ts*A7 *mid2::kan*ʳ cells were stained with anti-tubulin. Cells were examined with a fluorescence microscope and Z stack images compiled of 10 slices were composed. White arrow indicates a cell containing a curved spindle. Black bar represents 10μm. (Strain:AL164) **B** *skp1ts*A7 cells containing a copy of *mid2*⁺ under a thiamine-repressible promoter were grown overnight at 26°C or 36°C. Black bar represents 10μm. (Mid2OP) **C** Asynchronous cultures of *skp1ts*A7 *mid2*⁺-*HA* were used to prepare protein extract from 10^7 cells. Blots were probed with anti-HA antibodies and re-probed with antibodies against α tubulin as a loading control. (See strain list: Mid2 experiements in Materials and Methods for full genotypes)

5.7 Summary

In this chapter mitosis in *skp1^{ts}A7* cells has been examined. *skp1^{ts}A7* cells have aberrant chromosome segregation. Also *skp1^{ts}A7* cells bend their mitotic spindles, which eventually leads to collapse of the spindle. Spindle growth in *S. pombe* is normally divided into 3 phases: phase 1-the phase of spindle formation; phase 2-the phase of constant spindle length and phase 3-the phase of spindle elongation(Nabeshima *et al.*, 1998). In *skp1^{ts}A7* cells, initially the SPBs move apart, suggesting that cells entered phase 1, and subsequently reached phase 2, the period of constant spindle length. After this the SPBs begin to return towards each other at a velocity similar to the rate of microtubule growth in phase 3; a period when normal spindles finally elongate and anaphase B occurs. This suggests that the problems in *skp1^{ts}A7* mitosis occur in anaphase. The bent spindle co-localises with the nuclear membrane. These findings suggest that the nuclear envelope is restricting the extension of the spindle as it tries to extend. This implicates the SCF in a role governing mitotic changes to the nuclear envelope.

The Mid2 protein has recently been identified as a target of the SCF, (although the F-box is unknown) but does not influence spindle bending in *skp1^{ts}A7* cells. Deletions of *mid2^{+}* in a *skp1^{ts}A7* background showed clear spindle bending even though the *mid2^{+}* deletion phenotype of multiple septa (Tasto *et al.*, 2003) was also seen (Fig. 5.7.1). Overproduction of Mid2 in a *skp1^{ts}A7* strain at 36°C created rounded cells and Mid2 was not seen to be vastly accumulated in a *skp1^{ts}A7* strain.

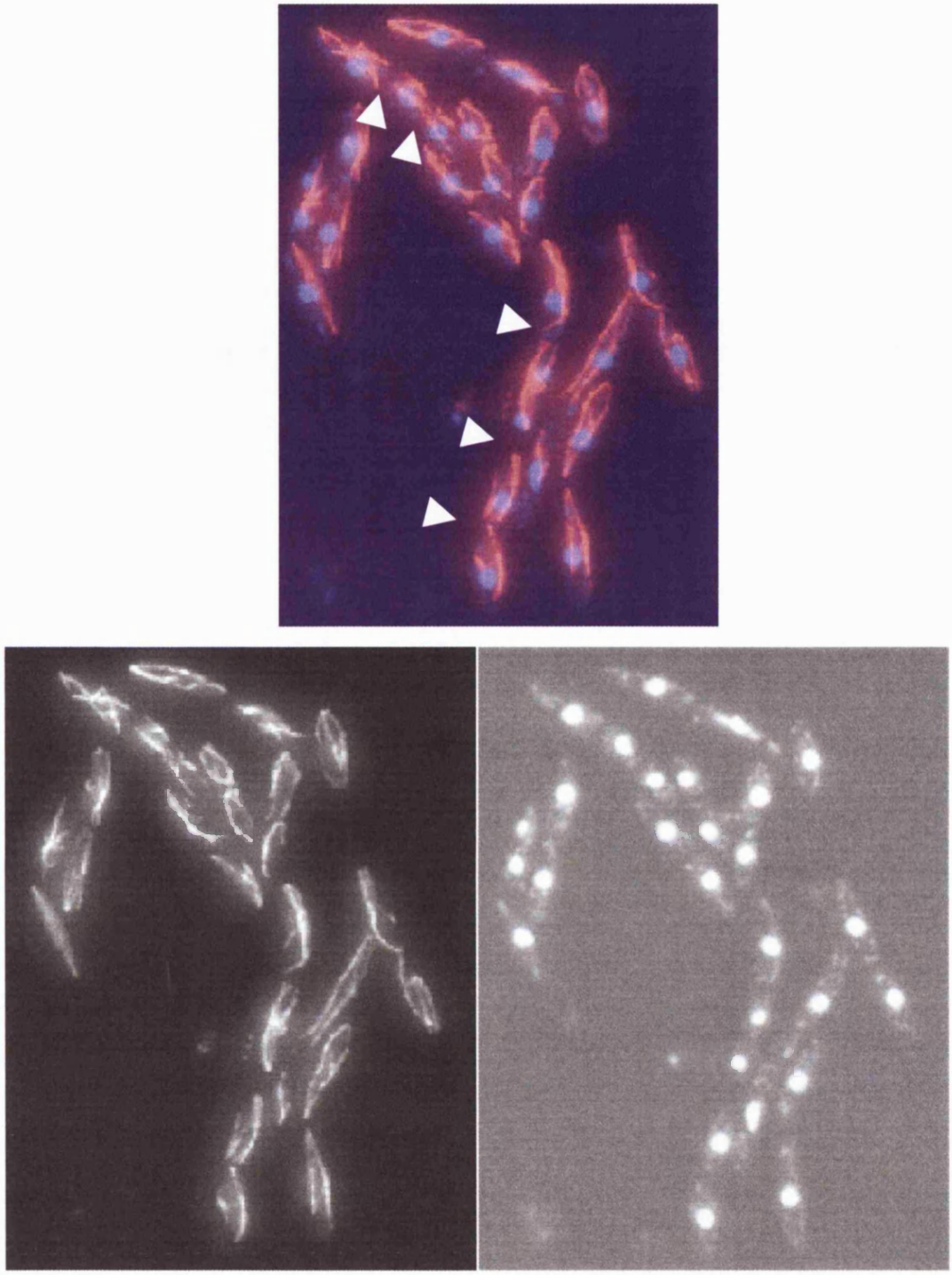

Fig. 5.7.1 The multiple septa of *mid2Δ skp1^{ts}A7*
mid2Δ skp1^{ts}A7 cells (AL164) were grown for 4 hours at 36°C. Cells were fixed in methanol and stained with anti-tubulin antibodies, followed by cy3 conjugated secondary antibodies. Cells were mounted in glycerol mounting medium containing DAPI. Upper panel shows merged images with white arrows indicating the location of septa. Lower panels show the anti-tubulin and DAPI respectively.

5.8 Discussion

In the previous chapter *skp1^{ts}A7* cells were shown to be delayed in G2. This was dependent on the DNA damage checkpoint. The majority of the cells were in interphase as judged by the presence of cytoplasmic microtubules. However a small proportion of the cells exhibited mitotic phenotypes indicating that they could enter mitosis. Mitosis at 36°C is, however, unusual with cells showing an assortment of defects. It is probable that these defects lead to cell death, as they include chromosome mis-segregation and 'cut' cells. This may result from bending of the mitotic spindle as it lengthens in an arch-like formation. Later this spindle snaps in the central region. The precise reason for this behaviour is unknown but it is feasible to imagine various explanations.

Mechanisms of spindle collapse

The bent spindles in *skp1^{ts}A7* cells, asks the question: how could these bent spindles be formed? What mechanism would give rise to this kind of effect? The curvature of the spindle and the manner in which this curving occurs, seen from the live imaging data (Fig. 5.2.1), suggests that the spindle microtubules are capable of sliding in order to extend the spindle (Mallavarapu *et al.*, 1999) but that the spindle is physically inhibited and this inhibitory force restricts elongation. This could be either a force pushing on the ends of the spindle or one that is obstructing movement of the spindle.

Conceptually there are several possible structures that could have this restraining effect on the spindle. These include the presence of unreplicated DNA or cohesin remaining at anaphase, faulty SPBs, stable astral microtubules, the presence of excess mitotic motors or a rigid nuclear membrane. All are discussed below.

Chromatin

Unreplicated chromatin or cohesion between sister chromatids could stop spindle elongation. As *skp1^{ts}A7* cells have a delayed S phase at 36°C (see Chapter 4), this is quite an appealing proposition. If *skp1^{ts}A7* had unreplicated regions of DNA as the spindle tried to elongate the remaining unreplicated regions of DNA could not be separated easily and separation would lead to

shearing of DNA. If the force of the spindle was not strong enough to shear the DNA, the spindle could be forced to bend as it is restrained by the DNA. The same would be true if there were unresolved cohesin bridges still holding the DNA together.

Cohesin is cleaved by the Separase protein Cut1 (Uzawa *et al.*, 1990) which is released from inhibition by Cut2/Securin (Funabiki *et al.*, 1996a; Funabiki *et al.*, 1996b) on degradation of this protein by APC after the mitotic checkpoint has been passed. In order to address the problem of cohesin cleavage in these mutants a strain in which cohesin was tagged with GFP could be used to check for loss of the signal during the metaphase to anaphase transition. Cohesin cleavage could also be assessed by immunoblotting in synchronised cells. To examine the replication of centromeres using a cen-GFP strain would be a method to examine the separation of chromatids and would also indicate to some extent if the DNA had been replicated. If two cen-GFP dots could be visualised this would imply that at the very least centromeres were replicated.

Spindle pole bodies

The SPBs of *S. pombe* duplicate by means of an appendage which links the two together. This occurs on the cytoplasmic side of the nuclear envelope and once these SPBs are mature they insert into the nuclear envelope. When the two SPBs are ready to separate at mitosis the half bridge is severed (Ding *et al.*, 1997). One possibility to explain the spindle bending in *skp1^{ts}A7* cells is that the two SPBs maintain some kind of latent connection that cannot expand. However this does not explain the recoil type motion whereby the spindle initially elongates but later the SPBs move back together (Fig. 5.3.2). The kind of movement seen in this film suggests that the SPB movement is dependent on the spindle elongating and driving the SPBs back towards each other.

Astral microtubules

The astral microtubules of *skp1^{ts}A7* cells were seen to be highly stable. Previous work (Gachet *et al.*, 2001) suggests that these microtubules are highly dynamic initially but are stabilised by interaction with the cortical actin ring around the nucleus. This brings about an orientation of the spindle within the

cell so that division occurs along the long axis of the cell. In *skp1*^{ts}*A7* cells these microtubules could be further stabilised. Improperly regulated they would form a negative force against the elongation of the spindle. However unless this force pushing against the elongating spindle increases over time this again could not in purely physical terms explain the formation of a complete circle by the spindle. A more plausible explanation for the length and stability of the astral microtubules in *skp1*^{ts}*A7* cells would be that due to the extreme length of the cells astrals require a longer growth period without collapse to search and reach the cortical actin ring of the cell in order for the microtubule to be stabilised. Also the astral microtubule is only a single microtubule and the spindle is composed of several microtubules sliding against each other. It seems likely that the force of the spindle would be far greater than any antagonistic force that the astral microtubules could produce. Therefore this is a physically unlikely mechanism by which to restrict the spindle elongation along the long axis of the cell.

Motor proteins

The mitotic spindle is often regarded as a machine involving the balance of forces of spindle polymerisation, depolymerisation and motor proteins, which separate chromatids. The motors are involved at many points such as extension of the spindle by sliding of microtubule filaments past one another using homo-tetrameric double-headed motor proteins of the Bim C family. There are also plus and minus end directed kinesin motor proteins which are probably involved in attachment of kinetochores end-on to polymerising or depolymerising microtubules in order to achieve movement of the cleaved chromatids to opposite poles in anaphase A. Members of the chromokinesin family are also thought to create force on the arms of the chromatids to create a polar ejection force and the dynein family of motors are thought to be involved in organising the location and position of the spindle through the SPBs by creating pulling forces on the astral microtubules attached to the cortex of the cell (reviewed by Inoue and Salmon, 1995; McIntosh *et al.*, 2002; Sharp *et al.*, 2000; Wittmann *et al.*, 2001). The picture of the spindle in mitosis is a highly complex one, it is therefore easy to envisage that if the levels of some of these motors were improperly balanced, for example the dyneins were over

accumulated, then the spindle poles could be driven together by inappropriate action of these motors. There are no known motor proteins that are targets of the SCF however it is not impossible that a motor protein involved in mitosis could be an SCF target. If this accumulated in mitosis it could act as a force against spindle elongation.

Nuclear envelope

The most appealing idea is that a change occurs in the nuclear membrane of cells undergoing mitosis. This would increase the elasticity of the nuclear membrane allowing it to be stretched more easily by the elongating spindle. If this change in the nuclear envelope relied on the degradation of an SCF substrate then its ability to stretch in mitosis might be inhibited by the presence of the undegraded substrate X that accumulated in *skp1^{ts}A7* cells. Under these circumstances, the spindle would begin elongation correctly but would be restricted by the lack of elasticity in the nuclear envelope. If it could not overcome this inelasticity it would take the path of least resistance during elongation which would be the circumference of the nuclear envelope. The co-localisation of the aberrant spindle in *skp1^{ts}A7* cells with the nuclear membrane enhances the appeal of this theory. Although there are no obvious precedents to suggest changes to the nuclear membrane in mitosis in yeast, in mammalian cells the nuclear envelope disassembles during mitosis. This is regulated by the joint action of phosphorylation of nuclear lamin proteins, the network underlying the nuclear envelope and a dynein based motor activity of microtubules which creates a shearing effect of the nuclear envelope (reviewed by Burke and Ellenberg, 2002). The yeast *cdc2* $^{+}$ kinase has shown to be effective at phosphorylating human lamins expressed in yeast suggesting that some kind of changes may also occur in the yeast nuclear envelope. For a diagrammatic representation of all the possible methods of restricting spindle elongation discussed see Fig. 5.8.1.

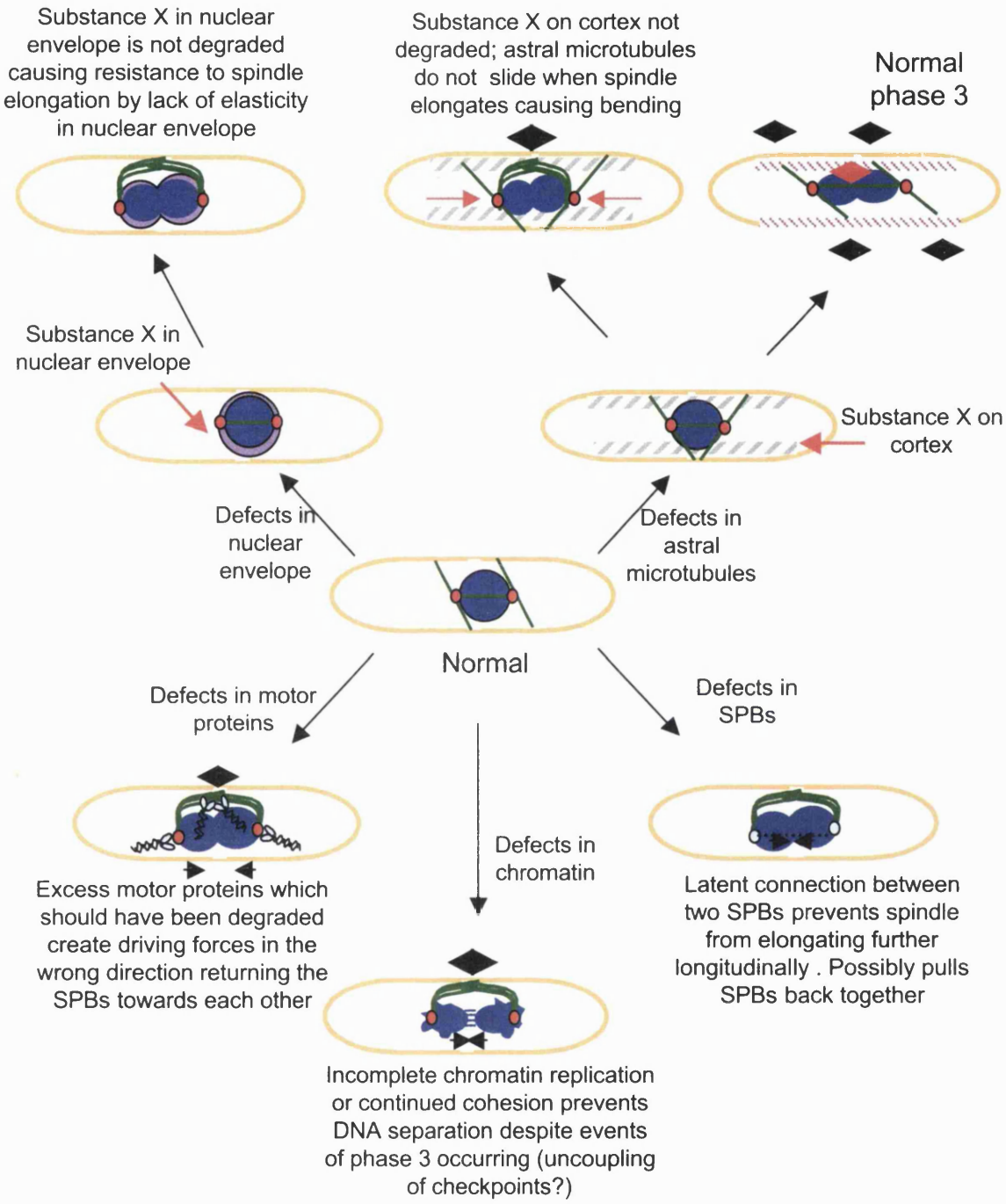

Fig. 5.8.1: Hypothetical models of the causes of spindle curvature in anaphase.
It is possible that defects in any or several of these crucial mitotic components could be responsible for the dramatic curvature observed in the *skp1*^{ts}*A7* spindle during mitosis.

Mid2 protein degradation and the SCF complex

Mid2 is involved in cytokinesis and the placement of septin rings in *S. pombe* in the final stages of mitosis. A deletion of *mid2*$^{+}$ shows multiple septa and nuclei without cytokinesis and cell separation. The *mid2*$^{+}$ deletion also shows a diffuse under-organised septin ring. The regulation of Mid2 is thought to be dependent on the SCF complex. Stabilised Mid2 caused a delay to the cell cycle and persistence of septin rings (Tasto *et al.*, 2003).

Deletion of Mid2 in the *skp1*^{ts}*A7* cells resulted in the formation of multiple septa as expected (Fig. 5.7.1) but did not suppress the temperature sensitivity or alleviate the mitotic spindle bending. This suggests that Mid2 accumulation in *skp1*^{ts}*A7* cells is not responsible for the presence of these phenotypes. Also Mid2 is not significantly accumulated this implies that whichever F-box protein is responsible for degradation of Mid2 is not affected in the *skp1*^{ts}*A7* mutant. The overexpression of Mid2 in *skp1*^{ts}*A7* cells did create the rounded cells seen by Tasto *et al.*, (2003) over-riding the elongation normally seen in *skp1*^{ts}*A7* cells. The phenotype appeared reminiscent of *pof1* mutants and these cells also occasionally have septation defects.

Pof1 binding is mildly affected in *skp1*^{ts}*A7* cells, therefore one hypothesis would be that perhaps Pof1 is responsible for the destruction of Mid2. However because Pof1 binding in a *skp1*^{ts}*A7* cell is not normally grossly affected, *skp1*^{ts}*A7* is able to breakdown Mid2. However under conditions where Mid2 is overproduced, the cell is flooded with Mid2 and this can no longer be broken down effectively by the defective Skp1/Pof1 complex. In opposition to this, the fact that deletion of *mid2*$^{+}$ in *skp1*^{ts}*A7* cells does not affect temperature sensitivity or give any beneficial growth effects in these cells makes this seem less likely.

The authors who describe Mid2 suggest that Pof6 may be responsible for the destruction of Mid2 as it has been shown to localise to the septum (Hermand *et al.*, 2003). However Pof6 localisation in my hands is at the nuclear membrane. The similarity between *pof1* mutants and Mid2 overproduction leads to the proposal that Pof1 may be the responsible F-box protein for Mid2 ubiquitination, possibly in conjunction with Pof6.

The evidence from Tasto *et al.*, (2003) that Mid2, a protein involved with cytokinesis, is degraded by the SCF finally gives credence to the existence of substrates of this complex outside of the G1/S phase boundary in *S. pombe*.

Chapter 6

Discussion

6.1 Insights into SCF function from *skp1*$^{+}$ mutants.

This thesis has described the creation and characterisation of *skp1* temperature sensitive mutants. The aim of creating these mutants was to allow a clearer insight into SCF function in the *S. pombe* cell. Since initiating this work it has become clear from the body of literature that Skp1 is not just a protein involved in the SCF; it forms complexes above and beyond those of the SCF.
In hindsight the choice of Skp1 for investigating SCF function may not be the most immediately obvious due to the fact that Skp1 is involved in functions above and beyond the SCF. A more appropriate target would have been the cullin proteins, which form the main scaffold of the SCF complex. Cullin proteins have not been described to act in complexes outside of the SCF so far. Despite this it is clear that Skp1 is an important cellular factor and that its correct function is relevant to the normal physiological behaviour of the cell. Therefore the creation of temperature sensitive mutants which may affect one particular factor of Skp1's behaviour more than others are helpful for dissecting the function of this protein.

In studying these mutants it has been established that Skp1 mutants have a G2 delay phenotype. The evidence for this is that around 70% of cells show a highly elongated phenotype, without mitotic defects. These cells have a 2C DNA content, suggesting that the cells have replicated their DNA and are continuing to grow in length without attempting mitosis. The correct function of Skp1 is required by the cell to prevent delay in the G2 phase of the cell cycle. In addition, the absence of proper Skp1 function in the cell leads to activation of the DNA damage checkpoint, and cells that enter mitosis cannot properly regulate spindle elongation resulting in severe mitotic defects.

As yet it is unclear if these defects in cells lacking Skp1 function are due to defective SCF function. If this was the case substrates of the SCF would be expected to accumulate in the *skp1* temperature sensitive cells. If these are non-SCF functions of Skp1 then one could expect that new complexes containing Skp1 would be involved. The SCF complex is a highly important regulatory complex for proteins within the cell. The targets of this complex discovered so far are cell cycle regulatory proteins. It therefore seems likely that the greatest functional importance of Skp1 is as part of the SCF complex. Complexes such as the vATPase RAVE and CBF3 have so far not been found to require ubiquitination activity. However this does not exclude the possibility that ubiquitination activity may also be present in these complexes. In short it is as yet unproved that Skp1 has a function that is completely unrelated to ubquitin ligase activity and therefore it seems most likely that the defects in *skp1^{ts}A7* cells will be due to a breakdown in SCF function.

6.2 Defects in *skp1^{ts}A7*: discrete events or sequential accumulation of defective phenotypes?

The defective phenotype of *skp1^{ts}A7* cells has several distinct characteristics that become apparent through different modes of study. What remains unclear is whether these phenotypes are sequentially accumulated or are discrete events. For example, do defective spindles become apparent only in those cells that have an inability to maintain the G2 delay seen in some *skp1^{ts}A7* cells? Alternatively are some *skp1^{ts}A7* cells incapable of activating the checkpoint and delaying in G2 resulting in inappropriate entry to mitosis and defective spindles? A further possibility is that the spindle defects occur by a mechanism completely unrelated to G2 delay and thus could occur in cells which either do or do not delay in G2.

One way to address this question of dependency of spindle defects upon a G2 delay would be to follow an entire cell cycle live in a *skp1^{ts}A7* cell carrying *atb2^{+}*-GFP. An alternative way to address this issue is to examine cells that do not undergo the G2 delay, for example the *skp1^{ts}A7rad3Δ* cells, for spindle defects. We performed preliminary analysis on these cells, which are partially rescued by deletion of *rad3^{+}* and do not appear to have severe morphological

defects. This suggests that the spindle defects may be dependent on G2 delay. However analysis is preliminary and in order to fully investigate the defects in these cells a live analysis would be required which would remove the possibility of fixation artefacts.

The phenotypes of G2 delay through DNA damage checkpoint activation and spindle defects could occur by accumulation of multiple different SCF substrates. This is an appealing theory as the population of *skp1^{ts}A7* cells is heterogeneous. It could therefore be postulated that whichever substrate accumulates the most determines the outcome of the phenotype: checkpoint activation or spindle defects. If, as discussed earlier, control of SCF degradation is partly dependent on which F-box protein is binding, then the capacity to bind to either one F-box (Pof3) or another (Pof1) could vary between cells (this variation could come about due to differential transcription in different cells, occurring from natural heterogeneity, resulting in different levels of Pof1 or Pof3 protein within the cell). The effect of this would be that Pof1 binding cells would not accumulate Pof1 substrate to the same extent as Pof3 binding cells might. This could explain the heterogeneous population of cells observed.

6.3 Are individual F-boxes compromised or is there a reduction in general SCF function?

A further question that arises from the generation of the *skp1^{ts}A7* strain is whether the mutant Skp1 is affected only in the function of one or two F-box proteins or if there is a general reduction in the effectiveness of the SCF. Our analysis of the crystal structure and binding assays suggest that only 2 out of the 16 F-box proteins, Pof1 and 3, are affected in their binding to Skp1^{ts}A7. This data taken together with the evidence that *skp1^{ts}A7* cells can still degrade the known SCF substrate, Rum1, strongly suggest that it is only certain F-box proteins that are affected by the mutation in this allele. If binding to Skp1^{ts}A7 is taken as the criterion to judge whether an individual SCF complex is functional or not we conclude that only the SCF^{pof3} and SCF^{pof1} complexes will be affected. This implies that the reduction in degradation will be proportional to the reduction in the amount of F-box protein bound suggesting that cells are sensitive to the levels of substrates as binding is reduced to around 50%.

Crucial to future work will be the identification of proteins accumulated in *skp1^{ts}A7* or *pof3Δ* or *pof1^{ts}* cells; this could be achieved by 2 dimensional chromatography of the proteins of these 3 different mutant strains and a wild type strain. Spots with increased intensity would be candidate substrates and could be identified by tryptic peptide digests. If all SCF targets were affected by the mutation it might be expected that many proteins would show a moderate increase. If only one or two F-box proteins were affected there would be a larger increase of a smaller subset of proteins.

Skp1 temperature sensitive mutants in budding yeast cells that have so far been analysed fall into two distinct categories. Those mutants that arrest in G1 with Sic1 accumulation such as *skp1-11* and *skp1-3* or those that arrest in G2 such as *skp1-12* or *skp1-4* with kinetochore defects (Bai *et al.*, 1996; Connelly and Hieter, 1996). These mutants show separation of the functions of Skp1 in G1 and G2 very clearly as these separate functions can be compensated for by the addition of the F-box protein affected i.e. by overexpression of *CDC4* or *CTF13* respectively. Although not a saturated screen, it is in a sense surprising that the *skp1* mutants generated in the *S. pombe* screen are not more diverse in the phenotypes they display. There is a uniform character to the initial phenotypes seen. It might therefore be that the functions of Skp1 throughout the cell cycle cannot be separated out as in an *S. cerevisiae* cell, possibly suggesting that in *S. pombe* the functions of the SCF are inter-dependent or rely on dimerisation of different F-boxes. How dimerisation could occur is unclear, as Skp1 has only one F-box binding site.

6.4 A model for Skp1 function from analysis of *skp1^{ts}A7* cells

The study of *skp1^{ts}A7* cells implies that there are functions for Skp1 in both G2 and M phase of the cell cycle. It is also possible that the defects that occur in these two phases of the cell cycle are dependent upon accumulation of an SCF substrate earlier in the cell cycle for example G1 or S phase and the occurrence of a delayed S phase in *skp1^{ts}A7* cells corroborates this (Fig 4.3.1).
To propose a unified model of the behaviour of Skp1 defective cells is difficult due to the modular nature of the SCF complex. However it could be proposed

that defects seen in *skp1^{ts}A7* cells are due to the accumulation of SCF substrates X, Y etc. The accumulation of these substrates would be due to the inability of defective Skp1 to adequately associate with the F-box proteins Pof1 and Pof3. The physiological consequences of these substrates accumulating are the activation of the DNA damage checkpoint and mitotic defects.
As discussed in Chapter 4 we propose activation of the DNA damage checkpoint occurs through over accumulation of a substrate, triggering signalling through Rad3 kinase. This can be understood in a manner analogous to overproduction of the Mph1 Spindle assembly checkpoint protein initiating signalling of the SAC in the absence of spindle damage. In Skp1 defective cells the checkpoint is activated unnecessarily and thus prevention of signalling through DNA damage checkpoint partially rescues the phenotype.
The second phase of Skp1 function, in M phase could be regarded as a consequence of accumulation of a different substrate. The accumulation of this substrate results in defective spindles that appear to be restricted by the nuclear membrane. One explanation for this phenomenon is that the nuclear envelope is required to undergo an SCF dependent change during mitosis to allow stretching of the nuclear membrane in conjunction with elongation of the spindle. This SCF dependent change would require degradation of a component of the nuclear membrane that increases its elasticity. In order to test this theory it would be interesting to examine the effects of deletions of certain nuclear envelope components in a *skp1^{ts}A7* cell. Alternatively FRAP (Fluorescence Recovery After Photobleaching) techniques could be used to monitor the elasticity of the nuclear membrane during different stages of mitosis to see if the membrane undergoes a change and also whether the rate of this change is affected in *skp1^{ts}A7* cells.
See Fig 6.4.1 for a diagram of Skp1's proposed function.

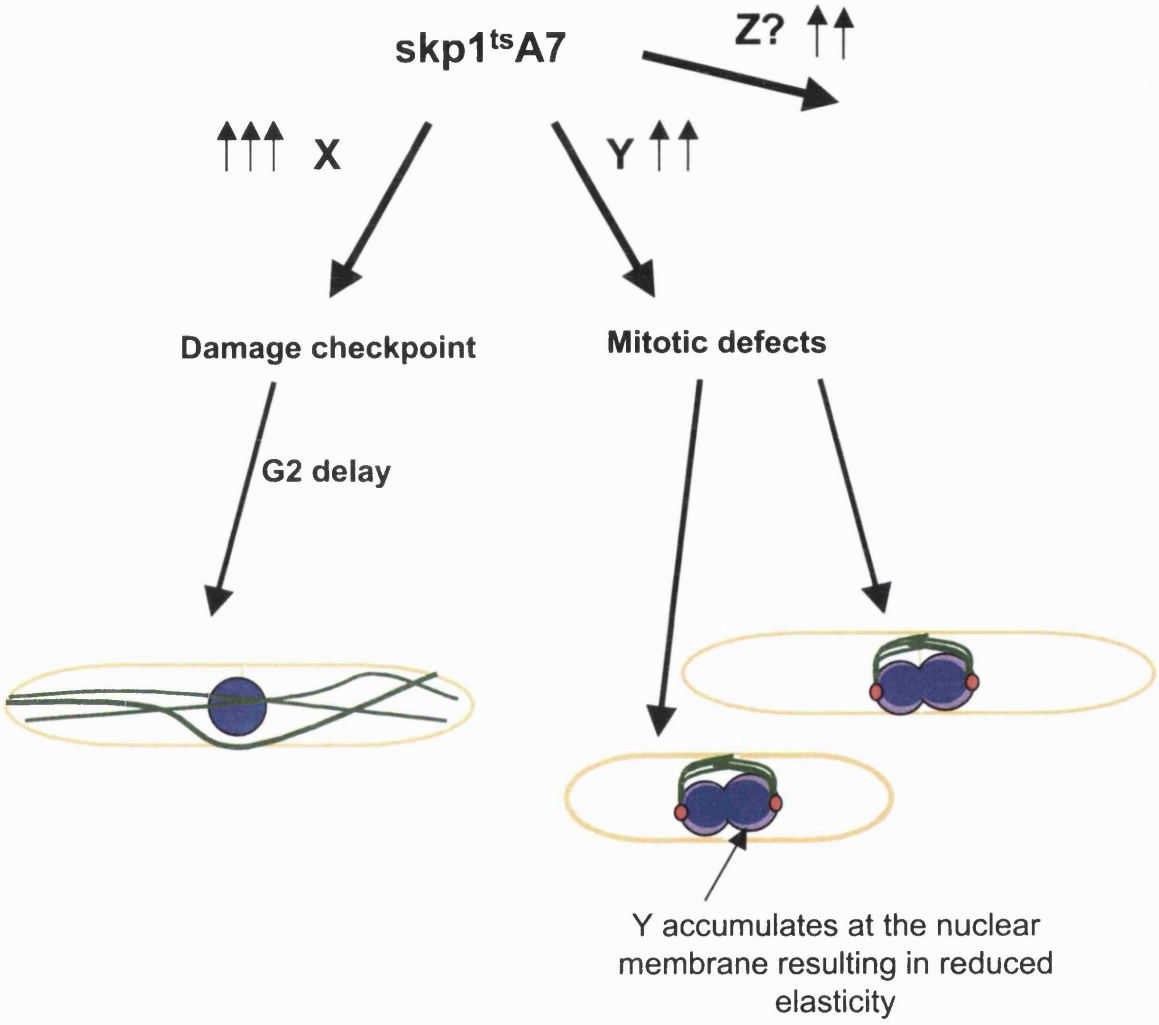

Fig. 6.4.1 general model to explain defective SCF function in *skp1^{ts}A7* cells

skp1^{ts}A7 cells incubated at 36°C accumulate a variety of substrates which result in the defects displayed by these cells. It is proposed that the accumulation of different substrates is responsible for the phenotypes seen in G2, activation of the DNA damage checkpoint, and M phase, mitotic spindle defects. This means that the mitotic defects are not dependent on G2 delay and could occur in cells which have not activated the DNA damage checkpoint.

6.5 The SCF in an evolutionary context

The SCF has been conserved across the species boundaries from yeast to humans. Unlike the APC whose substrates mainly concentrate around the mitosis period, the diversity of the SCF's substrates now being discovered is huge. Not only is the SCF known to be a key regulator of the G1 to S phase transition but it is involved in regulation of various signalling pathways and the potential list of substrates continues to expand. The advent of a modular ubiquitin ligase has been evolutionarily diversified with more and more proteins that could be involved in such ligases being discovered in the proteomes of higher eukaryotes. Given that regulated protein levels are essential for many switch like processes it is perhaps unsurprising that the cell requires a potentially enormous number of ubiquitin ligases. The ability of ubiquitin mediated proteolysis to completely remove a protein in a sharply defined period makes this a more reliable switch than regulated protein transcription. The end of a transcription period for a gene will result in residual protein in the cell unless some method of proteolysis removes it. A question that remains unanswered concerns why the cell should rely so heavily on one particular set of ubiquitin ligases. The absence of a central component is lethal in a haploid organism and in humans the absence of certain SCF functions would lead to accumulation of carcinogenic substrates. It is further interesting to ask why so many different complexes appear to depend on Skp1 as a central bridging molecule.

6.6 Future directions for understanding the SCF

Crucial to the further understanding of the role of Skp1 in the cell and the SCF complex as a whole is the identification of its substrates. The route to elaborating these is unclear as the SCF may have different targets dependent on growth conditions. The elucidation of target proteins through examination of individual F-box proteins is one potential method. Most of the F-box proteins in *S. pombe* are non-essential under normal vegetative growth conditions. However, it may be that some of these F-box proteins become essential in meiosis or growth under stress conditions. This is becoming apparent for

different activators of the APC or different cullin based ligase complexes at different stages of *C. elegans* embryonic development. The analysis of the targets of each individual F-box may be aided by examining the function of F-box deletions in different growth conditions. A further method for examining potential SCF substrates would be a large scale *in vitro* screen in which bacterially expressed proteins were tested assubstrates individually with a purified SCF complex. This would only be possible in smaller organisms such as the yeasts where the whole genome has been sequenced and large scale libraries of tagged proteins exist.

It is undoubtedly the case that there will be further substrates and roles for the SCF complex in this yeast. This is evidenced by the presence of multiple F-box protein ORFs in the *S. pombe* genome and the presence of examples of SCF mediated ubiquitination in mammalian, worm, fly, and budding yeast systems. It would seem therefore that the SCF is a ubiquitous ubiquitin ligase.

Chapter 7

Materials and methods

Introduction

This chapter details the experimental methods used throughout this thesis. It also gives details of the contents of buffers and the derivation of strains used.

7.1 solutions, buffers and media

All media and commonly used solution were provided by Cancer Research UK central services.

Media

L-Broth (LB)	170mM NaCl, 0.5%w/v yeast extract, 1% w/v bactotryptone.
YE5S	0.5% Difco yeast extract, 3% dextrose and 250mg/ml histidine, leucine, uracil, adenine and lysine.
EMM	14.7mM KH phthalate, 15mM Na_2HPO_4, 93.5mM NH_4Cl, 2% w/v glucose, salt and vitamin stocks. See: http://flosun.salk.edu/~forsburg/media.html for full details
EMM-NH_4Cl	As above – NH_4Cl
PBSA	170mM NaCl, 3mM KCl, 10mM Na_2HPO_4, 2mM KH_2PO_4 .

QIAGEN

Equilibration buffer	750mM NaCl, 50mM MOPS pH7.0, 15%v/v ethanol
Wash Buffer	50mM MOPS, 15%v/v ethanol
Elution buffer	1.25M NaCl, 50mM Tri-Hcl pH8.5, 15%v/v ethanol
P1	50mM glucose, 25mM Tris pH 8.0, 10mM EDTA
P2	200mM NaOH, 1%w/v SDS
P3	3M K Acetate

DNA manipulation

TE	10mM Tris-Hcl pH7.0, 0.1M EDTA.
10Xloading buffer	60%w/v sucrose, 0.1%w/v bromophenol blue.
TBE	45mM Tris base, 1mM EDTA
TAE	40mM Tris-acetate, 1mM EDTA
Taq Buffer	200mM Tris-Hcl pH6.8, 100mM KCl, 30mM $MgSO_4$, (0.5% Triton X-100)

Protein Biochemistry

STOP buffer	150mM NaCl, 50mM NaF, 10mM EDTA, 0.006% v/vNaN_3 pH8.0.

HB buffer	25mM MOPS pH7.2, 60mM β-glycerophosphate, 15mM-p-nitrophenyl-phosphate, 15mM $MgCl_2$, 15mM EGTA, 1mM dithiothreitol, 0.1mM sodium vanadate, 1% Triton X-100, 1mM PMSF, 20μg/ml leupeptin, 40μg/ml apoprotinin.
RIPA buffer	50mM Tris.Cl pH7.5, 150mM NaCl, 1% Nonidet P-40, 0.5% sodium deoxycholate, 0.1% SDS.
5X loading buffer (PAGE)	60mM Tris.Cl pH6.8, 25% glycerol, 2% SDS, 14.4mM 2-mercaptoethanol, 1% Bromophenol blue
SDS-PAGE buffer	25mM Tris, 250mM glycine pH8.3, 0.1%SDS
Transfer Buffer	39mM glycine, 48mM Tris base, 20% methanol
Sonication Buffer	50mM Sodium phosphate pH 8, 300mM NaCl

Immunofluorescence

PEM (pH6.9)	100mM PIPES, 1mM EGTA, 1mM $MgSO_4$
PEMS	PEM+ 1.2M sorbitol
PEMBAL (pH6.9)	PEM+ 1%BSA, 0.1% NaN_3, 100mM lysine hydrochloride

7.2 Yeast physiology

Nomenclature

A Fission yeast gene name consists of 3 italicised letters and a number e.g. *skp1*. A wild type allele may be denoted by a plus sign e.g. $skp1^{+}$. Temperature sensitive mutant alleles of a gene are indicated by a suffix of *ts* in superscript. An allele number is also used to identify different mutant alleles of the same gene e.g. $skp1^{ts}A7$. Proteins are named using the same three letters indicative of the gene but are not written in italics. The first letter is in upper case e.g. Skp1.

Gene deletions which have been achieved using a specific marker are shown by the gene name followed by :: and the replacement marker gene name. E.g. $fdh1::ura4^{+}$. A gene deletion can also be annotated by a Δ symbol. Sensitivity and resistance to the selectable marker kanamycin can be shown by an 's' or 'r' in superscript.

Budding yeast nomenclature

The gene names of budding yeast are typically shown as 3 upper case letters and a number in italics e.g. *SKP1*, a mutant allele is italicised and lower case e.g.*skp1*. Proteins names take the same format as fission yeast in this thesis.

Other nomenclature

Mammalian and *Xenopus* gene names and gene products are usually written as upper case letters. Genes are written in italicised upper case. Drosophila proteins are denoted in lower case letters with an upper case first letter and the gene names are italicised and lowercase.

Strain growth and maintenance

Techniques used to grow and maintain fission yeast strains and to store and revive cultures were performed as previously described (Moreno *et al.*, 1991). *S. pombe* cells were grown in either liquid media or on agar plates containing 1.6% agar. The contents of different media are shown above in section 7.1. Stocks of yeast strains were stored in Yellow Freezing Mix containing normal YE5S media containing 15-20% glycerol and maintained at –70 °C (Burke *et al.*, 2000) .

Selection media containing the drug 5-FOA was made by addtion of the drug at a concentration of 1mg/ml to hot, molten, YE5S agar. A sterile stirrer was added and bottles were placed on a magnetic stirrer with the lid replaced until the mixture was cool enough to pour.

Transformation of fission yeast

Transformations of plasmid DNA into yeast cells were carried out using lithium acetate and poly ethylene glycol (PEG) as previously described Ito *et al.*, (1983). Approximately 1 μg of plasmid DNA was used for these transformations.

PCR fragments for integration into the genome were transformed using Lithium acetate, PEG and DMSO previously described by Bahler *et al.*, (1998); Keeney and Boeke, (1994). Selective markers used in plasmid and integrant transformations were *LEU2*, *ura4*$^{+}$ and *kan*^{r}.

Synchronous cultures

G2 synchrony

Elutriations were carried our using a Beckman J6 centrifuge or a Beckman Coulter Avanti J-20 centrifuge as described by the manual and previously by Moreno *et al.*, (1991). YE5S medium was used and the rotor held at a temperature of 26°C throughout the elutriation. Elutriated cultures were then split and half the culture filtered and added to pre-warmed conditioned medium at 36°C. Synchrony was measured as the percentage of septated to non-septated cells at 26°C.

G1 synchrony

Nitrogen starvation block and release experiments used prototrophic strains. Cells were grown to mid log phase in rich medium, filtered and washed with MM medium minus nitrogen. Cells were then resuspended in the same nitrogen free, starvation medium. Cells were left in this medium for 14hrs at 26°C after which time they were filtered again and returned to rich medium and grown at 36°C. Synchrony was measured by flow cytometric analysis (FACS).

Flow cytometry

10^6-10^7 cells from relevant cultures were fixed in 70% ethanol. Cells were pelleted and rehydrated in 3ml 50mM Na_3citrate and then resuspended in 1ml 50mM Na_3citrate containing 0.1mg RNase A, 2μg/ml propidium iodide and incubated for 4hrs at 37°C. Before analysis cells were sonicated for 30s at setting 5 (soniprep 150 sonicator MSE). Flow cytometry was performed as described previously (Sazer and Sherwood, 1990) using a Becton-Dickinson FAC Scan with an excitation wavelength of 488nm and a detection wavelength of 510-550nm. Data analysis used the CELL QUEST software package.

Cell numbers and viability counts

20 or 200μl of sample was added to 10ml of Isoton (Beckman Coulter). Cells were sonicated as above and counted on a Sysmex Microcell counter F-800 in the white blood cell channel.

For viability counts cells were diluted in YE5S and plated out at 300 cells per plate and incubated at the permissive temperature (26°C) for each time point. Colonies that grew were counted and given as a percentage of the 300 plated cells.

Thiabendazole, Hydroxyurea and Ultra Violet light plating assays

Thiabendazole (TBZ) was added to plates at a concentration of 10μg/ml or 20μg/ml. Stock solutions were stored in DMSO at 1000x concentration, 4°C. Hydroxyurea (HU) was added to plates at a concentration of 5mM or 10mM. A fresh solution at 1M was made every time for use immediately.

Cells were serially diluted and spotted onto plates so that the first spot should contain $1x10^5$ cells and the last spot should contain ten cells. They were subsequently examined for growth at different temperatures.

For Ultra Violet light sensitivity strains were grown and counted as above then plated at 300 cells per plate. Plates were then exposed to UV light in a Stratalinker UV crosslinker 1800 at various doses for 30s and allowed to grow at the permissive temperature (26°C). Colonies were counted as a percentage of 300.

7.3 Fission yeast Strains

All tagging and expression from p3nmt promoter occur at endogenous loci. Plasmids are indicated by brackets.

Name	**Genotype**	**Derivation**
Wild Type strains		
CHP428	*h⁺ leu1⁻ura4⁻ his7⁻ ade6-m210*	Dr C. Hoffman
CHP429	*h⁻ leu1⁻ ura4⁻ his7⁻ ade6-m216*	Dr C. Hoffman
513	*h⁻ leu1⁻ ura4⁻*	lab stock
TP108-3D	*h⁺ leu1⁻ his2⁻ ura4⁻*	lab stock
Pertaining to *skp1^{ts}* mutant creation		

skp1Δ	CHP428/429 *diploid skp1::ura4*$^+$	this study
AL1	*h*$^-$ *leu1*$^-$ *ura4*$^-$ *skp1-ura4*$^+$	this study
AL1-A1	*h*$^-$ *leu1*$^-$ *ura4*$^-$ *skp1*^{ts}A1	this study
AL1-A2	*h*$^-$ *leu1*$^-$ *ura4*$^-$ *skp1*^{ts}A2	this study
AL1-A3	*h*$^-$ *leu1*$^-$ *ura4*$^-$ *skp1*^{ts}*A3*	this study
AL1-A4	*h*$^-$ *leu1*$^-$ *ura4*$^-$ *skp1*^{ts}*A4*	this study
AL2-A5	*h*$^-$ *leu1*$^-$ *ura4*$^-$ *skp1*^{ts}*A5*	this study
AL2-A6	*h*$^-$ *leu1*$^-$ *ura4*$^-$ *skp1*^{ts}*A6*	this study
AL2-A7	*h*$^-$ *leu1*$^-$ *ura4*$^-$ *skp1*^{ts}*A7*	this study
AL2-A8	*h*$^-$ *leu1*$^-$ *ura4*$^-$ *skp1*^{ts}*A8*	this study
AL45	*h*$^-$ *skp1*^{ts}*A7*	this study
AL14	*h*$^+$*his2*$^-$ *leu1*$^-$ *ura4*$^-$ *skp1*^{ts}*A7*	this study
AL155	*h*$^-$ *leu1*$^-$ *skp1-ura4::kan*^{r}	this study
TP619-94-2D	*h*$^-$ *leu1*$^-$ *ura4*$^-$ *rad3::ura4*$^+$ *skp1*^{ts}*94*	this study
TP619-94-5D	*h*$^-$ *leu1*$^-$ *ura4*$^-$ *his2*$^-$ *skp1*^{ts}*94*	this study
Pertaining to checkpoints		
AL31	*h*$^-$ *leu1*$^-$ *ura4*$^-$ *skp1*^{ts}*A7mad2::ura4*$^+$	this study
Chk1Δ	*h*$^+$ *leu1*$^-$ *ura4-D18 ade6.704 chk1::ura4*$^+$	this study
AL59	*h*$^-$ *leu1*$^-$ *ura4-D18ade6- skp1*^{ts}*A7 chk1::ura4*$^+$	this study
AL65	*h*$^-$ *leu1*$^-$ *ura4*$^-$ *skp1*^{ts}*A7 rad26::ura4*$^+$	this study
AL69	*h*$^-$ *leu1*$^-$ *ura4*$^-$ *skp1*^{ts}*A7 rad9::ura4*$^+$	this study
SKS1	*h*$^-$ *leu1*$^-$ *ura4-D18 ade6.704 rad3::ura4*$^+$	lab stock
AL20	*h*$^+$ *leu1*$^-$ *ura4-D18 his7- rad3::ura4*$^+$	this study
AL22	*h*$^-$ *leu1*$^-$ *ura4-D18 skp1*^{ts}*A7rad3::ura4*$^+$	this study
AL64	*h*$^-$ *leu1*$^-$ *ura4*$^-$ *skp1*^{ts}*A7 cds1::kan*^{r}	this study
SKP467-13	*h*$^-$ *leu1*$^-$ *ura4*$^-$ *chk1-myc*	Dr S. Katayama
AL144	*h*$^-$ *leu1*$^-$ *ura4*$^-$ *skp1*^{ts}*A7 chk1-myc*	this study
Fdh1Δ	*h*$^+$ *leu1*$^-$ *ura4*$^-$ *his2*$^-$ *fdh1::kan*^{r}	this study
TP624-10B	*h*$^-$ *ura4*$^-$ *fdh1::kan*^{r} *chk1::ura4*$^+$	this study
TP624-9C	*h*$^-$ *leu1*$^-$ *ura4*$^-$ *fdh1::kan*^{r} *cds1::kan*^{r}	this study
TP624-2C	*h*$^-$ *leu1*$^-$ *ura4*$^-$ *fdh1::kan*^{r} *cds1::kan*^{r} *chk1::ura4*$^+$	this study

TP612-10D	*h⁻ leu1⁻ ura4⁻ fdh1::kan^r rad3::ura4⁺*	this study
AL181	*h⁻ leu1⁻ ura4⁻ fdh1::kan^r skp1^ts A7*	this study
F-box tags		
SKP510	*h⁺leu1⁻ his2⁻ ade6.210 pof3-myc*	Dr S. Katayama
AL76	*h⁻ leu1⁻ ura4⁻ skp1^ts A7 pof3-myc*	this study
CLP9	*h⁻ leu1⁻ ura4⁻ pof1-myc*	C. Harrison
AL84	*h⁻ leu1⁻ ura4⁻ skp1^ts A7 pof1-myc*	this study
SKP414-17	*h⁻ leu1⁻ ura4⁻ pcu1-myc*	Dr S. Katayama
AL74	*h⁻ leu1⁻ ura4⁻ skp1^ts A7 pcu1-myc*	this study
SKP410-15	*h⁻ leu1⁻ ura4⁻ pop1-myc*	Dr S. Katayama
AL80	*h⁻ leu1⁻ ura4⁻ skp1^ts A7 pop1-myc*	this study
AL167	*h⁻ leu1⁻ ura4⁻ p3nmt-GFP-pof2⁺*	this study
AL169	*h⁻ leu1⁻ ura4⁻ p3nmt-GFP-pof2⁺ skp1^ts A7*	this study
AL95	*h⁻ leu1⁻ ura4⁻ pof5-myc*	this study
AL126	*h⁻ leu1⁻ ura4⁻ pof5-myc skp1^ts A7*	this study
AL166	*h⁻ leu1⁻ ura4⁻ p3nmt-GFP-pof6⁺*	this study
AL171	*h⁻ leu1⁻ ura4⁻ p3nmt-GFP-pof6⁺ skp1^ts A7*	this study
AL87	*h⁻ leu1⁻ ura4⁻ pof7-myc*	this study
AL127	*h⁻ leu1⁻ ura4⁻ pof7-myc skp1^ts A7*	this study
AL98	*h⁻ leu1⁻ ura4⁻ pof8-myc*	this study
AL124	*h⁻ leu1⁻ ura4⁻ pof8-myc skp1^ts A7*	this study
AL90	*h⁻ leu1⁻ ura4⁻ pof9-myc*	this study
AL123	*h⁻ leu1⁻ ura4⁻ pof9-myc skp1^ts A7*	this study
AL91	*h⁻ leu1⁻ ura4⁻ pof10-myc*	this study
AL120	*h⁻ leu1⁻ ura4⁻ pof10-myc skp1^ts A7*	this study
AL92	*h⁻ leu1⁻ ura4⁻ pof12-myc*	this study
AL129	*h⁻ leu1⁻ ura4⁻ pof12-myc skp1^ts A7*	this study
AL89	*h⁻ leu1⁻ ura4⁻ pof13-myc*	this study
AL131	*h⁻ leu1⁻ ura4⁻ pof13-myc skp1^ts A7*	this study
AL182	*h⁻ leu1⁻ ura4⁻ p3nmt-GFP-fdh1⁺*	this study

AL177	*h⁻ leu1⁻ ura4⁻ p3nmt-GFP-fdh1⁺ skp1ᵗˢA7*	this study
AL179	*h⁻ leu1⁻ ura4⁻ p3nmt-GFP-fdh1⁺ pcu1-myc*	this study
Mid2 experiments		
AL164	*h⁻ leu1⁻ ura4⁻ skp1ᵗˢA7 mid2::kanʳ*	this study
AL165	*h⁻ leu1⁻ ura4⁻ mid2::kanʳ*	this study
AL166	*h⁻ leu1⁻ ura4⁻ p3nmt-mid2⁺ skp1ᵗˢA7*	this study
Mid2OP	*h⁻ leu1⁻ ura4⁻ p3nmt-mid2⁺*	this study
Mid2 HA	*h⁻ leu1⁻ ura4⁻ mid2-HA*	this study
Mid2HAskp1ts	*h⁻ leu1⁺ ura4⁻ mid2-HA skp1ᵗˢA7*	this study
Rum1 experiments		
Rum1Δ	*h⁻ leu1⁻ ura4⁻ rum1::kanʳ skp1ᵗˢA7*	this study
AL158	*h⁻ leu1⁻ ura4⁻ rum1-HA skp1ᵗˢA7*	this study
AL159	*h⁻ leu1⁻ ura4⁻ rum1-HA*	this study
Miscellaneous		
Skp1nmt	*h⁻ p3nmt-HA-skp1⁺ ura4⁻ ade6⁻*	this study
354	*h⁺ leu1.32 ura4-D18 cut11-GFP-ura4⁺*	Dr R. west
AL190	*h⁻ leu1⁻ cut11-GFP-ura4⁺ skp1ᵗˢA7*	this study
AL149	*h⁻ leu1⁻ ura4⁻ cut12-CFP skp1ᵗˢA7*	this study
AL108	*h⁻ leu1⁻ ura4⁻ skp1ᵗˢA7 (atb2-GFP leu1⁺)*	this study

7.4 Molecular Biological techniques

Molecular biological techniques were used as described (Maniatis *et al.*, 1982) including growth and transformation of bacterial cells, gel electrophoresis of DNA in TBE and TAE buffer, restriction enzyme digests, minipreps and preparation of competent bacteria.

Nucleic Acid preparation and manipulation

Yeast genomic DNA was prepared based on the method described previously (Burke *et al.*, 2000).

Enzymic digestion of DNA with restriction enzymes was carried out as recommended by the suppliers (New England Biolabs)
DNA fragments were examined on 1%, 1.5% and occasionally where fragments were very small 2% (w/v) agarose in 1XTBE buffer. These gels were run at 100v in 1XTBE buffer in Embitech Runone Electrophoresis Cells.

Polymerase Chain Reaction

Mutagenic PCR

PCR under modified conditions was used to create fragments containing randomised mutations. This was based upon methods previously described to attain approximately one mutation per fragment (Cadwell and Joyce, 1992; Leung *et al.*, 1989). Generation of mutated PCR fragments were performed with Taq polymerase. An increased amount of one purine and one pyrimidine were used to prevent mutational bias. These were used as follows: dCTP and dTTP at a final reaction concentration of 1mM and dATP and dGTP at a final concentration of 0.2mM. Template was supplied at ~50ng per reaction and primers at ~100ng per reaction. In addition 5mM Mg^{2+} ions were supplied for each reaction.
A second set of mutagenic PCR conditions was used to create other mutated fragments. In these reactions the concentration of dGTP was increased to 2mM whilst the remaining dNTPs were supplied at 0.2mM per reaction. The total reaction volume was 100μl and contained 5 units of enzyme.

Non Mutagenic PCR

Normal PCR reactions were carried out using Vent (New England Biolabs), Expand High Fidelity (Roche) or LA Taq (Takara) polymerases with buffers supplied by the manufacturers. dNTPs were supplied at 0.2mM in reaction volumes of 50 or 100μl.
For colony PCR samples were prepared in a similar manner without the addition of enzyme. A toothpick of yeast colony was suspended in the reaction mix and heated to 95°C for 5 minutes. Subsequently enzyme was added and PCR started.

All PCRs were performed in a Peltier Thermal Cycler-200. All products were purified using Wizard DNA Clean Up System (Promega) according to the manufacturers instructions and run on DNA agarose gels to check for product size.

Sequencing

Oligonucleotide primers of 20 base pairs each were designed based on the known sequence of the *skp1*$^{+}$ gene in *S. pombe*. These primers were separated at intervals of 200 base pairs throughout the gene. PCR reactions including each of these primers and *skp1* mutant genomic DNA were carried out with ABI Prism Dye Terminator Cycle Sequencing Ready Reaction Kit and followed by automated read out using a Perkin Elmer sequencer, ABI prism 377.

Gene Disruption

All genes were disrupted using PCR generated fragments (Bahler *et al.*, 1998). The 1.8kb *ura4*$^{+}$ gene was amplified with flanking sequences corresponding to the 5' and 3' ends of the relevant genes. These fragments were transformed into a *ura4*$^{-}$ diploid made from CHP428 and CHP429 strains. *ura4*$^{+}$ colonies were selected on plates lacking uracil and then sporulated on plates lacking nitrogen. Asci from heterozygous diploids were dissected (Burke *et al.*, 2000) and germination of haploids monitored. Where a 2:2 ratio is seen with 2 growing spores lacking the ability to grow on ura- plates the disruption is deemed lethal to the cell. Genes were also disrupted in an identical manner but using the Kanamycin resistance gene.

Overexpression and N/C-terminal epitope tagging of genes in their chromosomal location.

Thiamine repressible promoters with epitope tags HA or GFP were integrated into the genome in front of the initiator ATG codon of genes by a PCR-based gene targeting method (Bahler *et al.*, 1998). In most cases the nmt1, strong promoter was used. This promoter is repressed in the presence of thiamine but due to its strength there is often transcriptional leak-through. In most cases the strains used were grown under repressed conditions (+thiamine) to drive the

promoter at low levels. In order to over produce the protein, cells were grown in MM without thiamine.
C-terminal tagging of genes with HA, Myc or GFP eptiopes was also carried out using PCR generated fragments as described Bahler *et al.*, (1998). All tagging was confirmed by PCR to look for increased gene size and western blotting with specific antibodies.

Transformation and isolation of plasmid DNA in *E. coli*

Competent *E. coli* stored at –70°C were thawed on ice and incubated 20 minutes with 10μg of plasmid DNA. Cells were heat shocked at 42°C for 90s after which 1ml of LB media was added. The cells were allowed to recover at 37°C for 30 minutes to 1 hour before being plated onto LB plates containing Ampicillin.

3-5ml of *E. coli* were grown overnight in LB + 100μg/ml ampicillin at 37°C. Cells were harvested by centrifugation at 4000rpm for 5 minutes and the pellet was resuspended in 150μl of solution P1 (QIAGEN) containing 100μg/ml of RNase A.
150μl of solution P2 (QIAGEN) was added and cells were left to incubate for 5 minutes at room temperature to allow alkaline lysis of the bacterial cell membranes and denaturation of both plasmid and bacterial DNA.
150μl of chilled solution P3 (QIAGEN) was added to neutralise alkaline conditions and increase salt concentration. Cells were left to incubate on ice for 15 minutes to allow full precipitation of bacteria protein and chromosomal DNA. The plasmid DNA which remains in solution was separated from the cell debris by centrifugation 13,000rpm for 30 mins. Plasmid DNA was then bound to a silica column (QIAGEN) previously equilibrated with equilibration buffer. The column was then washed twice with 1.5ml of wash buffer and the plasmid eluted from the column with 800μl of elution buffer. The Plasmid DNA was recovered by isopropanol precipitation.

7.5 Protein Biochemistry

Skp1 purification from bacterially expressed protein.

Complementary DNA of *skp1*$^{+}$ was cloned into the expression vector pET14b in frame with six copies of the histidine tag and under an IPTG inducible promoter. This plasmid was transformed into *E. coli* and selected by the ability to grow in the presence of the antibiotics, ampicillin and chloramphenicol. 100ml liquid cultures of E.coli were grown in LB with ampicillin and chloramphenicol overnight. 20mls of this culture was diluted into 1 litre of fresh medium, grown for an hour or until turbidity reached ~0.4 when measured with a wavelength of 600nm. IPTG was added (final concentration of 2mM) to induce the expression of Skp1.Cells were grown for a further 4 hours. The cell culture was then spun at 6000rpm for 10 mins to pellet the cells. The pellet was then resuspended in 3 volumes of its wet weight with sonication buffer and frozen in dry ice and ethanol followed by thawing in cold water. The solution was then kept on ice and sonicated at setting 15 (soniprep 150 sonicator MSE). The solution was given 5 pulses of 1 minute each with cooling intervals of 2 minutes between each pulse. The sonicated solution was spun for 20 minutes at 10, 000 rpm and supernatant used in Nickel columns (QIAGEN) according to instructions supplied by the manufacturers.

Western blot analysis

Fission yeast protein extract was either prepared using glass beads disruption or NaOH lysis. For glass bead disruption cells were lysed in either HB buffer or RIPA lysis buffer following the method previously described Moreno *et al.*, (1991). Following lysis with glass beads the extract was clarified and the protein concentration measured using the Bradford Assay (BioRad). 30μg of protein extracts were boiled in sample buffer for 4 minutes and then run on 10% SDS-polyacrylamide gels or 4-15% gradient SDS-Polyacrylamide gels (BioRad/Atto). For NaOH lysis of yeast cells, cell numbers were measured as described in the section on cell number and viability counting. Between 10^{6} -10^{8} cells were used per sample. Cells were harvested by centrifugation at 2500rpm and washed once with water. 500μl of chilled water and 500μl of 0.6M NaOH were then

added to the cells, which were incubated on ice for 10 minutes before centrifugation at 4°C for 2 minutes at 4000rpm in a bench top centrifuge. The supernatant was discarded and cell pellet resuspended in 40μl of sample buffer. This was then boiled for 4 minutes and 20μl run on an SDS-polyacrylamide gel as above.

Blotting of gels was carried out as follows, proteins were first transferred onto Immobilon™-P (Millipore) transfer membrane. After blocking for 1hr in 5% Milk PBSA solution with 0.01% Tween detergent, antibodies were added in the same solution. Membranes were incubated overnight at 4°C washed and secondary antibody of Horseradish peroxidase conjugated goat anti-rabbit or goat anti-mouse IgG (BioRad) were incubated with the blot. A chemiluminescence system (ECL Amersham) was used to detect the bound antibodies.

Immunoprecipitation

For immunoprecipitation analysis 2mg of soluble protein extract was prepared as described for western blot analysis using glass bead lysis and RIPA buffer. 2.5μg of polyclonal αskp1 antibody was incubated with the protein extract at 4°C for 1 hour before the addition of protein A sepharose beads (Affi-prep ® BioRad) pre-washed in RIPA buffer. Beads and extract were further incubated at 4°C for an hour. The protein A beads were then washed 8 times in RIPA buffer before the addition of 30μl of sample buffer. Samples were boiled for 4 minutes and then run on 5-20% SDS-polyacrylamide gels. 30μg of the corresponding extract untreated with antibody or beads was also run on a corresponding gel. Blots were transferred and probed as described above.

NIH image quantification

The computer program NIH image was used to quantify the intensity of bands resulting from Immunoprecipitation western blots. This program allows an image scanned into the computer to be analysed on the pixel density of any one area. Blots were directly scanned into the computer in Adobe Photoshop. A rectanglular area was drawn that fitted around a band on the western blot and the mean pixel density within that area was measured by the program. The

same rectangle was then used to measure the pixel density of a region beneath the band as background. The pixel density of the background region was subtracted from the pixel density of the band region to normalise the bands for background.

Antibodies used in western and immunoprecipitation analysis

C-Myc9E10	mouse mono	BabCO	1/1000 or1/2000
C-Myc	rabbit poly	BabCO	IP
HA12CA5	mouse mono	Clontech	1/1000
Cdc2 Y100	mouse mono	Dr H.Yamano	1/2000
GFP	mouse mono	Roche	1/1000
GFP	mouse mono	Clontech	1/1000
Skp1	Rabbit poly	This study	IP or 1/1000
α-tubulin	mouse mono	Sigma	1/1000 or1/2000

Phosphorylation shift assay

Strains containing chk1-myc could be assayed for a phosphorylation band shift (Walworth and Bernards, 1996). Extracts were prepared using the glass bead method described above and run on a specialised 10% SDS-polyacrylamide gel containing an increased concentration of acrylamide to bis-acrylamide, which allowed greater separtation of proteins.

The ratio of acrylamide was increased from 29:1 to 200:1 by the addition of pure 30% acrylamide solution to the gel mixture before pouring (Katayama *et al.*, 2002).

7.6 Microscopy

Visualisation of DNA, septa, mitochondria and vacuoles

Analysis of DNA and of cell septa, was performed by fixing 850μl of a culture of cells, with 150μl of formaldehyde for 10 minutes at 4°C. Cells were washed with PBSA and then viewed under a fluorescence microscope by addition of DAPI or

calcofluor stain. Mitochondria were visualised using 2-(4-dimethylaminostyryl)-1-methylpridinium iodide (DASPMI, Sigma) as described (Yaffe *et al.*, 1996).

Indirect immunofluorescence microscopy

Methods for indirect immunofluorescence were adapted from Hagan and Hyams, (1988)

5 X 10^7 cells were filtered and fixed in methanol at –70°C for 24hrs. After 3 washes in PEM buffer the cell wall was digested with 0.6mg/ml Zymolyase 20T in PEMS for 70 minutes. Cells were then pelleted and resuspended in 1%Triton-X100 in PEMS for 5 minutes. A further 3 washes in PEM were carried out before cells were incubated in PEMBAL for 30 minutes. Primary antibody (α-tubulin TAT-1, monoclonal 1:40) was added in 40μl PEMBAL and left overnight to incubate at room temperature. Primary antibody was washed out using PEMBAL and secondary antibody (Cy3 conjugated sheep α mouse IgG 1:500) added in 200μl of PEMBAL. Cells were incubated in the dark for 1-2 hours. After washes to remove the secondary antibody cells were resuspended in PBSA+0.2μg/ml sodium azide. Immunofluorescence images were viewed with a Zeiss Co, Axioplan 2 imaging microscope attached to a Hamamatsu ORCA-ER I digital camera and Pentium III processor. A laser scanning confocal microscope LSM510 (Zeiss Co.) was also used. Images were processed using Kinteic imaging advance 6 software and Adobe ® Photoshop versions 5.5, 6 or 7.

Direct immunofluorescence microscopy was also used on a strain containing cut11-GFP. Cells were fixed as described above and stained for tubulin to provide double staining.

Antibodies used for indirect immunofluorescence

Primary	anti α-tubulin (TAT1)	Dr. Keith Gull	monoclonal	1/40

Secondary:

cy3 conjugated sheep anti-mouse IgG	Sigma	monoclonal	1/500

Live cell Imaging

skp1^{ts}-A7 cells expressing the α-tubulin gene *atb2^{+}* GFP or the Spindle Pole Body marker gene *cut12^{+}* GFP from a multicopy plasmid under control of the nmt1 promoter were used. Cultures were grown to mid log phase 5X10^{6} cells/ml MM at 26°C filtered and washed with YE5S then transferred to YE5S media at 36°C for four hours in order to see the temperature sensitive phenotype. Cells were mounted on a thin layer of rich media agar beneath a cover slip. The microscope stage was pre-heated and stabilised at 36°C. Live images were taken using a Zeiss Co, Axioplan 2 imaging microscope attached to a Hamamatsu ORCA-ER I digital camera and Pentium III processor. The images were processed using Kinteic Imaging Advance 6 software and Adobe ® Photoshop versions 5.5, 6 or 7.

Bibliography

Abraham, R.T. (2001) Cell cycle checkpoint signaling through the ATM and ATR kinases. *Genes Dev*, **15**, 2177-2196.

Amon, A. (1999) The spindle checkpoint. *Curr Opin Genet Dev*, **9**, 69-75.

Aravind, L. and Koonin, E.V. (1999) Fold prediction and evolutionary analysis of the POZ domain: structural and evolutionary relationship with the potassium channel tetramerization domain. *J Mol Biol*, **285**, 1353-1361.

Aso, T., Haque, D., Barstead, R.J., Conaway, R.C. and Conaway, J.W. (1996) The inducible elongin A elongation activation domain: structure, function and interaction with the elongin BC complex. *EMBO J*, **15**, 5557-5566.

Bahler, J., Wu, J.Q., Longtine, M.S., Shah, N.G., McKenzie, A., 3rd, Steever, A.B., Wach, A., Philippsen, P. and Pringle, J.R. (1998) Heterologous modules for efficient and versatile PCR-based gene targeting in *Schizosaccharomyces pombe*. *Yeast*, **14**, 943-951.

Bai, C., Sen, P., Hofmann, K., Ma, L., Goebl, M., Harper, J.W. and Elledge, S.J. (1996) SKP1 connects cell cycle regulators to the ubiquitin proteolysis machinery through a novel motif, the F-box. *Cell*, **86**, 263-274.

Barral, Y., Jentsch, S. and Mann, C. (1995) G1 cyclin turnover and nutrient uptake are controlled by a common pathway in yeast. *Genes Dev*, **9**, 399-409.

Bartek, J. and Lukas, J. (2001) p27 destruction: Cks1 pulls the trigger. *Nat Cell Biol*, **3**, E95-98.

Bentley, N.J., Holtzman, D.A., Flaggs, G., Keegan, K.S., DeMaggio, A., Ford, J.C., Hoekstra, M. and Carr, A.M. (1996) The *Schizosaccharomyces pombe* rad3 checkpoint gene. *EMBO J*, **15**, 6641-6651.

Berndt, C., Bech-Otschir, D., Dubiel, W. and Seeger, M. (2002) Ubiquitin system: JAMMing in the name of the lid. *Curr Biol*, **12**, R815-817.

Blatch, G.L. and Lassle, M. (1999) The tetratricopeptide repeat: a structural motif mediating protein-protein interactions. *Bioessays*, **21**, 932-939.

Blondel, M., Galan, J.M., Chi, Y., Lafourcade, C., Longaretti, C., Deshaies, R.J. and Peter, M. (2000) Nuclear-specific degradation of Far1 is controlled by the localization of the F-box protein Cdc4. *EMBO J*, **19**, 6085-6097.

Boyartchuk, V.L., Ashby, M.N. and Rine, J. (1997) Modulation of Ras and a-factor function by carboxyl-terminal proteolysis. *Science*, **275**, 1796-1800.

Bridge, A.J., Morphew, M., Bartlett, R. and Hagan, I.M. (1998) The fission yeast SPB component Cut12 links bipolar spindle formation to mitotic control. *Genes Dev*, **12**, 927-942.

Brower, C.S., Sato, S., Tomomori-Sato, C., Kamura, T., Pause, A., Stearman, R., Klausner, R.D., Malik, S., Lane, W.S., Sorokina, I., Roeder, R.G., Conaway, J.W. and Conaway, R.C. (2002) Mammalian mediator subunit mMED8 is an Elongin BC-interacting protein that can assemble with Cul2 and Rbx1 to reconstitute a ubiquitin ligase. *Proc Natl Acad Sci U S A*, **99**, 10353-10358.

Burke, B. and Ellenberg, J. (2002) Remodelling the walls of the nucleus. *Nat Rev Mol Cell Biol*, **3**, 487-497.

Burke, D., Dawson, D. and Stearns, T. (2000) *Methods in Yeast Genetics*. Cold Spring Harbour Laboratory Press.

Cadwell, R.C. and Joyce, G.F. (1992) Randomization of genes by PCR mutagenesis. *PCR Methods Appl*, **2**, 28-33.

Caspari, T., Dahlen, M., Kanter-Smoler, G., Lindsay, H.D., Hofmann, K., Papadimitriou, K., Sunnerhagen, P. and Carr, A.M. (2000) Characterization of *Schizosaccharomyces pombe* Hus1: a PCNA-related protein that associates with Rad1 and Rad9. *Mol Cell Biol*, **20**, 1254-1262.

Cenciarelli, C., Chiaur, D.S., Guardavaccaro, D., Parks, W., Vidal, M. and Pagano, M. (1999) Identification of a family of human F-box proteins. *Curr Biol*, **9**, 1177-1179.

Connelly, C. and Hieter, P. (1996) Budding yeast SKP1 encodes an evolutionarily conserved kinetochore protein required for cell cycle progression. *Cell*, **86**, 275-285.

Deshaies, R.J. (1999) SCF and Cullin/Ring H2-based ubiquitin ligases. *Annu Rev Cell Dev Biol*, **15**, 435-467.

Ding, R., West, R.R., Morphew, D.M., Oakley, B.R. and McIntosh, J.R. (1997) The spindle pole body of *Schizosaccharomyces pombe* enters and leaves the nuclear envelope as the cell cycle proceeds. *Mol Biol Cell*, **8**, 1461-1479.

Doree, M. and Hunt, T. (2002) From Cdc2 to Cdk1: when did the cell cycle kinase join its cyclin partner? *J Cell Sci*, **115**, 2461-2464.

Duan, D.R., Pause, A., Burgess, W.H., Aso, T., Chen, D.Y., Garrett, K.P., Conaway, R.C., Conaway, J.W., Linehan, W.M. and Klausner, R.D. (1995) Inhibition of transcription elongation by the VHL tumor suppressor protein. *Science*, **269**, 1402-1406.

Edwards, R.J., Bentley, N.J. and Carr, A.M. (1999) A Rad3-Rad26 complex responds to DNA damage independently of other checkpoint proteins. *Nat Cell Biol*, **1**, 393-398.

Elledge, S.J. (1996) Cell cycle checkpoints: preventing an identity crisis. *Science*, **274**, 1664-1672.

Elsasser, S., Chi, Y., Yang, P. and Campbell, J.L. (1999) Phosphorylation controls timing of Cdc6p destruction: A biochemical analysis. *Mol Biol Cell*, **10**, 3263-3277.

Evans, T., Rosenthal, E.T., Youngblom, J., Distel, D. and Hunt, T. (1983) Cyclin: a protein specified by maternal mRNA in sea urchin eggs that is destroyed at each cleavage division. *Cell*, **33**, 389-396.

Fantes, P.A. (1977) Control of cell size and cycle time in *Schizosaccharomyces pombe*. *J Cell Sci*, **24**, 51-67.

Fantes, P.A. and Nurse, P. (1978) Control of the timing of cell division in fission yeast. Cell size mutants reveal a second control pathway. *Exp Cell Res*, **115**, 317-329.

Feldman, R.M., Correll, C.C., Kaplan, K.B. and Deshaies, R.J. (1997) A complex of Cdc4p, Skp1p, and Cdc53p/cullin catalyzes ubiquitination of the phosphorylated CDK inhibitor Sic1p [see comments]. *Cell*, **91**, 221-230.

Flick, J.S. and Johnston, M. (1991) GRR1 of *Saccharomyces cerevisiae* is required for glucose repression and encodes a protein with leucine-rich repeats. *Mol Cell Biol*, **11**, 5101-5112.

Freemont, P.S. (2000) RING for destruction? *Curr Biol*, **10**, R84-87.

Funabiki, H., Kumada, K. and Yanagida, M. (1996a) Fission yeast Cut1 and Cut2 are essential for sister chromatid separation, concentrate along the metaphase spindle and form large complexes. *EMBO J*, **15**, 6617-6628.

Funabiki, H., Yamano, H., Kumada, K., Nagao, K., Hunt, T. and Yanagida, M. (1996b) Cut2 proteolysis required for sister-chromatid seperation in fission yeast. *Nature*, **381**, 438-441.

Gachet, Y., Tournier, S., Millar, J.B. and Hyams, J.S. (2001) A MAP kinase-dependent actin checkpoint ensures proper spindle orientation in fission yeast. *Nature*, **412**, 352-355.

Galan, J.M. and Peter, M. (1999) Ubiquitin-dependent degradation of multiple F-box proteins by an autocatalytic mechanism. *Proc Natl Acad Sci U S A*, **96**, 9124-9129.

Galan, J.M., Wiederkehr, A., Seol, J.H., Haguenauer-Tsapis, R., Deshaies, R.J., Riezman, H. and Peter, M. (2001) Skp1p and the F-box protein Rcy1p form a non-SCF complex involved in recycling of the SNARE Snc1p in yeast. *Mol Cell Biol*, **21**, 3105-3117.

Ganoth, D., Bornstein, G., Ko, T.K., Larsen, B., Tyers, M., Pagano, M. and Hershko, A. (2001) The cell-cycle regulatory protein Cks1 is required for SCF(Skp2)-mediated ubiquitinylation of p27. *Nat Cell Biol*, **3**, 321-324.

Geyer, R., Wee, S., Anderson, S., Yates, J. and Wolf, D.A. (2003) BTB/POZ domain proteins are putative substrate adaptors for cullin 3 ubiquitin ligases. *Mol Cell*, **12**, 783-790.

Gong, L. and Yeh, E.T. (1999) Identification of the activating and conjugating enzymes of the NEDD8 conjugation pathway. *J Biol Chem*, **274**, 12036-12042.

Griffiths, D.J., Barbet, N.C., McCready, S., Lehmann, A.R. and Carr, A.M. (1995) Fission yeast rad17: a homologue of budding yeast RAD24 that shares regions of sequence similarity with DNA polymerase accessory proteins. *EMBO J*, **14**, 5812-5823.

Groisman, R., Polanowska, J., Kuraoka, I., Sawada, J., Saijo, M., Drapkin, R., Kisselev, A.F., Tanaka, K. and Nakatani, Y. (2003) The ubiquitin ligase activity in the DDB2 and CSA complexes is differentially regulated by the COP9 signalosome in response to DNA damage. *Cell*, **113**, 357-367.

Hagan, I.M. and Hyams, J.S. (1988) The use of cell division cycle mutants to investigate the control of microtubule distribution in the fission yeast *Schizosaccharomyces pombe*. *J Cell Sci*, **89 (Pt 3)**, 343-357.

Hardwick, K.G., Weiss, E., Luca, F.C., Winey, M. and Murray, A.W. (1996) Activation of the budding yeast spindle assembly checkpoint without mitotic spindle disruption. *Science*, **273**, 953-956.

Hartwell, L.H. and Weinert, T.A. (1989) Checkpoints: controls that ensure the order of cell cycle events. *Science*, **246**, 629-634.

He, X., Jones, M.H., Winey, M. and Sazer, S. (1998) Mph1, a member of the Mps1-like family of dual specificity protein kinases, is required for the spindle checkpoint in *S. pombe*. *J Cell Sci*, **111 (Pt 12)**, 1635-1647.

Heissmeyer, V., Krappmann, D., Hatada, E.N. and Scheidereit, C. (2001) Shared pathways of IkappaB kinase-induced SCF(betaTrCP)-mediated ubiquitination and degradation for the NF-kappaB precursor p105 and IkappaBalpha. *Mol Cell Biol*, **21**, 1024-1035.

Hermand, D., Bamps, S., Tafforeau, L., Vandenhaute, J. and Makela, T.P. (2003) Skp1 and the F-box protein Pof6 are essential for cell separation in fission yeast. *J Biol Chem*, **278**, 9671-9677.

Hershko, A. and Ciechanover, A. (1992) The ubiquitin system for protein degradation. *Annu Rev Biochem*, **61**, 761-807.

Hochstrasser, M. (1996) Ubiquitin-dependent protein degradation. *Annu Rev Genet*, **30**, 405-439.

Hoyt, M.A., Totis, L. and Roberts, B.T. (1991) *S. cerevisiae* genes required for cell cycle arrest in response to loss of microtubule function. *Cell*, **66**, 507-517.

Ikebe, C., Kominami, K., Toda, T. and Nakayama, K. (2002) Isolation and characterization of a novel F-box protein Pof10 in fission yeast. *Biochem Biophys Res Commun*, **290**, 1399-1407.

Inoue, S. and Salmon, E.D. (1995) Force generation by microtubule assembly/disassembly in mitosis and related movements. *Mol Biol Cell*, **6**, 1619-1640.

Irniger, S., Piatti, S., Michaelis, C. and Nasmyth, K. (1995) Genes involved in sister chromatid separation are needed for B-type cyclin proteolysis in budding yeast. *Cell*, **81**, 269-278.

Ito, H., Fukuda, Y., Murata, K. and Kimura, A. (1983) Transformation of intact yeast cells treated with alkali cations. *J Bacteriol*, **153**, 163-168.

Iwai, K., Yamanaka, K., Kamura, T., Minato, N., Conaway, R.C., Conaway, J.W., Klausner, R.D. and Pause, A. (1999) Identification of the von Hippel-lindau tumor-suppressor protein as part of an active E3 ubiquitin ligase complex [see comments]. *Proc Natl Acad Sci U S A*, **96**, 12436-12441.

Jaquenoud, M., Gulli, M.P., Peter, K. and Peter, M. (1998) The Cdc42p effector Gic2p is targeted for ubiquitin-dependent degradation by the SCFGrr1 complex. *EMBO J*, **17**, 5360-5373.

Jiang, J. and Struhl, G. (1998) Regulation of the Hedgehog and Wingless signalling pathways by the F-box/WD40-repeat protein Slimb. *Nature*, **391**, 493-496.

Kaiser, P., Flick, K., Wittenberg, C. and Reed, S.I. (2000) Regulation of transcription by ubiquitination without proteolysis: Cdc34/SCF(Met30)-mediated inactivation of the transcription factor Met4. *Cell*, **102**, 303-314.

Kamura, T., Burian, D., Yan, Q., Schmidt, S.L., Lane, W.S., Querido, E., Branton, P.E., Shilatifard, A., Conaway, R.C. and Conaway, J.W. (2001) Muf1, a novel Elongin BC-interacting leucine-rich repeat protein that can assemble with Cul5 and Rbx1 to reconstitute a ubiquitin ligase. *J Biol Chem*, **276**, 29748-29753.

Kamura, T., Koepp, D.M., Conrad, M.N., Skowyra, D., Moreland, R.J., Iliopoulos, O., Lane, W.S., Kaelin, W.G., Jr., Elledge, S.J., Conaway, R.C., Harper, J.W. and Conaway, J.W. (1999) Rbx1, a component of the VHL tumor suppressor complex and SCF ubiquitin ligase [see comments]. *Science*, **284**, 657-661.

Kamura, T., Sato, S., Haque, D., Liu, L., Kaelin, W.G., Jr., Conaway, R.C. and Conaway, J.W. (1998) The Elongin BC complex interacts with the conserved SOCS-box motif present in members of the SOCS, ras, WD-40 repeat, and ankyrin repeat families. *Genes Dev*, **12**, 3872-3881.

Kamura, T., Sato, S., Iwai, K., Czyzyk-Krzeska, M., Conaway, R.C. and Conaway, J.W. (2000) Activation of HIF1alpha ubiquitination by a reconstituted von Hippel-Lindau (VHL) tumor suppressor complex. *Proc Natl Acad Sci U S A*, **97**, 10430-10435.

Kaplan, K.B., Hyman, A.A. and Sorger, P.K. (1997) Regulating the yeast kinetochore by ubiquitin-dependent degradation and Skp1p-mediated phosphorylation. *Cell*, **91**, 491-500.

Karin, M. and Ben-Neriah, Y. (2000) Phosphorylation meets ubiquitination: the control of NF-[kappa]B activity. *Annu Rev Immunol*, **18**, 621-663.

Katayama, S., Kitamura, K., Lehmann, A., Nikaido, O. and Toda, T. (2002) Fission Yeast F-box Protein Pof3 Is Required for Genome Integrity and Telomere Function. *Mol Biol Cell*, **13**, 211-224.

Kawakami, T., Chiba, T., Suzuki, T., Iwai, K., Yamanaka, K., Minato, N., Suzuki, H., Shimbara, N., Hidaka, Y., Osaka, F., Omata, M. and Tanaka, K. (2001) NEDD8 recruits E2-ubiquitin to SCF E3 ligase. *EMBO J*, **20**, 4003-4012.

Keeney, J.B. and Boeke, J.D. (1994) Efficient targeted integration at leu1-32 and ura4-294 in *Schizosaccharomyces pombe*. *Genetics*, **136**, 849-856.

Kibel, A., Iliopoulos, O., DeCaprio, J.A. and Kaelin, W.G., Jr. (1995) Binding of the von Hippel-Lindau tumor suppressor protein to Elongin B and C. *Science*, **269**, 1444-1446.

Kile, B.T., Schulman, B.A., Alexander, W.S., Nicola, N.A., Martin, H.M. and Hilton, D.J. (2002) The SOCS box: a tale of destruction and degradation. *Trends Biochem Sci*, **27**, 235-241.

Kim, J., Kim, J.H., Lee, S.H., Kim, D.H., Kang, H.Y., Bae, S.H., Pan, Z.Q. and Seo, Y.S. (2002) The novel human DNA helicase hFBH1 is an F-box protein. *J Biol Chem*, **277**, 24530-24537.

Kim, S.H., Lin, D.P., Matsumoto, S., Kitazono, A. and Matsumoto, T. (1998) Fission yeast Slp1: an effector of the Mad2-dependent spindle checkpoint. *Science*, **279**, 1045-1047.

King, R.W., Peters, J.M., Tugendreich, S., Rolfe, M., Hieter, P. and Kirschner, M.W. (1995) A 20S complex containing CDC27 and CDC16 catalyzes the mitosis-specific conjugation of ubiquitin to cyclin B. *Cell*, **81**, 279-288.

Kishi, T. and Yamao, F. (1998) An essential function of Grr1 for the degradation of Cln2 is to act as a binding core that links Cln2 to Skp1. *J Cell Sci*, **111**, 3655-3661.

Kitagawa, K., Abdulle, R., Bansal, P.K., Cagney, G., Fields, S. and Hieter, P. (2003) Requirement of skp1-bub1 interaction for kinetochore-mediated activation of the spindle checkpoint. *Mol Cell*, **11**, 1201-1213.

Kitagawa, K., Skowyra, D., Elledge, S.J., Harper, J.W. and Hieter, P. (1999) SGT1 encodes an essential component of the yeast kinetochore assembly pathway and a novel subunit of the SCF ubiquitin ligase complex. *Mol Cell*, **4**, 21-33.

Koepp, D.M., Schaefer, L.K., Ye, X., Keyomarsi, K., Chu, C., Harper, J.W. and Elledge, S.J. (2001) Phosphorylation-dependent ubiquitination of cyclin E by the SCFFbw7 ubiquitin ligase. *Science*, **294**, 173-177.

Kominami, K., Ochotorena, I. and Toda, T. (1998) Two F-box/WD-repeat proteins Pop1 and Pop2 form hetero- and homo-complexes together with cullin-1 in the fission yeast SCF (Skp1-Cullin-1-F-box) ubiquitin ligase. *Genes Cells*, **3**, 721-735.

Kominami, K. and Toda, T. (1997) Fission yeast WD-repeat protein pop1 regulates genome ploidy through ubiquitin-proteasome-mediated degradation of the CDK inhibitor Rum1 and the S-phase initiator Cdc18. *Genes Dev*, **11**, 1548-1560.

Kroll, M., Margottin, F., Kohl, A., Renard, P., Durand, H., Concordet, J.P., Bachelerie, F., Arenzana-Seisdedos, F. and Benarous, R. (1999) Inducible degradation of IkappaBalpha by the proteasome requires interaction with the F-box protein h-betaTrCP. *J Biol Chem*, **274**, 7941-7945.

Kubai, D.F. (1975) The evolution of the mitotic spindle. *Int Rev Cytol*, **43**, 167-227.

Kuras, L., Rouillon, A., Lee, T., Barbey, R., Tyers, M. and Thomas, D. (2002) Dual regulation of the met4 transcription factor by ubiquitin-dependent degradation and inhibition of promoter recruitment. *Mol Cell*, **10**, 69-80.

Lammer, D., Mathias, N., Laplaza, J.M., Jiang, W., Liu, Y., Callis, J., Goebl, M. and Estelle, M. (1998) Modification of yeast Cdc53p by the ubiquitin-related protein rub1p affects function of the SCFCdc4 complex. *Genes Dev*, **12**, 914-926.

Lang, V., Janzen, J., Fischer, G.Z., Soneji, Y., Beinke, S., Salmeron, A., Allen, H., Hay, R.T., Ben-Neriah, Y. and Ley, S.C. (2003) betaTrCP-mediated proteolysis of NF-kappaB1 p105 requires phosphorylation of p105 serines 927 and 932. *Mol Cell Biol*, **23**, 402-413.

Latres, E., Chiarle, R., Schulman, B.A., Pavletich, N.P., Pellicer, A., Inghirami, G. and Pagano, M. (2001) Role of the F-box protein Skp2 in lymphomagenesis. *Proc Natl Acad Sci U S A*, **98**, 2515-2520.

Latres, E., Chiaur, D.S. and Pagano, M. (1999) The human F box protein beta-Trcp associates with the Cul1/Skp1 complex and regulates the stability of beta-catenin. *Oncogene*, **18**, 849-854.

Leung, D.W., Chen, E. and Goeddel, D.V. (1989) A method for random mutagenesis of a defined DNA segment using a modified polymerase chain reaction. *Technique*, **1**, 11-15.

Li, R. and Murray, A.W. (1991) Feedback control of mitosis in budding yeast. *Cell*, **66**, 519-531.

Li, X. and Nicklas, R.B. (1995) Mitotic forces control a cell-cycle checkpoint. *Nature*, **373**, 630-632.

Liakopoulos, D., Busgen, T., Brychzy, A., Jentsch, S. and Pause, A. (1999) Conjugation of the ubiquitin-like protein NEDD8 to cullin-2 is linked to von Hippel-Lindau tumor suppressor function. *Proc Natl Acad Sci U S A*, **96**, 5510-5515.

Lisztwan, J., Imbert, G., Wirbelauer, C., Gstaiger, M. and Krek, W. (1999) The von Hippel-Lindau tumor suppressor protein is a component of an E3 ubiquitin-protein ligase activity. *Genes Dev*, **13**, 1822-1833.

Lisztwan, J., Marti, A., Sutterluty, H., Gstaiger, M., Wirbelauer, C. and Krek, W. (1998) Association of human CUL-1 and ubiquitin-conjugating enzyme CDC34 with the F-box protein p45(SKP2): evidence for evolutionary conservation in the subunit composition of the CDC34-SCF pathway. *EMBO J*, **17**, 368-383.

Liu, C., Powell, K.A., Mundt, K., Wu, L., Carr, A.M. and Caspari, T. (2003) Cop9/signalosome subunits and Pcu4 regulate ribonucleotide reductase by both checkpoint-dependent and -independent mechanisms. *Genes Dev*, **17**, 1130-1140.

Lonergan, K.M., Iliopoulos, O., Ohh, M., Kamura, T., Conaway, R.C., Conaway, J.W. and Kaelin, W.G., Jr. (1998) Regulation of hypoxia-inducible mRNAs by the von Hippel-Lindau tumor suppressor protein requires binding to complexes containing elongins B/C and Cul2. *Mol Cell Biol*, **18**, 732-741.

Lyapina, S., Cope, G., Shevchenko, A., Serino, G., Tsuge, T., Zhou, C., Wolf, D.A., Wei, N. and Deshaies, R.J. (2001) Promotion of NEDD-CUL1 conjugate cleavage by COP9 signalosome. *Science*, **292**, 1382-1385.

Mallavarapu, A., Sawin, K. and Mitchison, T. (1999) A switch in microtubule dynamics at the onset of anaphase B in the mitotic spindle of *Schizosaccharomyces pombe*. *Curr Biol*, **9**, 1423-1426.

Maniatis, T., Fritsch, E. and Sambrooke, J. (1982) *Molecular Cloning: a laboratory Manual. Cold Spring Harbour Laboratory Press.*

Margottin, F., Bour, S.P., Durand, H., Selig, L., Benichou, S., Richard, V., Thomas, D., Strebel, K. and Benarous, R. (1998) A novel human WD protein, h-

beta TrCp, that interacts with HIV-1 Vpu connects CD4 to the ER degradation pathway through an F-box motif. *Mol Cell*, **1**, 565-574.

Margottin-Goguet, F., Hsu, J.Y., Loktev, A., Hsieh, H.M., Reimann, J.D. and Jackson, P.K. (2003) Prophase destruction of Emi1 by the SCF(betaTrCP/Slimb) ubiquitin ligase activates the anaphase promoting complex to allow progression beyond prometaphase. *Dev Cell*, **4**, 813-826.

Martin-Castellanos, C., Blanco, M.A., de Prada, J.M. and Moreno, S. (2000) The puc1 cyclin regulates the G1 phase of the fission yeast cell cycle in response to cell size. *Mol Biol Cell*, **11**, 543-554.

Marzluf, G.A. (1997) Molecular genetics of sulfur assimilation in filamentous fungi and yeast. *Annu Rev Microbiol*, **51**, 73-96.

Mathias, N., Johnson, S., Byers, B. and Goebl, M. (1999) The abundance of cell cycle regulatory protein Cdc4p is controlled by interactions between its F box and Skp1p. *Mol Cell Biol*, **19**, 1759-1767.

Mathias, N., Johnson, S.L., Winey, M., Adams, A.E., Goetsch, L., Pringle, J.R., Byers, B. and Goebl, M.G. (1996) Cdc53p acts in concert with Cdc4p and Cdc34p to control the G1-to-S-phase transition and identifies a conserved family of proteins. *Mol Cell Biol*, **16**, 6634-6643.

Matsuzawa, S.I. and Reed, J.C. (2001) Siah-1, SIP, and Ebi collaborate in a novel pathway for beta-catenin degradation linked to p53 responses. *Mol Cell*, **7**, 915-926.

Maxwell, P.H., Wiesener, M.S., Chang, G.W., Clifford, S.C., Vaux, E.C., Cockman, M.E., Wykoff, C.C., Pugh, C.W., Maher, E.R. and Ratcliffe, P.J. (1999) The tumour suppressor protein VHL targets hypoxia-inducible factors for oxygen-dependent proteolysis. *Nature*, **399**, 271-275.

McIntosh, J.R., Grishchuk, E.L. and West, R.R. (2002) Chromosome-microtubule interactions during mitosis. *Annu Rev Cell Dev Biol*, **18**, 193-219.

Michel, J.J. and Xiong, Y. (1998) Human CUL-1, but not other cullin family members, selectively interacts with SKP1 to form a complex with SKP2 and cyclin A. *Cell Growth Differ*, **9**, 435-449.

Millband, D.N., Campbell, L., Hardwick, K.G., The awesome power of multiple model systems: interpreting the complex nature of spindle checkpoint signaling. *Trends Cell Biol*, **12(5)**, 203-209

Miyake, S., Lupher, M.L., Jr., Andoniou, C.E., Lill, N.L., Ota, S., Douillard, P., Rao, N. and Band, H. (1997) The Cbl protooncogene product: from an enigmatic oncogene to center stage of signal transduction. *Crit Rev Oncog*, **8**, 189-218.

Moberg, K.H., Bell, D.W., Wahrer, D.C., Haber, D.A. and Hariharan, I.K. (2001) Archipelago regulates Cyclin E levels in Drosophila and is mutated in human cancer cell lines. *Nature*, **413**, 311-316.

Moreno, S., Klar, A. and Nurse, P. (1991) Molecular genetic analysis of fission yeast *Schizosaccharomyces pombe*. *Methods Enzymol*, **194**, 795-823.

Moreno, S. and Nurse, P. (1994) Regulation of progression through the G1 phase of the cell cycle by the rum1+ gene. *Nature*, **367**, 236-242.

Mundt, K.E., Porte, J., Murray, J.M., Brikos, C., Christensen, P.U., Caspari, T., Hagan, I.M., Millar, J.B., Simanis, V., Hofmann, K. and Carr, A.M. (1999) The COP9/signalosome complex is conserved in fission yeast and has a role in S phase. *Curr Biol*, **9**, 1427-1430.

Murakami, H. and Okayama, H. (1995) A kinase from fission yeast responsible for blocking mitosis in S phase. *Nature*, **374**, 817-819.

Murray, A.W., Solomon, M.J. and Kirschner, M.W. (1989) The role of cyclin synthesis and degradation in the control of maturation promoting factor activity. *Nature*, **339**, 280-286.

Musacchio, A. and Hardwick, K.G. (2002) The spindle checkpoint: structural insights into dynamic signalling. *Nat Rev Mol Cell Biol*, **3**, 731-741.

Nabeshima, K., Nakagawa, T., Straight, A.F., Murray, A., Chikashige, Y., Yamashita, Y.M., Hiraoka, Y. and Yanagida, M. (1998) Dynamics of centromeres during metaphase-anaphase transition in fission yeast: Dis1 is implicated in force balance in metaphase bipolar spindle. *Mol Biol Cell*, **9**, 3211-3225.

Nakayama, K., Nagahama, H., Minamishima, Y.A., Matsumoto, M., Nakamichi, I., Kitagawa, K., Shirane, M., Tsunematsu, R., Tsukiyama, T., Ishida, N., Kitagawa, M. and Hatakeyama, S. (2000) Targeted disruption of Skp2 results in accumulation of cyclin E and p27(Kip1), polyploidy and centrosome overduplication. *EMBO J*, **19**, 2069-2081.

Nash, P., Tang, X., Orlicky, S., Chen, Q., Gertler, F.B., Mendenhall, M.D., Sicheri, F., Pawson, T. and Tyers, M. (2001) Multisite phosphorylation of a CDK inhibitor sets a threshold for the onset of DNA replication. *Nature*, **414**, 514-521.

Nasmyth, K., Nurse, P. and Fraser, R.S. (1979) The effect of cell mass on the cell cycle timing and duration of S-phase in fission yeast. *J Cell Sci*, **39**, 215-233.

Nicklas, R.B. (1997) How cells get the right chromosomes. *Science*, **275**, 632-637.

Nurse, P., Thuriaux, P. and Nasmyth, K. (1976) Genetic control of the cell division cycle in the fission yeast *Schizosaccharomyces pombe*. *Mol Gen Genet*, **146**, 167-178.

O'Connell, M.J., Walworth, N.C. and Carr, A.M. (2000) The G2-phase DNA-damage checkpoint. *Trends Cell Biol*, **10**, 296-303.

Orian, A., Schwartz, A.L., Israel, A., Whiteside, S., Kahana, C. and Ciechanover, A. (1999) Structural motifs involved in ubiquitin-mediated processing of the NF-kappaB precursor p105: roles of the glycine-rich region and a downstream ubiquitination domain. *Mol Cell Biol*, **19**, 3664-3673.

Orian, A., Whiteside, S., Israel, A., Stancovski, I., Schwartz, A.L. and Ciechanover, A. (1995) Ubiquitin-mediated processing of NF-kappa B transcriptional activator precursor p105. Reconstitution of a cell-free system and identification of the ubiquitin-carrier protein, E2, and a novel ubiquitin-protein ligase, E3, involved in conjugation. *J Biol Chem*, **270**, 21707-21714.

Osaka, F., Saeki, M., Katayama, S., Aida, N., Toh, E.A., Kominami, K., Toda, T., Suzuki, T., Chiba, T., Tanaka, K. and Kato, S. (2000) Covalent modifier NEDD8 is essential for SCF ubiquitin-ligase in fission yeast. *EMBO J*, **19**, 3475-3484.

Patton, E.E., Peyraud, C., Rouillon, A., Surdin-Kerjan, Y., Tyers, M. and Thomas, D. (2000) SCF(Met30)-mediated control of the transcriptional activator Met4 is required for the G(1)-S transition. *EMBO J*, **19**, 1613-1624.

Patton, E.E., Willems, A.R., Sa, D., Kuras, L., Thomas, D., Craig, K.L. and Tyers, M. (1998a) Cdc53 is a scaffold protein for multiple Cdc34/Skp1/F-box proteincomplexes that regulate cell division and methionine biosynthesis in yeast [published erratum appears in Genes Dev 1998 Oct 1;12(19):3144]. *Genes Dev*, **12**, 692-705.

Patton, E.E., Willems, A.R. and Tyers, M. (1998b) Combinatorial control in ubiquitin-dependent proteolysis: don't Skp the F-box hypothesis. *Trends Genet*, **14**, 236-243.

Pintard, L., Kurz, T., Glaser, S., Willis, J.H., Peter, M. and Bowerman, B. (2003) Neddylation and Deneddylation of CUL-3 Is Required to Target MEI-1/Katanin for Degradation at the Meiosis-to-Mitosis Transition in C. elegans. *Curr Biol*, **13**, 911-921.

Regan-Reimann, J.D., Duong, Q.V. and Jackson, P.K. (1999) Identification of novel F-box proteins in Xenopus laevis. *Curr Biol*, **9**, R762-763.

Rhind, N. and Russell, P. (2000) Chk1 and Cds1: linchpins of the DNA damage and replication checkpoint pathways. *J Cell Sci*, **113 (Pt 22)**, 3889-3896.

Rouillon, A., Barbey, R., Patton, E.E., Tyers, M. and Thomas, D. (2000) Feedback-regulated degradation of the transcriptional activator Met4 is triggered by the SCF(Met30)complex. *EMBO J*, **19**, 282-294.

Russell, I.D., Grancell, A.S. and Sorger, P.K. (1999) The unstable F-box protein p58-Ctf13 forms the structural core of the CBF3 kinetochore complex. *J Cell Biol*, **145**, 933-950.

Russell, P. (1998) Checkpoints on the road to mitosis. *Trends Biochem Sci*, **23**, 399-402.

Salic, A., Lee, E., Mayer, L. and Kirschner, M.W. (2000) Control of beta-catenin stability: reconstitution of the cytoplasmic steps of the wnt pathway in Xenopus egg extracts. *Mol Cell*, **5**, 523-532.

Saurin, A.J., Borden, K.L., Boddy, M.N. and Freemont, P.S. (1996) Does this have a familiar RING? *Trends Biochem Sci*, **21**, 208-214.

Sazer, S. and Sherwood, S.W. (1990) Mitochondrial growth and DNA synthesis occur in the absence of nuclear DNA replication in fission yeast. *J Cell Sci*, **97 (Pt 3)**, 509-516.

Schadick, K., Fourcade, H.M., Boumenot, P., Seitz, J.J., Morrell, J.L., Chang, L., Gould, K.L., Partridge, J.F., Allshire, R.C., Kitagawa, K., Hieter, P. and Hoffman, C.S. (2002) *Schizosaccharomyces pombe* Git7p, a member of the *Saccharomyces cerevisiae* Sgtlp family, is required for glucose and cyclic AMP signaling, cell wall integrity, and septation. *Eukaryot Cell*, **1**, 558-567.

Schulman, B.A., Carrano, A.C., Jeffrey, P.D., Bowen, Z., Kinnucan, E.R., Finnin, M.S., Elledge, S.J., Harper, J.W., Pagano, M. and Pavletich, N.P. (2000)

Insights into SCF ubiquitin ligases from the structure of the Skp1-Skp2 complex. *Nature*, **408**, 381-386.

Schwob, E., Bohm, T., Mendenhall, M.D. and Nasmyth, K. (1994) The B-type cyclin kinase inhibitor p40SIC1 controls the G1 to S transition in *S. cerevisiae*. *Cell*, **79**, 233-244.

Seibert, V., Prohl, C., Schoultz, I., Rhee, E., Lopez, R., Abderazzaq, K., Zhou, C. and Wolf, D.A. (2002) Combinatorial diversity of fission yeast SCF ubiquitin ligases by homo- and heterooligomeric assemblies of the F-box proteins Pop1p and Pop2p. *BMC Biochem*, **3**, 22.

Semenza, G.L. (2000) HIF-1 and human disease: one highly involved factor. *Genes Dev*, **14**, 1983-1991.

Seol, J.H., Feldman, R.M., Zachariae, W., Shevchenko, A., Correll, C.C., Lyapina, S., Chi, Y., Galova, M., Claypool, J., Sandmeyer, S., Nasmyth, K. and Deshaies, R.J. (1999) Cdc53/cullin and the essential Hrt1 RING-H2 subunit of SCF define a ubiquitin ligase module that activates the E2 enzyme Cdc34. *Genes Dev*, **13**, 1614-1626.

Seol, J.H., Shevchenko, A. and Deshaies, R.J. (2001) Skp1 forms multiple protein complexes, including RAVE, a regulator of V- ATPase assembly. *Nat Cell Biol*, **3**, 384-391.

Sharp, D.J., Rogers, G.C. and Scholey, J.M. (2000) Microtubule motors in mitosis. *Nature*, **407**, 41-47.

Skowyra, D., Craig, K.L., Tyers, M., Elledge, S.J. and Harper, J.W. (1997) F-box proteins are receptors that recruit phosphorylated substrates to the SCF ubiquitin-ligase complex [see comments]. *Cell*, **91**, 209-219.

Skowyra, D., Koepp, D.M., Kamura, T., Conrad, M.N., Conaway, R.C., Conaway, J.W., Elledge, S.J. and Harper, J.W. (1999) Reconstitution of G1 cyclin ubiquitination with complexes containing SCFGrr1 and Rbx1 [see comments]. *Science*, **284**, 662-665.

Spiegelman, V.S., Slaga, T.J., Pagano, M., Minamoto, T., Ronai, Z. and Fuchs, S.Y. (2000) Wnt/beta-catenin signaling induces the expression and activity of betaTrCP ubiquitin ligase receptor. *Mol Cell*, **5**, 877-882.

Spruck, C., Strohmaier, H., Watson, M., Smith, A.P., Ryan, A., Krek, T.W. and Reed, S.I. (2001) A CDK-independent function of mammalian Cks1: targeting of SCF(Skp2) to the CDK inhibitor p27Kip1. *Mol Cell*, **7**, 639-650.

Spruck, C.H. and Strohmaier, H.M. (2002) Seek and destroy: SCF ubiquitin ligases in mammalian cell cycle control. *Cell Cycle*, **1**, 250-254.

Stebbins, C.E., Kaelin, W.G., Jr. and Pavletich, N.P. (1999) Structure of the VHL-ElonginC-ElonginB complex: implications for VHL tumor suppressor function. *Science*, **284**, 455-461.

Stemmann, O. and Lechner, J. (1996) The *Saccharomyces cerevisiae* kinetochore contains a cyclin-CDK complexing homologue, as identified by in vitro reconstitution. *EMBO J*, **15**, 3611-3620.

Stemmann, O., Neidig, A., Kocher, T., Wilm, M. and Lechner, J. (2002) Hsp90 enables Ctf13p/Skp1p to nucleate the budding yeast kinetochore. *Proc Natl Acad Sci U S A*, **99**, 8585-8590.

Stern, B.M. and Murray, A.W. (2001) Lack of tension at kinetochores activates the spindle checkpoint in budding yeast. *Curr Biol*, **11**, 1462-1467.

Sudakin, V., Ganoth, D., Dahan, A., Heller, H., Hershko, J., Luca, F.C., Ruderman, J.V. and Hershko, A. (1995) The cyclosome, a large complex containing cyclin-selective ubiquitin ligase activity, targets cyclins for destruction at the end of mitosis. *Mol Biol Cell*, **6**, 185-197.

Sutter, C.H., Laughner, E. and Semenza, G.L. (2000) Hypoxia-inducible factor 1alpha protein expression is controlled by oxygen-regulated ubiquitination that is disrupted by deletions and missense mutations. *Proc Natl Acad Sci U S A*, **97**, 4748-4753.

Suzuki, H., Chiba, T., Kobayashi, M., Takeuchi, M., Suzuki, T., Ichiyama, A., Ikenoue, T., Omata, M., Furuichi, K. and Tanaka, K. (1999) IkappaBalpha ubiquitination is catalyzed by an SCF-like complex containing Skp1, cullin-1, and two F-box/WD40-repeat proteins, betaTrCP1 and betaTrCP2. *Biochem Biophys Res Commun*, **256**, 127-132.

Tanaka, K., Kawakami, T., Tateishi, K., Yashiroda, H. and Chiba, T. (2001) Control of IkappaBalpha proteolysis by the ubiquitin-proteasome pathway. *Biochimie*, **83**, 351-356.

Tasto, J.J., Morrell, J.L. and Gould, K.L. (2003) An anillin homologue, Mid2p, acts during fission yeast cytokinesis to organize the septin ring and promote cell separation. *J Cell Biol*, **160**, 1093-1103.

Thomas, D., Kuras, L., Barbey, R., Cherest, H., Blaiseau, P.L. and Surdin-Kerjan, Y. (1995) Met30p, a yeast transcriptional inhibitor that responds to S-

adenosylmethionine, is an essential protein with WD40 repeats. *Mol Cell Biol*, **15**, 6526-6534.

Tsvetkov, L.M., Yeh, K.H., Lee, S.J., Sun, H. and Zhang, H. (1999) p27(Kip1) ubiquitination and degradation is regulated by the SCF(Skp2) complex through phosphorylated Thr187 in p27. *Curr Biol*, **9**, 661-664.

Uzawa, S., Samejima, I., Hirano, T., Tanaka, K. and Yanagida, M. (1990) The fission yeast cut1+ gene regulates spindle pole body duplication and has homology to the budding yeast ESP1 gene. *Cell*, **62**, 913-925.

Walworth, N., Davey, S. and Beach, D. (1993) Fission yeast chk1 protein kinase links the rad checkpoint pathway to cdc2. *Nature*, **363**, 368-371.

Walworth, N.C. and Bernards, R. (1996) rad-dependent response of the chk1-encoded protein kinase at the DNA damage checkpoint. *Science*, **271**, 353-356.

Wei, N., Chamovitz, D.A. and Deng, X.W. (1994) Arabidopsis COP9 is a component of a novel signaling complex mediating light control of development. *Cell*, **78**, 117-124.

Weiss, E. and Winey, M. (1996) The *Saccharomyces cerevisiae* spindle pole body duplication gene MPS1 is part of a mitotic checkpoint. *J Cell Biol*, **132**, 111-123.

West, R.R., Vaisberg, E.V., Ding, R., Nurse, P. and McIntosh, J.R. (1998) cut11(+): A gene required for cell cycle-dependent spindle pole body anchoring in the nuclear envelope and bipolar spindle formation in *Schizosaccharomyces pombe*. *Mol Biol Cell*, **9**, 2839-2855.

Wiederkehr, A., Avaro, S., Prescianotto-Baschong, C., Haguenauer-Tsapis, R. and Riezman, H. (2000) The F-box protein Rcy1p is involved in endocytic membrane traffic and recycling out of an early endosome in *Saccharomyces cerevisiae*. *J Cell Biol*, **149**, 397-410.

Winston, J.T., Koepp, D.M., Zhu, C., Elledge, S.J. and Harper, J.W. (1999a) A family of mammalian F-box proteins. *Curr Biol*, **9**, 1180-1182.

Winston, J.T., Strack, P., Beer-Romero, P., Chu, C.Y., Elledge, S.J. and Harper, J.W. (1999b) The SCFbeta-TRCP-ubiquitin ligase complex associates specifically with phosphorylated destruction motifs in IkappaBalpha and beta-catenin and stimulates IkappaBalpha ubiquitination in vitro [published erratum appears in Genes Dev 1999 Apr 15;13(8):1050]. *Genes Dev*, **13**, 270-283.

Wittmann, T., Hyman, A. and Desai, A. (2001) The spindle: a dynamic assembly of microtubules and motors. *Nat Cell Biol*, **3**, E28-34.

Wood, V., Gwilliam, R., Rajandream, M.A., Lyne, M., Lyne, R., Stewart, A., Sgouros, J., Peat, N., Hayles, J., Baker, S., Basham, D., Bowman, S., Brooks, K., Brown, D., Brown, S., Chillingworth, T., Churcher, C., Collins, M., Connor, R., Cronin, A., Davis, P., Feltwell, T., Fraser, A., Gentles, S., Goble, A., Hamlin, N., Harris, D., Hidalgo, J., Hodgson, G., Holroyd, S., Hornsby, T., Howarth, S., Huckle, E.J., Hunt, S., Jagels, K., James, K., Jones, L., Jones, M., Leather, S., McDonald, S., McLean, J., Mooney, P., Moule, S., Mungall, K., Murphy, L., Niblett, D., Odell, C., Oliver, K., O'Neil, S., Pearson, D., Quail, M.A., Rabbinowitsch, E., Rutherford, K., Rutter, S., Saunders, D., Seeger, K., Sharp, S., Skelton, J., Simmonds, M., Squares, R., Squares, S., Stevens, K., Taylor, K., Taylor, R.G., Tivey, A., Walsh, S., Warren, T., Whitehead, S., Woodward, J., Volckaert, G., Aert, R., Robben, J., Grymonprez, B., Weltjens, I., Vanstreels, E., Rieger, M., Schafer, M., Muller-Auer, S., Gabel, C., Fuchs, M., Dusterhoft, A., Fritzc, C., Holzer, E., Moestl, D., Hilbert, H., Borzym, K., Langer, I., Beck, A., Lehrach, H., Reinhardt, R., Pohl, T.M., Eger, P., Zimmermann, W., Wedler, H., Wambutt, R., Purnelle, B., Goffeau, A., Cadieu, E., Dreano, S., Gloux, S., Lelaure, V., Mottier, S., Galibert, F., Aves, S.J., Xiang, Z., Hunt, C., Moore, K., Hurst, S.M., Lucas, M., Rochet, M., Gaillardin, C., Tallada, V.A., Garzon, A., Thode, G., Daga, R.R., Cruzado, L., Jimenez, J., Sanchez, M., del Rey, F., Benito, J., Dominguez, A., Revuelta, J.L., Moreno, S., Armstrong, J., Forsburg, S.L., Cerutti, L., Lowe, T., McCombie, W.R., Paulsen, I., Potashkin, J., Shpakovski, G.V., Ussery, D., Barrell, B.G., Nurse, P. and Cerrutti, L. (2002) The genome sequence of *Schizosaccharomyces pombe*. *Nature*, **415**, 871-880.

Yaffe, M.B. and Elia, A.E. (2001) Phosphoserine/threonine-binding domains. *Curr Opin Cell Biol*, **13**, 131-138.

Yaffe, M.P., Harata, D., Verde, F., Eddison, M., Toda, T. and Nurse, P. (1996) Microtubules mediate mitochondrial distribution in fission yeast. *Proc Natl Acad Sci U S A*, **93**, 11664-11668.

Yamano, H., Kitamura, K., Kominami, K., Lehmann, A., Katayama, S., Hunt, T. and Toda, T. (2000) The spike of S phase cyclin Cig2 expression at the G1-S border in fission yeast requires both APC and SCF ubiquitin ligases. *Mol Cell*, **6**, 1377-1387.

Yaron, A., Hatzubai, A., Davis, M., Lavon, I., Amit, S., Manning, A.M., Andersen, J.S., Mann, M., Mercurio, F. and Ben-Neriah, Y. (1998) Identification of the receptor component of the IkappaBalpha-ubiquitin ligase. *Nature*, **396**, 590-594.

Zachariae, W. and Nasmyth, K. (1999) Whose end is destruction: cell division and the anaphase-promoting complex. *Genes Dev*, **13**, 2039-2058.

Zhang, H., Kobayashi, R., Galaktionov, K. and Beach, D. (1995) p19Skp1 and p45Skp2 are essential elements of the cyclin A-CDK2 S phase kinase. *Cell*, **82**, 915-925.

Zhao, X., Georgieva, B., Chabes, A., Domkin, V., Ippel, J.H., Schleucher, J., Wijmenga, S., Thelander, L. and Rothstein, R. (2000) Mutational and structural analyses of the ribonucleotide reductase inhibitor Sml1 define its Rnr1 interaction domain whose inactivation allows suppression of mec1 and rad53 lethality. *Mol Cell Biol*, **20**, 9076-9083.

Zheng, N., Schulman, B.A., Song, L., Miller, J.J., Jeffrey, P.D., Wang, P., Chu, C., Koepp, D.M., Elledge, S.J., Pagano, M., Conaway, R.C., Conaway, J.W., Harper, J.W. and Pavletich, N.P. (2002) Structure of the Cul1-Rbx1-Skp1-F boxSkp2 SCF ubiquitin ligase complex. *Nature*, **416**, 703-709.

Zhou, B.B. and Elledge, S.J. (2000) The DNA damage response: putting checkpoints in perspective. *Nature*, **408**, 433-439.

Zhou, C., Seibert, V., Geyer, R., Rhee, E., Lyapina, S., Cope, G., Deshaies, R.J. and Wolf, D.A. (2001) The fission yeast COP9/signalosome is involved in cullin modification by ubiquitin-related Ned8p. *BMC Biochem*, **2**, 7.

Zhou, C., Wee, S., Rhee, E., Naumann, M., Dubiel, W. and Wolf, D.A. (2003) Fission yeast COP9/signalosome suppresses cullin activity through recruitment of the deubiquitylating enzyme Ubp12p. *Mol Cell*, **11**, 927-938.

Zou, L. and Elledge, S.J. (2003) Sensing DNA damage through ATRIP recognition of RPA-ssDNA complexes. *Science*, **300**, 1542-1548.